The role of pre-mRNA splicing and splicing related proteins in the cold acclimation induced adjustment of photosynthesis and the acquisition of freezing tolerance in *Arabidopsis thaliana.*

Marc Rosembert

Thesis submitted to the Faculty of Graduate and Postdoctoral Studies
in partial fulfillment of the requirements for the Ph.D. degree in Biology

Thèse soumise à la Faculté d'Études Supérieures et Postdoctorales en vue de l'obtention du doctorat en Biologie

Ottawa-Carleton Institute of Biology
Institut de Biologie d'Ottawa-Carleton

Faculty of Science
Faculté des Sciences

University of Ottawa
Université d'Ottawa

Abstract

This thesis evaluated the role of Serine/Arginine-rich proteins, also known as SR proteins, in addition to LAMMER kinases in the cold acclimation response using *Brassica napus* and *Arabidopsis thaliana*. Transcription profile analyses of SR and LAMMER kinase genes in *Brassica napus* and *BnCBF* overexpressor lines showed that exposure to low temperatures led to increased transcript levels for nine SR genes and two kinases. *BnCBF* overexpression was found to exacerbate this response. This was associated with increases in SR protein abundance and phosphorylation status, suggesting that SR proteins play an essential role in cold acclimation. These findings prompted further studies to assess the role of SR proteins and kinases in the cold acclimation induced adjustment of photosynthesis, the acquisition of freezing tolerance and the transcriptional profile of *CBF*, *SPS* and *COR* genes, which play an important role in the transcriptional cascade allowing plants to undergo cold acclimation. Using *Arabidopsis* loss-of-function mutants of SR proteins and AME3 LAMMER kinase, it was shown that At-RSZ22 and At-SR45 are indispensable in the regulation of photosynthesis under non-acclimated and cold acclimation conditions. At-RSZ22a, At-SCL30 and At-RS41 were then proposed to play a crucial role in the cold acclimation induced adjustment of photosynthetic performance. Moreover, the deletion of At-AME3 kinase not only jeopardized the cold acclimation induced adjustment of photosynthetic performance, but also the acquisition of freezing tolerance. This was associated with attenuation of the transcription profile of key cold responsive genes and protein abundance of COR15 A/B and dehydrins. These findings prompted further physiological characterization of *ame3* mutants, and the elucidation of Serine/Arginine-rich proteins capable of interacting with this LAMMER kinase of interest. Under cold stress and

acclimation conditions, the deletion of At-AME3 LAMMER kinase impeded Photosystem I physiology and state-1 state-2 transitions. These findings were associated with decreases in Photosystem II and Photosystem I protein abundance. Yeast 2-hybrid assays showed that six SR proteins are capable of physically interacting with AME3. Taken together, the results of this study demonstrate that At-RSZ22 and At-SR45 are essential in the photosynthetic performance of *Arabidopsis*, that At-RSZ22a, At-SCL30 and At-RS41 play an essential role in the cold acclimation induced recovery of photosynthetic performance, and that At-AME3 plays an essential role in the cold acclimation response.

Résumé

Cette thèse avait pour but d'évaluer le rôle potentiel des protéines riches en Serine et Arginine (SR) ainsi que les kinases LAMMER dans le processus d'acclimatation aux basses températures par l'entremise de *Brassica napus* et *Arabidopsis thaliana*. Des études préliminaires évaluant le profil de transcription des gènes SR ainsi que les kinases LAMMER ont révélé une hausse au niveau de la transcription de neuf gènes SR et une kinase LAMMER suite à une exposition prolongée à de basses températures. Cette réponse fut exacerbée auprès des lignées mutantes de *Brassica napus* surexprimant *BnCBF.* De plus, les changements de profil d'expression de gènes SR et de kinases lors d'exposition prolongée à de basses températures furent associés à une augmentation du taux de phosphorylation et d'abondance de protéines SR ainsi que des changements au niveau de la localisation de certains sous-groupes de protéines SR. Ces résultats préliminaires ont incité des recherches plus poussées, afin de déterminer le rôle potentiel de ces protéines SR et At-AME3 dans l'ajustement de la performance photosynthétique induite par l'acclimatation au basses températures, l'acquisition de la tolérance aux basses températures, ainsi qu'au niveau de la transcription de gènes essentiels (*CBF, SPS, COR*) jouant un rôle important dans l'acclimatation aux basses températures par l'entremise de mutants d'*Arabidopsis thaliana* contenant des disruptions de gènes d'intérêt. Les résultats de cette étude ont démontré qu'At-RSZ22 et At-SR45 jouent un rôle essentiel dans la régulation de la photosynthèse dans *Arabidopsis*. At-RSZ22a, At-SCL30 et At-RS41 ont été suggérés de jouer un rôle dans l'ajustement de la performance photosynthétique lors de l'acclimatation aux basses températures. Cependant, l'absence d'une kinase, At-AME3, a résulté en une diminution marquée de la performance photosynthétique de cette plante transgénique après acclimatation. Cette atténuation au

niveau de la performance photosynthétique d'*at-ame3* fut accompagnée par une sévère déficience concernant l'acquisition de la tolérance aux basses températures, associée à une diminution de l'expression de gènes essentiels à la cascade de transcription reliée à l'acclimatation aux basses températures. Conséquemment, une baisse du niveau de COR15A/B et dehydrins a été observée chez *at-ame3* après acclimatation comparativement à *Arabidopsis thaliana* dans les mêmes conditions. Ces résultats ont poussé des études physiologiques approfondies, comparant *at-ame3* à *Arabidopsis thaliana*. Sous des conditions de stress et après acclimatation, les lignées mutantes d'*at-ame3* exhibent des réponses atténuées au niveau de la physiologie de photosystème I, les transitions « state-1 state-2 », qui ont été attribués à une diminution marquée de protéines associées aux Photosystèmes II et I. Une évaluation d'interactions potentielles entre At-AME3 et certaines protéines SR d'intérêt ont démontré qu'At-AME3 possède la capacité d'interagir physiquement avec six protéines SR d'intérêt, dont cinq ont été suggérés de jouer un role au niveau de la performance photosynthétique d'*Arabidopsis*. Dans l'ensemble, cette étude à démontré que les protéines SR jouent un rôle au sein de l'acclimatation, et qu'At-AME3 semble également contribuer à ce processus complexe.

Acknowledgements

First off, I would like to thank Dr. Leonid V. Savitch and Dr. Douglas A. Johnson for giving me the opportunity to work on this project, their guidance and their patience throughout this entire process. I would also like to thank my committee members, Dr. Linda Bonen and Dr. Owen Rowland for all their help and advice through this process. Special thanks go to all members of the Savitch and Singh labs, especially Dave Sprott and Ghislaine Allard for their invaluable technical assistance and advice. In addition, I would also like to thank Dr. Loreta Gudynaite-Savitch and Maher Mounzer for all their help with the planning, setup and analysis of yeast 2-hybrid experiments, and valuable advice. Last, but certainly not least, a very special thanks to all my friends and family for all the kind words of encouragement and support in the completion of this work.

Table of Contents

Figure Legends

Table Legends

List of Abbreviations

1-qL	Excitation pressure of Photosystem II
3w CA	3 weeks cold acclimated
5w CA	5 weeks cold acclimated
A	Cold acclimation conditions
AL	Actinic light
At	*Arabidopsis thaliana*
BL	Blue Light
Bn	*Brassica napus*
C	Control conditions
CA	Cold acclimated
CBF	C-repeat binding Factors
CET	Cyclic Electron Transport
Chl	Chlorophyll
COR	Cold responsive
DCMU	3-(3`,4`-dichlorophenyl)-1,1-dimethylurea
DREB	Drought Responsive Element Binding
ETR	Linear Electron Transport Rate
FBPase	Fructose 1,6-bisphosphatase
FR	Far Red Light
ICE	Inducer of CBF Expression
KIN1	Cold Induced 1
MT	Multiple Turnover Flash
NPQ	Non-photochemical quenching
OE	Overexpressor
PGR5	Proton Gradient 5
PSI	Photosystem I
PSII	Photosystem II

qN	ΔpH-dependent and ΔpH-independent non-photochemical quenching
qo	Basal quenching
Rubisco	Ribulose 1,5-bisphosphate Carboxylase/Oxygenase
ROS	Reactive Oxygen Species
S	Cold stress conditions
SBPase	Sedoheptulose 1,7 bisphosphatase
SPS	Sucrose Phosphate Synthase
SR	Serine/Arginine-rich proteins
SRPK	SR Protein Kinase
ST	Single Turnover Flash
STA1	Stabilized1
$\phi_{f,D}$	Proportion of reaction centre based non-photochemical quenching
ϕ_{PSII}	Quantum yield of PSII
ϕ_{NPQ}	Proportion of antennae based non-photochemical quenching

Chapter 1: General introduction

Due to their sessile nature, plants are unable to escape from the multitude of biotic and abiotic factors that cause a departure from optimal growth and development. Of these abiotic factors, cold stress, which includes both chilling (0-15ºC) and/or freezing (below 0ºC) temperatures, is a major environmental factor, causing adverse effects on growth and development of plants, thus limiting agricultural productivity. For example, in 2003-2004, frost damage to Saskatchewan wheat crops resulted in losses estimated at 500 million dollars, with similar losses reported regularly across the mid-latitude continental agricultural regions of the world (Baxter, 2014). Thus, major research efforts are being directed towards mitigating such losses, by gaining a better understanding how plants respond and adapt to cold temperatures.

1.1 *Transcriptional regulation of cold stress and acclimation*

The complex process of cold acclimation involves extensive biochemical and physiological changes, leading to alterations in membrane stability (Nishida and Murata, 1996), pigment synthesis to protect from photoxidative stress (Christie et al., 1994; Król et al., 1999; Schöner & Krause, 1990), as well as increases in cryoprotective and antifreeze proteins (Tomashow et al., 1999). Most of these alterations appear to be regulated through changes in gene expression (Medina et al., 2011). Significant progress made in the elucidation of transcriptional networks involved in cold acclimation have led to the identification of three major components involved in the CBF/DREB1-dependent cold stress

responses. These components have been identified as Inducer of CBF expression 1, or ICE1, C-repeat Binding Factors, or CBFs, followed by Cold Responsive (COR) genes (Figure 1.1).

Inducer of CBF Expression 1, or ICE1, is a MYC-type basic helix-loop-helix transcription factor that recognizes and binds to MYC cis-elements (CANNTG) found in the promoter region of C-repeat Binding Factor 3/Dehydration Responsive Element Binding protein 1A (CBF3/DREB1A). To date, ICE1 is the most upstream transcription factor involved in the cold signaling pathway. ICE1 has been shown to be constitutively expressed and localized in the nucleus. Moreover, ICE1 has been shown to positively regulate the expression of genes involved in cold stress response, as *ice1* mutants are hypersensitive to chilling stress and are incapable of undergoing cold acclimation (Chinnusamy et al., 2003). ICE2 is another basic helix-loop-helix transcription factor with a high amino acid similarity to ICE1. While the role of ICE2 has yet to be defined, *Arabidopsis thaliana* mutant lines overexpressing ICE2 were reported as having an increased expression level of CBF1, as well as an enhanced freezing tolerance, suggesting that ICE2 is a positive regulator of CBF1 expression (Fursova et al., 2009). While ICE1 has been shown to be constitutively expressed, CBF gene expression is induced solely upon cold treatment, suggesting that ICE1 requires further interaction with additional cold-induced factors, or post-translational regulation in order to be active (Huang et al., 2012). High expression of OSmotically responsive genes, or HOS1 and SIZ1 were identified as post-translational regulators of ICE1.

Figure 1.1: Schematic diagram of the cold acclimation pathway.

Under regular conditions, HOS1 suppresses Inducer of CBF Expression 1 (ICE1). However, once chilling temperatures are sensed, ICE1 is activated through SUMOylation by SIZ1 (Haake, 2002). It is currently unclear whether SIZ1 also SUMOylates ICE2. ICE2 and ICE1 will in turn induce the expression of C-repeat Binding Factors 1 and 3 (CBF1/CBF3), respectively. CBFs, which recognise Drought Responsive Elements (DREs)/CRT sequences found in the promoter region of several cold responsive (COR) genes, bind to them, in turn increasing the expression of these genes, leading to a physiological response associated with cold tolerance. In addition to the CBF regulon, low temperatures have been shown to induce transcriptional pathways that are not associated with the CBF regulon such as RAV1 (Related to ABI3/VP1), which has been shown to be involved in regulating plant growth and senescence. DREB2 and CBF4, which are involved in the ABA-independent and ABA-responsive pathways, respectively, also recognize and bind to CRT/DREB elements in COR genes, increasing their expression. Moreover, certain COR genes have been shown to possess ABA-responsive promoter elements (ABRE), which are bound by bZIP transcription factors. (Modified from Haake et al., 2002).

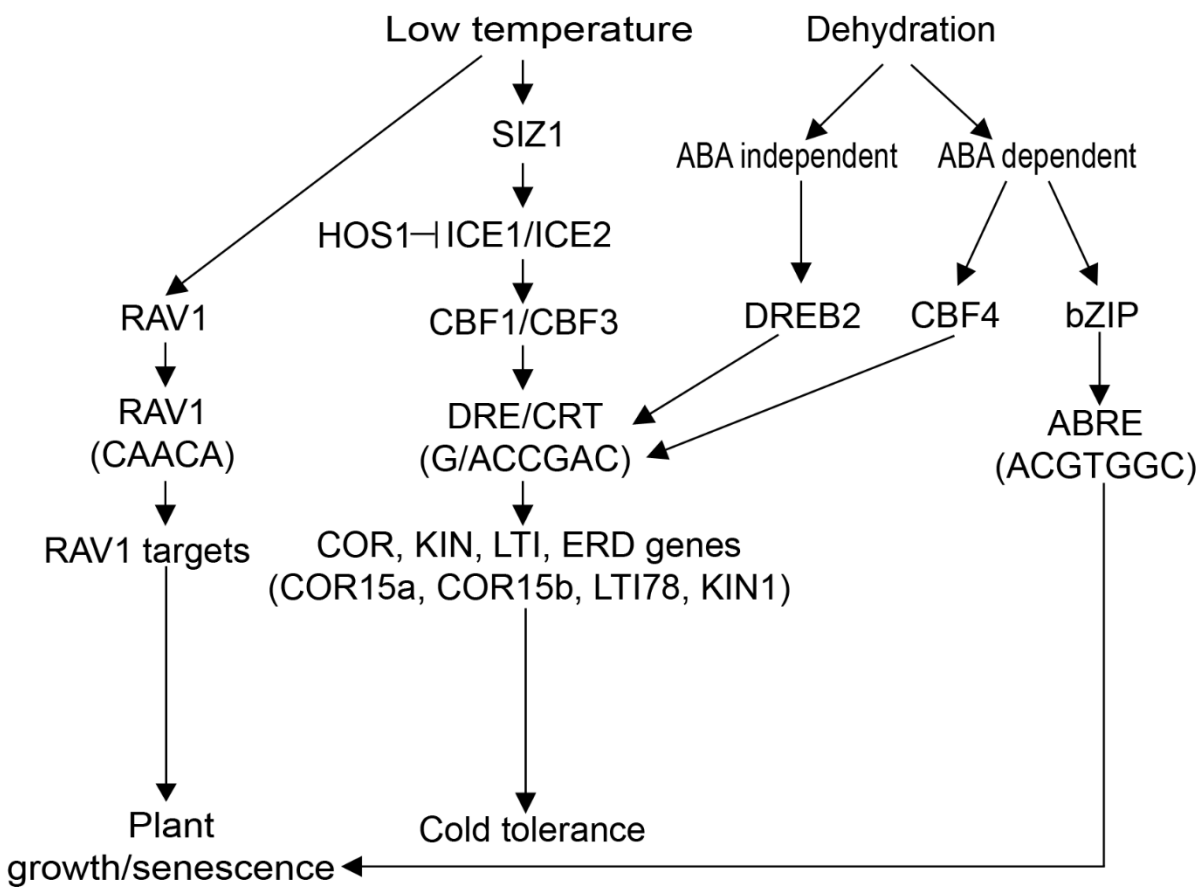
Low temperature
Dehydration
SIZ1
ABA independent
ABA dependent
HOS1⊣ICE1/ICE2
RAV1
CBF1/CBF3
DREB2
CBF4
bZIP
RAV1
(CAACA)
DRE/CRT
(G/ACCGAC)
ABRE
(ACGTGGC)
RAV1 targets
COR, KIN, LTI, ERD genes
(COR15a, COR15b, LTI78, KIN1)
Plant
growth/senescence
Cold tolerance

HOS1, or high expression of osmotically responsive genes 1, is a Really Interesting New Gene (RING)-type ubiquitin E3 ligase that negatively regulates cold responses. HOS1 functions as a cold response attenuator by physically interacting with ICE1 and triggering an ubiquitin-dependent proteolytic mechanism (Jung et al., 2014). Mutant lines deficient in HOS1 show an increase in ICE1, and subsequent accumulation of both CBF and cold responsive genes under normal conditions (Dong et al., 2006; Ishitani et al., 1998).

While the cold-induced ubiquitination and subsequent degradation of ICE1, mediated by HOS1 plays an important role in modulating cold stress responses, small ubiquitin-related modifier conjugation, or sumoylation appears to play an important role in the regulation of responses to abiotic stresses (Miura and Furumoto, 2013; Miura and Hasegawa, 2010). Sumoylation is a reversible post-translational modification that affects critical and diverse processes, including ubiquitin-mediated degradation (Miura et al., 2007). A study by Miura et al. (2007) has established that the *Arabidopsis* SUMO E3 ligase SIZ1 attenuates the ubiquitin-mediated degradation of ICE1 by sumoylating the transcription factor at Lysine residue 393, thus preventing HOS1 access to target residues. Therefore, SIZ1 was shown to antagonize HOS1 activity, hereby allowing ICE1 to bind to CBF3/DREB1A, resulting in the expression of its target genes.

1.1.1 CBF/DREB transcription factors

C-repeat (CRT)-binding factors (CBFs), also known as dehydration-responsive-element-binding proteins (DREBs) are a fundamental part of the signalling cascade resulting in the process of cold acclimation and the acquisition of freezing tolerance in cold-hardy plants. CBF/DREBs belong to the APETALA2/ETHYLENE RESPONSE FACTOR family

of transcription factors, defined by their AP2/ERF domain, which consists of 60-70 amino acids involved in DNA binding (Gilmour et al., 2004).

In *Arabidopsis*, four CBF/DREB proteins have been identified (Jaglo-Ottosen et al., 1998; Liu et al., 1998). The expression of CBF1, CBF2 and CBF3 were found to be induced by cold, but not by dehydration and high salinity stresses. Conversely, CBF4 expression is induced in response to high salinity (Sakuma et al., 2002) and dehydration (Haake, 2002) stresses, but not low temperatures. The identification of CBFs 1-4 in *Arabidopsis* was a major step towards understanding gene regulation with respect to cold acclimation, as CBFs have been shown to regulate approximately 12% of all its identified cold-inducible genes (Fowler, 2002), hereby confirming their relevance in cold acclimation.

1.1.2 CBF/DREB targets

CBF induction upon exposure to cold leads to the induction of a set of target genes, including a number of COR, KIN (cold-induced), LTI (low-temperature-induced) and ERD (early response to dehydration) (Zhu et al., 2007) genes, containing at least one copy of the conserved core sequence of CCGAC, known as C-repeat (CRT)/dehydration-responsive elements (DRE) (Jiang et al., 2013). Moreover, Low Temperature Responsive Elements (LTREs), characterized by their core sequence of CCGAAA, were identified in the promoter region of *Brassica napus BN115* (Jiang et al., 1996). CRT/DRE and LTRE elements, which are bound by C-repeat (CRT)-binding factors, or CBFs, also known as dehydration-responsive-element-binding proteins (DREBs) thus activating their expression. Most COR genes are members of the Late Embryogenesis Abundant (LEA) protein-encoding gene family. LEA proteins were first found to accumulate late in cotton seed development, when the embryo becomes desiccation tolerant (Galau and Dure, 1981). Related proteins were

identified in seeds as well as vegetative organs of other plant species under abiotic stress conditions such as low temperatures, high salinity and drought (Tunnacliffe et al., 2010). Most LEA proteins are highly hydrophilic intrinsically disordered proteins that do not aggregate during drying, freezing or boiling (Thalhammer and Hincha, 2013). While the exact mode of action of LEA proteins has remained elusive thus far, there is substantial evidence suggesting that some LEA proteins are able to stabilize membranes during freezing and desiccation conditions, as demonstrated in wheat (Danyluk et al., 1998), as well as in *Arabidopsis* (Thalhammer et al., 2014). In addition to the induction of COR genes, DNA microarray analyses have identified that the CBF regulon (Fowler and Thomashow, 2002) encodes for proteins belonging to a wide range of functional categories, such as signalling pathway components, biosynthetic proteins, osmoprotectants and other stress-related proteins, protease inhibitors, transcription factors as well as a large number of proteins of unknown function (Maruyama et al., 2004; Oono et al., 2006; Shinozaki et al., 2003; Vogel et al., 2005).

1.1.3 Effect of CBF/DREB overexpression

Analyses using *Arabidopsis* CBF overexpressor lines, as well as loss-of-function mutants have contributed in elucidating the role of CBFs in cold acclimation. Transgenic plants overexpressing CBF1 have been reported to have strong tolerance to freezing stress (Jaglo-Ottosen et al., 1998). Several reports have shown that CBF3 overexpression has improved tolerance to drought, high salinity and freezing stresses (Liu et al., 1998; Kasuga et al., 1999; Gilmour et al., 2000). Moreover, deletion of CBF2 led to an increase in expression of CBF1 and CBF3, consequently leading to an accumulation of CBF-target genes

under control and after cold acclimation conditions, as well as an increase in freezing tolerance. Taken together, these results suggest that CBF2 negatively regulates CBFs 1 and 3 (Novillo et al., 2007). In addition to playing a central role in the process of cold acclimation, CBFs appear to be involved in *Arabidopsis* growth and development, as overexpression of CBF1 has been shown to negatively impact plant growth under control conditions, similarly to cold acclimated plants (Achard et al., 2008). Other studies have shown that ectopic expression of CBFs is sufficient to activate the expression of COR genes and induce cold acclimation, even at warm temperatures (Chinnusamy et al., 2007). CBFs are known to regulate the expression of genes involved in transcription, Reactive Oxygen Species (ROS) detoxification, membrane transport, as well as genes presumed to play protective roles in the cell. CBF homologs have successfully been cloned from some cold-resistant plants, such as *Brassica napus*, and from cold-sensitive plants such as rice. Studies have shown that expression of transgenic *Arabidopsis* CBFs in different plant species can drive the expression of downstream genes, thus resulting in cold acclimation. Furthermore, the ectopic expression of CBFs from other species can also drive expression of CBF target genes in *Arabidopsis* (Shinozaki et al., 2006). In addition, studies using *CBF/DREB1* overexpressor plants have identified its involvement in several morphological and physiological processes pertaining to cold acclimation, such as the constitutive accumulation of soluble sugars as well as alterations in leaf morphology, namely increases in leaf thickness and cell density in *Arabidopsis* (Gilmour et al. 2004), as well as in *Solanum tuberosum* (Pino et al., 2008). These observations are in agreement with CBF/DREB1 overexpression studies done in *Brassica napus*, which have shown that the overexpression of *BNCBF5*, which shares a high homology with *Arabidopsis* CBF1 (Gao et al., 2002) and *BNCBF17*, which possesses two inserts in its acidic domain not found in any other *Brassica* and *Arabidopsis* CBF/DREBs (Gao et al.,

2002). Overexpression of *BNCBF5,* whose transcript levels rapidly increase in response to low temperatures, but remains for 48 hours and *BNCBF17*, whose transcript levels are rapidly induced in response to low temperatures, and decrease after two hours (Gao et al., 2002), led to an increase in *Brassica napus* cold responsive genes BN115, BN28 and BN47, which are orthologous with *Arabidopsis thaliana* COR15, 6.6 and 47 (Gao et al., 2002). The induction of these cold responsive genes led to multiple biochemical changes associated with cold acclimation, such as alterations in chloroplast photosynthetic development, enhancements in photosynthetic capacity and photochemical efficiency, increased level of photosynthetic pigments, and elevated activities of the Calvin cycle enzymes and key regulatory enzymes of starch and sucrose biosynthesis under non-acclimated conditions (Savitch et al., 2005). Furthermore, in a similar fashion to *Arabidopsis* transgenic lines overexpressing CBFs, *BNCBF5* overexpressors are marginally dwarfed compared to wild type, whereas *BNCBF17* are more severely dwarfed, and have developed waxier, thicker dark green leaves comparable to cold acclimated *Brassica napus* leaves.

1.1.4 CBF-independent pathways

While the CBF transcription pathway has been established as an integral component of the cold acclimation response in *Arabidopsis*, DNA microarray analyses have shown that approximately 12% of all cold responsive genes are regulated by the CBF regulon, suggesting the involvement of other cold regulatory pathways in the cold acclimation response (Fowler and Thomashow, 2002). This suggestion is supported by the *Arabidopsis eskimo1* mutant, which is constitutively freezing tolerant (Xin & Browse, 2000). Moreover, another study has shown that very few genes that are mediated by *Arabidopsis* ESK1 are also mediated by ICE1 and CBFs (Xin et al., 2007). In addition, a transcriptome profiling analysis of *Arabidopsis*

done by Fowler et al. (2002) has revealed that two transcription factors, ZAT12 and RAV1, were induced in parallel with the CBF transcriptional activators. While the authors have speculated that the low temperature regulation of these two transcription factors involves the action of the same regulatory proteins that activate CBFs, the parallel induction of CBF2, ZAT12 and RAV1 before the induction of known CBF targets such as COR47, COR6.6 and COR78/LTI78 suggests that those two transcription factors are not part of the CBF regulon. ZAT12 encodes for a transcription factor that was found to negatively regulate CBF expression in response to low temperatures, while coordinately regulating the expression of several COR genes involved in the CBF regulon in *Arabidopsis* (Vogel et al., 2005). Precisely how ZAT12 controls the expression of several genes shared by the CBF regulon while negatively regulating CBF expression has yet to be elucidated.

Related to ABI3/VP1, or RAV1, is a transcription factor belonging to the AP2 family of transcription factors. RAV1 is characterized by the presence of the B3 domain at the C-terminus, which recognizes and binds to the consensus CACCTG sequence, and the AP2 domain at the N-terminus, which recognizes and binds to the consensus CAACA sequence (Kagaya et al., 1999). RAV1 has been suggested to be involved in the initiation of leaf senescence (Woo et al., 2010), hypocotyl elongation of *Arabidopsis* (Ma et al., 2005) and negatively regulate plant growth (Hu et al., 2004) of *Arabidopsis*. Moreover, RAV1 has been suggested to regulate plant growth under cold temperatures, due to its induction under low temperatures, and its role in several developmental processes in *Arabidopsis* (Chinnusamy et al., 2007).

1.1.5 ABA-mediated regulation of cold acclimation

Abscisic acid (ABA) is a phytohormone known to play a critical role in response to various abiotic stress responses such as drought and high salinity (Shinozaki et al., 2003). Cellular ABA accumulates in response to such stresses, leading to a number of physiological adaptations, such as stomatal closure and growth inhibition (Knight et al., 2004). As exposure to low temperatures leads to cellular dehydration, one component of the cold acclimation response involves the accumulation of compatible solutes to minimize cellular dehydration, similarly to the drought tolerance response (Jiang et al., 2013). Thus, ABA is not only involved in the mediation of drought stress responses, but also appears to play a role in the cold acclimation response. Moreover, ABA is able to induce CBF gene transcription, in addition to subsequent COR genes hereby confirming its role with respect to the cold acclimation response in *Arabidopsis* (Knight et al., 2004).

So far, two ABA-induced pathways have been identified. One involves the use of basic leucine zipper (bZIP) family of transcription factors, which recognize and bind to ABA-responsive (ABRE) promoter elements, characterized by their core ACGTGGC sequence. ABA-responsive gene expression requires several ABREs or ABRE-like (ACGT) sequences as functional promoter elements (Maruyama et al., 2012). Several genes that are ABA responsive have been shown to respond to drought and/or cold stress. For instance, *Arabidopsis* LTI78, a cold responsive gene has been shown to possess both CRT/DRE and ABRE promoter elements, indicating its involvement in drought, high salinity and cold stress responses (Shinozaki et al., 2003). Moreover, the ABA-mediated cold acclimation response was shown to be induced by CBF4, a transcription factor with homology to CBFs 1-3. While the expression of CBF4 is not induced by cold, it is rapidly induced during drought stress

and ABA treatment (Haake et al., 2002). Moreover, CBF4 overexpression resulted in the constitutive expression of COR15A, COR78A and several CBF1-3 target genes, resulting in an increase in both freezing and drought tolerance (Haake, 2002).

In addition to the ABA-mediated pathway, DREB2, an ethylene-responsive element binding protein/AP2-type protein, was identified as a major transcription system regulating ABA-independent gene expression in response to dehydration (Shinozaki and Yamaguchi-Shinozaki, 2000). DREB2 recognizes and binds to DRE elements, leading to the expression of several genes that are involved in drought stress tolerance. Moreover, DNA microarray analyses have shown that genes regulated by DREB2 have homologous functions to CBF/DREB1 target genes (Maruyama et al., 2009; Nakashima et al., 2014).

1.2 *Post-transcriptional regulation of cold stress/acclimation*

In addition to transcriptional regulation by the CBF regulon as well as other pathways not involving CBFs, such as RAV1 and ABA-dependent/ABA-independent pathways, recent advances have revealed that post-transcriptional mechanisms such as pre-mRNA processing and RNA stability play critical roles during cold acclimation (Chinnusamy et al., 2007; Mazzucotelli et al., 2008). Pre-mRNA splicing is a crucial part of the nuclear processing of intron-containing genes coupled with nuclear export of mRNAs. Cold stress induces multiple genes involved in RNA metabolism (Lee et al., 2005), including pre-mRNA splicing factors and DEAD box helicases. Analyses of mutations of either cold-induced DEAD box helicase (*LOS4*) (Gong et al., 2005) or cold-induced pre-mRNA splicing factor (*STA1*) (Lee et al., 2006) indicated that by affecting mRNA export and pre-mRNA splicing, respectively, these

mutations led to chilling hypersensitivity, thus, supporting a strong connection between RNA metabolism and cold responses.

1.2.1 Pre-mRNA splicing and plant stress responses

The recent sequencing of the genome of the model plant *Arabidopsis thaliana* has revealed that the coding regions of approximately 80% of genes are interrupted by non-coding intervening sequences, or introns (Reddy, 2007). To produce functional messenger RNAs (mRNAs) that can be transported into the cytoplasm for subsequent translation, the primary transcripts, or precursor mRNAs, must be efficiently and accurately spliced. RNA splicing involves the excision of introns and the joining of exons, or coding sequences. It has also been shown that in addition to constitutive splicing, pre-mRNAs containing multiple introns can undergo alternative splicing, producing several structurally and functionally different proteins from the same precursor gene. Thus, the combination of constitutive splicing and alternative splicing greatly enhances transcriptome plasticity and proteome diversity in eukaryotes (Filichkin et al., 2010). Although it has been shown that alternative splicing has many critical roles in metazoan organisms (Black, 2003), studies of the functional significance of alternative splicing at the protein level in plants has remained largely unexplored. Recent estimates based on high-throughput studies suggest that 95-100% of all human multi-exon genes undergo alternative splicing (Richardson et al., 2011). In comparison, global analyses of alternative splicing (AS) events using the completed *Arabidopsis* genome estimate that the amount of genes which contain at least one intron and being capable of producing multiple RNAs range from approximately 42% (Filichkin et al., 2010) to more than 61% (Marquez et al., 2012; Syed et al., 2012). Furthermore, 63% of soybean genes were reported to undergo alternative splicing (Shen et al., 2014). These

estimates are based on plants grown under normal growth conditions, and are likely to increase as more splicing variants are identified in different tissues at different developmental stages and/or growth condition. Four main types of alternative splicing are known: exon skipping, where an exon is removed in a splicing event, alternative 5` and 3` splice sites, where alternative splice sites at either end of an intron are used, thus adding or removing sequences, and intron retention, where one or more introns are not removed from a pre-mRNA. Alternative splicing events have been shown to be spatially and developmentally regulated, and are frequently associated with environmental stresses in *Arabidopsis* (Mazzucotelli et al., 2008; Palusa et al., 2007; Reddy, 2007).

Both constitutive splicing, as well as alternative splicing events occur in a large RNA-protein complex called the spliceosome, consisting of several uridine-rich small nucleolar RNAs, or UsnRNAs, and over 300 associated proteins (Bessonov et al., 2008; Jurica & Moore, 2003; Reddy & Shad Ali, 2011). The plant spliceosomal core contains five small nuclear ribonucleoproteins (snRNPs), known as U1, U2, U4, U5 and U6 snRNPs, which have been shown to be highly conserved between metazoans and plants (Wang and Brendel, 2004). In addition to snRNPs, there are several non-snRNPs that play key roles in splicing regulation and spliceosome assembly. Among this group of essential non-snRNPs are Serine/Arginine-rich proteins (Reddy et al., 2011). Serine/Arginine-rich proteins, or SR proteins were originally identified in metazoans in 1990 as factors necessary for the splicing of pre-mRNA substrates in *in vitro* assays, as they were shown to restore splicing activity to splicing factor deficient cell extracts (Graveley, 2000). These proteins are part of a large and highly conserved family of structurally and functionally related non-snRNPs that play multiple roles in pre-mRNA splicing.

Figure 1.2: Structural features of *Arabidopsis* SR proteins and associated kinases.

Members of the SR subfamily are homologous to mammalian ASF/SF2 (SRSF1). Members of the RSZ subfamily are homologous to mammalian 9G8 (SRSF7), and SC35, the sole member of the SC35 subclass, is homologous to mammalian SC35 (SRSF2). SR proteins belonging to SCL, RS2Z and RS subclasses are plant specific, whereas SR45 and SR45a, which are characterized by an atypical SR protein structure, have been excluded from the *Arabidopsis* SR protein family. RRM (dark grey box) denotes RNA recognition motifs and pRRM (light grey) denotes a pseudo RRM. Zinc knuckles (light grey hexagons), found in the RSZ and RS2Z subfamilies are labeled as ZnK. The black circle represents the charged domain (CD) of the SCL subfamily, whereas black rectangles represent the Serine/Arginine-rich domains found in all SR proteins. Panel B denotes the structural features of LAMMER kinases and SRPKs, which phosphorylate either serine, threonine and/or tyrosine residues in the RS domain of SR proteins. LAMMER kinases are characterized by an RS domain (black box) and a unique LAMMERILG domain (light grey box), whereas SR protein kinases (SRPKs) are characterized by their two kinase domains (KD1 and KD2), separated by a spacer region (grey box), which is required for activity. The structural features of SR proteins are modified from Barta et al. (2010), while the structural features of LAMMER and SRPK kinases are modified from Colwill et al. (1996) and Ngo et al. (2005), respectively.

A

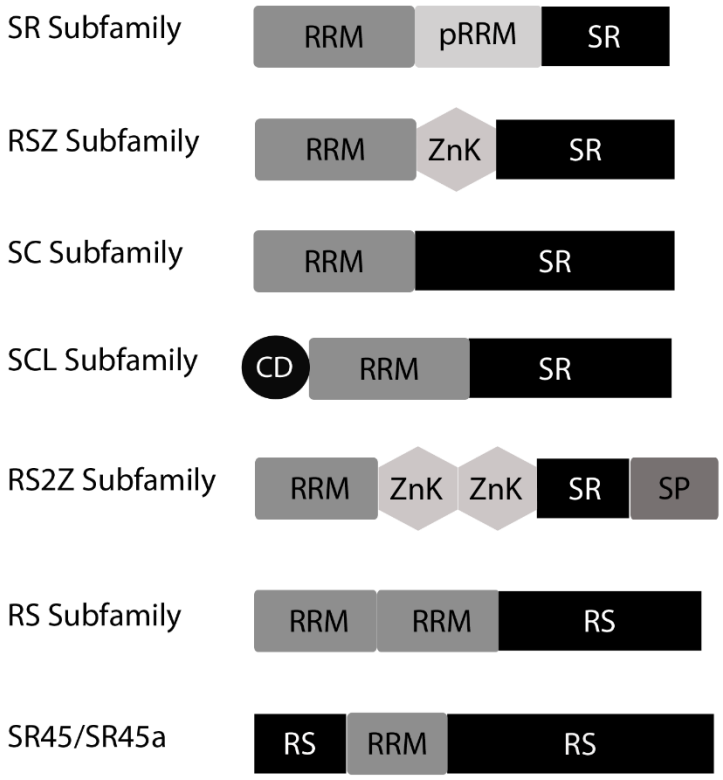
SR Subfamily
RRM
pRRM
SR
RSZ Subfamily
RRM
ZnK
SR
SC Subfamily
RRM
SR
SCL Subfamily
CD
RRM
SR
RS2Z Subfamily
RRM
ZnK
ZnK
SR
SP
RS Subfamily
RRM
RRM
RS
SR45/SR45a
RS
RRM
RS

B

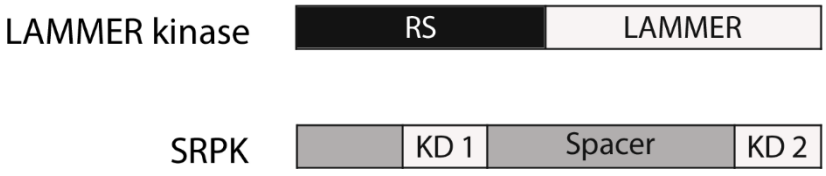
LAMMER kinase
RS
LAMMER
SRPK
KD 1
Spacer
KD 2

1.2.2 Serine/Arginine-rich proteins

SR proteins are characterized by their modular domain structure, composed of one or two RNA recognition motifs, or RRMs at the N-terminus, and an arginine/serine-rich dipeptide domain at the C-terminus (Fig. 1.2). Based on several phylogenetic and comparative analyses, there are 19 plant serine/arginine-rich proteins which are grouped into six different subfamilies. Of these six subfamilies, three have clear orthologs in humans. The remaining subfamilies are unique to plants and contain several novel structural features. The SR subfamily, characterized by two RNA recognition motifs, followed by the SR domain, consist of at-SR34, at-SR34a, at-SR34b and at-SR30 in *Arabidopsis*, and are homologous to SRSF1 (formerly ASF/SF2) in mammals. The RSZ subfamily, consisting of at-RSZ21, at-RSZ22 and at-RSZ22a in *Arabidopsis* are characterized by their zinc knuckles and are homologous to SRSF7 (formerly 9G8). Finally, at-SC35, the sole member of the SC subfamily, characterized by an RNA recognition motif and a SR domain is homologous to SRSF2 (formerly SC35) in metazoans. The remaining 10 SR proteins fall into plant specific subfamilies. At-SCL28, at-SCL30, at-SCL30a and at-SCL33 are members of the SCL (SC35-like) subfamily, which has an RNA recognition motif (RRM) like SRSF2. However, members of this plant-specific subfamily also possess a charged N-terminal extension rich in arginine, proline, serine, glycine and tyrosine residues. Members of the RS2Z subfamily, identified as at-RS2Z32 and at-RS2Z33 in *Arabidopsis* possess RRMs with significant similarity to human SRSF6, as well as a canonical RS domain. However, members of this subfamily also contain two Zn-knuckles, as well as an acidic C-terminal extension rich in serine and proline residues. These distinguishing features separate these SR proteins from the mammalian SRSF7 and its three plant orthologs, which only contain one zinc knuckle

(Barta, 2010). Members of the RS subfamily, At-RS31, At-RS31a, At-RS40 and At-RS41 contain two RRMs, similarly to the SR subfamily, but lack a phylogenetically conserved heptapeptide motif (SWDLKD) in their second RRM, a distinguishing feature of the SR subfamily. Moreover, members of the RS subfamily possess an RS domain with many RS dipeptides (Barta et al., 2010; Reddy and Ali, 2011). At-SR45, which was found to complement an animal *in vitro* splicing extract devoid of SR proteins (Ali et al., 2007) possesses a unique structure among identified SR proteins, consisting of two RS domains, with one located at the N-terminal and the second, located at the C-terminal. However, using the new criteria outlined by Barta (2010), At-SR45 falls outside of the proposed definition of an SR protein (Barta et al., 2010). In addition, At-SR45a, which has been identified as a homolog of Tra-2, no longer qualifies as an SR protein according to the criteria proposed by Manley and Krainer (Manley and Krainer, 2010).

1.2.3 Roles of SR proteins

SR proteins are prominently known for their role in constitutive and alternative pre-mRNA splicing through their contribution in spliceosomal assembly (Howard and Sanford, 2014). It is now known that the RRM confers RNA-binding specificity to SR proteins, allowing them to recognize short and degenerate sequences known as exonic splicing enhancers (ESEs) or exonic splicing silencers (ESSs), which are thought to be recognized by a unique set of one or several SR proteins (Duque, 2011). SR proteins can also recruit U1 snRNPs to the 5' splice site by interacting with both the pre-mRNA and the U1-70K protein (Graveley, 2000). SR proteins have also been shown to interact with U1-70K and U2AF35

in order to promote 3` splice site recognition by recruiting U2AF35 to the 3` splice site (Wu and Maniatis, 1993). Both 5` and 3` splice site recognition are mediated by protein-protein interactions with the RS domain of SR proteins. Splice site selection, leading to either constitutive or alternative splicing of a transcript, has been reported as being regulated in a concentration-dependent manner (Ali et al., 2007). Additionally, SR proteins are also responsible for facilitating the incorporation of the tri-snRNP complex, consisting of U4/6 and U5 snRNPs into the spliceosome (Roscigno and Garcia-Blanco, 1995). Taken together, several studies have shown that SR proteins are able to promote the recruitment of several members of the spliceosomal machinery, and are crucial in the formation of the final spliceosomal catalytic core.

In addition to their role in regulating constitutive and alternative splicing of pre-mRNA transcripts, SR proteins have been reported as being able to regulate their own transcripts. A comprehensive analysis of the splicing patterns of SR genes in response to various signals has shown that most of the precursor mRNAs from the 17 SR genes and two SR-like genes (At-SR45 and At-SR45a) in *Arabidopsis* can undergo alternative splicing, based on environmental and developmental stimuli, producing 95 different transcripts, with only four SRs (*At-RSZ22, At-RSZ22, At-RSZ22a* and *At-SCL28*) showing no signs of alternative splicing (Mazzucotelli et al., 2008; Palusa et al., 2007). Abiotic stresses such as heat and cold have strongly altered the alternative splicing profile of most SR genes, suggesting that changes in gene expression under heat and cold stress could partly be attributed to the alternative splicing of SR genes (Palusa et al., 2007). While the alternative splicing of SR genes under abiotic stress conditions would suggest that alternative splice forms play an important role, the functional significance of these alternatively spliced

products is currently unknown. In addition to their role in constitutive and alternative splicing, studies characterizing At-SR45, an SR-like protein, have shown that SR proteins could potentially be involved in developmental processes, as loss of function *sr45* mutants have been shown to exhibit several phenotypes, including delayed flowering, reduced root growth, and abnormal flower organs, in addition to altered responses to both glucose and abcissic acid (Ali et al., 2007).

The bulk of SR proteins are located in nuclear speckles, and are recruited to sites of pre-mRNA synthesis by means of phosphorylation (Huang & Steitz, 2005). However, in a similar fashion to hnRNPs, a subset of SR proteins were found to continuously shuttle between the cytosol and the nucleus (Cáceres et al., 1998), suggesting that this subset of SR proteins might play additional roles in mRNA transport and/or cytoplasmic events such as mRNA localization, mRNA stability, and translation regulation (Sanford et al., 2005). In accordance with this hypothesis, SRp20/9G8 was shown to be involved in mRNA export of intronless mRNAs (Huang et al., 2003; Huang & Steitz, 2001). Moreover, SR proteins were shown to be involved in the mediation of mRNA stability, as ASF/SF2 was shown to mediate the stability of PKCI-1 (protein kinase C-interacting protein) transcripts, which contain specific binding sites for ASF/SF2, in chicken fibroblasts (Lemaire et al., 2002). In addition, overexpression of SC35 and ASF/SF2 SR proteins leads to an enhancement of degradation of alternatively spliced messages by means of the nonsense mediated decay (NMD) pathway (Zhang & Krainer, 2004). ASF/SF2 was also reported to be associated with 80S ribosomes and polysomes in cytoplasmic extracts (Sanford et al., 2004). Moreover, when tethered to reporter mRNAs, ASF/SF2 was shown to increase the translational output of these transcripts in *Xenopus* oocytes (Sanford et al., 2004), suggesting that SR proteins might be involved in

regulating mRNA translation. Moreover, the RS domain has also been shown to affect SR protein subcellular localization by acting as a nuclear localization signal by means of interaction with the nuclear import receptor, transportin-SR (Cáceres et al., 1997; Kataoka et al., 1999; Lai et al., 2000). Taken together, these studies reveal an expanded role of SR proteins beyond the modulation of pre-mRNA splicing. However, in contrast to their established roles in pre-mRNA splicing, the molecular mechanisms behind the post-splicing regulation mediated by SR proteins are still poorly understood (Howard and Sanford, 2014).

1.2.4 Post-translational regulation of Serine/Arginine-rich proteins

One of the common strategies to regulate protein function involves post-translational modifications, such as phosphorylation (Barrero-Gil and Salinas, 2013). The observations that approximately 10% (~2800 genes) of the *Arabidopsis* genome encodes for protein kinases, and that the protein kinase superfamily is larger in plants than other eukaryotes (Lehti-Shiu and Shiu, 2012) have served in highlighting the relevance of phosphorylation in plants. Among the variety of mechanisms that regulate pre-mRNA splicing, reversible phosphorylation of splicing-related proteins is now known to play a prominent role (Fluhr, 2008). Moreover, post-translational modifications of SR proteins play a critical role in the regulation of their activity (Mermoud et al., 1994; Misteli et al., 1998; Xiao & Manley, 1997), and their localization (Cho et al., 2011; Ma et al., 2010). Phosphorylation of the RS domain of SR proteins increases RNA binding specificity (Tacke et al., 1997). Moreover, it has been shown to play a role in specific protein-protein interactions occurring within the spliceosomal complex (Howard and Sanford, 2014; Xiao and Manley, 1997). Furthermore, SR protein kinases have been demonstrated as playing a role in splice site selection (Zhong et al., 2009). Collective studies used to assess the dynamics of SR proteins have shown that similarly to

metazoan SR proteins, most *Arabidopsis* SR proteins are localized in highly dynamic, specialized subnuclear domains called speckles (Ali & Reddy, 2006; Tillemans et al., 2006). Nuclear speckles are thought to serve as storage, assembly and/or modification sites for splicing factors (Reddy and Ali, 2011). Phosphorylation of SR proteins, which occurs on Serine residues located in their RS domain (Lai et al., 2003; Zahler et al., 1992), is essential for their release from speckles, as the inhibition of SR protein phosphorylation led to enlarged speckles (Ali and Reddy, 2008a). Their release from speckles leads to the shuttling of SR proteins to active transcription sites (Cáceres et al., 1997; Misteli et al., 1998). Some SR proteins have also been reported to interact with U2AF, as well as U11-35K (Lopato et al., 2006; Wu and Maniatis, 1993) hereby facilitating spliceosomal assembly. Moreover, phosphorylation has also been reported to increase the binding specificity of RS40 to RNA, in turn reducing non-specific interactions between hypophosphorylated RS domains and RNA (Tacke et al., 1997). While it is well established that SR protein phosphorylation is essential in activities pertaining to pre-mRNA metabolism, studies have indicated that phosphorylation of SR proteins leads to functions beyond their role as splicing regulators. For instance, phosphorylation of *Arabidopsis* RSZ22 was reported to have led to its shuttling from the nucleus to the cytosol, suggesting its involvement in mRNA processing beyond splicing (Rausin et al., 2010; Tillemans et al., 2006). While the role of at-RSZ22 in the cytosol has yet to be determined, metazoan SR proteins have been reported to be associated with nonsense mediated decay of mRNA transcripts (Zhang and Krainer, 2004), as well as the translation of mRNA transcripts (Sanford et al., 2004), lending credence to the potential role of the phosphorylation of SR proteins with respect to functions beyond pre-mRNA splicing.

Taken together, these observations would suggest that in the absence of transcription, SR proteins aggregate into speckles and that phosphorylation is required for their recruitment to splicing sites, which are thought to be scattered throughout the nucleoplasm. While the number of protein kinases encoded by the *Arabidopsis* genome is estimated at over 10% (Lehti-Shiu and Shiu, 2012), or approximately 2800 genes, analyses of conserved phosphorylated motifs in proteins with RS domains have led to the identification of two major protein kinase families that are capable of phosphorylating serine residues in the RS domain of SR proteins. Those families are the LAMMER-type kinases and SR Protein-specific Kinases, or SRPKs, which differ in their substrate specificity.

1.2.4.1 LAMMER kinases

LAMMER kinases are dual-specificity protein kinases that are able to phosphorylate serine, threonine, and tyrosine residues (Colwill et al., 1996). Intriguingly, all three members of the LAMMER protein kinase family share an enriched RS dipeptide domain at the N-terminal region, similarly to SR proteins. The C-terminus contains the kinase domain, which is also highly conserved between members of the LAMMER kinase family. In addition to a strong degree of homology across the kinase domain, all members of this family contain a unique EHLAMMERILG motif in a subdomain of the kinase domain. Although this region is not conserved in general among kinases (Colwill, 1997), studies have suggested that this unique motif lies in a position where it might contact substrates and effectors (Yun et al., 1994, Nikolakaki et al., 2002).

In *Arabidopsis*, three LAMMER kinases, known as AME1, AME2 and AME3 have been identified. Studies by Bender and Fink have shown that AME2 was able to supress mating defects in fus3, kss1 and ste signal transduction mutants of *Saccharomyces cerevisiae*

by activating STE12, a transcription factor known to play a role in mating in haploid cells and pseudohyphal growth in diploid cells (Bender and Fink, 1994). Moreover, AME1, which is closely related to AME2, was unable to supress mating defects of the same mutant lines tested, suggesting differences in functions. These data are corroborated by the findings of Golovkin and Reddy (1999), who have shown that AME1, but not AME2, was able to undergo auto-phosphorylation and can heavily phosphorylate *Arabidopsis* At-RSZ21, At-RSZ22, At-RS2Z33, which are plant-specific SR proteins, and At-SR45, an SR-like protein. This was corroborated by a later study that has shown that At-AME1 is also capable of phosphorylating At-RSZ22 (Ahsan et al., 2013), in addition to proteins involved in flowering (Hornyik et al., 2010), drought and low temperature responses (Kaye et al., 1998). Interestingly, AME1 appears to be lacking an RS domain at the N-terminus, contrarily to other LAMMER kinases, suggesting that other structural features other than the RS domain are also important in the interaction of AME2 and other proteins. While there are no reports indicating that AME2 is capable of phosphorylating SR proteins *in vitro*, At-AME3 is able to undergo auto-phosphorylation (Nemoto et al., 2011), was reported as being capable of phosphorylating At-RSZ22 (Ahsan et al., 2013), as well as CAP160, PPI-2 and FPA, similarly to AME1. Furthermore, a recent high throughput yeast 2-hybrid assay has shown that AME3 is capable of physically interacting with At-RS21, At-SCL30 and At-RS2Z33 (Fig. 1.3) (*Arabidopsis* Interactome Mapping Consortium, 2011).

1.2.4.2 SRPKs

In addition to LAMMER kinases, SR-specific protein kinases, or SRPKs have been shown to mediate phosphorylation of SR proteins. The SRPK kinase family phosphorylates serine residues in the RS domains of SR proteins, and appear to have a strict requirement for

an arginine-serine-arginine (RSR) motif (Gui et al., 1994; Stojdl & Bell, 1999; H. Y. Wang et al., 1998). SRPKs are predominantly localized in the cytoplasm and are crucial for initiating nuclear import of Serine/Arginine-rich proteins in a phosphorylation-dependent manner (Fluhr, 2008). Structural analyses have shown that SRPK kinases contain a bipartite kinase catalytic core, separated by a unique spacer sequence that controls its cytoplasmic localization (Zhong et al., 2009).

In *Arabidopsis thaliana*, two SR protein kinases (SRPK1, SRPK4) and two SRPK-like protein kinases have been identified. While the role of SRPK 1, and the two SRPK-like kinases have yet to be discovered in plants, yeast 2-hybrid analyses have shown that SRPK4 interacts with at-SCL33 and at-RS2Z33 *in vitro* (de la Fuente van Bentem et al., 2006). Moreover, although SRPK4 has been shown to exhibit low autophosphorylation activity, it is able to strongly phosphorylate At-RS31 in a radioactive *in vitro* kinase assay (de la Fuente van Bentem et al., 2006), as well as At-SCL30 (de la Fuente van Bentem, 2008). Further analyses have revealed that SRPK4 phosphorylates an RpSP motif in At-RS31, which is conserved among other RNA metabolism-related proteins, suggesting that SRPK4 could be one of the kinases that phosphorylate these sites. Transcript levels of SRPK4 have been shown to increase 1.5-fold in response to multiple environmental stress factors, such as senescence, heat and osmotic stress, but the significance of this increase with respect to splicing remains unclear (Zimmermann et al., 2005).

Figure 1.3: Interaction network of LAMMER, SRPK and SRPK-like proteins reported to interact with SR proteins.

Each node presented in blue represents either LAMMER kinases or SRPK and SRPK-like kinases, while Serine/Arginine-rich proteins are represented as red nodes. Grey nodes represent proteins that were observed to interact with LAMMER kinases. Blue lines correspond to a predicted functional interacting partner of At-AME3, based on evidence from yeast 2-hybrid analyses, while red lines denote results from *in vitro* phosphorylation assays, as reported by Golovkin and Reddy (1999) and de la Fuente van Bentem (2006, 2008) The interaction map was based on data generated using STRING v10 (Szklarczyk et al., 2015) (http://www.string-db.org/)

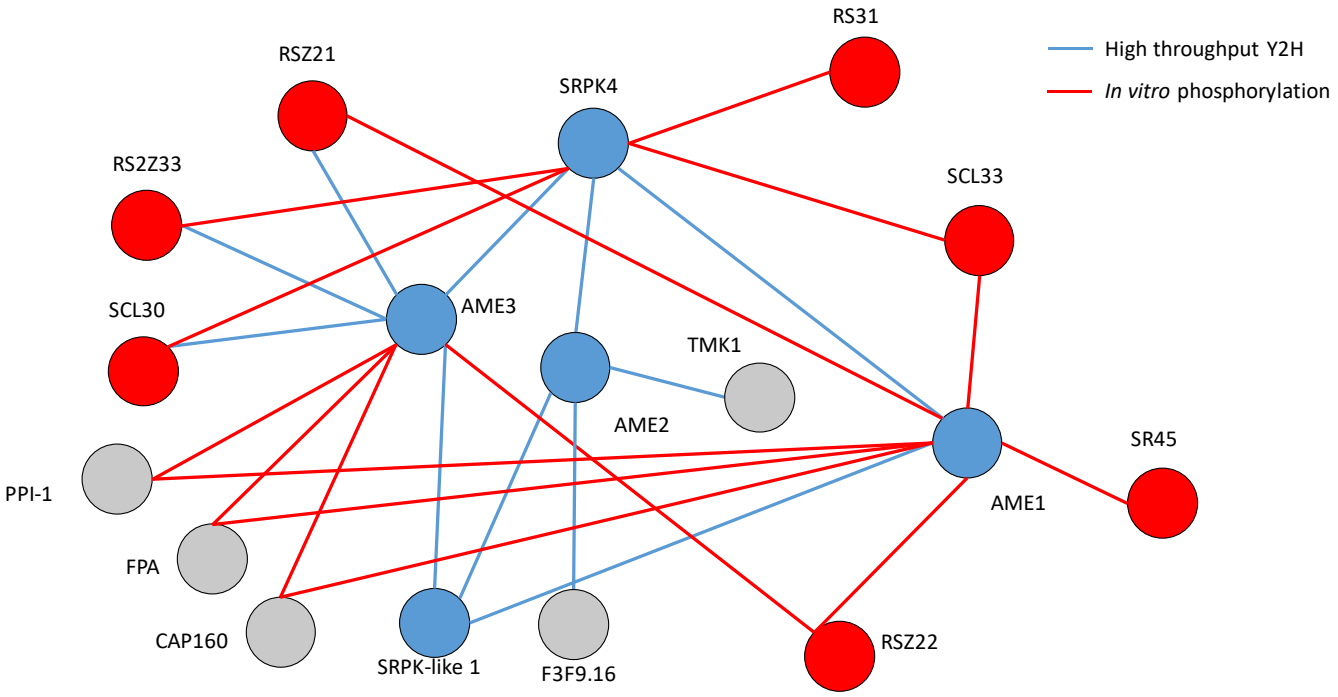
RS31
RSZ21
SRPK4
High throughput Y2H
In vitro phosphorylation
RS2Z33
SCL33
SCL30
AME3
TMK1
AME2
SR45
PPI-1
AME1
FPA
CAP160
SRPK-like 1
F3F9.16
RSZ22

Table 1.1: Summary table highlighting the nomenclature, classification and predicted protein sizes of both constitutive and alternative splice forms of Serine/Arginine-rich (SR) and associated kinases.

Protein sizes were extracted from TAIR (www.arabidopsis.org) Modified from Duque (2011).

Mammalian orthologs	Subfamily	Gene/Protein	Gene locus	Protein size (kDa)
		SR30	At1g09140	30.4/29.1
ASF/SF2 (SRSF1)	SR	SR34	At1g02840	33.7/32.0/33.7
		SR34a	At3g49430	31.5/19.8
		SR34b	At4g02430	19.6/31.5
9G8 (SRSF7)	RSZ	RSZ21	At1g23860	21.5/21.5
		RSZ22	At4g31580	22.5/22.5
		RSZ22a	At2g24590	21.9
SC35 (SRSF2)	SC	SC35	At5g64200	35.2/35.2
Plant specific	SCL	SCL28	At5g18810	28.0
		SCL30	At3g55460	29.6
		SCL30a	At3g17530	30.2
		SCL33	At1g55310	33.3/25.5/34.7
	RS2Z	RS2Z32	At3g53500	26.8/31.8
		RS2Z33	At2g37340	29.2/27.8/32.9
	RS	RS31	At3g61860	31.2
		RS31a	At2g46610	29.7/26.4
		RS40	At4g25500	40.3/35.5/36.4/40.3
		RS41	At5g52040	41.3/41.4/38.2/37.4
SR-like		SR45	At1g16610	45.3/44.6/46.6
		SR45a	At1g07530	45.0/14.7
LAMMER kinases		AME1	At4g24740	49.6/37.9
		AME2	At3g53570	54.2/54.2/52.7/54.2
		AME3	At4g32660	46.2/41.2/45.4
SRPK		SRPK1	At3g23000	48.3
		SRPK4	At3g53030	59.4
SRPK-like		SRPK-like 1	At2g17530	49.7/39.6/49.7
		SRPK-like 2	At5g22840	61.2

1.3 *Physiological regulation of cold stress and acclimation*

The use of chlorophyll a fluorescence measurements to examine photosynthetic performance and stress in algae and plants has played a major role in understanding the fundamental mechanisms of photosynthesis, plant responses to environmental changes, genetic variation and ecological diversity (Murchie and Lawson, 2013). Light energy absorbed by chlorophyll, a pigment-protein complex found in Photosystems I and II, and within the light harvesting complexes, can be used to drive photochemistry in which an electron is transferred from the reaction centre P_{680}, to Q_A, the primary quinone acceptor of PSII.

However, excess light energy absorbed by chlorophyll can also undergo two alternative pathways: it can be dissipated as heat or re-emitted as fluorescence (Figure 1.4). These three processes do not exist in isolation, but rather in competition with each other, such that any increase in the efficiency of one of these processes will result in a decrease of the other two (Baker, 2008; Murchie and Lawson, 2013). Thus, measuring changes pertaining to the yield of chlorophyll fluorescence can be used to monitor changes in heat dissipation, as well as PSII photochemistry (Henriques, 2009).

Figure 1.4: Model depicting the fates of light energy absorbed by photosystem II (PSII).

Light energy absorbed by chlorophyll found in photosystems I and II can be used to drive photochemistry. Alternatively, absorbed light energy can be dissipated as heat, or fluorescence. All three processes are in competition, indicating that an increase in either processes will result in a reduction of the other two (Figure modified from Baker, 2008). Chlorophyll a fluorescence measurements provide a non-intrusive method used in the evaluation of photosynthetic performance and efficiency. Panel B depicts a schematic diagram highlighting the possible energy partitioning of absorbed light energy into fractions utilised for Photosystem II photochemistry (Φ_{PSII}), heat dissipation through antenna-based quenching (Φ_{NPQ}), reaction centre quenching ($\Phi_{f,D}$), linear electron transport (ETR), and excitation pressure of Photosystem II (1-qL) within the thylakoid membrane of *Arabidopsis thaliana* (Figure modified from Ivanov et al., 2012).

A

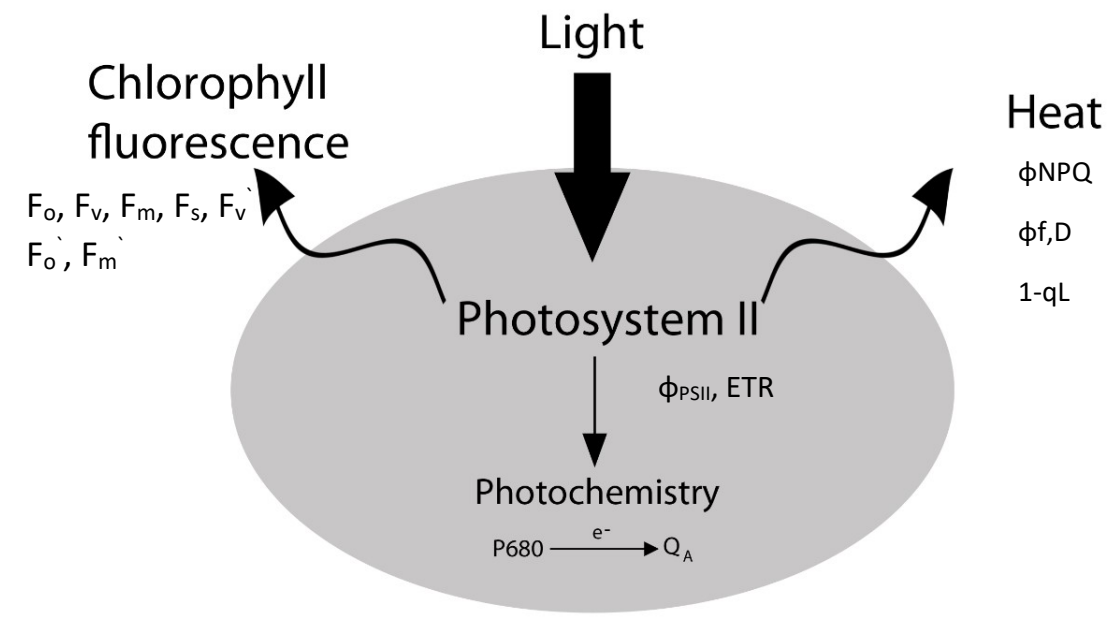
Light
Chlorophyll fluorescence
Fo, Fv, Fm, Fs, Fv`
Fo`, Fm`
Heat
ϕNPQ
ϕf,D
1-qL
Photosystem II
ϕPSII, ETR
Photochemistry
P680 e- QA

B

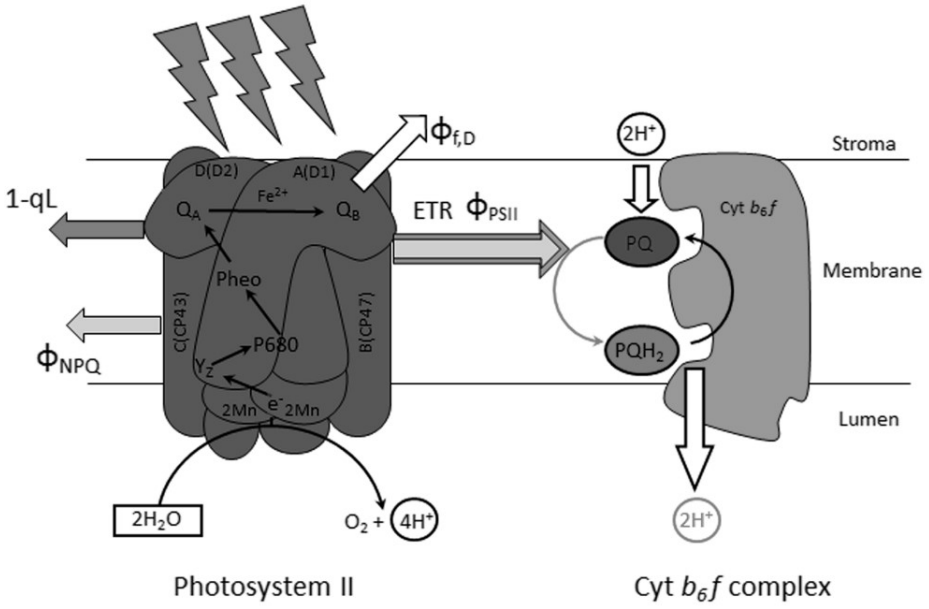
ϕf,D
2H+
Stroma
D(D2)
A(D1)
Fe2+
1-qL
QA
QB
ETR ϕPSII
Cyt b6f
PQ
Membrane
Pheo
C(CP43)
B(CP47)
ϕNPQ
P680
YZ
PQH2
2Mn
e-
2Mn
Lumen
2H2O
O2 + 4H+
2H+
Photosystem II
Cyt b6f complex

Studies done on chilling sensitive plants, as well as cold hardy plants have shown that short term exposure to chilling temperatures leads to a series of disruptions in all major components of photosynthesis, from linear electron transport, to components of the carbon reduction cycle (Allen and Ort, 2001). This attenuation in photosynthetic carbon reduction can be attributed to alterations in the biophysical properties of thylakoid membrane lipids and decreases in enzymatic reaction rates involved in CO_2 reduction to triose phosphate, and reduced electron transport rates (Ensminger et al., 2006). This imbalance between the capacity to harvest light energy and energy expended for both electron transport and carbon, sulphur and nitrogen reduction can result in the generation of reactive oxygen species (ROS), such as $^1O_2$ and O_2^-, in turn leading to photoinhibition and photooxidative damage to Photosystem II (Aro et al., 1993; Ivanov et al., 2012; Long, 1994), and Photosystem I (Ivanov et al., 2012; Sonoike et al., 1997). This reduction in photosynthesis has been associated with irreversible inactivation and subsequent loss of Ribulose 1,5-bisphosphate carboxylase/oxygenase (Rubisco) (Bruggermann et al., 1992), fructose 1,6-bisphosphatase (FBPase) and sedoheptulose 1,7 bisphosphatase (SBPase) (Sassenrath and Ort, 1990; Sassenrath et al., 1991; Holaday et al., 1992), accumulation of phosphorylated metabolites such as triose phosphates (Leegood and Furbank, 1986; Sharkey et al., 1986), a rapid accumulation of soluble sugars due to impediments in phloem export (Krapp and Stitt, 1995; Strand et al., 1997), and limitations in the transcription of nuclear encoded photosynthetic genes such as the small subunit of Rubisco (*rbcS*) and chlorophyll a/b-binding proteins (*cab*) (Catt and Ort, 1995; Kreps and Simon, 1997).

This in turn results in an over-reduction of the plastoquinone pool as well as other components of the intersystem electron transport pool (Hüner et al., 1998, 2013a). These changes, also known as excitation pressure, can be detected as an accumulation of closed PSII centres and quantified *in vivo* as an increase in 1-qP or 1-qL (Hendrickson et al., 2004; Hüner et al., 1998, 2013a) (Fig. 1.5B). Conversely, a decrease in PSII activity is observed, as linear electron rates (ETR) and photosystem II photochemistry rates decrease under cold stress conditions (Hüner et al., 1993; Savitch et al., 2001, 2009). If the absorbed energy exceeds both the capacity for non-photochemical quenching and the capacity for photochemistry, this can result in an accumulation of Reactive Oxygen Species (ROS), in turn leading to photooxidative damage and photoinhibition of Photosystem II and Photosystem I (Aro et al., 1993; Ivanov et al., 2012; Long et al., 1994; Savitch et al., 2001, 2011; Sonoike, 2011; Sonoike et al., 1997; Zhang and Scheller, 2004). However, plants have evolved a wide variety of mechanisms allowing them to restore photostasis, thus mitigating damages caused by this imbalance and maintaining an optimal electron flow.

One of the mechanisms used in restoring photostasis involves non-photochemical quenching mechanisms, used in the dissipation of excess energy not used in photosynthesis as heat, either through Photosystem II antennae, or the reaction centre (Fig. 1.5). Antennae-based non-photochemical quenching involves the conversion of violaxanthin, a light harvesting pigment, into antheraxanthin and zeaxanthin, two xanthophyll pigments which are incapable of absorbing energy, by means of the xanthophyll cycle (Hüner et al., 2008). In conjunction with the xanthophyll cycle, PsbS, a Photosystem II subunit belonging to the light harvesting complex superfamily, also plays an essential role in dissipating excess energy through the formation of a chlorophyll-zeaxanthin heterodimer (Hüner et al., 2008; Li et al.,

2002). Reaction centre quenching is another strategy used in the dissipation of excess energy as heat. This method is thought to be achieved through the conversion of open, photochemically active PSII reaction centres, into closed, photochemically inactive PSII reaction centres, which dissipate energy as heat, and prevent further damage to other active PSII reaction centres (Ensminger et al., 2006; Ivanov et al., 2001; Krause and Weis, 1991).

On a short time scale (within minutes of exposure to high excitation pressure), state transitions provide a means by which plants are able to adjust photosynthetic rates once exposed to these stresses involves a reduction in efficiency in the energy transfer to photosystem II by diverting energy to photosystem I (Ensminger et al., 2006). An imbalance in the excitation of PSII relative to PSI leads to a reduction of plastoquinone (PQ). This reduction in PQ leads to the phosphorylation of photosystem II light harvesting complex proteins by STN7, a protein kinase located in the thylakoid membrane (Minagawa, 2011). Consequently, this results in a dissociation and subsequent migration of a population of the peripheral light harvesting complex proteins from PSII to Psa-H, a subunit of PSI (Lunde et al., 2000). Thus, this transition results in a balanced excitation of both photosystems and optimal electron transport under high light and/or low temperature exposure, as some light energy is diverted to PSI at the expense of PSII. Conversely, an increase in excitation of PSI relative to PSII results in the oxidation of plastoquinone (Ensminger et al., 2006), in turn leading to the inactivation of STN7. Furthermore, the phosphorylated light harvesting complex proteins bound to PSI-H are dephosphorylated by TAP38/PPH1 (Minagawa, 2011), a phosphatase located in the thylakoid membrane. This leads to the dissociation of LHCII proteins from Psa-H and subsequent migration back to PSII, hereby restoring the imbalance in excitation between photosystems (Ensminger et al., 2006; Scheller and Haldrup, 2005).

Furthermore, dissipating excess energy as heat through the antennae and reaction centre quenching also provide a means to reduce the amount of energy absorbed by Photosystem II (Horton et al., 2008; Hüner and Grodzinski, 2011). On a longer time scale, the physical size of light harvesting complexes can be modulated by regulating the transcription and subsequent translation of *Lhcb* genes (Ensminger et al., 2006; Hüner et al., 2013b).

At the level of Photosystem I, the water-water cycle, or Mehler reaction, which uses O_2 and converts it into hydrogen peroxide (H_2O_2) by transferring excess electrons coming from Photosystem II back to O_2 (Figure 1.5) (Asada, 1999). In addition to its photoprotective role, the Mehler reaction also plays a role in the generation of extra ATP relative to NADPH (Vanlerberghe et al., 2015). Another strategy used in the dissipation of excess energy involves photorespiration. In contrast to the Calvin cycle, where Rubisco catalyses the carboxylation of Ribulose-1,5- Bisphosphate (RuBP) to produce 3-phosphoglycerate (3PGA), photorespiration involves the oxygenation of Ribulose-1,5- Bisphosphate by Rubisco, in order to generate phosphoglycolate (2PG). Phosphoglycolate is considered an inhibitor of enzymes in the carbon metabolism (Peterhansel et al., 2013), and is eventually converted to 3-phosphoglycerate, a Calvin cycle intermediate, via a number of enzymatic reactions. During this photorespiratory cycle, CO_2, NH_3 and NADP are produced, at the expense of ATP hydrolysis (Badger et al., 2000; Bauwe et al., 2010; Takahashi and Badger, 2011). Photorespiration is a photoprotective process, as it reduces photosynthetic performance by generating 2PG, which is eventually converted to 3PGA via a wasteful process that consumes ATP and NADPH (Wingler et al., 2000).

One of the strategies used in the photoprotection of photosystem I involves cyclic electron transport by means of the NDH and PGR5 dependent pathways, two partially

redundant routes (Shikanai, 2007). The NDH cyclic electron transport pathway depends on the chloroplast NADH Dehydrogenase, a large multisubunit complex consisting of over 30 subunits associated with PSI to form a supercomplex in *Arabidopsis* (Shikanai, 2014). This supercomplex has been shown to play a role in alleviating oxidative stresses by accepting electrons from Ferredoxin (Fd), which are cycled back to the plastoquinone pool, to be transported once more through the cytochrome b_6f (Johnson, 2011; Vanlerberghe et al., 2015). The second pathway, the PGR5-dependent cyclic electron transport pathway, involves Proton Gradient Regulation 5, or PGR5. PGR5 encodes a thylakoid membrane protein that plays a role in cyclic electron transport. Both cyclic electron transport pathways are thought to play a role in the generation of a proton motive force, across the thylakoid membrane, in turn driving ATP synthesis, but not NADPH. It should be noted that although both cyclic electron transport pathways are active under optimal growth conditions, the PGR5 pathway has been reported to play a more dominant role at the expense of the NDH-H pathway in corn (Savitch et al., 2011) as well as in *Arabidopsis* (Ivanov et al., 2012) under cold acclimation conditions.

In addition to NDH and PGR5 dependent pathways, chlororespiration is another strategy used to divert excess energy. Chlororespiration has been shown to take place via plant plastid terminal oxidase, or PTOX, which can catalyse the oxidation of plastoquinol and reduction of O_2 to H_2O. Furthermore, PTOX has been shown to increase in abundance under exposure to low temperatures, and has been shown to play a role as an alternate electron sink under exposure to low temperatures (Ivanov et al., 2012; Vanlerberghe et al., 2015). Taken together, by diverting excess electrons not being used in carbon assimilation both

cyclic electron transport pathways, and the PTOX-dependent electron transport pathway play an important role in mitigating reactive oxygen species (ROS) formation.

Conversely, leaves from cold hardy plants grown at low temperatures exhibit a strong recovery of photosynthetic activity (Savitch et al., 2001). This strong recovery in photosynthetic capacity can be attributed to the various photoprotective mechanisms taking place to mitigate reactive oxygen species (ROS) formation (Fig, 1.5C), in conjunction with increases in the expression and activity of Calvin cycle enzymes. This increase in photosynthetic capacity is achieved through the upregulation of carbon metabolism enzymes, such as Rubisco, sedoheptulose-1,7-biphosphate, or SBPase (Holaday et al., 1992; Hurry et al., 1994, 1995; Strand et al., 1997, 1999; reviewed in Yamori et al., 2014). Moreover, an increase in enzymes related to sucrose synthesis, such as Sucrose Phosphate Synthase (SPS) has also been observed in response to low temperature (Yamori et al., 2014). Large amounts of these proteins are produced to compensate for the decreased enzymatic activities under these conditions. Alternatively, compensation for decreased activity under cold conditions can also be achieved by shifting protein expression to produce isoforms with enhanced cold stability (Yamori et al., 2014). For example, exposure to low temperatures lead to the enhancement of splicing variants of Rubisco activase in *Lolium perene* (Jurczyk et al., 2016). In addition to the cold acclimation induced stimulation of photosynthetic capacity, an increased resistance to low temperature induced photoinhibition, as well as the acquisition of freezing tolerance has been observed in spinach (Boese and Hüner, 1990), winter wheat, winter rye (Gray et al., 1996) *Arabidopsis* (Savitch et al., 2001) and *Brassica napus* (Savitch et al., 2005).

Figure 1.5: Schematic diagram representing an overview of the energy partitioning of absorbed light by photosystem I and Photosystem II under optimal growth conditions and after cold acclimation conditions.

Under optimal growth conditions, (Panel A) the rate of consumption of electrons through carbon, N and S reduction can keep pace with the rate at which the photophysical processes used absorb light energy, resulting in a preferential reduction of the plastoquinone (PQ) pool. Thus, under these conditions, photostasis is reached, and linear electron flow from Photosystem II to Photosystem I takes precedence over cyclic electron flow. Exposure to low temperatures, however (Panel B), results in an imbalance, as the temperature sensitive dark reactions of photosynthesis are unable to keep up with the temperature insensitive light reactions of photosynthesis. This results in an increase in excitation pressure (1-qL), and if left unchecked, can result in the formation of reactive oxygen species. In order to restore photostasis, plants have developed a variety of mechanisms, such as reaction centre ($\phi_{f,D}$) and antennae quenching (ϕ_{NPQ}), which dissipate excess energy as heat via the reaction centre and PSII antennae, respectively. Cyclic electron transport through the NDH and PGR5 pathways provide means of diverting excess electrons from the linear electron flow by recirculating them, allowing the reduction of the plastoquinone pool. State transitions (not shown) also provide a means to regulate photosynthetic performance, by diverting excess energy from PSII to PSI. Photorespiration (not shown), which involves the oxygenation of Ribulose-1,5-Bisphosphate by Rubisco also acts as a safety valve. Other short term responses such as chlororespiration via Plastid Terminal oxidase, or PTOX, is also capable of diverting electrons by oxidizing the plastoquinone pool, while the Mehler reaction (not shown) will divert electrons from PSI to generate reactive oxygen species.

Leaves of cold hardy plants grown and developed at low temperatures (Panel C) exhibit a strong recovery of photosynthetic performance, as evidenced by a recovery in linear electron transport rates (ETR), and decreases in excitation pressure (1-qL), reaction centre ($\phi_{f,D}$) and antennae quenching (ϕ_{NPQ}). This recovery in photosynthetic performance can be attributed to adjustments in Calvin cycle enzymes and alterations in carbon partitioning, a long term acclamatory response used to restore photostasis. This is in conjunction with the short term strategies used to restore photostasis, including chlororespiration via PTOX, and an increase in cyclic electron transport via the PGR5 pathway. Figure reproduced from Ivanov et al. (2012), with permission.

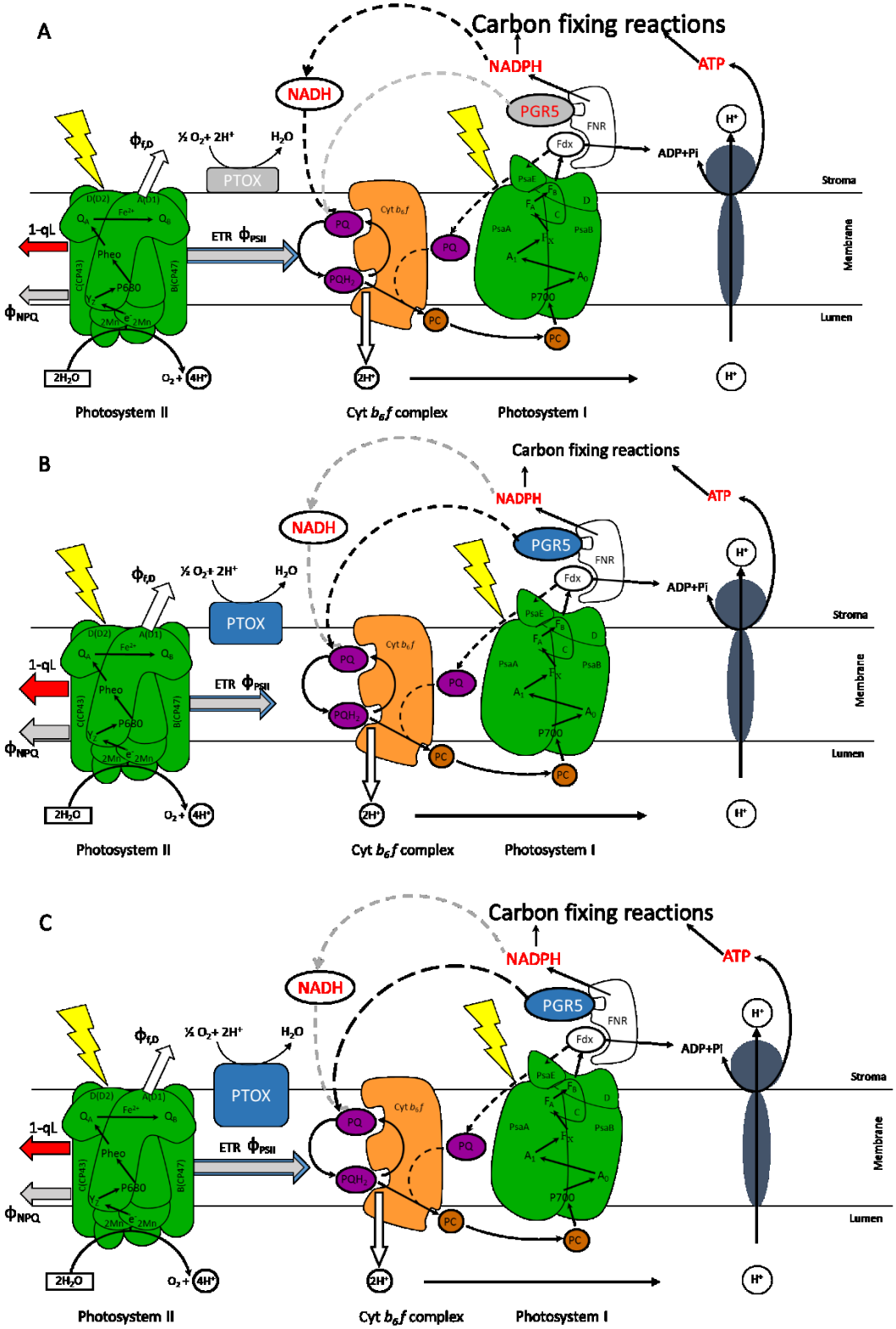
A
Carbon fixing reactions
NADPH
ATP
NADH
PGR5
FNR
Fdx
ADP+Pi
PTOX
½ O2+ 2H+
H2O
ETR ΦPSII
1-qL
ΦNPQ
Stroma
Membrane
Lumen
Photosystem II
Cyt b6f complex
Photosystem I
B
Carbon fixing reactions
NADPH
ATP
NADH
PGR5
FNR
Fdx
ADP+Pi
PTOX
½ O2+ 2H+
H2O
ETR ΦPSII
1-qL
ΦNPQ
Stroma
Membrane
Lumen
Photosystem II
Cyt b6f complex
Photosystem I
C
Carbon fixing reactions
NADPH
ATP
NADH
PGR5
FNR
Fdx
ADP+Pi
PTOX
½ O2+ 2H+
H2O
ETR ΦPSII
1-qL
ΦNPQ
Stroma
Membrane
Lumen
Photosystem II
Cyt b6f complex
Photosystem I

These physiological changes are associated with changes at the morphological level, as the cold acclimation of the aforementioned plants results in a dwarf, compact phenotype, in addition to alterations in leaf morphology, which include increases in leaf thickness and weight compared to their non-acclimated counterparts (Kurepin et al., 2013). The observed increases in leaf thickness can be attributed to increases in leaf mesophyll cell sizes (Gorsuch et al., 2010; Huner et al., 1981), and/or increases in the number of palisade mesophyll layers (Dahal et al., 2012; Dahal et al., 2014).

1.4 *Thesis organization*

The following thesis is separated into six chapters, where chapters 2-5 represent four individual studies. The second chapter of this thesis investigates the effect of low temperature stress, cold acclimation, and *BnCBF* overexpression on the transcription profile of SR genes, protein abundance and localization. The third chapter describes experiments to assess the role of a subset of SR proteins and one LAMMER kinase in the cold acclimation induced recovery of photosynthetic performance, as well as the acquisition of freezing tolerance by comparing chlorophyll a fluorescence and electrolyte leakage measurements between wild type *Arabidopsis*, SR and LAMMER kinase loss of function mutants under non-acclimated and after cold acclimation conditions. The fourth chapter is a detailed photochemical characterization of photosynthesis between wild type *Arabidopsis* and At-AME3 undergoing cold acclimation to assess the extent of limitations imposed by At-AME3 loss of function mutants in terms of photosynthetic performance. The fifth chapter focusses on defining potential SR proteins that can physically interact with At-AME3 LAMMER kinase using yeast 2-hybrid assays, while the sixth chapter consists of a summary of results attempting to

define the role of SR proteins and At-AME3 LAMMER kinase in the overall photosynthetic performance of *Arabidopsis thaliana*, the cold acclimation induced recovery of photosynthetic performance, and the acquisition of freezing tolerance.

Chapter 2: The effect of cold stress, acclimation and CBF overexpression on Serine/Arginine-rich protein gene expression, protein abundance and localization in *Brassica napus.*

Leonid V. Savitch, Ekaterina Ponomareva, David P. Sprott, Marc Rosembert, Adilah Bahadoor, Maxim Golovkin, Douglas A. Johnson, Jas Singh

For the second chapter, the identification of *Brassica napus* SR genes and associated kinases were performed by Ekaterina Ponomareva (AAFC, University of Ottawa) and David P. Sprott (AAFC). Moreover, RNA extractions and subsequent transcription profile analyses of SR genes in wild type *Brassica napus* and *BnCBF* overexpressor lines presented in Figure 2.2 were done by E. Ponomareva and D.P. Sprott. Protein extractions, 2D gels, SDS-PAGE and Western blot analyses presented in Figure 2.3, Panels A and B were done by D.P. Sprott. Adilah Bahadoor (AAFC) contributed in the protein extraction, SDS-PAGE and subsequent Western blots presented in Figure 2.3, Panel E.

Marc Rosembert's contribution to this chapter consists of enriched nuclei isolations, which were used for SDS-PAGE and Western Blot analyses to determine SR protein abundance and phosphorylation status under control and after cold acclimation conditions, as presented in Figure 2.3, Panel C. In addition, Marc has contributed to the preparation of enriched nuclei extracts from non-acclimated wild type *B. napus*, as well as *BnCBF5* and *BnCBF17* overexpressor lines which were used in SDS-PAGE and Western blots to determine the abundance of SR proteins belonging to 9G8, ASF/SF2 and Sc35 subclasses, as presented in Figure 2.3, Panel D.

This chapter was written as a manuscript, in preparation for submission by Leonid V. Savitch, Ekaterina Ponomareva, David P. Sprott, Marc Rosembert, Adilah Bahadoor, Douglas A. Johnson, Maxim Golovkin and Jas Singh, titled "**Cold and Cold-Attributed Factors Affecting Splicing-Related Gene Expression in *Brassica napus*".** I have written the first draft of this manuscript, along with all revised versions. Subsection 2.3, stating the hypotheses and research objectives of the study was added for the thesis.

2.1 Abstract

Exposure to low temperatures is one of the principal causes of complex physiological, morphological and biochemical changes in plants. Many intricate gene-reprogramming responses are involved in cold stressed plants with noticeable and extensive deviations of the entire transcriptional processes. In this study, we address the effects of cold and cold-related C-repeat binding factors (*BnCBF)* overexpression on plant *Brassica napus* splicing-related genes. The emphasis is on Serine Arginine-rich (SR) proteins, key players in pre-mRNA splicing and known plant splicing-related kinases. Gene-specific RT-PCR analyses on *Brassica napus* leaf tissue revealed a significant drop in transcript levels of *Bn-{SCL33, SR30*, *SC35*, RS2Z33; *RS31* and RSZ21*},* SR-like *Bn-SR45a* and splicing-related kinases *Bn-{AME1*, *AME2*, *SRPK1* and *SRPK-like 2}* genes in response to cold stress and cold acclimation conditions. Conversely, a dramatic cold temperature dependent increase in gene expression was evident for *Bn-{RSZ22*, *RS2Z32*, *SR40}* and less severe, for *Bn-{SCL30*, *SCL30a*, SR41; *SR34b*, *RSZ22a},* one SR-like gene *(Bn-SR45)* and two splicing-related kinases *Bn-{AME3* and *SRPK-like 1}* genes. Remarkably, expression profiles remained ubiquitously steady for two *Brassica* SR protein genes, *Bn-SR34* and splicing factor *Bn-SRL1*. At the proteomic level SDS-PAGE and 2D-analyses of total protein extracts plus enriched nuclei fractions revealed noticeable alterations in SR protein abundance and phosphorylation status. Moreover, deviations in subcellular compartmentalization patterns of plant SR proteins orthologous to mammalian ASF/SF2, SC35 and 9G8 SR proteins were also detected. In transgenic *Brassica* overexpressing the *BnCBF* gene and mimicking cold effects (Savitch et al., 2005) we have noticed a rather comparable pattern of changes in transcription

of SR proteins, as well as parallel trends in splicing-related protein abundance and phosphorylation status. These correlations, altogether, are emphasizing the remarkable orchestrated consistency in plant responses to cold.

2.2 Introduction

Cold stress, which includes both chilling (0-15ºC) and/or freezing (below 0ºC) temperatures, is a major environmental factor, causing adverse effects on growth and development of plants, thus limiting agricultural productivity. For example, in Alberta, a 20-23% yield loss of *Brassica napus* due to low temperatures resulted in losses estimated at a billion dollars in 2011 (Naseem and Singla, 2013). Thus, major research efforts are being directed to mitigate such losses. Cold temperature acclimation occurs only in cold-hardy plants trying to achieve the point of freezing tolerance, hence, responding with an extensive array of physiological, morphological and biochemical changes (Boese and Hüner, 1990; Dahal et al., 2012a, 2012b; Hüner et al., 2013a; Savitch et al., 2001, 2005). These physiological changes, like the substantial increase in photosynthesis activity, are closely associated with array of morphological alterations that often results in a distinct and well recognisable compact dwarf phenotype, typical for any cold geographical areas (Dahal et al., 2014; Ensminger et al., 2006). Cold exposure is changing morphological features in leaves, for example, as it increases their thickness and weight (Boese and Hüner, 1990; Dahal et al., 2012a, 2012b; Savitch et al., 2001; Strand et al., 1999); promote alterations in membrane stability (Nishida and Murata, 1996), changes pigmentation synthesis in order to shield from photoxidative stress (Christie et al., 1994; Król et al., 1999; Schöner and Heinrich Krause, 1990), induces upsurge of cryo-protective and antifreeze proteins (Tomashow et al., 1999).

DNA microarray analyses have shown that these changes, which allow the plant to adapt to low temperatures are associated with major changes in gene expression (Hannah et al., 2005; Matsui et al., 2008a; Medina et al., 2011; Shinozaki et al., 2003). Mutation studies of genes involved RNA metabolism (Gong et al., 2005) and pre-mRNA splicing factor (Lee et al., 2006) under cold stress have led to plant hypersensitivity to chilling, providing a strong link between RNA metabolism and cold responses.

Serine/Arginine-rich (SR) proteins, first studied in animals, are mostly prominent for their role in both constitutive and alternative pre-mRNA splicing (Howard and Sanford, 2014; Reddy and Ali, 2011; Roscigno and Garcia-Blanco, 1995; Wu and Maniatis, 1993). In plants, namely the research model plant *Arabidopsis thaliana*, there are seventeen SR and two SR-like proteins (genes) identified, in contrast to eleven in metazoans (Golovkin and Reddy, 1998, 1999; Lazar et al., 1995; Lopato et al., 1996, 1999a, 1999b). Hereafter, plant SR proteins are getting functionally characterized, with recognised multi-plural set of mammalian SR orthologues, ASF/SF2, SC35 and 9G8, and twelve plant-specific SR and SR-like proteins, all accredited with current nomenclature (Barta et al., 2010). Moreover, some studies have confirmed a multi-functional play of SR proteins, beyond the modulation of pre-mRNA splicing. They are causatively confirmed to participate in supporting stability (Lemaire et al., 2002), mRNA transport and changes in subcellular compartmentalisation (Huang et al., 2003), translation regulation (Sanford et al., 2005). The plausible cause of post-splicing interference for SR proteins is still poorly understood (Howard and Sanford, 2014). There are other studies to mention here that are also pointing out the significance of post-transcriptional mechanisms and pre-mRNA processing and stability is playing in plant cold acclimation (Chinnusamy et al., 2007; Mazzucotelli et al., 2008).

Experimental evidence on post-translational modifications, e.g., phosphorylation, of SR proteins have been steadily accumulating, leading to the definition of multiple roles, such as the regulation of their own activity (Misteli et al., 1998; Xiao and Manley, 1997) and changes in intrinsic patterns of nuclear localization (Cho et al., 2011). The dynamic phosphorylation of RS domain(s) of SR proteins was shown to elevate its RNA binding specificity (Tacke et al., 1997), affecting specific protein-protein interactions within the spliceosome complex (Xiao and Manley, 1997). Splicing-related kinases, first recognized in mammals, are able to meaningfully impact the convoluted process of splice site selection, key to splicing and overall processing (Zhong et al., 2009). Many SR proteins in *Arabidopsis* are heavily phosphorylated *in vivo,* steadily or interchangeably (de la Fuente van Bentem et al., 2006). Two major protein kinase families were identified as major players that differ in their substrate specificity. Both can phosphorylate RS domain serine residues, namely SRPKs and LAMMER-type kinases. All from LAMMER group are of dual-specificity, able to phosphorylate serine, threonine, and tyrosine residues (Colwill et al., 1996). In *Arabidopsis*, there are three known LAMMER kinases: AME1, AME2 and AME3, with two of them proven of auto-phosphorylation and phosphorylation of multiple SR proteins, including At-{RSZ21, RSZ22, SCL30, RS2Z33 and At-SR45}, those are AME1 (Golovkin and Reddy, 1999) and AME3 (Ahsan et al., 2013; *Arabidopsis* Interactome Mapping Consortium, 2011; Nemoto et al., 2011). Another kinase family, SRPK, differ in its abilities as enabled to phosphorylate only serine residues within specific arginine-serine-arginine (RSR) motif (Wang et al., 1998). In *Arabidopsis thaliana*, there are two recognized representatives: SRPK1, SRPK4, and two associated as SRPK-like protein kinases. For SRPK4 experiments have proven it can undergo auto-phosphorylation and phosphorylation of At-RS31 and At-SCL30 proteins (de la Fuente van Bentem et al., 2006, 2008). With

studies progressing, LAMMER and SRPK kinases were suggested to play an essential role in defining SR protein functions, hence, plausible participation in cold stress and acclimation responses. As regulators of constitutive and alternative splicing, Serine/Arginine-rich proteins are instrumental in regulating various processes in response to abiotic stresses such as low temperature stress.

The C-repeat binding factors (CBFs), previously known as dehydration-responsive-element-binding proteins (DREBs), are vital to cold-hardy plants signalling the path of complex cellular biochemical cascades toward cold acclimation, assuring plants acquisition of freezing tolerance status (Jaglo-Ottosen et al., 1998; Liu et al., 1998). CBF regulon established through microarray analyses of a vast array of Cold Responsive (COR) genes is comprised of many functionally different proteins, including signalling pathway components; biosynthetic proteins; osmo-protectants; many stress-related proteins like protease inhibitors, transcription factors; and a large number of proteins with yet unknown functions (Hannah et al., 2005; Vogel et al., 2005; Yamaguchi-Shinozaki and Shinozaki, 2006). The ectopic expression of some CBFs alone was shown to be sufficient to activate expression of COR genes and help induce plant cold acclimation at warm temperatures (Gilmour et al., 2004). Heterologous by origin, CBFs were all able to affect the expression of target genes in a model plant *Arabidopsis* (Yamaguchi-Shinozaki and Shinozaki, 2006). Transgenic plants of different species origin when overexpressing the *CBF (DREB1),* have clearly revealed a strong association with cold-acclimation-related morphological and physiological progressions, e.g., constitutive accumulation of soluble sugars, enhanced photosynthetic performance, alterations in leaf morphology, increases in leaf thickness and cell density (Dahal et al., 2012b; Gilmour et al., 2004; Hüner et al., 2014; Kurepin et al.,

2013; Pino et al., 2008; Savitch et al., 2005). Hence, the CBF regulon plays a pivotal role in cold stress transcriptional responses. In *Brassica napus,* two independent transgenic lines (*BNCBF5* and *BNCBF17*) overexpressing *Brassica CBF/DREB1*-like were reported to closely mimic the responses associated with cold stress (Dahal et al., 2012a, 2014; Hüner et al., 2014; Kurepin et al., 2013; Savitch et al., 2005). A sound experimental advantage of these *Brassica* transgenic plants is a constitutive nature of its cold response status giving a pair of comparison to experimental work with wild type plants physiological cold-induced changes.

This work is focusing mainly on *Brassica napus* plant that is prized as one of the most important principal sources of vegetable oil in the world. The accent is on cold and its effects triggered in plants exposed to low temperatures for a short or prolonged time. The emphasis is on the key splicing-related players, the Arginine-serine rich SR/SR-like plant proteins and splicing-associated LAMMER and SRPK/SRPK-like kinases. Experimental data presented here is encompassing the transcriptome and proteomic analyses of wild type *Brassica* plants and two transgenic plant lines with confirmed overexpression of cold-related C-repeat binding factor (*BnCBF)*. As expected, cold stress and acclimation conditions have led to major changes in splicing-related gene expression profiles and SR protein abundance, phosphorylation and subcellular compartmentalisation. These observations help to further elucidate a possibly major role of SR/SR-like proteins and the associated LAMMER and SRPK kinases in plants cold acclimation.

2.3 Hypotheses and objectives

It was hypothesized that 1) exposure to cold stress and/or cold acclimation conditions results in changes in the transcription profile of SR genes and associated kinases, 2) that these changes are associated with changes in SR protein abundance and phosphorylation

status, 3) that exposure to low temperatures has an effect on the localization of SR proteins and 4) that *Brassica napus* CBF overexpressor lines are capable of constitutively mimicking changes in SR and kinase expression, protein levels and phosphorylation status.

The objectives of this study were to 1) address whether cold stress and/or cold acclimation conditions have an effect on SR, LAMMER, SRPK and SRPK-like gene expression in *Brassica napus* by means of RT-PCR analyses, 2) whether these changes in transcript levels are associated with changes in SR protein abundance and phosphorylation status, 3) Assess whether CBF overexpression would have an effect on the transcription level of SR, LAMMER, SRPK and SRPK-like genes using *BnCBF5* and *BnCBF17* overexpressor lines and 4) whether *BnCBF* overexpression would have an effect on SR protein abundance, phosphorylation status and localization.

2.4 Materials and methods

2.4.1 Brassica napus growth conditions

Seeds of wild-type *Brassica napus* cv. Westar and transgenic *Brasssica napus* cv. Westar overexpressing *Brassica* cv. Jet Neuf *CBF/DREB1*-like transcription factors *BNCBF5* or *BnCBF17* (Gao et al., 2002;Savitch et al., 2005) were germinated in pots and grown for three weeks in a Conviron E-15 cabinet (Controlled Environments Ltd. Winnipeg, Manitoba) under controlled environmental conditions with a temperature regime of 20°C/16°C (day/night), a 16-h photoperiod and a photon flux density (PFD) of 250 µmol $m^{-2}s^{-1}$ for control (non-acclimating) conditions. The soil composition is a mix of top soil, peat moss, pumice and perlite at 4:1:1:1 volume ratio. Water-soluble industry standard micronutrients fertilizer "J.K. Peters 20:20:20 plus" (Everris/ICL, Mississauga, Canada) was utilized at the recommended rate of 100g $100L^{-1}$ once a week. To study the effect of low temperature stress and cold acclimation three weeks old/four leaf stage plants (leaf size of 2-4 cm across) were transferred to a temperature regime of 4°C/4°C (day/night) with light conditions identical to the control grown plants. During growth at low temperature the leaves previously developed at 20°C were considered cold-stressed while the new leaves developed at 4°C were considered cold acclimated. Effect of cold stress on 20°C developed leaves was monitored after 2 weeks of plant growth at 4°C while the effect of cold acclimation on 4°C developed leaves was monitored after 5 weeks of plant growth at 4°C. To avoid potential fluctuations in gene expression due to circadian rhythms, fully developed, non-senescent leaf tissue from both wild type *Brassica napus* and *BnCBF* overexpressors grown under every condition tested were collected at 10:00AM, frozen in liquid nitrogen and stored at -80°C for subsequent experiments. *BnCBF5* and *BnCBF17* overexpressors were obtained by

transforming cotyledons from *Brassica napus* cv. Westar with competent *Agrobacterium tumefaciens* strain GV3109pmp90 containing chimeric fusions of the coding regions of *BnCBF5* and *BnCBF17*, placed under the control of the Cauliflower Mosaic Virus-enhanced 35S promoter, as outlined in Savitch et al., (2005).

2.4.2 RNA isolations and reverse transcriptase reactions

RNA used for PCR analyses were extracted using a phenol/guanidine isothiocyanate solution (TRIzol® Reagent, Life Technologies) and chloroform, per the manufacturer's instructions. To remove genomic DNA contaminants, DNAse treatments were carried out using Invitrogen Ambion DNAse I (Burlington, ON, Canada) according to the manufacturer's instructions. Sample quality ($A_{260/280}$) and yield were assessed using the Pharmacia Biotech GeneQuant RNA/DNA Calculator (Cambridge, England). All reverse transcription (RT) reactions were carried out using the Superscript II Reverse Transcription kit from Invitrogen (Burlington, ON, Canada). One µg of mRNA template, 1 µL of 100 µM oligo dT, 0.5 µL of RNase inhibitors and water were added in a final volume of 11 µL, and were incubated for 10 minutes at 70°C, then cooled on ice. Superscript II 5X buffer, along with dNTPs, 0.1 M DTT and Superscript II (Invitrogen) were then added, and samples were incubated for 1 hour at 42°C. All RT reactions were carried out using an Eppendorf Mastercycler epigradient S thermocycler (Eppendorf Canada, Mississauga, ON).

2.4.3 PCR reactions

cDNA from previous RT reactions were used to assess the expression profile of Serine/Arginine-rich (SR) genes in wild type *Brassica napus* leaves, as well as *BnCBF5* and

BnCBF17 overexpressor lines under control, cold stress and cold acclimation conditions. Two µL of template cDNA was added to a master mix of PCR reagents consisting of 5 µL of 10X PCR buffer (Invitrogen), 1.5 µL of 50 mM $MgCl_2$ (final concentration of 1.5mM) (Invitrogen), 1 µL each of forward and reverse primers corresponding to SR genes of interest (Table 2.1), and 38 µL of dH_2O to a final volume of 50 µL. Primer sequences corresponding to SR genes of interest were based on *Brassica napus* Expressed Sequence Tags (ESTs) deposited to the NCBI database by AAFC-Saskatoon. To avoid the detection of various splice forms, all primers were designed to amplify only the first exon. The first exon of each SR gene of interest was targeted as it does not change between splicing variants. To avoid the amplification of off-target signals, PCR optimizations were performed using non-acclimated wild type cDNA with every primer pair under varying $MgCl_2$ concentrations, ranging from 1 mM to 4.5 mM in 0.5 mM increments. Moreover, optimal annealing temperatures were assessed by means of PCR reactions with annealing temperature gradients, ranging from 58°C to 72°C, in 2°C increments. PCR reactions involving no reverse transcriptase (no RT) were used as negative controls to ensure that there was no DNA contamination (data not shown). Every primer used in these experiments were designed using SeqMan (DNASTAR, Madison, WI). All PCR reactions were run on Eppendorf epigradient S or Mastercycler pro S thermocyclers, using the following parameters: an initial denaturation step at 90°C for two minutes, followed by 30 cycles at 90°C for 30 sec, 58°C annealing step for 30 seconds, and two minute extensions at 72°C.

Table 2.1: RT-PCR primers used in the assessment of the expression profile of Serine/Arginine-rich (SR) genes and associated kinases in wild type *Brassica napus* and *BnCBF5* and *17* overexpressor lines grown under control, cold stress and cold acclimation conditions.

Primer sequences were based on *Brassica napus* ESTs deposited by AAFC-Saskatoon to the NCBI database, and designed to cover the first exon of all SR genes and associated kinases, which is common to all alternatively spliced forms.

Gene of interest	*Arabidopsis* homolog	Forward primer sequence	Reverse primer sequence
Bn-RSZ21	AT1G23860	GAGTTTATGTCGGGAATCTGGA	CGGCGAGGTGGAGGTGGAC
Bn-RSZ22	AT4G31580	TGTGTACGTGGGAAACTTG	ACGAGCAGGAGGAGGTGAA
Bn-RSZ22a	AT2G24590	GCGAGTTACTGAGCGTGAGC	GGGCTCTTTCTGTATCTAGGAGG
Bn-SR30	AT1G09140	TCCTCGTGATGCAGATGATG	TAATATGGGCTGCGACTCACACTC
Bn-SCL30	AT3G55460	TCGATTGCAGACCAGAAGAGC	TCATAGCCAGGGGAATAGGAC
Bn-SCL30a	AT3G13570	TATGGTGGGGGTGGGGGTCGTG	TGGCTTCTTCCTGTTCTCTTCTGC
Bn-RS31	AT3G61860	ATGAGGCCGGTGTTCGTC	GCAGCGTATCTATCATCTCTTTCA
Bn-RS2Z32	AT3G53500	AGCGTGACTATGCCTTTGTTGA	TGATCTATCCTCCACGCTTCTCT
Bn-RS2Z33	AT2G37340	TGACGCGAGACATTACTTGG	GTCTTGAGGGCTGCTACCACCATC
Bn-SCL33	AT1G55310	CTAGAGGAGGAGGCCGTTATGGTG	GGCTTATGCTGCGGCTCTTACTTC
Bn-SR34	AT1G02840	GGATCCTCGGGATGCTGATGATG	CTGCGGCTAAGACTGCGGCTGTGG
Bn-SR34b	AT4G02430	CACCTCGTCCTCCATGTTATTGCTTTGTTG	AGCCTCTAGCCCATGGGTTTTTGAA
Bn-SC35	AT5G64200	ATTCGCGTGGTTTTGCATTTGTTC	CGACTGCGCCTCTCATCATCATAA
Bn-RS40	AT4G25500	GAGGCCTTGACCGCATTGAA	ACGCCTCGATCTCTTGTAA
Bn-RS41	AT5G52040	GGGTTGATATGAAAGCTGGGTT	TATCACGGCGTCTATCGGGACT
Bn-SR45	AT1G16610	AGTCGGTCCAGGTCTCTTTCTTC	AACAGGCTTAGGAGGTGGAGGTAG
Bn-SR45a	AT1G07350	AAAAGCGTCGTGGAAGGTCTGTGT	ATCTGTCCCGTGCTCTGTAATCA
Bn-AME1	AT4G24740	GAAAGAGATGGTGGCAGTGAAA	TCCTGTCGCTCATAAGTTGTGCT
Bn-AME2	AT3G53570	CCATCCACGGTATTTCATCCTC	CAAGCTCCCGAACAAGGTCAA
Bn-AME3	AT4G32660	GGAAGCGATGGGAGGGTTTTGT	TCGGGCTTGAGGTCGGTGTG
Bn-SRPK1	AT3G23000	CCTTTCTCCGGTGGTCGTTACATC	GCCGTTTGCGTTCCCCTCAG
SRPK-like 1	AT2G17530	GGTGGCCGTTACATTGCTCAG	TTGCGTTTCCTTCAGGCTTTTCTA
SRPK-like 2	AT5G22840	TGAAGGAACAGAGGATTAC	CCCAAATACTCAAAGACCA
Bn-SRL1	AT5G37370	GATGGGTGGAAACTGCCGTGGTC	TGCGGTTCATCCCTTTCGTTTCTG
Bn-Elf1	AT1G18070	AGCCCCTTCGTCTTCCACTTCAG	TGGGCTCCTTCTCAATCTCCTTAC

2.4.4 Protein extractions for SDS-PAGE electrophoresis

Enriched nuclei fractions were isolated based on a modified nuclei isolation protocol from Henfrey and Slater (Henfrey and Slater, 1988) (Figure 2.1). 10 grams of frozen leaf tissue from wild type *Brassica napus*, *BnCBF5* and *BnCBF17* overexpressors grown under control and cold acclimation conditions were ground in 40 mL of isolation buffer (20mM Tricine, pH 8.4, 10mM EDTA, pH 8.0, 5mM $MgCl_2$, 10mM KCl, 0.4M sorbitol, 20mM NaF, 1mM DTT, 0.2mM PMSF, 10mM 2-Mercaptoethanol, 1/100mL protease inhibitor cocktail) using a Waring Laboratory Blender. Sodium Fluoride (NaF) was added to the isolation buffer to preserve the phosphorylation status of the extracted proteins. The homogenate was then passed through a funnel lined with Miracloth (Bio-Rad) to remove debris. For total protein extracts, 20% SDS was added to the homogenate, to a final concentration of 2% and stored at -20 ºC, to be used for subsequent SDS-PAGE/Western blot assays. Samples used for enriched nuclear fractions were spun at 10 000 x g for 20 minutes, at a temperature of 4ºC. 800 µL of the resulting supernatant, representing the cytosolic fraction was transferred to a microcentrifuge tube containing 200 µL of 20% SDS, for a final concentration of 2% (v/v) and stored at -20ºC for subsequent solubilisation. The cytosolic fractions were collected from wild type *Brassica napus* samples grown under control and cold acclimation conditions for subsequent compartmentalization studies. The pellet, representing nuclear and chloroplast fractions was resuspended in isolation buffer containing Triton X-100, at a final concentration of 1% to selectively break chloroplasts. The samples were incubated on ice for 5 minutes and then spun at 3000 x g for 10 minutes, at a temperature of 4ºC. The resulting supernatant, corresponding to the chloroplast stromal fraction, was discarded, while the pellet

was washed twice in nuclei isolation buffer supplemented with 1% Triton X-100, and spun at 3000 x g for 10 minutes, at a temperature of 4ºC. The supernatant was discarded, and the pellet was resuspended in nuclei isolation buffer, and passed through a column consisting of 40%, 60%, 80% Percoll/Isolation buffer solutions, with a 2.3M sucrose cushion at the bottom. The column was then spun at 15 000 x g for 30 minutes at 4ºC, and the 40% and 60% Percoll layers, containing broken and intact chloroplasts, respectively, were discarded. The 80% Percoll layer, containing intact nuclei, was collected and spun at 5000 x g for 5 minutes at 4ºC. The resulting supernatant, consisting of 80% Percoll, was discarded and the pellet was washed twice in isolation buffer and spun at 5000 x g for 5 minutes at 4ºC. The pellet was then resuspended in isolation buffer supplemented with 2% (v/v) SDS, and stored at -20 ºC for subsequent solubilisation. Sample solubilisation was done by heating samples at 95ºC twice for five minutes. Once samples were solubilized, protein concentrations were assessed using a BioRad Dc protein detection kit and then quantified using the Evolution 300 (Thermo Fisher) UV-visible spectrophotometer and VisionPRO software.

Figure 2.1: Schematic diagram representing the enriched nuclear protein isolation protocol.

Leaves from wild type *Brassica napus* and *BnCBF* overexpressor lines grown under control and after cold acclimation conditions were collected to be used for enriched nuclei isolations. These enriched nuclei extracts were subsequently used to assess the protein expression profile and phosphorylation status of SR proteins.

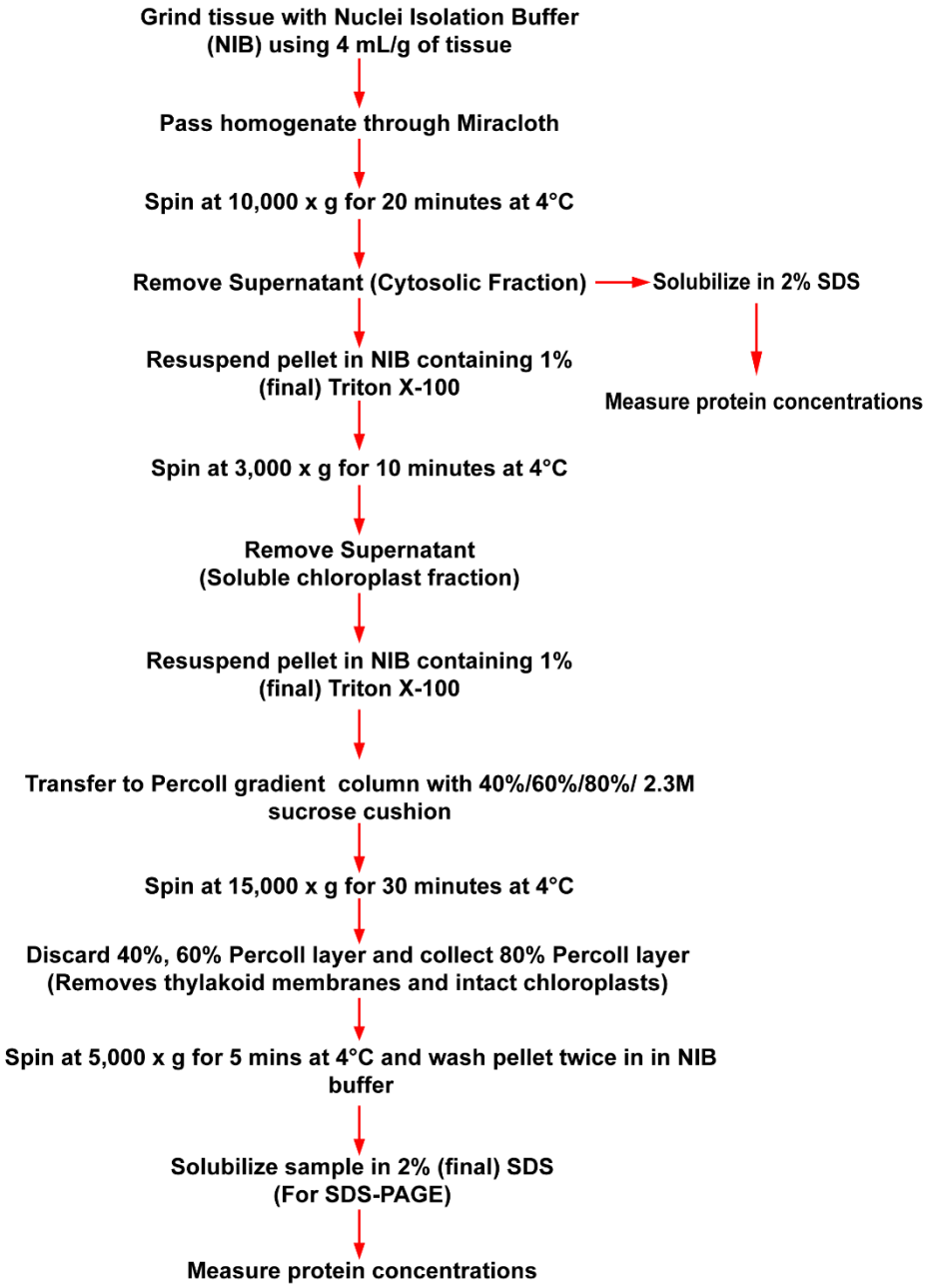
Grind tissue with Nuclei Isolation Buffer (NIB) using 4 mL/g of tissue
Pass homogenate through Miracloth
Spin at 10,000 x g for 20 minutes at 4°C
Remove Supernatant (Cytosolic Fraction)
Solubilize in 2% SDS
Measure protein concentrations
Resuspend pellet in NIB containing 1% (final) Triton X-100
Spin at 3,000 x g for 10 minutes at 4°C
Remove Supernatant (Soluble chloroplast fraction)
Resuspend pellet in NIB containing 1% (final) Triton X-100
Transfer to Percoll gradient column with 40%/60%/80%/ 2.3M sucrose cushion
Spin at 15,000 x g for 30 minutes at 4°C
Discard 40%, 60% Percoll layer and collect 80% Percoll layer (Removes thylakoid membranes and intact chloroplasts)
Spin at 5,000 x g for 5 mins at 4°C and wash pellet twice in in NIB buffer
Solubilize sample in 2% (final) SDS (For SDS-PAGE)
Measure protein concentrations

2.4.5 Sample preparation for 2D gel electrophoresis

Frozen leaf tissue from wild type *Brassica napus* and *BnCBF17* overexpressors grown under control and after cold acclimation conditions, respectively, were ground to a fine powder using a mortar and pestle, in the presence of polyvinylpolypyrolidone (PVPP), and resuspended in grinding buffer (1M Tris, pH 8.0, 0.5M EDTA, pH 8.0, 10mM PMSF, 10mM DTT, Protease inhibitor cocktail (Sigma-Aldrich, St. Louis, USA). The samples were then spun down at 21 000 x g for 30 minutes, at a temperature of 4ºC for 30 minutes to remove cell walls and debris. 9 mL of acid denaturing solution (11% (w/v) of TCA dissolved in acetone, 0.05% DTT) were added for every mL of grinding buffer used, and proteins were precipitated by incubating for 1 hour at -20ºC. The extracts were then centrifuged at 21 000 x g for 30 minutes, at a temperature of 4ºC. The resulting supernatant was decanted, and the pellets were washed twice by resuspension in an acetone solution, supplemented with 0.005% (w/v) DTT, and incubation for 60 minutes at -20ºC, followed by centrifugation for 30 minutes at 21 000 x g at 4ºC. After the second wash step, the supernatant was discarded, and the pellets were dried at room temperature for approximately 20 minutes. The pellets were then resuspended in rehydration buffer (8M urea, 2M thiourea, 2% (w/v) CHAPS, 50mM DTT, 0.1% (w/v) carrier ampholytes, pI range 3-10, 0.0005% Bromophenol Blue) at room temperature for 60 minutes. Protein concentrations were determined using a Bradford assay kit (Bio-Rad), and quantified using the Evolution 300 (Thermo Fisher) UV-visible spectrophotometer and VisionPRO software. To ensure equal protein loading, and sample integrity, an aliquot of each sample was added to 6X loading buffer (50 mM Tris-HCl, 0.002% Bromophenol Blue, 2.5% Glycerol, 2% SDS, and 143 mM 2-Mercaptoethanol), and

loaded on discontinuous polyacrylamide gel systems consisting of 4% (w/v) stacking and 12.5% (w/v) separating gels. Electrophoresis was performed using a Mini-Protean II apparatus (Bio-Rad) at a constant voltage of 100 V for approximately 2.5 h, until the dye front had run off the gel. The gel was incubated overnight in a Coomassie Blue staining solution (0.1% (w/v) Coomassie G-250 (Bio-Rad), 10% (v/v) Acetic acid, 50% (v/v) Methanol), then destained for three hours in a destaining solution (40% (v/v) Methanol, 10% (v/v) acetic acid), with gentle agitation, until the background staining is removed. Visual inspection of the large subunit of Rubisco (RBCSL) on the stained gel was used as a reference (data not presented) to ascertain equal loading if and necessary, adjustments to protein amounts were made. For SDS gels of enriched nuclear extracts, a visual inspection of the stained gel was used as a reference.

2.4.6 SDS-PAGE and 2D gel electrophoresis conditions

100 µg of total protein extracts from wild type *Brassica napus* or *BnCBF* overexpressors were loaded on hydrated ReadyStrip pH 3-10 IPG strips (Bio-Rad). Isoelectric focusing was performed using a PROTEAN IEF cell (Bio-Rad) under the following conditions: voltage was increased linearly to 250 V for 20 minutes, followed by a linear increase to 4000 V during 2 hours. Samples were then run at 4000 V for approximately 2 hours, until 10 000 V-hrs were reached. Strips were then incubated in Equilibration buffer I (375 mM Tris base, 6 M Urea, 2% SDS, 20% Glycerol, 2% DTT), followed by another incubation in Equilibration buffer II (375 mM Tris base, 6 M Urea, 2% SDS, 20% Glycerol, 2.5% iodocetamine). The strips were then put on top of 12.5% (w/v) polyacrylamide gels, and run at 100V for approximately 2 hours, until the dye front has run off the gel.

Loading buffer (6X solution; 50 mM Tris-HCl, 0.002% Bromophenol Blue, 2.5% Glycerol, 2% SDS, and 143 mM 2-Mercaptoethanol) was added to aliquots of total protein extracts, cytosolic and enriched nuclei fractions from wild type *Brassica* and *BnCBF* overexpressor lines grown under control, cold stress and cold acclimation, prior to loading. Samples were loaded in equal amounts, consisting of 40 µg per lane for total protein extracts, 20 µg per lane for cytosolic fractions and enriched nuclei fractions, into discontinuous polyacrylamide gel systems consisting of 4% (w/v) stacking and 12.5% (w/v) separating gels. Electrophoresis was performed using a Mini-Protean II apparatus (Bio-Rad) at a constant voltage of 100 V for approximately 2.5 h, until the dye front had run off the gel. The Kaleidoscope prestained protein standards (BioRad) were used as a molecular marker.

2.4.7 Gel transfer conditions and immunoblotting

SDS-PAGE gels that were used for immunoblotting were transferred from the SDS-polyacrylamide gel onto Immun-Blot polyvinylidene fluoride (PVDF) membranes (0,2µm pore size; Bio-Rad) by means of tank blotting (Towbin et al., 1979). Electrophoretic transfers were done at a constant voltage of 100 V for 1.5 h using Mini-Protean II apparatuses, at 4°C. Once the transfer has finished, membranes were incubated overnight in 2% (w/v) ECL Advance Blocking Agent (GE/Amersham Biosciences) in a 1X Tris Buffer Saline solution with 0.1% Tween-20 (1X TBST).

Membranes were subsequently probed with primary antibodies raised against 1H4, Sc35, 9G8 and ASF/SF2 (Santa Cruz Biosciences) or mAb104 for an hour at room temperature. 1H4 antibodies were raised against an epitope common to all mammalian SR proteins. Sc35 antibodies recognize an epitope from mammalian Sc35 while 9G8 and ASF/SF2 antibodies recognize epitopes found in SR proteins belonging to mammalian 9G8

and ASF/SF2 subclasses, respectively. mAb104 antibodies, which recognize phosphoepitopes in mammalian SR proteins were used for the detection of phosphorylated SR proteins. mAb104 hybridoma were purchased from ATCC (Manassas, VA), and cells were cultured in Isco's modified Dulbecco's medium, according to the provided protocol. Dilutions used were 1:100, 1:500, 1:200 and 1:500, respectively. For membranes probed with mAb104, the undiluted cell culture supernatant was used. Membranes were then washed twice in 1X TBST for 15 minutes, and incubated with secondary antibodies. The blots were then probed using goat anti-rabbit IgG conjugated with horseradish peroxidase from Sigma (Sigma Chemical Co., St. Louis, MO, USA) as a secondary antibody. Anti-mouse IgG secondary antibodies (Sigma Chemical Co., St. Louis, MO, USA) conjugated with horseradish peroxidase were used on membranes probed with 1H4, at a dilution of 1:100000. Anti-Rabbit IgG secondary antibodies were used on membranes probed with Sc35, 9G8 and ASF/SF2 primary antibodies, at dilutions of 1:1 000 000, 1: 3 000 000, and 1: 1 000 000, respectively. Anti-mouse IgM secondary antibodies were used at a dilution of 1:3 000 000 on membranes probed with mAb104 antibodies. An ECL Advanced chemiluminescent detection system from Amersham (ECL Advanced Western Blotting Detection Kit, Amersham Pharmacia Biotech, Buckinghamshire, UK) was used for the detection of proteins of interest for all SDS-PAGE Western blots.

2.5 Results

2.5.1 Expresssion profile of Serine/Arginine-rich (SR) genes and associated kinases in wild type Brassica napus, BnCBF5 and BnCBF17 overexpressors

A preliminary analysis assessing the overall transcript profile of SR genes and associated kinases in wild type *Brassica napus* has shown that out of all the SR genes and kinases tested, only one, SR34, showed no changes in expression when comparing control, cold stress and cold acclimation conditions (Figure 2.2. Panels A-B, Table 2.2). Moreover, the expression levels of SRL1, a splicing factor and housekeeping gene Elf1 were also unaltered under cold stress and acclimation conditions. When Bn-SRPK4 transcript levels were assessed, no amplification was detected in *BnCBF5* and *BnCBF17* overexpressors under every condition tested; this data is not included in the study. Exposure to cold stress and acclimation conditions led to a reduction in transcript levels of Bn-SR30 (homologous to ASF/SF2), Bn-RSZ21 (homologous to 9G8), Bn-SC35 (homologous to SC35), Bn-RS2Z33, Bn-SCL33, Bn-RS31 (plant specific), Bn-SR45a, as well as Bn-AME1 and Bn-AME2 LAMMER kinases, Bn-SRPK1, SRPK-like 2 kinase genes in wild type *Brassica napus*. Conversely, an increase in expression was observed for Bn-RSZ22, Bn-RSZ22a, which belong to the RSZ subfamily (homologous to 9G8), Bn-SR34b, (homologous to ASF/SF2). Plant specific SR genes Bn-SCL30, Bn-SCL30a, Bn-RS2Z32, Bn-RS40 and Bn-RS41, as well as SR-like Bn-SR45 have also shown an increase in expression under cold stress and acclimation conditions. Moreover, Bn-AME3 and SRPK-like 1 were also found to be upregulated in response to cold.

Figure 2.2: Effect of exposure to low temperatures and *BnCBF* overexpression on the expression profile of Serine/Arginine-rich (SR) genes (A) and associated LAMMER kinases (B) in leaves of wild type *Brassica napus* plants and *BnCBF* overexpressor lines grown under control, cold stress and cold acclimation conditions.

Lanes designated as C, S, A represent samples grown under control, cold stress and cold acclimation conditions, respectively. Housekeeping gene Elongation Factor 1 (Bn-Elf1) expression was monitored as a loading control. RT-PCR products shown in this preliminary figure were amplified for 30 cycles. These data were provided by Ekaterina Ponomareva and David P. Sprott and the figure was assembled by Dr. Leonid V. Savitch.

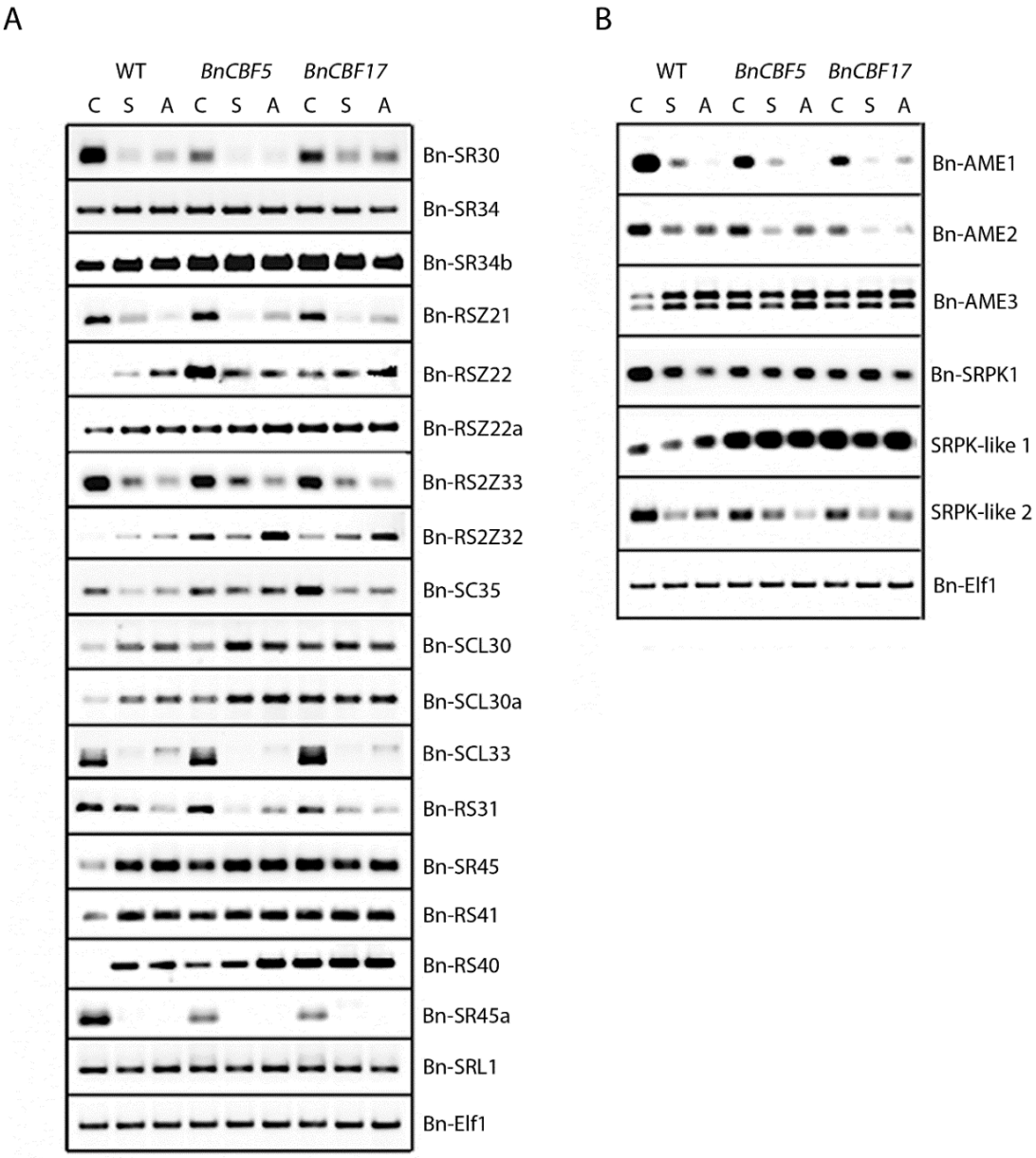
A
WT
BnCBF5
BnCBF17
C S A C S A C S A
Bn-SR30
Bn-SR34
Bn-SR34b
Bn-RSZ21
Bn-RSZ22
Bn-RSZ22a
Bn-RS2Z33
Bn-RS2Z32
Bn-SC35
Bn-SCL30
Bn-SCL30a
Bn-SCL33
Bn-RS31
Bn-SR45
Bn-RS41
Bn-RS40
Bn-SR45a
Bn-SRL1
Bn-Elf1
B
WT
BnCBF5
BnCBF17
C S A C S A C S A
Bn-AME1
Bn-AME2
Bn-AME3
Bn-SRPK1
SRPK-like 1
SRPK-like 2
Bn-Elf1

Table 2.2: Summary table portraying the assessment of the expression profile of Serine/Arginine-rich (SR) genes and associated Clk/Sty kinases in Wild Type *Brassica napus*, *BnCBF5* and *BnCBF17* overexpressor lines grown under control, cold stress and cold acclimation conditions.

Arrows pointing downwards represent genes that were found to be downregulated under cold stress and cold acclimation conditions relative to plants grown under control conditions, whereas arrows pointing upwards represent an increase in expression relative to plants grown under control conditions. Expression levels denoted as NC represent genes exhibiting no discernable changes in expression under cold stress and cold acclimation conditions relative to wild type plants. This modified table was provided by the Savitch lab.

Mammalian orthologs	Subfamily	Gene/Protein	Expression level		
			WT	*BnCBF5*	*BnCBF17*
ASF/SF2 (SRSF1)	SR	SR30	↓	↓	↓
		SR34	**NC**	**NC**	**NC**
		SR34b	↑	↑	↑
9G8 (SRSF7)	RSZ	RSZ21	↓	↓	↓
		RSZ22	↑	↑	↑
		RSZ22a	↑	↑	↑
SC35 (SRSF2)	SC	SC35	↓	↓	↓
Plant specific	SCL	SCL30	↑	↑	↑
		SCL30a	↑	↑	↑
		SCL33	↓	↓	↓
	RS2Z	RS2Z32	↑	↑	↑
		RS2Z33	↓	↓	↓
	RS	RS31	↓	↓	↓
		RS40	↑	↑	↑
		RS41	↑	↑	↑
SR-like		SR45	↑	↑	↑
		SR45a	↓	↓	↓
		SRL1	**NC**	**NC**	**NC**
LAMMER kinases		AME1	↓	↓	↓
		AME2	↓	↓	↓
		AME3	↑	↑	↑
SRPK		SRPK1	↓	↓	↓
SRPK-like		SRPK-like 1	↑	↑	↑
		SRPK-like 2	↓	↓	↓

The alterations in SR and kinase gene transcripts observed in wild type *Brassica napus* under cold stress and acclimation conditions raised the question as to whether *BnCBF* overexpression would have a similar effect on the expression profile of SR genes. Similar to wild type *Brassica napus* under cold stress and acclimation conditions, *BnCBF5* and *BnCBF17* overexpression had no effect on *Bn-SR34* and *Bn-SRL1* transcript levels, as no changes in expression were detected under control, cold stress and acclimation conditions.

Under non-acclimated conditions, *BnCBF* overexpressor lines appear to partially mimic the expression profile of cold acclimated wild type *Brassica napus*, as transcript levels for *Bn-RSZ22, Bn-RSZ22a, Bn-SR34b, Bn-SCL30, Bn-SCL30a, Bn-RS2Z32, Bn-RS40, Bn-RS41, Bn-SR45,* as well as *Bn-AME3* and *SRPK-like 2* are greater in *BnCBF* overexpressors under control conditions compared to their wild type counterparts grown under the same condition, and are closer to transcript levels observed in cold acclimated wild type *Brassica napus*. Moreover, *Bn-SR45a*, *Bn-AME1* and *Bn-AME2* kinases exhibit greater reduction under control conditions in *BnCBF* OEs under control conditions compared to wild type *Brassica* grown under control conditions. While *BnCBF* overexpression led to an enhancement or a suppression in transcript levels of several SR genes under control conditions, *Bn-RSZ21*, *Bn-RS2Z33*, *Bn-SCL33* transcript levels remained identical to wild type *Brassica napus* under control conditions.

Similarly to the expression profile of SR genes observed in wild type *Brassica napus*, cold stress and cold acclimation conditions led to a decrease in the expression of *Bn-SR30* (homologous to mammalian ASF/SF2), *Bn-RSZ21* (homologous to mammalian 9G8), and *Bn-SC35* (homologous to mammalian SC35) in *BnCBF5* and *17* overexpressors. Furthermore, a decrease in transcript levels of plant specific SR genes *Bn-RS2Z33, Bn-*

SCL33, Bn-RS31, Bn-SR45a, as well as *Bn-AME1* and *Bn-AME2* LAMMER kinases, *Bn-SRPK1, SRPK-like 2* kinase genes were also observed in both *BnCBF5* and *BnCBF17* overexpressors. Conversely, as observed in wild type *Brassica napus*, exposure to cold stress and acclimation conditions led to an increase in expression of *Bn-RSZ22, Bn-RSZ22a* and *Bn-SR34b* in *BnCBF5* and *BnCBF17* overexpressors. Plant specific SR genes *Bn-SCL30, Bn-SCL30a, Bn-RS2Z32, Bn-RS40, Bn-RS41*, SR-like *Bn-SR45*, as well as *Bn-AME3* and *SRPK-like 2* were also found to be upregulated in response to cold.

Interestingly, the increase in expression of SR genes and associated kinases mentioned above was exacerbated in *BnCBF5* and *BnCBF17* overexpressors grown under the same conditions. This trend can be observed with the transcript profile of *Bn-SR34b, Bn-RS40* and *Bn-SR45*, which have been shown to increase in expression under cold stress and acclimation conditions in wild type *Brassica*. These three SR genes appear to be expressed at greater levels in both *BnCBF5* and *BnCBF17* under low temperature stress in comparison to their wild type *Brassica* counterparts. Moreover, some genes that have been shown to be suppressed under cold stress and cold acclimation conditions show a greater suppression under *BnCBF* overexpression. This trend can be seen with *Bn-SR45a*, as well as *Bn-AME1* and *Bn-AME2* kinases, whose expression levels exhibit greater reduction under control conditions in both *BnCBF5* and *BnCBF17* compared to wild type under the same condition.

Taken together, these results would suggest that both low temperatures and *BnCBF* overexpression influence the expression profile of several SR genes, as well as their associated kinases in *Brassica napus* plants undergoing cold acclimation. However, not all SR genes are affected by low temperatures and/or *CBF* overexpression, as the expression level of *Bn-SR34* has remained consistent under every condition tested. In addition, the

expression levels of *Bn-RS2Z33* and *Bn-RSZ21* which remained the same in both wild type *Brassica* and *BnCBF* overexpressors exposed to low temperatures, suggesting that exposure to low temperatures, but not *BnCBF* overexpression, play a role in modulating their expression. Moreover, these differences in SR gene expression in *BnCBF* overexpressors would suggest that *BnCBF* overexpression only partially mimics cold acclimation responses with respect to SR gene expression. It should be noted that the expression profile of some SR genes (Bn-SR30, Bn-RSZ21, Bn-RSZ22, Bn-RS2Z32, Bn-Sc35, Bn-SR45, Bn-RS40) under non-acclimated and stress conditions are not in agreement with changes in splicing patterns of these SR genes in response to cold stress observed by Palusa et al. (2007). Discrepancies between the findings presented in this study and the report by Palusa et al. could be attributed to differences in experimental design, which are discussed later in this study (Refer to the discussion).

2.5.2 Effect of cold stress, acclimation and BnCBF overexpression on SR protein abundance

The next objective consisted of addressing whether these alterations in gene expression can be correlated with changes in protein abundance in wild type *Brassica napus*, as well as *BnCBF5* and *BnCBF17* overexpressors. Total protein extracts from wild type *B. napus*, *BnCBF5* and *BnCBF17* overexpressor leaf tissue grown under control, cold stress and cold acclimation conditions were probed with 1H4, a primary antibody raised against Serine/Arginine epitopes common to all SR proteins. In wild type *B. napus*, exposure to low temperatures led to a gradual increase in SR protein abundance, as no bands were detected under non-acclimated conditions, followed by the presence of three bands, with the lower band detected in the 20-25kDa range, followed by two bands detected between 40-45 kDa,

under cold stress and acclimation conditions. Similarly to the observed changes in SR gene expression, *BnCBF* overexpression led to an increase in SR protein abundance under non-acclimated conditions, as the three bands which were detected in cold stressed and acclimated wild type *Brassica* samples were observed in both *BnCBF5* and *BnCBF17* samples grown under control conditions, with an increase in abundance under cold stress and acclimation conditions, as shown in Figure 2.3, Panel A.

Figure 2.3: Effects of low temperature and *BnCBF* overexpression on the protein abundance, phosphorylation status and localization of Serine/Arginine-rich proteins in wild type *Brassica napus* and *BnCBF* overexpressor lines grown under control, cold stress and cold acclimation conditions.

All blots shown represent qualitative results. Lanes designated as C, S and A are representative of samples grown under control, cold stress and cold acclimation conditions, respectively. Panel A depicts Western blots of SDS-PAGE gels of total protein extracts probed with 1H4 antibodies raised against SR domain-containing proteins and mAb104 antibodies raised against common phosphoepitopes shared by SR proteins. A representative Western blot of 2D gels of crude extracts and enriched nuclei from wild type *B. napus* grown under control conditions and cold acclimated *BnCBF17* overexpressors probed with 1H4 antibodies is shown in Panel B. Panel C represents the protein expression profile and phosphorylation status of SR proteins in enriched nuclear fractions from wild type *B. napus* and *BnCBF* overexpressors grown under control and after cold acclimation conditions probed with 1H4 and mAb104 antibodies. Panel D depicts Western blots probed with 9G8, ASF/SF2 and Sc35, which recognize SR proteins that are homologous to mammalian 9G8, ASF/SF2 and Sc35 in enriched nuclei sample preparations from wild type *B. napus* and *BnCBF5/BnCBF17* overexpressor lines grown under control conditions. Panel E represents Western blots from wild type *B. napus* cytosolic fractions extracted from leaf tissue grown under control and after cold acclimation conditions, compared to enriched nuclei sample preparations from the same leaves. The samples were probed with 1H4, which recognizes SR domains common to all SR proteins, as well as ASF/SF2, 9G8 and Sc35, which recognizes SR proteins homologous to mammalian ASF/SF2, 9G8 and Sc35 SR proteins.

Data presented in Panels A and B were obtained by David P. Sprott and data from Panel E were obtained by Adilah Bahadoor. Panels A and B were assembled by Dr. Leonid V. Savitch.

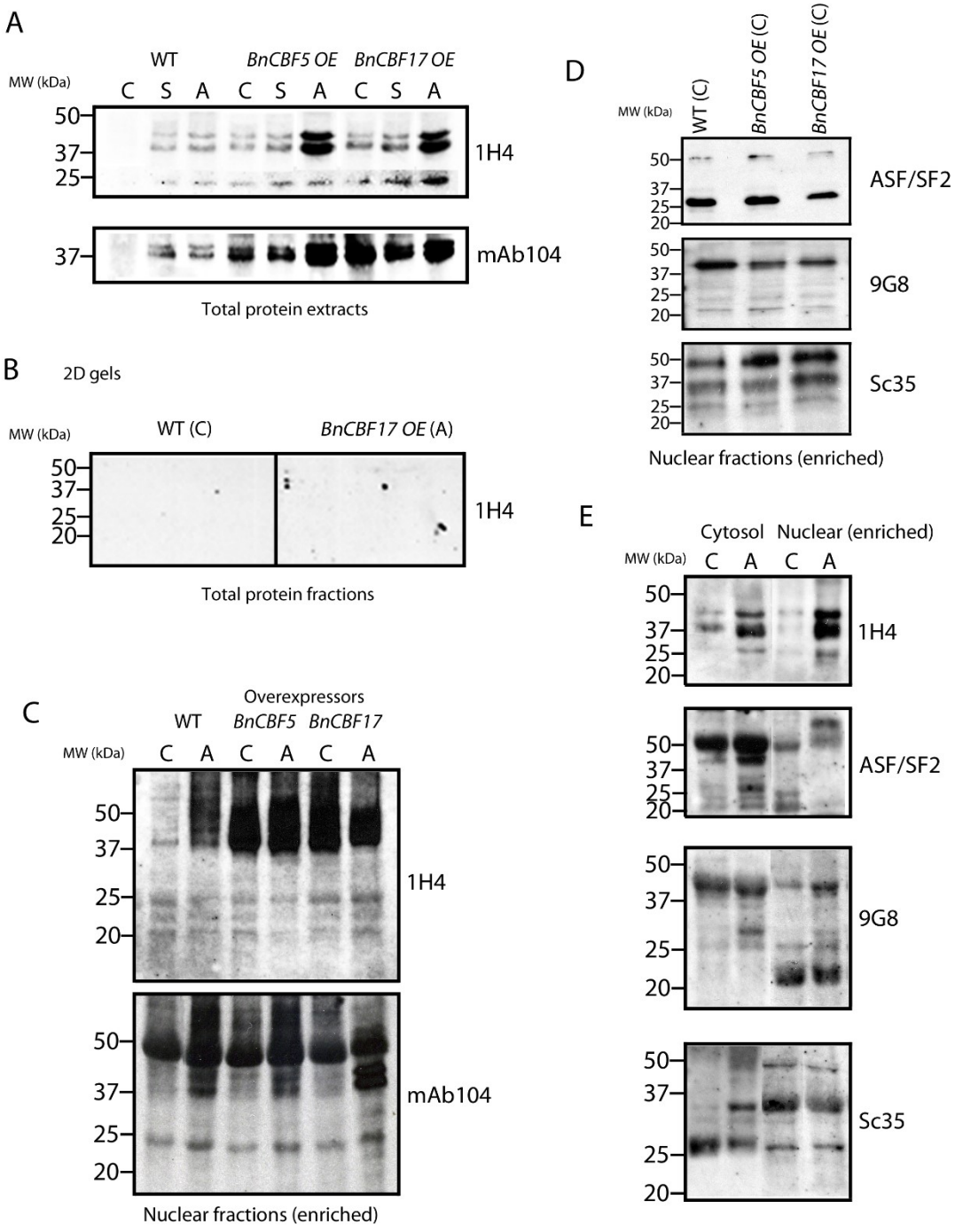
A
WT
BnCBF5 OE
BnCBF17 OE
MW (kDa)
C S A C S A C S A
50
37
25
1H4
37
mAb104
Total protein extracts
B
2D gels
MW (kDa)
WT (C)
BnCBF17 OE (A)
50
37
25
20
1H4
Total protein fractions
C
Overexpressors
WT
BnCBF5
BnCBF17
MW (kDa)
C A C A C A
50
37
25
20
1H4
50
37
25
20
mAb104
Nuclear fractions (enriched)
D
MW (kDa)
WT (C)
BnCBF5 OE (C)
BnCBF17 OE (C)
50
37
25
20
ASF/SF2
50
37
25
20
9G8
50
37
25
20
Sc35
Nuclear fractions (enriched)
E
Cytosol
Nuclear (enriched)
MW (kDa)
C A C A
50
37
25
20
1H4
50
37
25
20
ASF/SF2
50
37
25
20
9G8
50
37
25
20
Sc35

While the abundance of LAMMER, SRPK and SRPK-like kinases could not be assessed, due to a lack of commercially available antibodies raised against them, the phosphorylation status of SR proteins targeted by these kinases could be assessed using mAb104, an antibody raised against SR phosphoepitopes (Roth et al., 1990). As shown in Figure 2.3, Panel A, probing leaf samples from wild type *Brassica napus*, as well as *BnCBF5* and *BnCBF17* overexpressors grown under control, cold stress and cold acclimation conditions has revealed that SR proteins undergo an increase in phosphorylation under exposure to cold stress and acclimation conditions, as no bands were detected in samples grown under control conditions, followed by the presence of two bands ranging from 37kDa to 45kDa in samples grown under cold stress and acclimation conditions. Moreover, *BnCBF* overexpression led to a constitutive increase in the phosphorylation status of SR proteins, as stronger bands ranging between 37 and 45kDa were detected in both *BnCBF5* and *BnCBF17* samples grown under control conditions compared to cold stress and acclimated wild type *B.napus* samples. Exposure to cold stress and acclimation conditions have exacerbated the phosphorylation profile of SR proteins in *BnCBF* overexpressors, as the two bands detected in *BnCBF5* and *BnCBF17* samples are heavily phosphorylated when compared to samples from wild type plants grown under the same conditions (Figure 2.3, Panel A). Taken together, both short and long-term exposure to low temperatures led to an increase in SR protein abundance, as detected by 1H4 antibodies, which detect all SR proteins in wild type *Brassica napus*. This increase in SR protein abundance also led to an increase in phosphorylation, as evidenced by mAb104 detection. Moreover, similarly to the transcription profile analyses,

BnCBF overexpression led to an enhancement in SR protein abundance and phosphorylation status under control, cold stress and acclimation conditions.

Although there are 17 known SR proteins and 2 SR-like proteins in *Arabidopsis*, total protein extracts of wild type *Brassica napus* and *BnCBF* overexpressors probed with 1H4 led to the detection of only three bands. To improve SR protein detection, enriched nuclear fractions were isolated from wild type *Brassica napus* and *BnCBF* overexpressors grown under control and cold acclimation conditions, using a modified extraction protocol from Henfrey and Slater, (1988) (refer to Materials and methods, section 1.3.4). Similarly to the total protein extracts presented in Figure 2.3, Panel A, these isolated nuclei fractions were probed with 1H4 and mAb104, and presented in Figure 2.3, Panel C. In contrast with total protein extracts that were previously used, enriched nuclei samples from wild type *B.napus* probed with 1H4 have shown the presence of three bands ranging from 20 to 25 kDa, and three bands with a molecular weight ranging from 37 to 50kDa. Cold acclimation led to an overall increase in abundance of the upper bands observed at 37-50kDa, while the abundance of the three lower bands detected between 20 and 25kDa remained consistent. Concomitantly, *BnCBF* overexpression greatly increased the abundance of SR proteins ranging from 37kDa to 50kDa under control conditions compared to wild type samples grown under similar conditions. A similar trend was observed in cold acclimated *BnCBF* samples, as both cold acclimated *BnCBF5* and *BnCBF17* samples had an increase in abundance of SR proteins ranging from 37kDa to 50kDa compared to cold acclimated wild type samples. While *BnCBF* overexpression greatly enhanced the abundance of SR proteins ranging from 37kDa to 50kDa, it did not appear to have a significant impact on the protein abundance of

SR proteins ranging from 20 to 25kDa, as their abundance remained comparable to wild type *Brassica* samples.

Assessing the phosphorylation status of SR proteins in enriched nuclei samples with mAb104 has revealed the presence of four bands, with one at approximately 25kDa, followed by two faint bands at approximately 37kDa and a heavily phosphorylated band at 50kDa (Figure 2.3, Panel C). The presence of these bands is in contrast with the absence of bands observed in total protein extracts from wild type *Brassica* plants grown under control conditions (Figure 2.3, Panel A). Moreover, cold acclimation led to an increase in the phosphorylation of two bands located at approximately 37kDa. An increase was observed for the phosphorylated band at 25kDa while the band with the strongest signal remained heavily phosphorylated under cold acclimation conditions. In accordance with the phosphorylation profile of total protein extracts (Figure 2.3, Panel A, mAb104), *BnCBF* overexpression led to an overall enhancement of the phosphorylation status of some SR proteins, as the same three bands (ranging from 25 to 37kDa) which were previously identified in wild type *Brassica* were also phosphorylated in *BnCBF* overexpressors under control conditions (Figure 2.3, Panel C, mAb104). Cold acclimation led to an increase in the phosphorylation of three SR proteins, ranging from 25 to 37kDa, with *BnCBF17* overexpressors showing the most pronounced effect. In addition, like wild type *Brassica* samples, *BnCBF* overexpression did not alter the phosphorylation of the band located at 50kDa, as it remained heavily phosphorylated under every condition tested.

To identify which SR proteins had increased in abundance under cold stress and acclimation conditions, total protein extracts, as well as enriched nuclei fractions from wild type *Brassica napus* grown under control conditions and cold acclimated *BnCBF17* were

used for 2D gel analyses in conjunction with mass spectroscopy. As total protein and enriched nuclei fractions had shown similar results, a representative blot was presented in Figure 2.3, Panel B. Although Western blots probed with 1H4 revealed the presence of one spot at approximately 37kDa in wild type *Brassica* grown under non-acclimated conditions, the corresponding spot could not be seen on a corresponding Coomassie-stained gel run in parallel, and therefore could not be used for mass spectroscopy analyses (Figure 2.3, Panel B). Conversely, total protein extracts from cold acclimated wild type *BnCBF17* leaves probed with 1H4 have revealed the presence of six spots, with three spots located at approximately 22kDa, two spots with a molecular weight of approximately 40kDa and one spot detected at approximately 45 kDa. The six SR proteins identified by 1H4 in cold acclimated *BnCBF17* samples were excised from a Coomassie-stained gel that was run in parallel and sent for mass spectroscopy analyses to confirm the identity of these SR proteins that have increased in abundance (data not shown). While the same six spots were observed in samples from cold acclimated wild type *Brassica napus* leaves, as well as in *BnCBF* overexpressors under every condition tested, only spots corresponding to cold acclimated *BnCBF17* overexpressors were excised and sent for mass spectroscopy analyses, as those samples had the greatest protein abundance of all samples tested. Although no SR proteins were identified, total protein extracts, as well as enriched nuclei samples run on 2D gels probed with 1H4 revealed the presence of 6 spots under cold acclimation conditions compared to the three bands that were previously detected in the same total protein extracts run on SDS-PAGE gels probed with 1H4 antibodies.

In summary, exposure to low temperatures, as well as *BnCBF* overexpression led to an increase in abundance of a subset of SR proteins in enriched nuclear fractions, as shown by 1H4 antibodies. These results corroborate trends that were observed in total protein extracts probed with 1H4. Conversely, exposure to low temperatures, but not *BnCBF* overexpression, led to an increase in the phosphorylation profile of SR proteins in the nuclear fraction. These findings are in contradiction with the phosphorylation profile of SR proteins from total protein fractions. As total protein extracts include SR proteins that are located in the cytosol, these results would suggest that the phosphorylation profile of SR proteins located in the cytosol are affected by both exposure to low temperatures and *BnCBF* overexpression, whereas low temperatures, but not *BnCBF* overexpression, increased the phosphorylation status of SR proteins located in the nucleus.

While SDS-PAGE gel analyses on total protein and enriched nuclear protein fractions probed with 1H4 and mAb104 showed an overall increase in SR protein abundance and phosphorylation status under cold acclimation conditions, attempts at identifying potential SR proteins involved in cold acclimation have been unsuccessful so far. As an alternative, enriched nuclear fraction samples from wild type *Brassica napus* collected under non-acclimated conditions, as well as *BnCBF5* and *BnCBF17* grown under control conditions were probed with ASF/SF2, 9G8 and Sc35 antibodies, which recognize plant SR proteins homologous with mammalian ASF/SF2, 9G8 and Sc35, respectively. As shown in Figure 1.5, Panel D, antibodies raised against mammalian ASF/SF2, which recognize ASF/SF2 homologs in plants (Bn-SR30, Bn-SR34, Bn-SR34a and Bn-SR34b) revealed the presence of four bands, ranging between 25 kDa and 50kDa. No changes in protein abundance was

observed in non-acclimated *BnCBF5* overexpressors, while a decrease in abundance of the band at 25kDa was observed in non-acclimated *BnCBF17* overexpressors probed with ASF/SF2. A 50 kDa band was detected by ASF/SF2 antibodies in non-acclimated wild type and *BnCBF* overexpressors. This band does not correspond with predicted SR protein sizes belonging to the ASF/SF2 subclass, which range from 19.6 to 33.7 kDa (Table 1.1). As these antibodies were raised to detect epitopes in mammalian ASF/SF2, it is possible that the detection of this signal could be attributed to non-specific binding.

Samples probed with 9G8, which recognizes plant SR proteins homologous with mammalian 9G8 (Bn-RSZ21, Bn-RSZ22, Bn-RSZ22a) revealed the presence of five bands ranging from 20-50 kDa in wild type *Brassica* under non-acclimated conditions (Fig. 2.3D) control conditions. A decrease in protein abundance of the 37 kDa band was observed in non-acclimated *BnCBF5* and *BnCBF17* samples, the protein abundance of the three lower bands remained comparable to non-acclimated wild type *Brassica napus*. Bands of greater molecular weight than the expected size range of 9G8 were also observed under every condition tested. As observed with nuclei samples probed with ASF/SF2, it is possible that the signal detected could be attributed to non-specific binding.

Samples probed with antibodies raised against Sc35-like proteins that recognize and bind to SC35 showed the presence of three bands, with one band located at approximately 25 kDa, one at 37 kDa and one located at 50 kDa. An increase in protein abundance at 50 kDa was observed in non-acclimated *BnCBF5* samples, while an increase in abundance of the 37 kDa and 50 kDa bands were observed in non-acclimated *BnCBF17* enriched nuclear extracts probed with Sc35. As there is currently only one member of the SC35 subclass (Table 1.1), the detection of two additional bands was not expected. As seen with ASF/SF2

and 9G8 antibodies, the detection of these additional bands could be attributed to non-specific binding.

Taken together, comparing the protein profile of ASF/SF2, 9G8 and Sc35 SR proteins in wild type *Brassica napus* and *BnCBF* overexpressors has shown that *BnCBF* overexpression did not result in major changes in the protein profile of SR proteins belonging to these subclasses in the nucleus. These results are in contradiction with the increase in SR protein signal detected by 1H4 antibodies in *BnCBF* overexpressors under non-acclimated conditions (Figure 2.3, Panel C). As 1H4 antibodies can detect an epitope common to all SR proteins, it is possible that the increase in signal detected by 1H4 and not ASF/SF2, 9G8 and Sc35 antibodies could be attributed to the detection of plant-specific SR proteins.

Moreover, results from Figure 2.3, Panel D are also in contradiction with total protein extracts probed with 1H4 antibodies, where an overall increase in proteins detected by 1H4 antibodies was observed in non-acclimated *BnCBF* overexpressors compared to non-acclimated wild type *Brassica napus*. As total protein extracts include the cytosolic fraction, these results have led to the suggestion that the increase in signal detected by 1H4 in total protein extracts could be attributed to an increase in SR proteins in the cytosol.

These findings prompted further studies to address whether SR protein localization was affected by exposure to low temperatures. Thus, cytosolic and enriched nuclear fractions from wild type *Brassica* leaves grown under non-acclimated and cold acclimation conditions were probed with 1H4, 9G8, ASF/SF2, and Sc35 antibodies, and presented in Figure 2.3, Panel E. Under non-acclimated conditions, three bands were detected by 1H4 antibodies, ranging from approximately 30kDa to 50kDa (Fig. 2.3, Panel E). Exposure to low temperatures led to an increase in abundance of those three bands in the cytosolic fraction.

As seen in Figure 2.3, panel C, an overall increase in SR proteins was detected in enriched nuclei fractions probed with 1H4. Under non-acclimated conditions, stronger bands were detected by 1H4 in the cytosolic fraction compared to the nuclear fraction. This data suggests that cold acclimation leads to an overall increase in SR proteins, including plant-specific SR proteins. These results are corroborated by the overall increase in SR proteins detected in total protein extracts (Fig. 2.3A) and enriched nuclear extracts (Fig. 2.3C). As 1H4 antibodies have been suggested to detect plant specific SR proteins, this data would suggest that plant-specific SR proteins accumulate in the cytosol and the nucleus. This data is corroborated by an overall increase in plant-specific SR gene transcripts under cold acclimation conditions (Figure 2.2; Table 2.2). Taken together, these observations would suggest that plant-specific SR proteins can shuttle from the nucleus to the cytosol under cold acclimation conditions.

Five bands, ranging from 20 to 50 kDa were detected in cytosolic fraction samples probed with ASF/SF2. Cold acclimation conditions led to an increase in abundance of SR proteins belonging to ASF/SF2 subclass in the cytosolic fraction. This correlates with an increase in SR34b transcripts, which belongs to the ASF/SF2 subclass (Figure 2.2; Table 2.2) A different protein profile was observed in nuclei samples probed with ASF/SF2 as two bands were detected at approximately 20-25 kDa and one band located at approximately 50 kDa was detected under control conditions. Cold acclimation conditions have led to a decrease in ASF/SF2 subclass proteins in nuclei samples as the lower bands, located between 20 and 37kDa, could no longer be detected in those samples. Moreover, cold acclimation conditions have led to the appearance of a band that is greater than 50 kDa, which was not detected in both cytosolic fractions. One explanation for the detection of an upper band exclusively in cold acclimated samples could be attributed to non-specific binding, as these

antibodies recognize an epitope found in mammalian ASF/SF2 SR proteins. Moreover, the presence of this large band could be due to protein aggregation within the cold acclimated enriched nuclei sample probed with ASF/SF2. Taken together, these data would suggest that SR34b, could potentially accumulate and localize in the cytosol under cold acclimation conditions by means of nucleocytoplasmic shuttling.

Four bands, ranging between 25-37 kDa were detected in cytosolic fractions probed with 9G8 under control conditions. An increase in abundance was detected in cold acclimated cytosolic fraction samples probed with 9G8 compared to wild type samples. Nuclei fraction samples probed with 9G8 have a similar protein expression profile as cytosolic fraction samples, apart from the presence of two strong bands at approximately 20kDa whose abundance did not change under cold acclimation conditions. Bands detected in cytosolic fraction samples appear to increase under cold acclimation conditions, while an overall decrease in protein abundance was observed in nuclei fraction samples probed with 9G8 under cold acclimation conditions. The increased detection of 9G8 subclass SR proteins in the cytosol under cold acclimation conditions were associated with an increase in RSZ22 and RSZ22a transcripts (Figure 2.2; Table 2.2) under cold acclimation conditions. These results would suggest that RSZ22 and RSZ22a shuttle to the cytosol and accumulate there under cold acclimation conditions.

A strong band was detected at 25 kDa, followed by two upper bands in the 30-35 kDa range in cytosolic samples probed with Sc35 antibodies. Cold acclimation conditions have led to an overall increase with respect to the band located at 35 kDa. Conversely, while nuclei fraction samples also show one band at approximately 25kDa, followed by two bands in the 30-35 kDa range, the band detected at approximately 35 kDa is stronger than the band

detected in the cytosolic fraction. Cold acclimation conditions do not appear to alter the protein profile detected by Sc35 antibodies in enriched nuclei fractions. These results are in contradiction with the observed decrease in SC35 transcripts under cold acclimation conditions. A possible explanation for this discrepancy could be attributed to an increased stability of the SC35 transcript, even if it is downregulated under cold acclimation conditions. It should also be noted that because the bands detected in cytosolic and nuclear fractions were probed with mammalian SC35, it is possible that the signal detected could be attributed to non-specific binding.

In summary, investigating changes in the localization of SR protein subclasses in wild type *Brassica* undergoing cold acclimation has shown that exposure to low temperatures led to differences in the localization of SR protein subclasses, as well as changes in protein abundance between the cytosolic and nuclear fractions. Changes in SR proteins belonging to the ASF/SF2 and 9G8 subclasses were associated with an increase in transcript levels of a subset of SR genes belonging to these subclasses. It should be noted that discrepancies in protein sizes and intensity was observed between non-acclimated nuclear extracts probed with ASF/SF2, 9G8 and Sc35 antibodies presented in Figure 2.3, Panel D and Panel E. While it is unclear as to why these differences have been observed, they could be attributed to non-specific binding of these antibodies designed to detect mammalian SR proteins belonging to ASF/SF2, 9G8 and SC35 subclasses. Moreover, it is possible that differences in sample solubilisation between extractions resulted in the presence of a non-denatured protein in Western blots. One example of such an anomaly can be seen in cytosol and enriched nuclei extracts probed with ASF/SF2 antibodies. A band was detected at 50kDa in both fractions under non-acclimated and after cold acclimation conditions. Interestingly, an unexpected

band at approximately 60 kDa was detected in the cold acclimated enriched nuclear fraction sample.

2.6 Discussion

This study aimed to address whether exposure to low temperatures, as well as overexpressing two CBF/DREB1-like transcription factors would influence the transcription profile, protein abundance and localization of Serine/Arginine-rich proteins and associated kinases in *Brassica napus* undergoing cold acclimation. As shown in Figure 2.3, exposure to low temperatures have resulted in the upregulation of *Bn-RSZ22, Bn-RSZ22a, Bn-SR34b, Bn-SCL30, Bn-SCL30a, Bn-RS2Z32, Bn-RS40* and *Bn-RS41*, as well as SR-like Bn-SR45 in *Brassica napus* grown under cold stress and acclimation conditions. In addition, one SRPK-like kinase (*SRPK-like 1*) and one LAMMER kinase (*Bn-AME3*) were also found to be upregulated in cold stress and cold acclimation conditions. These findings are in partial agreement with reports indicating that exposure to cold stress conditions leads to the differential expression of several SR genes, including *At-SR34b*, *At-RS40*, and *At-SR45* in *Arabidopsis thaliana* (Ali and Reddy, 2008b; Palusa et al., 2007; Reddy and Ali, 2011). The differences between the expression profiles reported in Palusa et al. (2007) and this study could be attributed to several factors. This study looked at the expression profile of SR genes and kinases in four week old, fully developed *Brassica napus* leaves, while Palusa's study looked at the splicing patterns of SR gene transcripts in various tissues, including leaves, of two week old plants grown on MS plates. Therefore, it is possible that differences in the expression profile of *Brassica napus* RSZ22, RS2Z32 and RS40 which, unlike *Arabidopsis*, show very faint expression under non-acclimated conditions relative to cold stress and acclimated samples (Fig. 2.2; Fig A2.2) could be attributed to differences between species.

Under cold stress and acclimation conditions, differences in experimental conditions could contribute to the differences in gene expression profile between *Brassica napus* and *Arabidopsis thaliana* SR genes. For instance, in this study, Bn-SR30 was shown to be downregulated under cold stress and acclimation conditions (Fig. 2.2) while Palusa et al. (2007) showed no change in splicing patterns for At-SR30 after 24h at low temperatures. However, it is important to note that while both studies have looked at the effects of cold stress on SR transcript levels, this study looked at the effect of long term cold stress (2 weeks), as well as the effect of cold acclimation on new leaves that are grown and developed at low temperatures for five weeks. As SR proteins are known to be regulated by stress cues at the transcriptional, post-transcriptional and posttranslational level (Barta et al., 2008; Iida and Go, 2006), it is possible that SR30 is required under short term cold stress, but not under prolonged exposure to cold stress, or cold acclimation conditions.

Only one band was observed for every SR gene and associated kinase tested, except for *Bn-AME3* where two bands were observed. While it is known that SR genes can undergo alternative splicing and produce various transcripts under abiotic stress conditions (Mazzucotelli et al., 2008), the purpose of this study was to assess whether exposure to low temperatures and/or *BnCBF* overexpression would result in changes in the overall transcription profile of SR genes in *Brassica napus*. Thus, to avoid the detection of several alternatively spliced transcripts for every SR gene and associated kinase tested, each primer was designed to amplify the first exon, which remains unchanged in each splicing variant of every SR gene and associated kinase, apart from AME3. The third alternatively spliced form of AME3 (At4g32660.3) has a shorter first exon than the other two splicing variants, resulting in the amplification of a second band not seen in every other SR gene and associated kinases.

Moreover, no amplification was observed in PCR reactions where no reverse transcriptase (non-RT) was performed (data not shown), suggesting that the bands that were amplified were not due to DNA contamination.

In contrast, low temperature exposure led to a reduction in the expression of *Bn-RSZ21, SR30* and *Bn-SC35*. Plant-specific SR genes *Bn-RS2Z33, Bn-SCL33, Bn-RS31*, SR-like *Bn-SR45a*, as well as *Bn-AME1* and *Bn-AME2* LAMMER kinases, *Bn-SRPK1*, *SRPK-like 2* kinase genes have shown a reduction in gene expression. The observed downregulation of this subset of SR genes is in agreement with previous reports observing the downregulation of *At-RSZ21* (Fowler and Thomashow, 2002; Oono et al., 2006), *At-RS31* (Palusa et al., 2007), *At-SR30* and *At-SR45a* (Fowler & Thomashow, 2002; Oono et al., 2006; Tanabe et al., 2007) in *Arabidopsis* under cold stress conditions. Moreover, transcript levels of one SR gene (*Bn-SR34*) and one splicing factor (*Bn-SRL1*) remained unaffected by cold stress and acclimation conditions, suggesting that these genes are not responsive to cold, and that they might not play a role in modulating splicing of transcripts involved in cold stress and acclimation responses. While the differential expression of *SRL1* under cold stress and acclimation has yet to be reported, *Arabidopsis SRL1* was shown to be involved in salt stress tolerance (Forment et al., 2002).

Taken together, assessing the overall gene transcript levels of SR genes and associated kinases has shown that short term exposure to low temperatures (cold stress) leads to major changes in the transcription profile of SR genes, as well as their associated kinases in *Brassica napus* undergoing cold acclimation. This observation is supported by various studies assessing differential splicing and expression of SR genes in response to abiotic stresses, including low temperatures, in *Arabidopsis* (Ali and Reddy, 2008b; Palusa et al.,

2007; Reddy and Ali, 2011), as well as rice (Zhang et al., 2013). Furthermore, these observed changes in SR and kinase gene expression remained in newly developed, cold acclimated *Brassica napus* leaves (Figure 2.2). While these findings are in agreement with transcriptome profiling analyses (Fowler & Thomashow, 2002; Hannah et al., 2005; Oono et al., 2006; Vogel et al., 2005), and one study assessing changes in *Arabidopsis* SR gene splice variants under abiotic stress conditions, including low temperature stress (Palusa et al., 2007; Reddy and Ali, 2011) in *Arabidopsis thaliana* under control, cold stress and acclimation conditions, no studies to date that have assessed the overall transcription profile of SR genes as well as their associated kinases under cold stress and acclimation conditions in *B. napus*.

These extensive changes in both SR genes and associated kinase gene expression have raised the question as to whether *BnCBF5* and *BnCBF17,* two *Brassica CBF/DREB1*-like overexpressor lines which have previously been shown to partially mimic cold acclimation responses (Dahal et al., 2012; Kurepin et al., 2013; Savitch et al., 2005), would result in alterations in the transcription profile of SR genes, as well as their associated kinases. As shown in Figure 2.2, transcription profile analyses from *BnCBF* overexpressor lines have shown that *BnCBF* overexpression led to a reduction in the transcript levels of a subset of SR genes, including *Bn-SR30, Bn-RSZ21, Bn-SC35, Bn-RS2Z33, Bn-SCL33, Bn-RS31, Bn-SR45a*, as well as *Bn-AME1, Bn-AME2* LAMMER kinases and *Bn-SRPK1*, *SRPK-like 2* kinase genes under non-acclimated conditions. Moreover, exposure to low temperatures have led to an even greater reduction in transcript levels of these genes when compared to wild type *Brassica napus* grown under similar conditions.

Conversely, *BnCBF* overexpression led to an increase in the expression of *Bn-RSZ22, Bn-RSZ22a, Bn-SR34b, Bn-SCL30, Bn-SCL30a, Bn-RS2Z32, Bn-RS40, Bn-RS41, Bn-SR45*,

as well as *Bn-AME3* and *SRPK-like 1* under non-acclimated conditions when compared to wild type *Brassica napus* grown under non-acclimated conditions. Although low temperature exposure led to an increase in transcript levels of those SR genes, this response was exacerbated in both *BnCBF* overexpressors in comparison to wild type *Brassica napus* grown under the same conditions. Taken together, these results would suggest that in addition to low temperatures, *BnCBF* overexpression can also lead to constitutive changes in the transcription profile of SR genes. These results are similar to transcriptome profile analyses of *Arabidopsis CBF* overexpressors, which have been shown to constitutively express a wide variety of genes, including SR genes (Fowler and Thomashow, 2002). Moreover, promoter region analyses of SR genes, as well as associated kinases have shown the presence of CRT/DRE, LTRE, RAV1 and ERD1 promoter elements (Appendix Table A2.1) (Hannah et al., 2005; Vogel et al., 2005), lending credence to the suggestion that CBFs, as well as cold-induced transcription factors working in parallel with the CBF regulon also play a role in the regulation of SR genes, which play a key role in post-transcriptional regulation of genes involved in the response associated with cold acclimation.

While *BnCBF* overexpression led to an overall enhancement with respect to changes observed in SR/kinase gene transcripts, the transcription profile of *Bn-RSZ21* and *Bn-RS2Z33* was not enhanced by *BnCBF* overexpression under control, cold stress and acclimation conditions. These differences in SR gene expression observed in *BnCBF* overexpressors in comparison to wild type *Brassica napus* would suggest that both *BnCBF5* and *BnCBF17* overexpressors are able to partially mimic the changes in transcription profile of SR genes and associated kinases occurring in wild type *Brassica napus* plants undergoing cold acclimation. These results are in agreement with previous studies (Dahal et al., 2012; Kurepin

et al., 2013; Savitch et al., 2005) that have shown that *BnCBF* overexpressors are able to partially mimic cold acclimation responses.

RT-PCR analyses assessing the expression profile of SR genes and associated kinases in wild type *Brassica napus*, as well as *BnCBF* overexpressor lines have shown that low temperature exposure and *BnCBF* overexpression result in changes in the expression profile of several SR genes. However, it was still unclear whether these changes in transcript levels correlated with changes in SR protein abundance and/or phosphorylation status. As shown in Figure 2.3, Panels A and C, crude extracts, as well as enriched nuclei samples probed with 1H4 antibodies raised against SR epitopes common to mammalian SR proteins have revealed that exposure to low temperatures led to an overall increase in SR protein abundance in *Brassica napus* undergoing cold acclimation. Moreover, the observed changes in SR protein abundance were correlated with an observed increase in SR protein phosphorylation, as evidenced by wild type *Brassica napus* total protein extracts and enriched nuclei samples grown under control, cold stress and acclimation conditions probed with mAb104 antibodies raised against phosphoepitopes common to Serine/Arginine-rich proteins (Roth et al., 1990).

In addition, *BnCBF* overexpression has resulted in a constitutive increase in Serine/Arginine-rich protein abundance under control conditions, compared to wild type *Brassica napus* grown under similar conditions in total protein extracts, as well as in enriched nuclei fractions probed with 1H4 antibodies, as both *BnCBF* overexpressor lines grown under control conditions exhibit SR protein abundances comparable to cold acclimated wild type *Brassica napus* (Fig. 2.3, Panels A, C). Cold stress and cold acclimation conditions have led to increases in abundance under cold acclimation conditions. Interestingly, *BnCBF*

overexpression was correlated with a constitutive increase in abundance in the phosphorylation status of SR proteins in total protein extracts, but not in enriched nuclei samples, as shown by mAb104 Western blots.

Taken together, these results suggest that similarly to the transcription profile of SR genes, exposure to low temperatures, as well as *BnCBF* overexpression influence SR protein abundance and phosphorylation status. As recent studies have shown that *Arabidopsis* AME3 is capable of autophosphorylation (Nemoto et al., 2011), and is able to phosphorylate At-RSZ22 and At-SCL30, (Ahsan et al., 2013; *Arabidopsis* Interactome Mapping Consortium, 2011) the strong increase in Bn-*AME3* expression (Fig. 2.2) in response to cold stress/acclimation and *BnCBF* overexpression, which coincides with the strong increase in phosphorylation observed under the same conditions (Fig. 2.3) would suggest that Bn-AME3 plays a role in the mediation of phosphorylation of SR proteins in *Brassica napus* plants undergoing cold acclimation.

Attempts at identifying individual SR proteins that have increased in abundance in response to cold stress/acclimation and *BnCBF* overexpression have been unsuccessful. As an alternative, enriched nuclei samples were from wild type *Brassica napus* and *BnCBF* overexpressors were probed with antibodies raised against mammalian 9G8, ASF/SF2 and Sc35 to assess whether exposure to low temperatures and/or *BnCBF* overexpression would result in changes in plant 9G8, ASF/SF2 and Sc35-like SR protein subclasses. *BnCBF* overexpression under non-acclimated conditions resulted in the decrease in abundance of a subset of SR proteins belonging to the ASF/SF2 and 9G8 subfamilies (Figure 2.3, Panel D). These findings are in contradiction with the observed increase in protein abundance in enriched nuclear samples probed with 1H4 (Figure 2.3, Panel C). One possible explanation

would be that the overall increase in protein abundance observed in both wild type *Brassica napus* and *BnCBF* overexpressors are plant specific proteins, as this subclass of Serine/Arginine-rich proteins would be detected only by 1H4. In addition, increases in abundance were observed for proteins ranging from 37 to 45 kDa in size (Figure 2.3, Panel C). Based on known SR protein sizes (Table 1.1), the lower band could correspond to either RS40 or RS41, whereas the upper band, of approximately 45 kDa in size, could potentially correspond with SR45. This observed increase in SR protein abundance also correlates with the increase in RS40, RS41 and SR45 transcripts under cold stress and acclimation conditions (Figure 2.2, Panel A).

These results prompted further studies to address whether low temperatures would influence SR protein localization. There is limited knowledge pertaining to plant SR protein dynamics. So far, a study has shown that *Arabidopsis* RSZ22 can undergo nucleocytoplasmic shuttling (Rausin et al., 2010). While other studies have shown that the localization of Serine/Arginine-rich proteins has been shown to be altered based on physiological stresses, such as heat stress in *Arabidopsis* (Ali and Reddy, 2006, 2008a; Tillemans et al., 2006), there currently is no evidence that cold acclimation conditions influence the localization of Serine/Arginine-rich proteins in *Brassica napus*.

To address whether SR protein localization is altered in response to cold, cytosolic and enriched nuclear fractions from both control and cold acclimated *Brassica napus* were probed with 1H4, Sc35, 9G8 and ASF/SF2 antibodies (Figure 2.3, Panel E). Comparisons between cytosolic and nuclear fractions from samples probed with 1H4 show no discernable differences, as an increase in protein abundance was observed under cold acclimation conditions in both fractions. As 1H4 antibodies, can detect epitopes common to all SR

proteins, these results would suggest that SR proteins, including plant specific SR proteins are in the cytosol, as well as in the nucleus. Cold acclimation conditions result in an increased abundance of these proteins. These results were supported by an overall increase in transcription of plant-specific SR proteins under cold acclimation conditions (Fig. 2.2; Table 2.2). An increase in protein abundance was observed in cold acclimated cytosolic fraction extracts probed with ASF/SF2. Conversely, cold acclimation conditions have led to an overall decrease in ASF/SF2-like SR proteins in enriched nuclei samples probed with ASF/SF2 antibodies. These observations were associated with a increase in Bn-SR34b transcript levels under cold acclimation conditions. This led to the suggestion that Bn-SR34b might be involved in shuttling between the nucleus and cytosol. Both cytosolic and enriched nuclei extracts probed with 9G8 antibodies have shown an overall accumulation of SR proteins belonging to this subclass under cold acclimation conditions. This was associated with an increase in Bn-RSZ22 and Bn-RSZ22a transcript levels under cold acclimation conditions. These results suggested that under cold acclimation conditions, members of the SR, RSZ and SC subclasses, probed by ASF/SF2 and 9G8 antibodies, respectively, localize and accumulate in the cytosol. Moreover, differences in the protein profile of cytosolic and enriched nuclei fractions probed with ASF/SF2 and 9G8 suggest that plant SR proteins belonging to these subclasses can shuttle between the cytosol and nucleus. These results are in agreement with studies which have shown that *Arabidopsis* RSZ22 (Rausin et al., 2010), metazoan 9G8 (Swartz et al., 2007), and ASF/SF2 (Sanford et al., 2004) are able to shuttle between the cytosol and nucleus, thus suggesting their involvement in processes other than the modulation of constitutive and alternative splicing, such as mRNA export, mRNA stability and translation (Howard & Sanford, 2014; Twyffels et al., 2011). Interestingly, cold acclimation conditions led to an overall increase in Sc35-like SR proteins in the cytosol, and

no change in abundance in enriched nuclear fractions. These results suggest that plant SR proteins belonging to the Sc35 subclass can accumulate in the cytosol, in addition to the nucleus. Conversely, Sc35 transcript levels were observed to decrease under cold acclimation conditions (Fig. 2.2; Table 2.2). This discrepancy between Sc35 transcript levels and protein abundance might be due to an increase in transcript stability for Sc35 under cold acclimation conditions as post-transcriptional modifications such as RNA stability have been reported to play critical roles in response to cold acclimation (Chinnusamy et al., 2007; Mazzucotelli et al., 2008). These results suggest that plant Sc35 can shuttle from the nucleus to the cytosol, unlike mammalian Sc35, which contains a nuclear retention signal in its RS domain (Cazalla et al., 2002).

2.7 Conclusion

In summary, results of this study have shown that exposure to low temperatures results in major changes in the transcription profile of Serine/Arginine-rich genes, as well as associated kinases in *Brassica napus* undergoing cold acclimation. These changes in transcription profile are correlated with alterations in SR protein abundance, phosphorylation status and localization. Furthermore, *BnCBF* overexpression was shown to exacerbate changes in transcription profile of SR genes and associated kinases, as well as changes in protein abundance and phosphorylation status previously observed in wild type *Brassica napus*. While this study has shown that both low temperatures and *CBF* overexpression have an effect on the transcription profile, protein abundance and localization of SR proteins in *Brassica napus* undergoing cold acclimation, SR protein function in the process of cold acclimation has yet to be addressed. Future directions could involve generating knockout lines of those SR genes of interest kinases, and assessing their ability to undergo key

physiological changes related to cold acclimation, such as increased photosynthetic performance and the acquisition of freezing tolerance (Discussed in Chapter 3).

Chapter 3: Roles of Serine/Arginine-rich proteins and At-AME3 LAMMER kinase on the cold acclimation-induced adjustment of photosynthetic performance, acquisition of freezing tolerance and the CBF transcriptional cascade.

Marc Rosembert, David P. Sprott

Marc Rosembert's contributions to the third chapter include the transfer of heterozygous T-DNA insertion mutant lines to homozygous mutant lines, as shown in Table 2.3. All RNA, genomic DNA extractions and RT-PCR analyses used in the identification of homozygous mutant lines (Figure 3.3) were performed by Marc. The evaluation of excitation pressure of Photosystem II (1-qL), linear electron transport rates (ETR), yield of Photosystem II (Φ_{PSII}), antenna (Φ_{NPQ}) and reaction centre ($\Phi_{f,D}$) based portion of non-photochemical quenching of leaves from wild type *Arabidopsis* grown and developed under non-acclimated conditions as well as after three weeks and five weeks of growth under low temperature conditions (Table 3.4) was done by Marc. The evaluation of homozygous mutant lines grown under control conditions and after five weeks of cold acclimation with respect to their photochemical efficiency (F_v/F_m), excitation pressure of Photosystem II (1-qL), linear electron transport rates (ETR), yield of Photosystem II (Φ_{PSII}), antenna (Φ_{NPQ}) and reaction centre ($\Phi_{f,D}$) based portion of non-photochemical quenching presented in Figures 3.4 and A3.1 were also performed by Marc.

The capacity of *at-ame3* (Figure 3.5) as well as SR loss-of-function mutants (Fig. A2.2) to acquire freezing tolerance by means of electrolyte leakage assays done on wild type and *ame3* mutants grown under non-acclimated conditions and after cold acclimation conditions (Fig. 3.5) as well as five weeks cold acclimated wild type *Arabidopsis* and SR mutant lines (Fig. A3.2) was evaluated by Marc Rosembert. qPCR analyses presented in Figures 3.6 and A2.3 were done by David P. Sprott (AAFC), using primers designed by M. Rosembert and D.P. Sprott. Total protein extracts from leaf tissue from wild type and *ame3* mutants grown under non-acclimated conditions and after cold acclimation conditions, which were used in the determination of COR15 and dehydrins accumulation were prepared by Marc Rosembert, and presented in Fig. 3.7. Marc has also evaluated morphological differences between wild type and *ame3* mutants grown under optimal growth conditions (Figs. 3.7-3.8), and done all statistical analyses presented in each figure presented in this chapter.

This chapter was also prepared to be converted into two manuscripts, in preparation for submission by Marc Rosembert, Loreta Gudynaite-Savitch, David P. Sprott, Jas Singh, Douglas A. Johnson and Leonid V. Savitch titled **"The effect of Splicing-Related Proteins**

in the cold acclimation induced recovery of photosynthetic performance of *Arabidopsis thaliana".* I have written the original draft.

The second manuscript, in preparation for submission by Marc Rosembert, David P. Sprott, Jas Singh, Douglas A. Johnson and Leonid V. Savitch titled **"The effect of a splicing related protein kinase in the acquisition of freezing tolerance of *Arabidopsis thaliana*"**. I have written the first draft. Subsection 3.3, stating the hypotheses and research objectives for this study is included for the thesis.

3.1 Abstract

Cold acclimation induces a wide variety of changes at the physiological, morphological and cellular level in cold hardy plants, leading to alterations in photosynthetic performance, membrane stability and the accumulation of cryoprotective/antifreeze proteins. These diverse changes can be attributed to an extensive reprogramming at the transcriptional level. In addition to modifications at the transcriptional level, post transcriptional regulation is thought to play an extensive role in the cold acclimation response. This study aimed to address the potential role of a subset of *Arabidopsis* Serine Arginine-rich (SR) proteins and one known splicing-related LAMMER kinase (AME3) in the cold acclimation induced recovery of photosynthetic performance by means of chlorophyll a fluorescence assays. These assays have led to the suggestion that three SR proteins (At-RSZ22A, At-SCL30, At-RS40), in addition to AME3 LAMMER kinase, play an essential role in the cold acclimation induced recovery of photosynthetic performance. Interestingly, two SR proteins (At-RSZ22 and At-SR45) have been suggested to play an essential role in the overall photosynthetic performance of *Arabidopsis thaliana* as loss-of-function mutants of these SR genes were impaired with respect to their photosynthetic performance under optimal growth conditions, as well as after five weeks of cold acclimation. Conversely, At-SR34, At-SR34B and At-

RS41 do not appear to play essential roles in the overall photosynthetic performance of *Arabidopsis thaliana*. At-AME3 loss-of-function mutants were also jeopardized with respect to the acquisition of freezing tolerance, based on electrolyte leakage assays. This was associated with a decrease in the transcript levels of SPS, CBF and COR genes involved in the CBF transcriptional pathway, and a decrease in protein abundance of BN115 and dehydrins. Taken together, these findings have shown the involvement of a subset of SR proteins, in addition to a LAMMER kinase in the cold acclimation induced recovery of photosynthetic performance, in addition to the overall photosynthetic performance of *Arabidopsis thaliana,* while At-AME3 plays an important role in the acquisition of freezing tolerance.

3.2 Introduction

Every plant possesses its optimal range of growth temperature, allowing maximal growth and development rates. At the level of photosynthesis, optimal growth conditions allow the slower (milliseconds to seconds intervals), temperature sensitive enzymatic reactions responsible for the reduction of CO_2 to triose phosphate, as well as nitrate and sulphur assimilation to keep up with the extremely rapid (picoseconds to millisecond intervals) temperature-independent photochemical and photophysical processes where Photosystems I and II trap light energy (Ensminger et al., 2006). Therefore, both the proportion of light used for photochemical reactions and linear electron flow are optimal, whereas a minimal proportion of absorbed light energy is dissipated as heat through the antennae and reaction centre. Furthermore, as there is equilibrium with respect to energy flow between the photochemical and biochemical reactions of photosynthesis, the excitation pressure of photosystem II is minimal (Ensminger et al., 2006; Ivanov et al., 2012).

A shift from warm growth conditions to chilling temperatures (5°C) leads to the inactivation of ribulose-1,5-bisphosphate carboxylase (Rubisco), stromal fructose-1,6-bisphosphatase (sFBPase) and sedoheptulose-1,7-biphosphatase both in chilling sensitive and chilling tolerant plant species (Strand et al., 1999). This in turn leads to a pronounced reduction in rates of the enzymatic reactions used in the reduction of CO_2 into triose phosphate. Consequently, an imbalance is created, as the rate at which the energy absorbed through photosystem II and injected into linear electron transport exceeds the rates of temperature-dependent biochemical reactions, in turn resulting in an increase in the excitation of photosystem II (Dahal et al., 2014). Moreover, an increase in the excitation pressure of PSII results in an increase in heat dissipation rates, which can be measured as heat dissipated through the antennae, or through the reaction centre. Conversely, a decrease in PSII activity is observed, as linear electron rates and photosystem II photochemistry rates decrease under cold stress conditions (Hüner et al., 1993). If the absorbed energy exceeds both the capacity for non-photochemical quenching and the capacity for photochemistry, photooxidative damage to Photosystem II (Aro et al., 1993; Ivanov et al., 2012; Long, 1994), as well as Photosystem I (Ivanov et al., 2012; Sonoike et al., 1997) can occur.

In addition to impediments with respect to photosynthetic performance, exposure to low temperatures results in a reduction of membrane fluidity (Miura and Furumoto, 2013; Orvar et al., 2000). Reductions in temperature result in the formation of extracellular ice crystals. As these ice crystals form outside of the cell, the water potential outside of the cell diminishes, resulting in transient losses in intracellular solutes, or plasma membrane leakiness (Steponkus, 1984). This in turn can result in mechanical stress to the membrane, and subsequent damage (Steponkus, 1984; Thomashow, 1999). Prolonged exposure to low

temperatures can result in a reduction in leaf expansion, leaf chlorosis, wilting and may lead to death of tissues, or necrosis in chilling sensitive plants, such as *Lycopersicon esculentum* and *Oryza sativa* (Mahajan and Tuteja, 2005).

Conversely, cold hardy species are able to sense this stress response and adapt, thus allowing them to extend their temperature range for survival during acute temperature stress (Guy et al., 2008). This adaptive response, termed cold acclimation, is the result of an extensive reprogramming at the transcriptional level, resulting in alterations in a wide array of molecular, biochemical and physiological processes, including a recovery of photosynthesis and pigment synthesis to protect from photoxidative stress (Christie et al., 1994; Król et al., 1999; Schöner and Heinrich Krause, 1990), alterations in lipid membrane composition to improve membrane stability (Nishida and Murata, 1996), increases in osmolytes playing a role in the reduction of cellular dehydration (Guy et al., 2008), increases in sucrose and other compatible solutes which play a cryoprotective role in the cell (Guy et al., 1992; Mahajan and Tuteja, 2005) and antifreeze proteins (Thomashow, 1999), resulting in the acquisition of freezing tolerance. At the plant and leaf level, a compact dwarf phenotype, with thicker leaves compared to non-acclimated leaves (Boese and Hüner, 1990; Dahal et al., 2012b; Gorsuch et al., 2010; Hüner et al., 1981; Strand et al., 1999) has been reported. It should be noted that cold acclimation requires long term growth and development at low temperatures, compared to cold stress, which can be induced in non-acclimated plants exposed to low temperatures (Dahal et al., 2012b).

While the extent of signaling pathways resulting in the acquisition of freezing tolerance are not fully understood, several key components of the signal transduction pathways have been identified. One well known signal transduction pathway controlling the expression of

cold inducible genes involves C-repeat Binding Factors (CBFs) 1, 2 and 3 (Gilmour et al., 1998; Liu et al., 1998). Under non-acclimating conditions, HOS1 negatively regulates Inducer of CBF Expression 1 and 2 (ICE1/ICE2). However, exposure to low temperatures activates a protein kinase which phosphorylates ICE1 and ICE2, leading to the rapid induction of CBF transcription factors. First, CBFs 1 and 3 are induced, followed by CBF2 (Medina et al., 2011; Novillo et al., 2007). In turn, CBFs recognize and bind to CRT/DRE promoter elements found in a variety of cold responsive genes, including COR, LTI and KIN, leading to an accumulation of cold-induced stress proteins, encoded by COR genes (Guy, 1990; Thomashow et al., 1998, 1999).

While it is well understood that CBFs, which are found only in plants, play a critical role in the transcriptional regulation of cold stress responses, there is a strong connection between RNA metabolism and cold stress responses (Refer to Chapter 1, Section 1.3). Serine/Arginine-rich (SR) proteins are prominently known for their role in constitutive and alternative pre-mRNA splicing through their contribution in spliceosomal assembly (Roscigno and Garcia-Blanco, 1995; Wu and Maniatis, 1993). Studies using mammalian systems have defined roles for SR proteins in mRNA transport and localization (Huang et al., 2003), mRNA stability (Lemaire et al., 2002) and translation regulation (Sanford et al., 2005). Furthermore, post-translational regulation of SR proteins via phosphorylation has been shown to play a critical role in the regulation of their activity (Misteli et al., 1998; Xiao and Manley, 1997), as well as their localization (Cho et al., 2011). Although *Brassica* SR proteins (*Bn-RSZ22, Bn-RSZ22a, Bn-SR34b, Bn-SCL30, Bn-SCL30a, Bn-RS2Z32, Bn-RS40, Bn-RS41*), one SR-like (*Bn-SR45*) and LAMMER kinases (*Bn-AME3* and *Bn-SRPK-like 1*) have been suggested to play a role in RNA metabolism in *Brassica napus* and *BnCBF*

overexpressor lines undergoing cold acclimation (Refer to Chapter 2), their role in this complex stress response has yet to be defined.

3.3 Hypotheses and objectives

It was hypothesized that RSZ22, RSZ22a, SR34b, SCL30, SCL30a, RS2Z32, RS40, RS41, SR45, AME3 LAMMER kinase and SRPK-like 1 play a role either in 1) the cold acclimation induced enhancement of photosynthetic performance, 2) the acquisition of freezing tolerance and/or 3) the transcription, splicing and/or post-splicing activities of cold responsive genes, including *SPS*, *CBF* and *COR* genes which are involved in the cold acclimation-induced transcriptional cascade.

The objectives of this study were to 1) generate homozygous *at-rsz22, at-rsz22a, at-sr34b, at-scl30, at-scl30a, at-rs2z32, at-rs40, at-rs41*, *at-sr45, at-ame3* and *at-srpk-like 1 Arabidopsis* loss-of-function mutant lines, 2) assess the effect of these mutations in the cold acclimation induced enhancement of photosynthetic performance by monitoring changes in chlorophyll a fluorescence, 3) assess the effect of these mutations in the acquisition of freezing tolerance by monitoring electrolyte leakage and 4) assess the transcription profile of key cold responsive genes involved in the cold acclimation induced transcriptional response by means of qPCR analyses. It should be noted that *Arabidopsis* loss-of-function mutants were used in this study due to the lack of *Brassica* SR mutants. *Arabidopsis* is a suitable model for this study due to the high sequence homology between SR, LAMMER, SRPK and SRPK-like genes in *Arabidopsis thaliana* and *Brassica napus.*

3.4 Materials and methods

3.4.1 Arabidopsis thaliana growth conditions

Seeds of wild type (ecotype Columbia) and transgenic *Arabidopsis thaliana* heterozygous SALK T-DNA insertion lines disrupting either *At-RSZ22* (At4g31580; CS815114), *At-RSZ22a* (At2g24590; SALK_120499) *At-RS41* (At5g52040; CS803022, SALK_035417), *At-SR34b* (At4g02430; SALK_072651), *At-RS40* (At4g25500; CS853681, SALK_118875), *At-SCL30* (At3g55460; CS805508), *At-SCL30a* (At3g13570; SALK_041849) *At-SR34* (At1g02840; SALK_102166), *At-RS2Z33* (At2g37340; SALK_051525), *At-RS31* (At3g61860; SALK_029586), *At-SCL33* (At1g55310; SALK_058566), *At-SR45* (At1g16610; SALK_121702, SALK_002537) *At-SR45a* (At1g07350; SALK_054457, SALK_012034) Serine/Arginine-rich proteins, *At-AME3* (At4g32660; CS835176), a LAMMER-type protein kinase, or *SRPK-like 1* (At2g17530; SALK_006436, SALK_006427) protein kinase were purchased from the ABRC (arabidopsis.org). Seeds were germinated in soil flats and seedlings were grown for four weeks in a Conviron E-15 cabinet under controlled environmental conditions with a temperature regime of 20°C/16°C (day/night), a 16-h photoperiod and a photon flux density (PFD) of 250 µmol $m^{-2}s^{-1}$ for control (non-acclimating) conditions. Non-acclimated four-week-old plants were then transferred to a temperature regime of 4°C/4°C (day/night) with light conditions identical to the control grown plants. During growth at low temperatures the leaves previously developed at 20°C were considered cold-stressed while the new leaves developed at 5°C were considered cold acclimated. The effect of cold acclimation on 20°C on newly developed leaves was monitored after three weeks and after five weeks of plant growth at 4°C. Leaf tissue from wild type *Arabidopsis,* as well as the aforementioned mutants

was collected after three weeks and five weeks of growth and development at low temperatures. All leaf tissue was collected at 10:00 AM, frozen in liquid nitrogen, and stored at -80°C for the identification of potential homozygous lines by means of RT-PCR analyses.

Leaf tissue from wild type *Arabidopsis thaliana* and the aforementioned transgenic lines grown under control conditions and after five weeks cold acclimation were used in the identification of potential homozygous SR transgenics. Initial chlorophyll a fluorescence analyses were performed using leaves from wild type *Arabidopsis thaliana* grown under control conditions, three weeks and five weeks cold acclimation. For subsequent chlorophyll a fluorescence measurements, electrolyte leakage assays and qPCR analyses, non-acclimated and five weeks cold acclimated leaf tissue from wild type (ecotype Columbia) and homozygous transgenic *Arabidopsis thaliana* lines lacking either *at-sr34* (SALK_102166), *at-sr34b* (SALK_072651), *at-rsz22* (CS815114), *at-rsz22a* (SALK_120499), *at-scl30* (CS805508), *at-rs40* (CS853681, SALK_118875), *at-rs41* (CS803022, SALK_035417), *at-sr45* (SALK_121702, SALK_002537) and *at-ame3* (CS835176) LAMMER kinase were used.

Furthermore, detailed electrolyte leakage freeze tests were achieved using leaf tissue from non-acclimated and five weeks cold acclimated wild type *Arabidopsis* compared to leaf tissue from *at-ame3* knockouts grown under the same conditions. To progressively monitor *cor* gene transcript levels by means of qPCR in *at-ame3* knockouts compared to wild type *Arabidopsis*, leaf tissue was collected under non-acclimated conditions. Newly developed leaves grown under low temperatures were also collected after three weeks exposure (3w CA) and five weeks (5w CA) exposure.

3.4.2 RNA and genomic DNA extractions

Total RNA was extracted for RT-PCR and qPCR analyses using the FastRNA® Pro Green Kit (Qbiogene, Inc., CA), according to the manufacturer's instructions. Leaf tissue was homogenized using the FastPrep® Instrument (Qbiogene, Inc, CA), at a speed setting of 6.5 for 45 seconds. RNA yield, purity and quantity were measured using the Pharmacia Biotech GeneQuant RNA/DNA Calculator (Cambridge, England). DNAse treatments were carried out using the Invitrogen Ambion DNAse I (Burlington, ON, Canada) according to the manufacturer's instructions. Subsequently, RNA samples were loaded on a 1% formaldehyde gel to assess sample quality, and visualized using a BioRad gel doc and Image Lab imaging software. Genomic DNA extractions were achieved using CTAB (Hexadecyl trimethyl-ammonium bromide), as described by Richards et al. (1994). Sample quantity and yield were assessed using the Pharmacia Biotech GeneQuant RNA/DNA Calculator (Cambridge, England).

3.4.3 RT-PCR, qPCR and genotyping analyses

All reverse transcription (RT) reactions were carried out as described in Chapter 2. PCR optimization steps ($MgCl_2$ gradient and annealing temperature gradient), using cDNA from non-acclimated wild type *Arabidopsis thaliana* as a template and the primer pairs indicated in Table 3.1 were also carried out as described in Chapter 2. To avoid the amplification of multiple splicing variants, each SR primer was designed to amplify the first exon, which does not change between splicing variants, apart from the third splicing variant of At-AME3 (At4g32660.3), which contains a shorter first exon. To ensure that amplification that was observed is not due to DNA contamination, PCR reactions with no RT templates

(non-RT) were also performed (data not shown). All PCR reactions were run on Eppendorf epigradient S or Mastercycler pro S thermocyclers, using the following parameters: an initial denaturation step at 90°C for two minutes, followed by 30 cycles at 90°C for 30 sec, 58°C annealing step for 30 seconds, and two minute extensions at 72°C. The amplified products were then run on 1% TAE-Agarose gels and visualized under UV light using an Alpha Innotech light cabinet and AlphaImager visualization software. All qPCR reactions were carried out using Applied Biosystems SYBR® Green PCR Master Mix (2x), in accordance with the manufacturer's instructions. Forward and reverse primers used in all qPCR reactions are highlighted in Table 3.2. No-RT negative controls were also performed (data not shown). Amplification was performed using a StepOne Plus Real-Time PCR System (Applied Biosciences). The amplification cycles were carried out as follows: the initial denaturing step was done at 95°C for 10 minutes, followed by 40 cycles at 95°C for 15 seconds for denaturation, 60°C for 45 seconds for annealing, and extensions were done at 72°C for 1 minute. The data was then analyzed using StepOne software version 2.2.

Table 3.1: RT-PCR primers used in the identification of potential SR or LAMMER kinase homozygous knockouts.

Gene of interest	TAIR accession number	Forward primer sequence	Reverse primer sequence
At-RSZ22	AT4G31580	TGTGTACGTGGGAAACTTG	ACGAGCAGGAGGAGGTGAA
At-RSZ22a	AT2G24590	GCGAGTTACTGAGCGTGAGC	GGGCTCTTTCTGTATCTAGGAGG
At-SCL30	AT3G55460	TCGATTGCAGACCAGAAGAGC	TCATAGCCAGGGGAATAGGAC
At-SCL30a	AT3G13570	TATGGTGGGGGTGGGGGTCGTG	TGGCTTCTTCCTGTTCTCTTCTGC
At-RS31	AT3G61860	ATGAGGCCGGTGTTCGTC	GCAGCGTATCTATCATCTCTTTCA
At-RS2Z33	AT2G37340	TGACGCGAGACATTACTTGG	GTCTTGAGGGCTGCTACCACCATC
At-SCL33	AT1G55310	CTAGAGGAGGAGGCCGTTATGGTG	GGCTTATGCTGCGGCTCTTACTTC
At-SR34	AT1G02840	GGATCCTCGGGATGCTGATGATG	CTGCGGCTAAGACTGCGGCTGTGG
At-SR34b	AT4G02430	CACCTCGTCCTCCATGTTATTGCTTTGTTG	AGCCTCTAGCCCATGGGTTTTTGAA
At-RS40	AT4G25500	GAGGCCTTGACCGCATTGAA	ACGCCTCGATCTCTTGTAA
At-RS41	AT5G52040	GGGTTGATATGAAAGCTGGGTT	TATCACGGCGTCTATCGGGACT
At-SR45	AT1G16610	AGTCGGTCCAGGTCTCTTTCTTC	AACAGGCTTAGGAGGTGGAGGTAG
At-SR45a	AT1G07350	AAAAGCGTCGTGGAAGGTCTGTGT	ATCTGTCCCGTGCTCTGTAATCA
At-AME3	AT4G32660	GGAAGCGATGGGAGGGTTTTGT	TCGGGCTTGAGGTCGGTGTG
At-SRPK-like 1	AT2G17530	GGTGGCCGTTACATTGCTCAG	TTGCGTTTCCTTCAGGCTTTTCTA
At-Elf1	AT1G18070	AGCCCCTTCGTCTTCCACTTCAG	TGGGCTCCTTCTCAATCTCCTTAC

Table 3.2: Primer list of genes involved in the cold acclimation transcriptional pathway used in expression analyses of SR and *at-ame3* LAMMER kinase knockouts.

Gene of interest	TAIR accession number	Forward primer sequence (5`-3`)	Reverse primer sequence (5`-3`)
ice1	AT3G26744	GGA GAA ATA GTG ACG GTG AGA GAG	GAA GTT ATG TAT CCA ACA ACA ACA ACC TC
hos1	AT2G39810	CCG CGA GAT CGA TAT CTC TTC CTA	TCA TCT TGC TGC GAA TCT ACG TCT CC
cbf1	AT4G25490	CGT ACT ACT TAA ACC TTA TCC AGT TTC	AAT AAT CTC CGC CTT GAG CGT CGT
cbf3	AT4G25480	GCT CCG ATT ACG AGT CTT CGG TTT	AAA CTT ACG ACC CGC CGC TTT
Sps	AT1G04920	CAG GCT TTA CGT TGC CAT GTC GTT	CTC TTG TGA AGC CCA CCA AGC AAT
cor15a	AT2G42540	TTC TCA GGA GCT GTT CTC ACT GGT	TTT GTG GCA TCC TTA GCC TCT CCT
cor15b	AT2G42530	ACG TAG GAG CAA AGC AGA GTG GTG	TGT GGC ATT CTT AGC CTC TTC TGC
kin1	AT5G15960	CAA TGT TCT GCT GGA CAA GGC CAA	TTC ACG AAG TTA ACA CCT CCC GCT
lti78	AT5G52310	AAG TGA TCG ATG CAC CAG GCG TAA	ACG ACA GGA AAC ACC TTT GTC CCT

For the identification of homozygous lines, eight leaves were harvested at random from *At-RSZ22*, *At-RSZ22a, At-RS41*, *At-SR34b* , *At-RS40*, *At-SCL30*, *At-SCL30a*, *At-SR34*, *At-RS2Z33*, *At-RS31*, *At-SCL33*, *At-SR45* and *At-SR45a* Serine/Arginine-rich mutants, *At-AME3*, a LAMMER protein kinase mutant, or *SRPK-like 1* kinase mutant lines grown under non-acclimated conditions, as well as leaves grown and developed at low temperatures for five weeks. Homozygous mutant lines identified by the absence of bands corresponding to the gene of interest under control conditions, and after five weeks of cold acclimation were harvested for seeds and propagated for another screen. This process was repeated until the band(s) corresponding to genes of interest were absent in leaf tissue from 10 plants. Seeds were then harvested from the corresponding plants, to be used for subsequent experiments. Furthermore, 18 leaves per batch of previously identified homozygous *at-ame3* mutants, as well as wild type *Arabidopsis*, grown under control conditions were collected at random, and used for genotyping experiments. The genotyping experiment was repeated once, on a different batch of plants. Thus, genotyping experiments are representative of 36 different *at-ame3* plants. Two paired PCR reactions were setup for genotyping experiments. Primer pairs LP (5`-TATGCAGAAGGCTTCATCGAC-3`) and RP (5'-TGGTGAAAACAGAGGAATTGC-3'), were used to amplify the genomic region flanking the T-DNA insert in At-AME3 kinase knockouts. The second primer pair, consisting of LB3 (5`-TAGCATCTGAATTTCATAACCAATCTCGATACAC-3`) and RP, were used to amplify a region within the insertion site. All PCR reactions were run on Eppendorf epigradient S or Mastercycler pro S thermocyclers, using the same parameters as described above. The amplified products were then run on 1% TAE-Agarose gels and visualized under UV light using a ChemiDoc XR+ light cabinet (BioRad) and ImageLab visualization

software (Figure 3.3B). All three primers used in genotyping experiments were designed using the T-DNA Primer Design tool (http://signal.salk.edu/tdnaprimers.2.html).

3.4.4 SDS-PAGE analyses

Total protein extractions, sample solubilisation, SDS-PAGE electrophoresis and transfer were performed as described in Chapter 2. To ensure equal protein loading, and sample integrity, an aliquot of each sample was added to 6X loading buffer (50 mM Tris-HCl, 0.002% Bromophenol Blue, 2.5% Glycerol, 2% SDS, and 143 mM 2-Mercaptoethanol), and loaded on discontinuous polyacrylamide gel systems consisting of 4% (w/v) stacking and 12.5% (w/v) separating gels. Electrophoresis was performed using a Mini-Protean II apparatus (Bio-Rad) at a constant voltage of 100 V for approximately 2.5 h, until the dye front had run off the gel. The gel was incubated overnight in a Coomassie Blue staining solution (0.1% (w/v) Coomassie G-250 (Bio-Rad), 10% (v/v) Acetic acid, 50% (v/v) Methanol), then destained for three hours in a destaining solution (40% (v/v) Methanol, 10% (v/v) acetic acid), with gentle agitation, until the background staining is removed. Visual inspection of the large subunit of Rubisco (RBCSL) was used as a reference protein to ascertain equal loading. Stained gels are unavailable. The membranes were probed with antibodies raised against the K segment, located in the C-terminus of dehydrin proteins (Agrisera, Sweden), at a dilution of 1:5000, or with antibodies raised against *Brassica napus* BN115, which is homologous to *Arabidopsis thaliana* COR15A and COR15B, at a dilution of 1:1000. All membranes were incubated for an hour at room temperature, followed by two 15 minute washes in a 1X TBST. Immunodetection was achieved by incubating membranes in 2% blocking buffer with goat anti-rabbit IgG secondary antibodies (Sigma Chemical Co., St. Louis, MO, USA), conjugated with horseradish peroxidase, at a dilution of 1:3 000 000.

Blots were incubated for 1 hour, followed by 2 15-minute washes in 1X TBST. Amersham ECL Prime Western blotting detection reagents (GE Healthcare/Amersham Pharmacia Biotech, Buckinghamshire, UK) was used for the detection of dehydrins and COR15A/B on film.

3.4.5 Chlorophyll a fluorescence measurements

To identify optimal conditions for the cold acclimation induced recovery of photosynthetic performance, chlorophyll a fluorescence of dark adapted leaves from wild type *Arabidopsis thaliana* grown under control conditions, control grown leaves measured at 5ºC, three weeks cold acclimated and five weeks cold acclimated were measured using a PAM 101 modulated fluorescence system (Heinz Walz, Effletrich, GmbH) (Schreiber et al. 1986), at light intensities of 350 μmol photons m^{-2} s^{-1}.

Non-acclimated, or control samples designate leaf tissue collected from plants grown for four weeks at 20°C. To measure the effect of low temperatures on the photosynthetic performance of non-acclimated plants, leaves from non-acclimated plants were dark adapted and subsequently measured at 5°C using a temperature and airflow controlled cuvette. These samples were considered Control at 5°C. Three weeks cold acclimated samples designate newly developed leaves grown from plants grown under non-acclimated conditions for four weeks, then transferred to low temperatures for three weeks. Five weeks cold acclimated samples designate newly developed leaves from plants that were grown under non-acclimated (20°C) conditions for four weeks and transferred to low temperatures for five weeks. Non-acclimated samples were dark adapted at 20°C while control at 5°C, three weeks and five weeks cold acclimated samples were dark adapted at 5°C using a temperature, light and airflow-controlled cuvette. As the best recovery of photosynthetic performance was

observed after five weeks of cold acclimation, this condition was used as a comparison to non-acclimated conditions to identify potential SR knockouts that are impaired in their capacity to adjust their photosynthetic performance in response to cold acclimation conditions.

Chlorophyll a fluorescence of wild type *Arabidopsis thaliana* leaves, as well as leaves from homozygous *at-sr34* (SALK_102166), *at-sr34b* (SALK_072651), *at-rsz22* (CS815114), *at-rsz22a* (SALK_120499), *at-scl30* (CS805508), *at-rs40* (CS853681, SALK_118875), *at-rs41* (CS803022, SALK_035417), *at-sr45* (SALK_121702, SALK_002537) and *at-ame3* (CS835176) mutant lines grown under control conditions (four weeks at 20°C) and after cold acclimation conditions (four weeks growth at 20°C, then transferred to 4°C for five weeks) were measured as described above. To maintain consistency between measurements, all chlorophyll a fluorescence measurements were performed between 12:00PM and 3:00PM. For all chlorophyll fluorescence measurements, five leaves were collected at random from wild type *Arabidopsis*, as well as all mutant lines tested, under non-acclimated and after cold acclimation conditions. Furthermore, each experiment was repeated three times, thus all chlorophyll fluorescence data is representative of averaged values from 15 leaves. Standard error (SE) were calculated for each of the fluorescence parameter measured.

Chlorophyll fluorescence parameters were defined in accordance with the nomenclature of van Kooten and Snel (1990) (Figure 3.1). F_o was defined as the lowest level of chlorophyll fluorescence after the weak pulse light which does not drive photosynthesis is turned on. F_m was measured as the maximum level of fluorescence after a flash of 10,000 μmol photons m^{-2} s^{-1} was applied, causing reaction centres to close and all the light energy to be given off as fluorescence. The difference between the maximal (F_m) and minimal (F_o) fluorescence, defined as variable fluorescence, or F_v, can be calculated and used to approximate the maximum quantum yield of photosystem II, known as F_v/F_m. This ratio is based on the model proposed by Butler (1978).

Following the first flash, actinic light of 350 μmol photons m^{-2} s^{-1} which is capable of driving photosynthesis, was turned on. Light pulses of 10,000 μmol photons m^2 s^{-2}, with a duration of 800 ms were applied at 40 sec intervals, resulting in the closing of reaction centres. Transient increases in fluorescence, recorded as peaks on the fluorescence trace designate F_m`. Light pulses were applied until steady state, designated as F_s was reached. At this point, actinic light was turned off, and F_o', which is determined as the minimal level of fluorescence after actinic light is turned off was measured.

Figure 3.1: A typical chlorophyll fluorescence trace.

Once the leaf has been adapted to the dark for 30 minutes, it is then placed in a chamber to measure chlorophyll fluorescence. A far-red dim light is turned on to measure background fluorescence with all PSII centres opened in the absence of light, or F_o. A saturating flash of light is then applied, causing all of the PSII reaction centres to be closed. This allows the measurement of the maximum fluorescence level in the dark or F_m. A light is then turned on at this point to drive photosynthesis, with saturating flashes of light at an intensity of 10, 000 μmol m^{-2} s^{-1}, at a certain interval that is determined by the user. After a certain point, the fluorescence will reach a point called steady state (F_s), and the saturating flashes of light will be measured at approximately the same intensity. These values are represented as F_s and F_m`, respectively. Once steady state is reached, the light is turned off (AL light off), which allows measurement of the background fluorescence in darkness after exposure to light, $F_o$`.

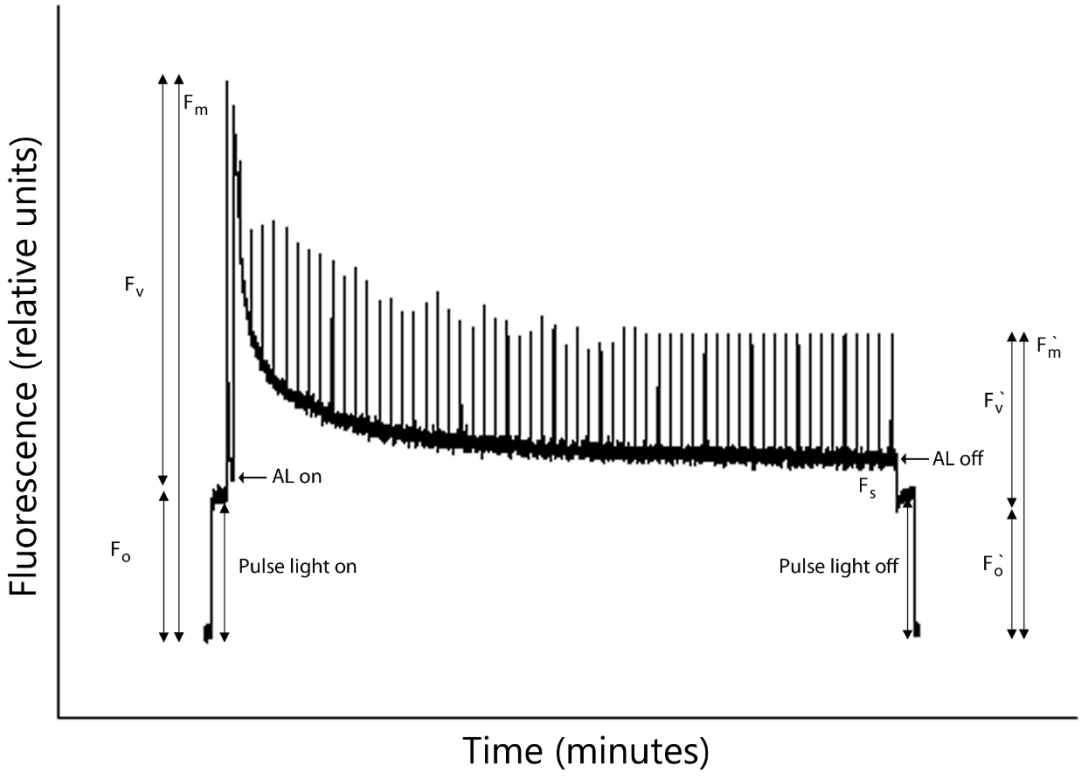
Fluorescence (relative units)
Time (minutes)
F_m
F_v
F_o
AL on
Pulse light on
AL off
F_s
Pulse light off
F_m`
F_v`
F_o`

The excitation pressure of PSII, or the relative reduction state of Photosystem II at the growth temperature and growth irradiance measured was designated as 1-qL (Kramer et al., 2004), and is calculated using the following equation:

$$1 - qL = 1 - (\frac{F_m^` - F_s}{F_m^` - F_o^`} \times \frac{F_o^`}{F_s}) \qquad (1)$$

The operating efficiency of photosystem II is calculated as:

$$\Phi_{PSII} = (F_m^` - F_s)/F_m^` \qquad (2)$$

This parameter measures the proportion of the light absorbed by chlorophyll associated with photosystem II that is used in photochemistry (Maxwell and Johnson, 2000). Moreover, the operating efficiency of PSII can be used to estimate the linear electron transport rate (ETR), using the following equation:

$$ETR = \Phi_{PSII} \times PPFD \times A_{leaf} \times fraction_{PSII} \qquad (3)$$

Where PPFD represents the photosynthetically active photon flux density, or light intensity incident on the leaf. A_{leaf} represents the amount of light absorbed by the leaf. As 84% of incident PPFD is assumed to be absorbed by mature green leaves, A_{leaf} is assumed to be 0.84. Similarly, $fraction_{PSII,}$ representing the percentage of light absorbed by photosystem II is frequently assumed to be 0.5, as light is assumed to be absorbed equally by Photosystems I and II (Baker, 2008; Maxwell and Johnson, 2000; Murchie and Lawson, 2013). The fraction of light that is absorbed by Photosystem II antennae and thermally dissipated by a ΔpH-

dependent (or driven) gradient in the thylakoid membrane, or xanthophyll-related processes can be quantified using the following equation, proposed by Hendrickson et al (2004).

$$\phi_{NPQ} = \frac{F_s}{F_m'} - \frac{F_s}{F_m} \qquad (4)$$

Additionally, $\phi_{f,D}$ can be used to quantify the fraction of light absorbed by PSII antennae that is emitted as heat by the reaction centre, otherwise known as reaction centre quenching, using the following equation, also proposed by Hendrickson et al (2004).

$$\phi_{f,D} = \frac{F_s}{F_m} \qquad (5)$$

3.4.6 Leaf electrolyte leakage freeze tests

The determination of electrolyte leakage from plant tissues after freezing and thawing, by means of conductivity measurements, is a frequently used method to assess freezing tolerance. This method mainly monitors the ability of the plasma membrane to function as a semi-permeable barrier towards intracellular ions (Ehlert and Hincha, 2008), assuming that the degree of tissue injury is correlated with damage of the plasma membrane of mesophyll cells (Mishra et al., 2011; Steponkus, 1984).

Leaf electrolyte leakage assays were performed as described by Savitch et al., (2005), using wild type *Arabidopsis* grown under optimal growth conditions, and after five weeks of cold acclimation. In addition, cold acclimated leaf tissue corresponding to SR mutant lines of interest were used. Three leaves from wild type or mutant lines grown under every condition tested were collected at random for electrolyte leakage assays. Each experiment was repeated three times; therefore, electrolyte leakage values are representative of 9 leaves. All leaves collected were placed in 15mL Falcon tubes, and subsequently submerged in a

Lauda RM20 low temperature water bath, set at 0°C for 1h. The temperature was then lowered to -2°C for 30 min. To initiate nucleation, a small piece of ice was added to each tube. The temperature was held at -2°C for another hour, and then lowered at a rate of 2°C h^{-1}. Samples were removed at -2°C intervals and 6mL of sterilized deionized (MilliQ) was added to each tube, and shaken overnight in a cold room set at a temperature of 4°C. The leaves were then removed from the tubes, and the conductivities of the supernatants were measured. In order to measure the electrolyte leakage maximum, each leaf was then frozen at -80°C overnight by means of an ultra-low temperature freezer, and returned to their respective tubes containing the initial 6mL of water (which were kept frozen once the conductivities were measured, in order to prevent microbial growth), and shaken for 3 hours. Leaves were then discarded, and conductivity measurements were taken. All conductivity measurements were achieved using an accumet excel XL30 conductivity meter (Fisher Scientific).

3.4.7 Statistical analyses

Leaves from wild type *Arabidopsis thaliana*, as well as leaves from *at-rsz22, at-rsz22a, at-rs41*, *at-sr34b*, *at-rs40*, *at-scl30*, *at-sr34*, *at-sr45* and *at-ame3* grown under control, three weeks and five weeks of cold acclimation conditions, and used in subsequent chlorophyll fluorescence and electrolyte leakage assays. For chlorophyll fluorescence assays, five leaves per batch were harvested at random for wild type and all mutant lines, at every growth condition tested, and considered a technical replicate. Each experiment was repeated in triplicate, where each leaf collected for one experiment was considered a biological replicate. Therefore, chlorophyll fluorescence experiments are representative of leaf tissue collected

from fifteen different plants. For electrolyte leakage assays, three leaves per batch were chosen at random from the previously mentioned plants for each data point, at every growth condition tested. Similarly to chlorophyll fluorescence assays, each leaf collected at random was considered a technical replicate. Each experiment was repeated using plants grown on three separate occasions, which were considered as biological replicates. Therefore, each data point measured for electrolyte leakage experiments are representative of leaf tissue from nine different plants. For qPCR analyses used to assess the role of SR proteins in the transcription profile of genes involved in the cold induced transcriptional cascade, two leaves were harvested at random from wild type *Arabidopsis*, grown under non-acclimated and after five weeks of cold acclimation, as well as leaf tissue from cold acclimated *at-rsz22, at-rsz22a, at-rs41*, *at-sr34b*, *at-rs40*, *at-scl30*, *at-sr34*, *at-sr45* and *at-ame3* mutant lines. Three technical replicates were done per leaf, therefore results presented are representative of averaged values from two biological replicates, with three technical replicates per sample. Moreover, three leaves, collected at random from wild type *Arabidopsis* and *at-ame3* mutants grown under non-acclimated, after three and five weeks of cold acclimation were used in qPCR analyses. Each leaf was considered a biological replicate, and three technical replicates were performed. Western blots used in the determination of dehydrins and COR15 A/B abundance are representative of protein extractions from three leaves harvested at random from wild type *Arabidopsis* and *at-ame3* mutants grown under non-acclimated and cold acclimation conditions. Variance analyses were performed by means of one-way ANOVA, while Tukey's Honest Significant Difference was used as post-hoc statistical analysis to determine means that are significantly different from each other. All statistical analyses were performed in R version 3.1.1.

3.5 Results

3.5.1 Identification of homozygous SR protein and LAMMER kinase T-DNA insertion mutants

Using RT-PCR as a screening tool for the identification of homozygous SR and LAMMER kinase knockouts to be used for subsequent experiments have led to the successful identification of *at-sr34* (SALK_102166), *at-sr34b* (SALK_072651), *at-rsz22* (CS815114), *at-rsz22a* (SALK_120499), *at-scl30* (CS805508), *at-rs40* (CS853681, SALK_118875), *at-rs41* (CS803022, SALK_035417) and *at-sr45* (SALK_121702, SALK_002537) homozygous mutant lines. Moreover, an *at-ame3* (CS835176) homozygous kinase knockout has also been identified (Figure 3.2A), and confirmed through genotyping (Figure 3.2B). Conversely, due to the persistent presence of bands in RT-PCR screens, homozygous SALK lines corresponding to *At-SCL30a* (SALK_041849) *At-RS2Z33* (SALK_051525), *At-RS31* (SALK_029586), *At-SCL33* (SALK_058566), *At-SR45a* (SALK_054457, SALK_012034) as well as *At-SRPK-like 1* (SALK_6436, SALK_6427) could not be identified. These results could be attributed to the location of the T-DNA inserts for these homozygous mutants, as evidenced by At-SRPK-like 1, whose T-DNA inserts were located within the third intron, and At-SCL33, whose T-DNA insert was located within the last intron (Table 3.3).

Figure 3.2: DNA amplification of At-AME3 in 6 At-AME3 homozygous knockout (1-6) lines and wild type (WT) *Arabidopsis thaliana*.

Lanes 1-6 represent potential AME3 homozygous lines from the first generation in comparison to wild type samples, designated as WT. Housekeeping gene elf1 expression was used as a loading control. Lanes expressing elf1a and not At-AME3 were considered as homozygous knockouts to be harvested for seeds and retested. Conversely, lanes showing an expression profile similar to wild type were discarded. Panel B depicts the genotyping of third generation *at-ame3* knockouts using LP/RP and LB3/RP primer combinations. Lane 1 represents PCR reactions for wild type *Arabidopsis* and lanes designated as 2-19 represent PCR reactions for 18 *at-ame3* knockouts that were tested to confirm homozygosity. M designates the molecular marker.

A

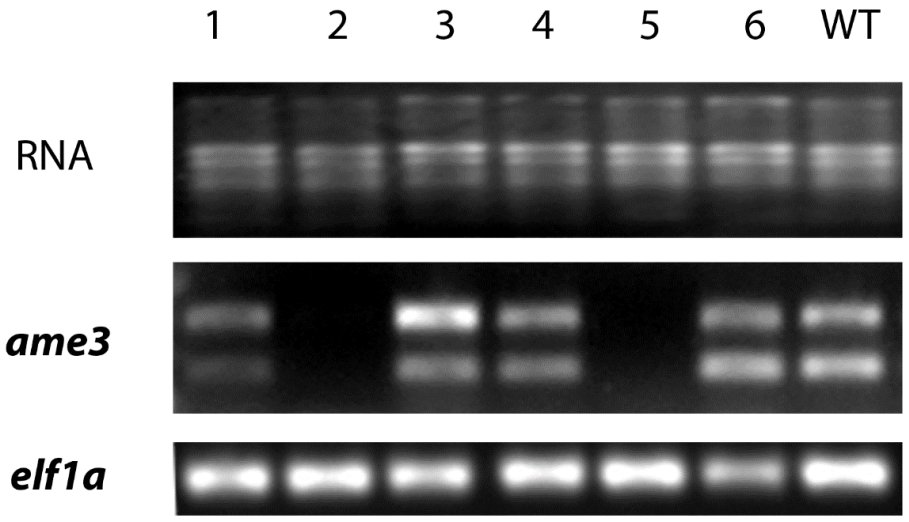
1
2
3
4
5
6
WT
RNA
ame3
elf1a

B

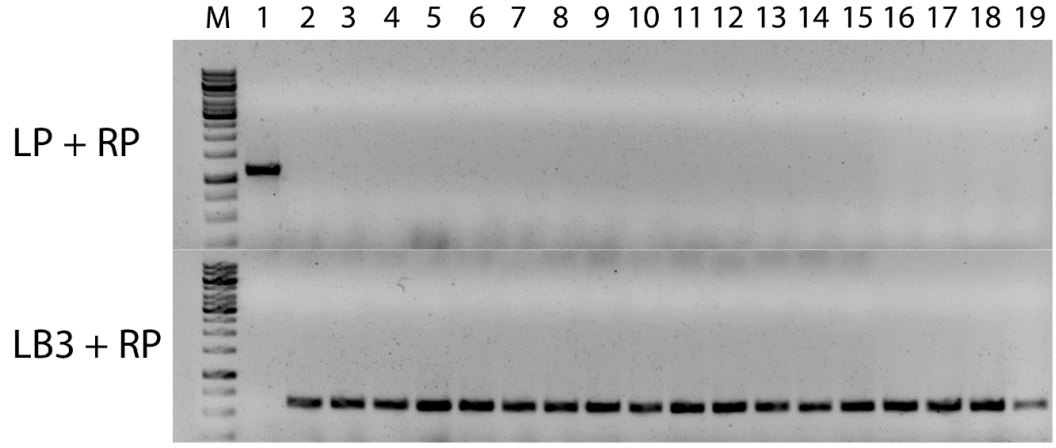
M 1 2 3 4 5 6 7 8 9 10 11 12 13 14 15 16 17 18 19
LP + RP
LB3 + RP

Table 3.3: Summary table of *Arabidopsis* SR/kinase knockouts screened by RT-PCR.

Mutant lines highlighted in bold characters denote mutant lines that were identified as homozygous T-DNA insertion lines. HM designates a certified homozygous line by SALK.

SALK number	Accession number	SR knockout	Insertion site
72651	At4g02430	***sr34b***	Within 4th intron
102166	At1g02840	***sr34***	Within 3rd exon; Certified HM line (SALK)
815114	At4g31580	***rsz22***	300 bp in 3`UTR
120499	At2g24590	***rsz22a***	300 bp in 5`UTR
805508	At3g55460	***scl30***	Within promoter region
002537	At1g16610	***sr45***	Within promoter region
121702	At1g16610	***sr45***	300 bp Within 5`UTR
803022	At5g52040	***rs41***	Within first intron
035417	At5g52040	***rs41***	Within promoter region
118875	At4g25500	***rs40***	Within promoter region
853681	At4g25500	***rs40***	Within 3rd exon; Certified HM line (SALK)
835176	At4g32660	***ame3***	Within promoter region
041849	At3g13570	*scl30a*	Within promoter region
029586	At3g61860	*rs31*	Within promoter region
051525	At2g37340	*rs2z33*	Within promoter region
058566	At1g55310	*scl33*	Within last intron
054457	At1g07350	*sr45a*	300bp within 5`UTR
012034	At1g07350	*sr45a*	300bp within 5`UTR
6436	At2g17530	*Srpk-like 1*	Within 3rd intron
6427	At2g17530	*Srpk-like 1*	Within 3rd intron

3.5.2 Role of Serine/Arginine-rich proteins and AME3 LAMMER kinase on the cold acclimation induced photosynthetic adjustment

The overall photosynthetic performance of wild type *Arabidopsis thaliana* was first evaluated, at a growth irradiance of 350 PFD, to be used as a baseline for the subsequent evaluation of the photosynthetic performance of SR and *at-ame3* mutant lines. A 34% increase in PSII excitation pressure (1-qL) in non-acclimated leaves measured at 5ºC compared to non-acclimated controls (Table 3.4) was measured. This was associated with a 55% increase in antennae quenching (Φ_{NPQ}) and a marginal increase in reaction centre quenching ($\Phi_{f,D}$). Furthermore, these observed increases in heat dissipation and antennae quenching have led to 25% decreases in the proportion of light used in photochemistry (Φ_{PSII}) and linear electron transport rates (ETR) (Table 3.4). Newly developed leaves exposed to low temperatures for three weeks were observed to exhibit a partial recovery in photosynthetic performance, as evidenced by a 30% decrease in PSII excitation pressure (1-qL) compared to cold stressed leaves. This was associated with a 10% decrease in antennae-based (Φ_{NPQ}) non-photochemical quenching, a marginal change in reaction centre-based ($\Phi_{f,D}$) non-photochemical quenching, and 8% increases in the fraction of light used in PSII photochemistry (Φ_{PSII}) and linear electron transport rates (ETR) compared to cold stressed leaves. Furthermore, in accordance with previous reports (Savitch et al., 2001) leaves developed at low temperatures for five weeks have shown an even greater recovery, as shown by a 2% difference in excitation pressure of Photosystem II (1-qL) between five weeks cold acclimated leaves and non-acclimated wild type *Arabidopsis thaliana* leaves (Table 3.4). This result was associated with a 9% difference in linear electron transport rates (ETR) and

proportion of light used in photochemical reactions (Φ_{PSII}) when compared to non-acclimated wild type *Arabidopsis thaliana*. While linear electron transport rates, excitation pressure of PSII and the proportion of light used for photochemistry are close to wild type values, leaves grown and developed under low temperature conditions were observed to exhibit increased antennae based quenching, as evidenced by the 39% increase in antennae quenching (Φ_{NPQ}) values in cold acclimated leaves compared to non-acclimated controls. It should be noted that while an increase in antennae quenching was observed in cold acclimated leaves, this value was less than the antennae quenching values recorded under cold stress conditions, and after three weeks of growth at low temperatures (Table 3.4). The maximum photochemical efficiency (F_v/F_m) was observed to decrease in non-acclimated leaves measured at 5ºC, followed by a gradual recovery in newly developed leaves grown for three weeks and five weeks of cold acclimation (data not shown). Based on the cold acclimation induced adjustment of photosynthesis observed in wild type *Arabidopsis* at 350 PFD, *at-rsz22, at-rsz22a, at-rs41*, *at-sr34b*, *at-rs40*, *at-scl30*, *at-sr34*, *at-sr45* and *at-ame3* loss of function mutants were tested for their inability to undergo this process.

Screening knockouts of interest for their inability to undergo a cold acclimation induced adjustment of photosynthetic performance has shown that the deletion of *at-sr34*, *at-sr34b,* and *at-rs41* had no effect on photosynthetic performance, as these loss-of-function mutant lines performed similarly to wild type ($P>0.05$) *Arabidopsis thaliana* under control and after cold acclimation conditions, at a Photon Flux Density (PFD) of 350µmol m^{-2} s^{-1}. Conversely, *at-rsz22*, as well as *at-sr45* mutants were hindered with respect to photosynthetic performance under non-acclimated conditions in comparison to wild type *Arabidopsis* grown under the same conditions (Fig. 3.3). While *at-sr45* mutants exhibited marginal decreases in

photochemical efficiency (F_v/F_m) relative to wild type, an 18% increase in excitation pressure of Photosystem II (1-qL) was observed compared to non-acclimated wild type *Arabidopsis* leaves. This increase in excitation of PSII led to a 24% decrease in linear electron transport rates (ETR) as well as energy used for photochemistry (ϕ_{PSII}), followed by a 37% increase in antennae-based quenching (ϕ_{NPQ}). Heat dissipation through the reaction centre ($\phi_{f,D}$) remained comparable to non-acclimated wild type *Arabidopsis thaliana*. The deletion of *at-rsz22* had resulted in an 18% decrease in the operating efficiency of Photosystem II and linear electron transport rates relative to non-acclimated wild type *Arabidopsis thaliana*. These results were associated with a 38% increase in antennae-based quenching values compared to its wild type counterpart. Furthermore, the impediments in photosynthetic performance observed under optimal growth conditions persisted in newly developed leaves grown under cold acclimation conditions from *at-rsz22* and *at-sr45* mutants, as evidenced by 23% and 28% increases in excitation pressure of PSII (1-qL), 10% and 28% reductions in linear electron transport rates and photochemical efficiency, respectively, compared to cold acclimated wild type *Arabidopsis* leaves. Moreover, these findings were associated with 31% and 28% increases in antennae based heat dissipation. Differences in reaction centre based quenching were marginal for both mutant lines.

Table 3.4: Comparison of chlorophyll a florescence parameters from wild type *Arabidopsis thaliana* measured under non-acclimated, non-acclimated measured at low temperature, three weeks and five weeks of cold acclimation.

Values with two asterisks (**) denote statistical significance, with a p-value lesser than or equal to 0.05 ($P \leq 0.05$) in comparison to non-acclimated wild type *Arabidopsis*, while values with three asterisks (***) designate statistical significance, with a p-value lesser than or equal to 0.01 ($P \leq 0.01$) in accordance with Tukey's Honest Significant Difference test.

	Non acclimated	**Control at 5ºC**	**3w Cold Acclimated**	**5w Cold Acclimated**
Excitation pressure (1-qL)	0.362 ± 0.004	0.549 ± 0.025***	0.382 ± 0.026	0.368 ± 0.011
Linear electron transport rates (ETR)	88.36 ± 1.65	66.40 ± 1.774***	71.54 ± 1.44	80.31 ± 3.56
Quantum yield of Photosystem II (Φ_{PSII})	0.601 ± 0.01	0.458 ± 0.015***	0.487 ± 0.01***	0.546 ± 0.026
Antenna-based quenching (Φ_{NPQ})	0.137 ± 0.006	0.305 ± 0.029***	0.275 ± 0.0120***	0.226 ± 0.03**
Reaction centre-based quenching ($\Phi_{f,D}$)	0.232 ± 0.006	0.237 ± 0.0170	0.235 ± 0.007	0.224 ± 0.011

While *at-rsz22* and *at-sr45* mutants were impaired with respect to their photosynthetic performance, the remaining mutant lines have shown negligible ($P>0.05$) differences in photosynthetic performance relative to wild type under non-acclimated conditions. The cold acclimation-induced enhancement of photosynthetic performance, however, was jeopardized to various degrees in *at-rsz22a*, *at-scl30, at-rs40* and *at-ame3* mutants. These previously mentioned knockouts exhibited 18%, 32%, 24% and 40% increases in PSII excitation pressure, which were associated with 24%, 54%, 33% and 67% decreases in linear electron transport rates and photochemical efficiency, respectively. Interestingly, *at-rsz22a, at-scl30* and *at-rs40* loss-of-function mutants exhibited enhanced heat dissipation through antennae quenching, at 46%, 46% and 52%, respectively, while *ame3* was the only mutant that was observed to possess an enhancement in heat dissipation via reaction centre quenching, which was 53% greater than cold acclimated wild type *Arabidopsis*. Furthermore, it should be noted that both *scl30* and *ame3* have shown severe photoinhibition under cold acclimation conditions, as evidenced by 10% and 51% reductions in maximum photochemical efficiency (F_v/F_m) (Figure 3.3A).

Figure 3.3: Effects of the deletion of Serine/Arginine-rich proteins or At-AME3 kinase on maximum photochemical efficiency (F_v / F_m), excitation pressure of photosystem II (1-qL), linear electron transport rates (ETR), yield of photosystem II (Φ_{PSII}), antenna-based portion of non-photochemical quenching (Φ_{NPQ}), and PSII reaction centre-based portion of non-photochemical quenching ($\Phi_{f,D}$) under control conditions and after five weeks of cold acclimation.

Control conditions denote plant growth for four weeks at 20°C, while cold acclimation conditions denote newly developed leaves from plants that were grown for four weeks under non-acclimated conditions, then transferred to 4°C growth conditions for five weeks. All leaves were measured at a Photon Flux Density (PFD) of 350µmol m^{-2} s^{-1}. White bars designate samples grown under control conditions whereas grey bars represent cold acclimated samples. All bars represent averaged values from 15 recordings + SE. Letters a-d denote statistical significance between parameters measured under control conditions compared to cold acclimation conditions, in accordance with Tukey's Honest Significant Difference test. Bars containing the letter a designate a p-value of $P \leq 0.05$ and b denoting a p-value of $P \leq 0.01$ between their non-acclimated and cold acclimated counterparts. Bars assigned with the letter c designate a statistically significant result with a p-value of $P \leq 0.01$ when compared to wild type samples, whereas the letter d designates a statistically significant difference of $P \leq 0.01$ between samples from mutant lines and wild type *Arabidopsis thaliana* grown under cold acclimation conditions.

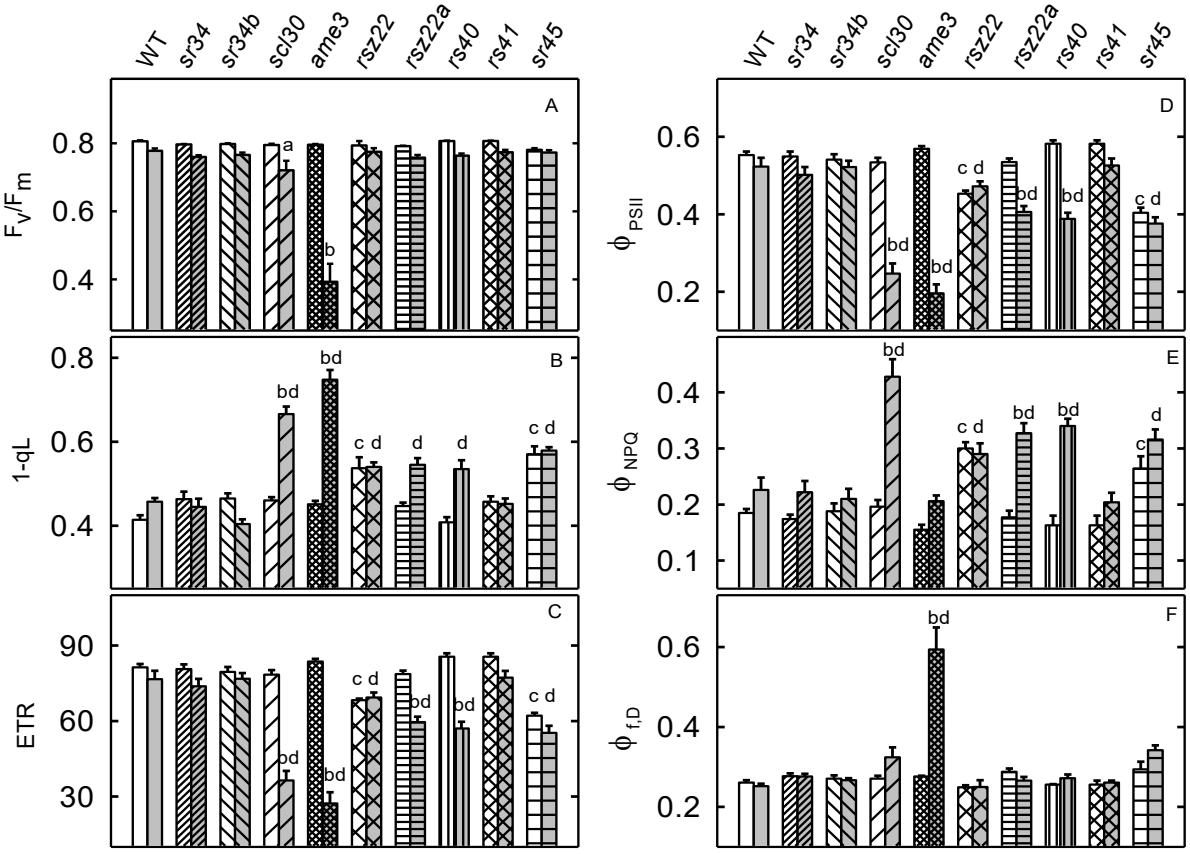
WT
sr34
sr34b
scl30
ame3
rsz22
rsz22a
rs40
rs41
sr45
A
B
C
D
E
F
F_V/F_m
1-qL
ETR
ϕ_{PSII}
ϕ_{NPQ}
$\phi_{f,D}$

In summary, chlorophyll fluorescence results suggest that At-SR34, At-SR34b and At-RS41 do not play a role in the photosynthetic performance in *Arabidopsis thaliana*. Conversely, At-RSZ22 and At-SR45 are suggested to play an important role(s) in the photosynthetic performance of *Arabidopsis* under non-acclimated growth conditions as well as under cold acclimation conditions, while *at-rsz22a*, *at-scl30*, *at-rs40* and *at-ame3* play an important role in the cold acclimation-induced adjustment of photosynthetic performance in *Arabidopsis thaliana*, but not under optimal growth conditions. Furthermore, differences in the location of T-DNA insertions had no effect on the observed photosynthetic performance of the mutant lines which were tested (Appendix Fig A3.1).

3.5.3 Role of SR proteins and At-AME3 on acquisition of freezing tolerance

As exposure to low temperatures lead to losses in membrane integrity and subsequent solute leakage, a key function of cold acclimation involves a variety of mechanisms which allow the membrane to withstand freezing temperatures. Some of the mechanisms associated with the acquisition of freezing tolerance include a retailoring of the membrane lipid composition (Guy et al., 2008), the gradual accumulation of sugars as well as proteins playing a cryoprotective role in the plant cell (Thomashow, 1999). Therefore it is expected that prolonged exposure of newly developed cold acclimated leaves will result in a gradual increase in freezing tolerance relative to non-acclimated control plants which can be measured via electrolyte leakage assays (Lee and Zhu, 2010; Wilson and Jacobs, 2004). Thus, leaves from wild type *Arabidopsis* grown and developed in low temperatures are expected to exhibit a greater resistance to freezing temperatures due to the accumulation of cryoprotectants, reflected by a lower Lethal Temperature 50 (LT_{50}) value compared to its non-acclimated counterpart. LT_{50} represents the temperature resulting in the leakage of 50%

of electrolytes from the plant leaf value. Using electrolyte leakage assays as a screening tool to monitor changes in freezing tolerance between cold acclimated SR and AME3 LAMMER kinase knockouts has shown that, in a similar fashion to wild type *Arabidopsis thaliana*, *at-rsz22, at-sr34b, at-rsz22a, at-scl30, at-rs40* and *at-rs41* mutant lines possess the capacity to acquire freezing tolerance, as evidenced by their recorded LT_{50} temperatures ranging between -9°C and -10°C after five weeks of cold acclimation (Appendix Fig. A3.2). These observed values were comparable to wild type *Arabidopsis*, which was observed to reach LT_{50} at -9°C. In comparison, the acquisition of freezing tolerance has been severely impeded in *At-AME3* kinase knockouts (Figure 3.4). Non-acclimated conditions have led to recorded LT_{50} values of -5°C, which is comparable to wild type *A. thaliana.* While exposure to low temperatures have led to an increase in freezing tolerance in wild type *Arabidopsis* leaves as shown by an observed LT_{50} of -9°C, *ame3* mutants had an observed LT_{50} temperature of -3°C, which was observed to be worse than wild type *Arabidopsis thaliana* plants grown under control conditions (Figure 3.4).

Figure 3.4: Freezing survival of leaves non-acclimated wild type *Arabidopsis thaliana* and At-AME3 knockouts compared to 5 weeks cold acclimated wild type and At-AME3 knockouts, as determined by electrolyte leakage assays.

The acquisition of freezing tolerance was assessed by means of electrolyte leakage assays for fully developed leaves of wild type *Arabidopsis thaliana* (circles) and *at-ame3* mutant lines (triangles) tested under control (white) and after five weeks cold acclimation (black) conditions. Each point represents the mean of 3 recordings from 3 independent experiments ± SE (n=9).

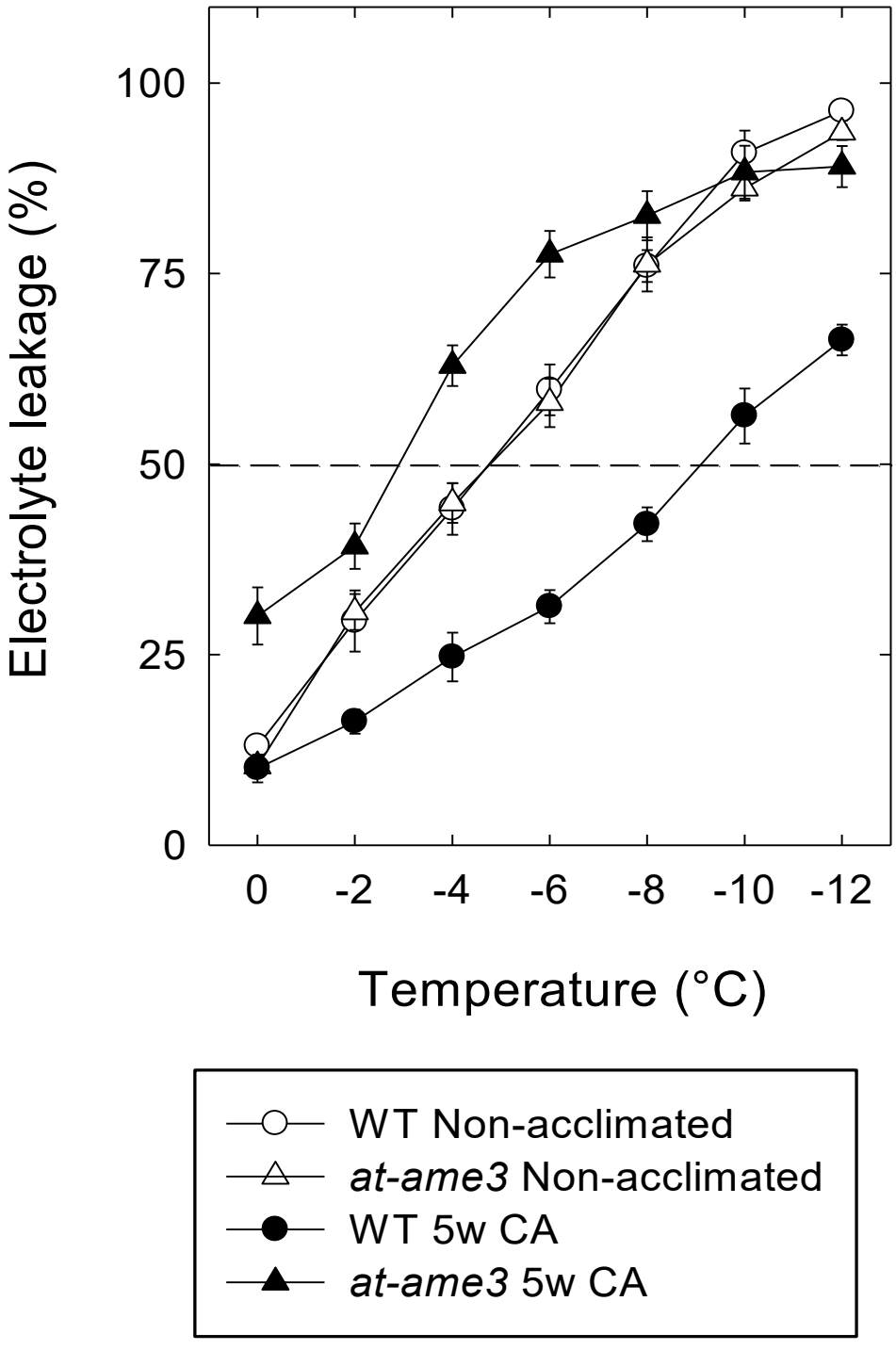
Electrolyte leakage (%)
100
75
50
25
0
0
-2
-4
-6
-8
-10
-12
Temperature (°C)
WT Non-acclimated
at-ame3 Non-acclimated
WT 5w CA
at-ame3 5w CA

3.5.4 Role of Serine/Arginine-rich proteins and At-AME3 LAMMER kinase in the regulation of the cold induced transcriptional cascade

The inability to acquire freezing tolerance, which was observed in *ame3* mutants raised the question as to whether the expression levels of genes involved in the transcriptional cascade leading to the acquisition of freezing tolerance has been altered in *ame3* mutants, as well as *at-rsz22, at-sr34, at-sr34b, at-rsz22a, at-scl30, at-rs40* and *at-rs41* compared to wild type *Arabidopsis* undergoing cold acclimation. It is well established that under non-acclimated conditions, HOS1 suppresses Inducer of CBF Expression 1 (ICE1). However, once chilling temperatures are sensed, ICE1, which is constitutively expressed, is activated, and will in turn induce the expression of C-repeat Binding Factors 1 and 3 (CBF1/CBF3), respectively. CBFs, which recognize Drought Responsive Elements (DREs)/CRT sequences found in the promoter region of several cold responsive (COR) genes, such as COR15A and COR15B, KIN1 and LTI78, will bind to them, in turn increasing the expression of these genes. In addition to the induction of cold responsive genes, exposure to low temperatures have also been associated with the induction of *Sucrose Phosphate Synthase* (*SPS*) (Refer to Chapter 1, Section 1.3). Thus, exposure to low temperatures leading to a physiological response associated with cold tolerance. Therefore, it is expected that exposure to low temperatures would result in the induction of *CBF1* and *CBF3* transcript levels. As CBFs 1 and 3 are induced, it is expected that an increase in *SPS* transcript levels, as well as downstream targets of *CBF1* and *CBF3*, namely *COR15A*, *COR15B*, *KIN1* and *LTI78*, would be observed. Furthermore, as long term exposure to low temperatures lead to an accumulation of transcripts from the CBF transcription pathway, it is expected that prolonged exposure to low temperatures would result in an enhancement in the induction of key cold responsive

genes, including *SPS*, *CBFs*, and *COR* genes. Due to the known role of SR proteins and LAMMER kinases pertaining to RNA metabolism, we hypothesized that this subset of SR proteins might play a role in the pre-mRNA splicing and/or post-splicing activities of these previously mentioned genes, which are involved in the cold acclimation induced transcriptional cascade.

An initial screen was performed, with the purpose of quickly assessing any differences in transcript levels in SR and AME3 mutant lines under cold acclimation conditions compared to wild type. While some variability was observed in the transcript levels of cold responsive genes monitored in *At-RSZ22, At-SR34b, At-RSZ22a, At-SCL30, At-RS40* and *At-RS41* mutants under cold acclimation conditions compared to wild type *Arabidopsis*, these findings did not correlate with a decrease in electrolyte leakage for these mutant lines (Appendix Fig. A3.3). Conversely, transcript levels of genes involved in the cold acclimation induced transcriptional cascade was reduced in *ame3* mutants, prompting a more detailed comparison with respect to transcript levels of cold responsive genes between wild type *Arabidopsis* and *ame3* mutants undergoing cold acclimation.

Monitoring transcript levels of genes involved in the acquisition of freezing tolerance has shown that exposure to low temperatures have led to minimal changes in ICE1 transcript levels in wild type *Arabidopsis* (Fig. 3.5B). Conversely, exposure to low temperatures have led to a gradual decrease in *HOS1* transcript levels in wild type *Arabidopsis* (Figure 3.5C). As HOS1 is a negative regulator of ICE1 (Refer to Chapter 1) this gradual decrease in *HOS1* transcript levels allows *ICE1*, which is constitutively expressed, to induce the expression of CBF transcription factors, which was observed as an increase in both *CBF1* and *CBF3* expression in leaves from wild type *Arabidopsis* grown and developed after three weeks at

low temperatures (Fig. 3.5D-E). Prolonged exposure to low temperatures have exacerbated the expression of *CBF1* and *CBF3* transcripts. The observed increase in *CBF* transcript levels was associated with an observed increase in *SPS* transcript levels (Fig. 3.5F, p.138) as well as the expression of downstream targets of *CBF1* and *CBF3*, such as *COR15A*, *COR15B*, *KIN1* and *LTI78* (Fig. 3.5G-J). Furthermore, as *At-AME3* transcript levels were shown to be induced under exposure to low temperatures in *Brassica napus*, it is also expected that exposure to low temperatures would result in an increase in *At-AME3* transcript levels. As expected, leaves from wild type *Arabidopsis* grown at low temperatures for three weeks have shown an increase in transcript levels of *At-AME3* kinase (Fig. 3.5A) relative to non-acclimated leaves. Prolonged exposure to low temperatures have led to a gradual increase in *At-AME3* transcript levels, as seen in transcript levels for *At-AME3* in leaves that were cold acclimated for five weeks (Fig. 3.5A).

In comparison to wild type *Arabidopsis*, leaves from non-acclimated and cold acclimated *at-ame3* mutants have shown marginal *At-AME3* transcript levels (Fig. 3.5A). While cold acclimated leaves from *at-ame3* knockouts have shown a decrease in *HOS1* expression, similarly to wild type, *at-ame3* mutants express *HOS1* at lower levels than wild type *Arabidopsis* under every condition tested (Fig. 3.5C). Furthermore, *at-ame3* constitutively expresses *ICE1* at lower levels than wild type. While long term exposure to low temperatures led to marginal changes in *ICE1* transcript levels in wild type *Arabidopsis*, a decrease in *ICE1* expression was observed in *at-ame3* knockouts (Fig 3.5B). As expected, exposure to low temperatures have led to an increase in CBF1 and CBF3 transcripts, in turn leading to an increase in *COR15A*, *COR15B*, *KIN1* and *LTI78* transcript levels in wild type *Arabidopsis thaliana*.

This suppression of *ICE1* observed in *at-ame3* mutants led to a reduction of both *CBF1* and *CBF3* transcripts in leaves collected after exposure to low temperatures for three and five weeks (Fig. 3.5D-E), in turn leading to a suppression of downstream targets of *CBFs*, such as *COR15A* and *COR15B, KIN1* and *LTI78* (Fig 3.5G-J). Furthermore, an increase in *SPS* transcript levels was not observed in *ame3* mutants undergoing cold acclimation. As the expression of these genes are known to be positively correlated with the acquisition of freezing tolerance (Strand et al., 2003; Thalhammer and Hincha, 2013; Thalhammer et al., 2014), the observed suppression in transcript levels of cold responsive genes and *SPS* observed in *ame3* knockouts would lend credence to its observed inability to acquire freezing tolerance previously shown by means of electrolyte leakage assays (Fig. 3.5). Moreover, *at-ame3* mutants are hindered in their capacity to accumulate dehydrins as well as cold induced COR15A/B proteins under cold acclimation conditions compared to wild type *Arabidopsis* (Fig. 3.6), as exposure to low temperatures have led to an increase in dehydrins and COR15A/B abundance in leaves from wild type *Arabidopsis thaliana* (Fig. 3.6), while no changes in dehydrins and COR15 A/B protein abundance were observed in leaves from *ame3* mutants under control conditions compared to five weeks cold acclimated samples.

Figure 3.5: Effect of At-AME3 kinase deletion on the expression level of genes involved in the cold stress responsive transcriptional cascade in *Arabidopsis thaliana*.

Leaves of non-acclimated wild type *Arabidopsis* (white bars) and *ame3* mutants (diagonal lines), as well as newly developed, cold acclimated leaves grown for three weeks (grey bars, crossed lines) and after five weeks of cold acclimation (black bars, horizontal lines) were used in transcription profile analyses of *AME3* (A), *ICE1* (B), *HOS1* (C), *CBF1* (D), *CBF3* (E), Sucrose Phosphate Synthase (*SPS*) (F), *COR15A* (G), *COR15B* (H), *KIN1* (I) and *LTI78* (J) by means of qPCR. All bars represent averaged expression values +SE from three biological replicates, each with three technical replicates (n=9) normalized against the mean transcript levels of elongation factor 1α (elf1). The data presented in this figure was provided by David P. Sprott and the figure was assembled by Dr. Leonid V. Savitch.

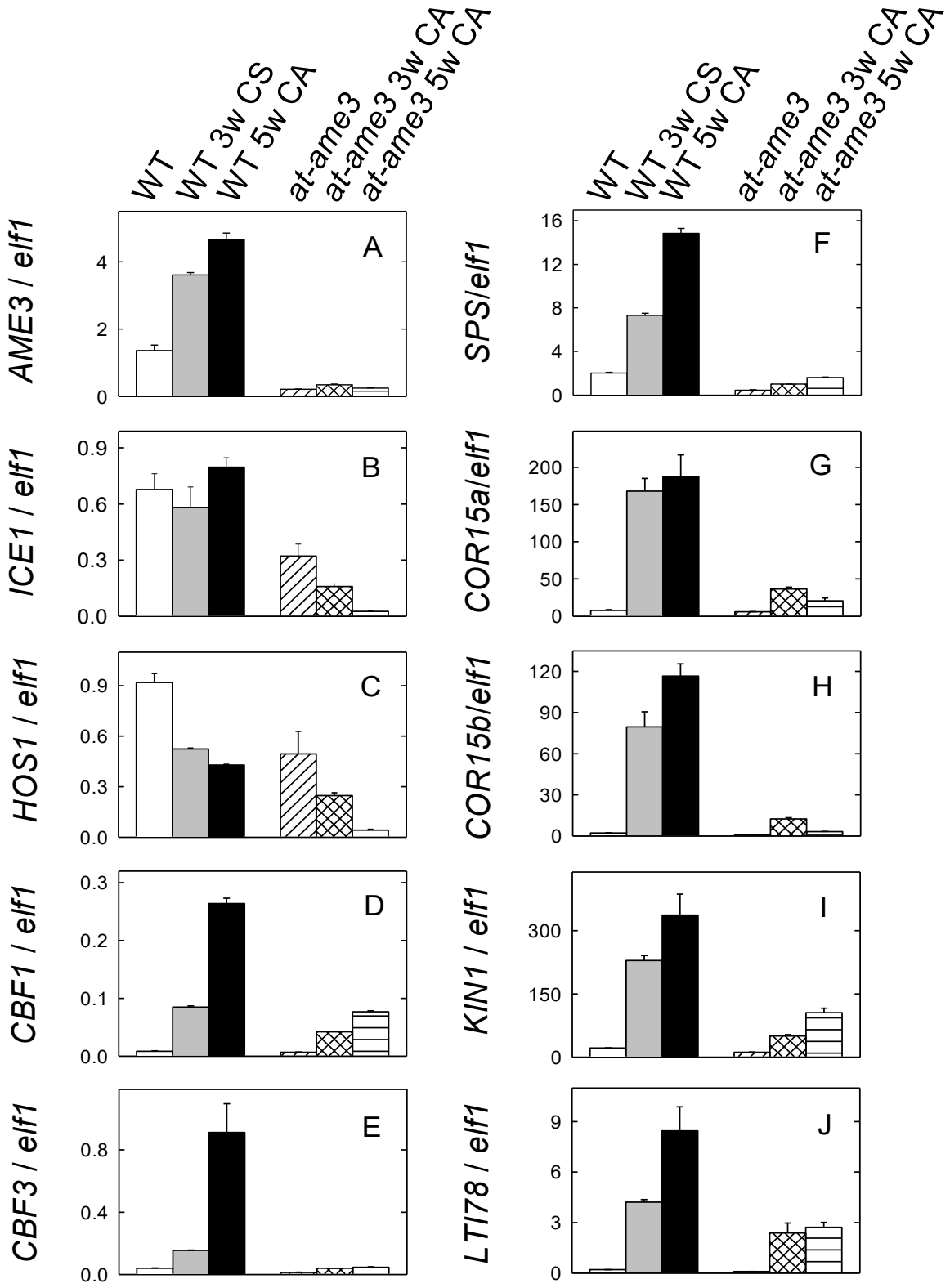
WT
WT 3w CS
WT 5w CA
at-ame3
at-ame3 3w CA
at-ame3 5w CA
AME3 / elf1
ICE1 / elf1
HOS1 / elf1
CBF1 / elf1
CBF3 / elf1
SPS/elf1
COR15a/elf1
COR15b/elf1
KIN1 / elf1
LTI78 / elf1
A
B
C
D
E
F
G
H
I
J

Figure 3.6: Protein abundance profile of Dehydrins and COR15A/B in wild type *Arabidopsis* and *ame3* loss-of-function mutant under non-acclimated and cold acclimated conditions.

Solubilized samples were loaded on an equal protein basis, consisting of 20µg of protein per lane. Stained gels used to assess equal loading are unavailable. All blots shown are representative of 3 biological replicates. All molecular weights are represented in kilodaltons (kDa). Panel A depicts a Western blot of an SDS-PAGE gel of total protein extracts from wild type and *ame3* mutant lines under non-acclimated (20°C) and cold acclimated (5°C) for 5 weeks probed with antibodies raised against dehydrins, as well as *Brassica napus* BN115, which is homologous to *Arabidopsis thaliana* COR15A and COR15B..

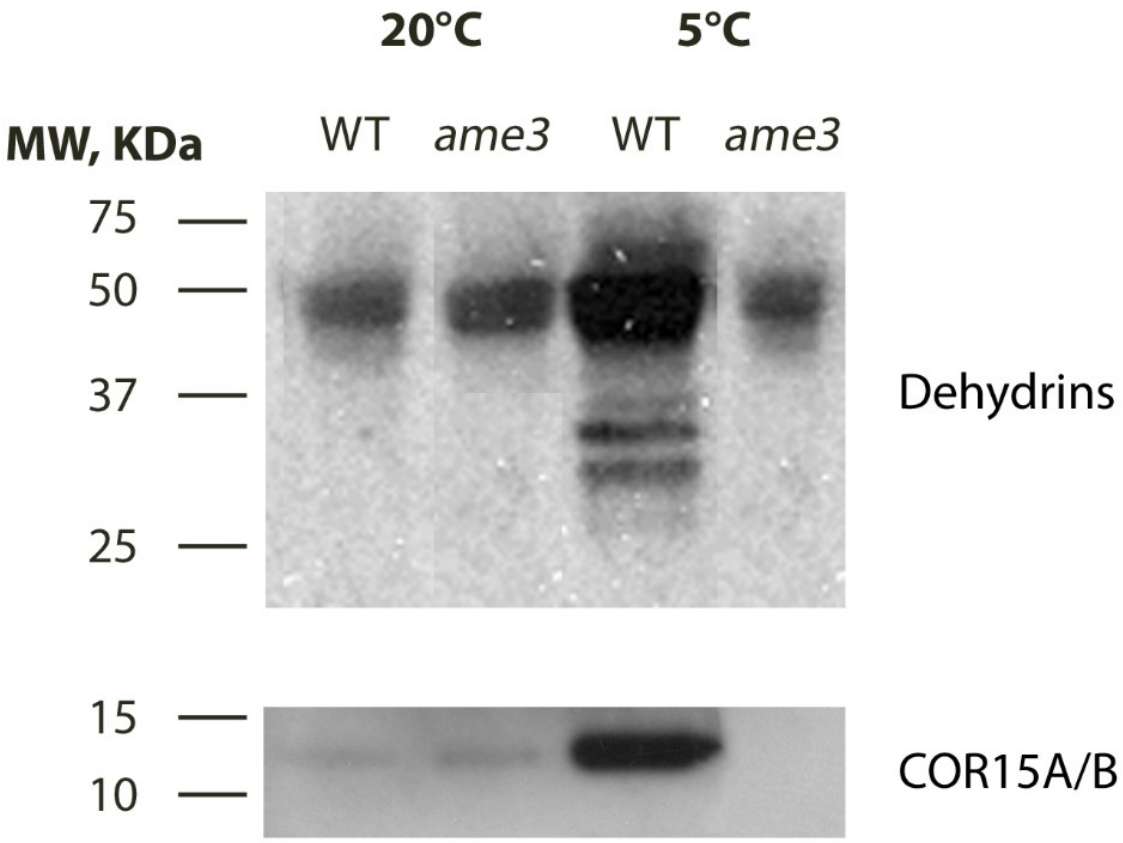
20°C
5°C
MW, KDa
WT
ame3
WT
ame3
75
50
37
25
Dehydrins
15
10
COR15A/B

The deletion of At-AME3 kinase also resulted in phenotypic differences when compared to wild type Arabidopsis thaliana, as well as the other mutant lines tested in this study. Under control conditions, wild type plants were observed to have flat leaves while, *ame3* mutants exhibit curved leaves (Fig. 3.7). Three weeks exposure to low temperatures led to the growth and development of cold acclimated leaves in wild type plants, which are thicker and darker in color than their non- acclimated counterparts but leaves from *ame3* mutants appear photobleached (Fig. 3.7). Longer exposure to low temperatures leads to a greater proportion of cold acclimated leaves in wild type *Arabidopsis*, while this was not observed in *ame3* mutants. *ame3* mutants were also associated with a reduced silique formation compared to wild type plants (Fig. 3.8).

Taken together, these phenotypic differences between wild type *Arabidopsis* and *ame3* mutants would suggest that the role of *ame3* could extend beyond its involvement in processes pertaining to the cold acclimation induced enhancement of photosynthetic performance and the acquisition of freezing tolerance.

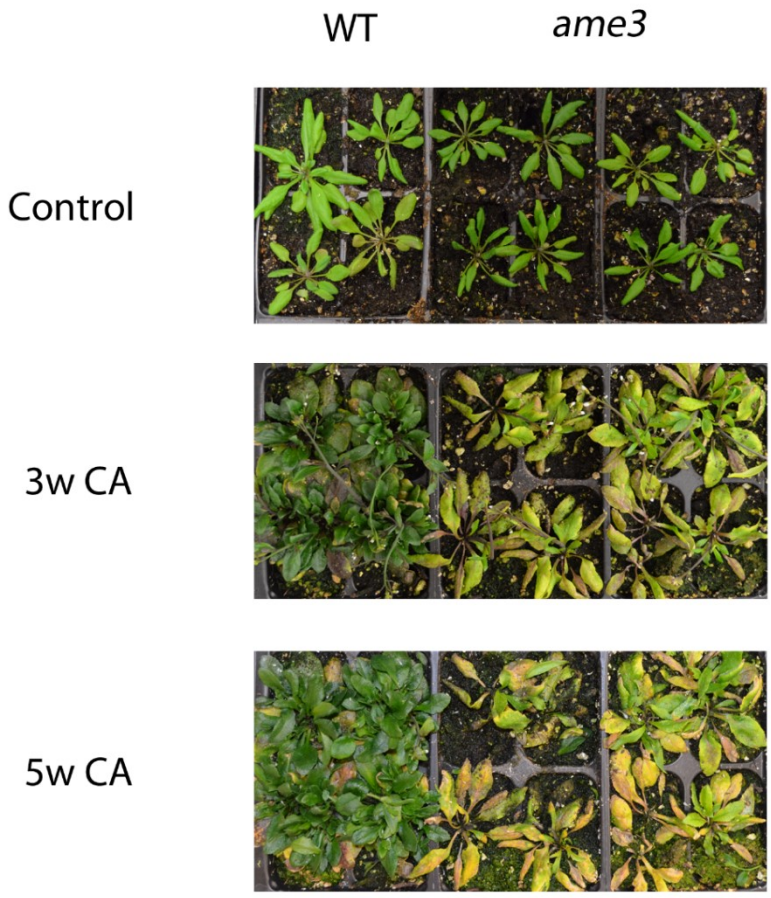

Figure 3.7: Effect of the deletion of At-AME3 kinase on the phenotype of *Arabidopsis* plants grown under optimal growth conditions, three weeks and five weeks growth and development at 5^{o}C.

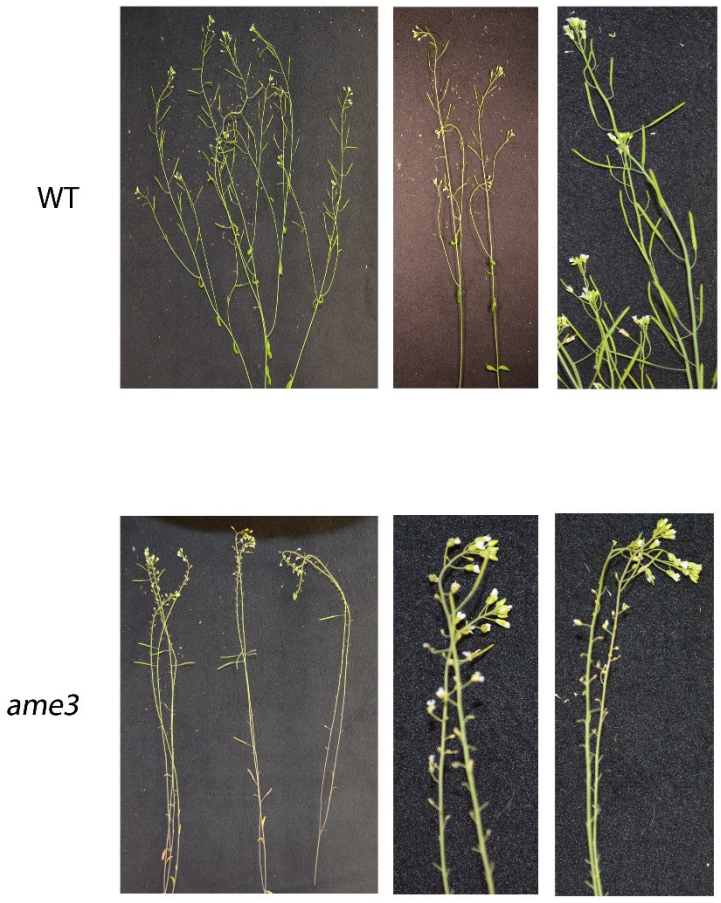

Figure 3.8: Effect of the deletion of At-AME3 LAMMER kinase on silique development in *Arabidopsis* after four weeks growth and development under optimal growth conditions.

3.6 Discussion

As key factors in the early recognition of splice sites, Serine/Arginine-rich proteins, as well as LAMMER kinases, are widely recognized as instrumental in the regulation of both constitutive and alternative splicing (Barta et al., 2008; Long and Caceres, 2009; Reddy and Golovkin, 2008), as well as various roles in post-splicing activities, such mRNA transport, stability and translational regulation (Huang et al., 2003; Lemaire et al., 2002; Sanford et al., 2004, 2005). While it is generally understood that this family of highly conserved splicing regulators are involved in abiotic stress responses (Ali and Reddy, 2008b; Palusa et al., 2007), functional data pertaining to the role of SR proteins as well as LAMMER kinases remains scarce. The first functional studies involving plant SR proteins have reported that overexpression of At-SR30 influences splice site selection of U1-70K, At-RS31, At-SR34, as well as its own transcript (Lopato et al., 1999a). In addition, At-SR30 overexpression was shown to result in a bushy phenotype, along with delays in the transition from the vegetative to the flowering stage (Lopato et al., 1999a). A later study has shown that transgenic plants overexpressing At-RS2Z33 influenced the splice site selection of At-SR30 and At-SR34, while leading to developmental and morphological changes such as the formation of twin embryos and an elongated cell shape compared to wild type plants (Kalyna et al., 2003). At-SR45 was also suggested to negatively regulate glucose signalling during early seedling development by negatively regulating the ABA pathway, as shown by *sr45-1* loss-of-function mutants which display enhanced levels of endogenous glucose and ABA, as well as reduced transcript levels of *RBCS*, which encodes for the small subunit of ribulose-1,5-bisP carboxylase, and *CAB1*, which encodes for a chlorophyll a/b-binding protein (Carvalho et al., 2010; Duque, 2011). Moreover, phosphorylation has been shown to play a prominent role

not only in splice site recognition (Zhong et al., 2009), but in the modulation of alternative splicing, as seen by a tobacco LAMMER kinase, PK12. This LAMMER kinase, which is homologous to At-AME1, was shown to alter the alternative splicing patterns of At-SR30, At-SR34 and U1-70K (Savaldi-Goldstein et al., 2003), as well as the subcellular localisation of SR-like SR45 under stress conditions (Ali and Reddy, 2006). SR45 was shown to be preferentially organized in enlarged nuclear speckles upon heat shock, as opposed to its relocation to a diffuse nucleoplasmic pattern upon exposure to low temperature (Ali and Reddy, 2006). While these findings have provided valuable functional clues with respect to the role of SR proteins and LAMMER kinases, the role of these splicing regulators in cold stress and acclimation responses has yet to be elucidated. *Brassica napus* SR proteins (*Bn-RSZ22, Bn-RSZ22a, Bn-SR34b, Bn-SCL30, Bn-SCL30a, Bn-RS2Z32, Bn-RS40, Bn-RS41*), SR-like (*Bn-SR45)* and LAMMER kinases (*Bn-AME3* and *Bn-SRPK-like 1*) have been suggested to play a role in RNA metabolism in wild type *Brassica napus* and *BnCBF* overexpressor lines undergoing cold acclimation (Refer to Chapter 2). Thus, it was hypothesized that this subset of SR proteins and LAMMER kinases might be involved in either the cold acclimation induced enhancement of photosynthetic performance and/or the acquisition of freezing tolerance, two processes among several others that play a role in the cold acclimation response. Moreover, as SR proteins and LAMMER kinases have been shown to be involved in mRNA metabolism and post-splicing activities, it was hypothesized that this subset of SR proteins and LAMMER kinases might play a role in the transcription, splicing and/or post-splicing activities of cold responsive genes involved in the cold acclimation induced transcriptional cascade.

If these SR proteins and At-AME3 LAMMER kinase are involved in the low temperature induced adjustment of photosynthetic performance, it was expected that loss-of-function mutants would be impaired in their photosynthetic performance under cold acclimation conditions. No discernable changes in chlorophyll a fluorescence parameters between leaves from wild type *Arabidopsis* and *at-sr34*, *at-sr34b* and *at-rs41* mutant lines were observed (Fig. 3.3). These results suggested that this subset of serine/arginine-rich proteins may not be involved in mechanisms of post-transcriptional regulation contributing to the adjustment of photosynthetic performance in *Arabidopsis thaliana* plants undergoing cold acclimation. While these genes do not appear to play a role in the photosynthetic adjustment occurring in newly developed leaves under cold acclimation conditions in *Arabidopsis*, based on chlorophyll fluorescence results, the possibility that these SR proteins play a role in the regulation of genes involved in other processes occurring during cold acclimation cannot be ruled out, as this study has focused solely on the potential role of SR proteins in the cold acclimation induced adjustment of photosynthesis, the acquisition of freezing tolerance and/or the expression profile of key cold responsive genes involved in the transcriptional cascade associated with cold acclimation.

While the SR protein knockouts mentioned above were shown to behave similarly to wild type *Arabidopsis* undergoing cold acclimation, *at-rsz22* and *at-sr45* mutants were observed to be impaired with respect to their photosynthetic performance under non-acclimating conditions (Fig. 3.3). Furthermore, this trend was maintained in newly developed, five weeks cold acclimated leaves (Fig. 3.3), suggesting that *at-rsz22* and *at-sr45* play an essential role in the regulation of photosynthetic machinery under optimal growth conditions, as well as under cold acclimation conditions. While there is no data suggesting

that *at-rsz22* is impaired with respect to its photosynthetic performance, a previous study has shown that *at-sr45* mutants are hypersensitive to ABA and glucose (Ali et al., 2007). Under 3% glucose growth, *at-sr45* mutants expressed reduced level of *RBCS,* which encodes for the small subunit of Rubisco and *CAB1*, which encodes for a subunit of the light harvesting complex II (LHCBII) (Carvalho et al., 2010, 2016). This study is expanding on current knowledge of the role(s) of SR proteins by presenting a new role for At-RSZ22 and At-SR45 in the overall photosynthetic performance of *Arabidopsis* under non-acclimated conditions, as well as after cold acclimation conditions.

While newly developed leaves from wild type *Arabidopsis thaliana* grown at low temperatures for five weeks were demonstrated to exhibit a cold acclimation induced enhancement of their photosynthetic performance relative to non-acclimated leaves, five weeks cold acclimated leaves from *at-rsz22a, at-scl30, at-rs40* and *at-ame3* mutants exhibited increases in excitation pressure of PSII (1-qL) which was associated with decreases in the proportion of light used in photochemistry (ϕ_{PSII}), linear electron transport rates (ETR) and increased heat dissipation (ϕ_{NPQ} and $\phi_{f,D}$) (Figure 3.3). Interestingly, *at-scl30* and *at-ame3* were drastically affected with respect to their ability to adjust their photosynthetic rates under exposure to cold acclimation conditions, as evidenced by their significantly lowered photochemical efficiency, linear electron transport rates and increased heat dissipation values when compared to wild type plants grown under similar conditions. These results led to the suggestion that this subset of SR proteins and At-AME3 might play an essential role in the post-transcriptional regulation and/or post-splicing activities of genes related to the photosynthetic adjustment of *Arabidopsis thaliana* undergoing cold acclimation. Moreover, quantifying the partitioning of the total amount of light absorbed by Photosystem II under

cold acclimation conditions has shown that *at-rsz22a*, *at-scl30, at-rs40* and mutant lines dissipate heat mostly through Photosystem II antennae, as evidenced by their higher antennae based quenching (ϕ_{NPQ}) values under cold acclimation conditions. These increased heat dissipation parameters through the PSII antennae were expected, as there is a growing body of evidence suggesting that non-photochemical quenching generally occurs within the PSII antenna pigment bed (Niyogi et al., 1998).

Conversely, only *at-ame3* mutants were found to dissipate excess energy within the reaction centre, based on their enhanced reaction centre quenching ($\phi_{f,D}$) values. These findings would suggest that in addition to hindering the photosynthetic performance under cold acclimation conditions, the deletion of *ame3* led to the use of an alternate method (reaction centre quenching) for dissipating excess light energy. While transgenic *Arabidopsis* lines impaired in the production of functional violaxanthin de-epoxidase (Li et al., 2000) were found to compensate for defects in NPQ by means of alternative mechanisms under cold acclimation conditions (Havaux and Kloppstech, 2001), no study has shown that Serine/Arginine-rich proteins, as well as LAMMER kinases, who are known to play an essential role in pre-mRNA metabolism, play a role in the cold acclimation induced recovery of photosynthesis in *Arabidopsis.*

In addition to the low temperature induced adjustment of photosynthetic performance occurring in cold hardy plants, exposure to low temperatures results in a variety of changes, including alterations in cell membrane fluidity (Nishida and Murata, 1996; Steponkus, 1984), the accumulation of various metabolites (Zhu et al., 2007) and proteins playing a cryoprotective role within the cell (Thomashow, 1999), resulting in an increase in freezing tolerance. Therefore, should At-RSZ22, At-SR34B, At-RSZ22A, At-SCL30, At-RS40, At-

RS41, as well as At-AME3 LAMMER kinase play a role in the acquisition of freezing tolerance occurring in *Arabidopsis thaliana* undergoing cold acclimation, it is expected that their deletion would have a negative effect on the capacity of these mutant lines to acquire freezing tolerance under prolonged exposure to low temperatures. Only *at-ame3* mutants appear to be jeopardized in their capacity to acquire freezing tolerance, based on LT_{50} values of leaves from *at-ame3* mutants exposed to cold acclimation conditions being comparable to its non-acclimated counterpart, as well as non-acclimated wild type *Arabidopsis thaliana* (Fig. 3.4). These results have led to the suggestion that At-AME3 LAMMER kinase plays a role in the acquisition of freezing tolerance in *Arabidopsis thaliana* undergoing cold acclimation.

One of the key modifications allowing the adaptation to a prolonged exposure to low temperatures involves the transcriptional activation and suppression of genes in response to low temperatures (Thomashow, 1999; Zhu et al., 2007). C-repeat (CRT)-binding factors (CBFs) are a fundamental part of the signaling cascade (Jaglo-Ottosen et al., 1998; Liu et al., 1998), leading to the induction of a variety of cold responsive genes including COR15A, COR15B, KIN1 and LTI78, which have been reported to play a role in the acquisition of freezing tolerance (Guy et al., 2008; Kurkela and Franck, 1990; Thalhammer et al., 2014; Trischuk et al., 2014). In addition to the expression of COR genes, another key factor in cold acclimation involves the accumulation of sugars, namely sucrose (Guy et al., 1992; Strand et al., 2003). This cold-induced stimulation of sucrose synthesis is correlated with an increase in sucrose phosphate synthase expression. If At-RSZ22, At-SR34B, At-RSZ22A, At-SCL30, At-RS40, At-RS41, as well as At-AME3 play a role in the transcriptional cascade leading to the induction of CBFs, SPS and COR genes, it was expected that their deletion would result

in alterations in the transcription profile of these genes. Only *at-ame3* mutants have shown attenuated transcript levels of key cold responsive genes involved in the transcriptional cascade associated with cold acclimation under control conditions, three weeks cold stress and five weeks cold acclimation conditions compared to wild type *Arabidopsis* (Fig. 3.5). This attenuation in the transcript level of cold responsive genes was associated with a decrease in dehydrins, COR15A and COR15B protein accumulation in *at-ame3* mutants compared to wild type *Arabidopsis thaliana* undergoing cold acclimation (Fig. 3.6) hereby supporting the inability for the acquisition of freezing tolerance observed in *at-ame3* mutants compared to wild type *Arabidopsis* (Fig 3.4).

Taken together, using chlorophyll a fluorescence measurements, in conjunction with electrolyte leakage freeze tests and transcription profile analyses of genes involved in the low temperature induced transcriptional cascade were used as screening tools to address the role of a subset of SR and LAMMER kinase mutant lines under control and cold acclimation conditions. Results from these analyses have led to the suggestion that At-RSZ22, At-RSZ22A, At-SCL30, At-RS40, and At-SR45 play a role in the cold acclimation induced recovery of photosynthesis, as their deletion had a negative effect on the recovery of photosynthetic performance typically observed in cold hardy plants undergoing cold acclimation to various degrees. While the deletion of this subset of Serine/Arginine-rich proteins has impaired their photosynthetic performance to varying degrees, their deletion was not associated with a disruption in their capacity to acquire freezing tolerance, as shown by electrolyte leakage freeze tests (Appendix Fig. A3.2), supported by the transcription profile analyses of key cold responsive genes associated with the low temperature induced transcriptional cascade. Due to the involvement of SR proteins in both constitutive and

alternative splicing (Ali and Reddy, 2008b; Reddy, 2001, 2007), as well as in mRNA transport and localization (Huang and Steitz, 2005; Huang et al., 2003), stability (Lemaire et al., 2002) and translation regulation (Sanford et al., 2005), it is possible that this subset of Serine/Arginine-rich proteins play a role either in the pre-mRNA regulation and/or post-splicing activities pertaining to the enhancement of photosynthetic performance, but not the acquisition of freezing tolerance, which are associated with long term growth and development at low temperatures.

Moreover, the deletion of At-AME3, a LAMMER kinase, has greatly jeopardized not only its photosynthetic performance, as evidenced by chlorophyll a fluorescence measurements, but also its capacity to acquire freezing tolerance, as shown by electrolyte leakage freeze tests and supported by the observed reduction in transcript levels of members of the CBF transcriptional pathway and SPS, in conjunction with the attenuation of dehydrins and COR15A/B protein accumulation under cold acclimation conditions. As there is a strong correlation between sucrose biosynthesis, photosynthetic performance and acquisition of freezing tolerance (Strand et al., 2003), the observed attenuation of SPS, in conjunction with the attenuated COR gene expression and subsequent decrease in dehydrin and COR15A/B protein abundance could provide an explanation with respect to the inhibition in photosynthetic performance recovery and failure in the acquisition of freezing tolerance observed in *ame3* mutants under cold acclimation conditions.

Phosphorylation has been shown to play a role in the splice site recognition of SR proteins (Zhong et al., 2009) and alternative splicing (Savaldi-Goldstein et al., 2003). Furthermore, as previous reports have indicated that At-AME3 is able to phosphorylate At-RSZ22 (Ahsan et al., 2013) and interact with At-RSZ21, At-SCL30, At-RS2Z33, At-SRPK4,

and At-SRPK-like 1 (STRING V10 (http://string-db.org); Arabidopsis Interactome Mapping Consortium, 2011; Szklarczyk et al., 2014) (Refer to Chapter 1), it is possible that this severe inhibition with respect to the photosynthetic adjustment occurring in cold acclimated plants, along with the acquisition of freezing tolerance occurring in *at-ame3* mutants can be attributed to a defect in the posttranslational regulation of SR proteins or other potential proteins involved either in the photosynthetic performance adjustment and/or the acquisition of freezing tolerance observed in *Arabidopsis* plants undergoing cold acclimation.

3.7 Conclusion

In conclusion, investigation of the potential involvement of SR proteins and associated kinases in the improvement of photosynthetic performance associated with cold acclimation has shown that *at-sr34* and *at-sr34b* do not play an essential role in the photosynthetic performance of *Arabidopsis thaliana*. Conversely, *at-rsz22* and *at-sr45* play an important role in the regulation of photosynthesis under non-acclimated, as well as under cold acclimation conditions. Furthermore, at-*rsz22a, at-scl30, at-rs41* and *at-ame3* play a crucial role in the cold acclimation induced adjustment of photosynthetic performance. Investigating the potential involvement of SR proteins of interest and At-AME3 kinase in the acquisition of freezing tolerance has shown that *ame3* plays a role in the acquisition of freezing tolerance, as this process was severely jeopardized in loss-of-function mutant lines. This finding was associated with an attenuated transcription profile of key cold responsive genes and subsequent protein abundance of COR15A/B and dehydrins. While these results have shown that the deletion of At-AME3 has a severe impact on two major processes occurring in plants undergoing cold acclimations, these findings raised several questions, namely, how do

LAMMER kinases affect both processes? Does this kinase interact with other SR proteins, or is it involved in the posttranslational regulation of non-SR proteins? To address the question as to whether At-AME3 interacts with SR proteins, future studies should involve yeast 2-hybrid assays (Refer to Chapter 5).

Chapter 4: The role of At-AME3 in the photosynthetic performance of *Arabidopsis thaliana* undergoing cold acclimation

Marc Rosembert, David P. Sprott

The growth and development of wild type plants, as well as *ame3* homozygous mutants under optimal growth conditions, in addition to low temperature conditions in order to compare the photosynthetic performance of these aforementioned plants with respect to maximal photochemical efficiency (Table 4.1), and to generate light response curves comparing the yield of Photosystem II (Φ_{PSII}), antenna (Φ_{NPQ}) and reaction centre ($\Phi_{f,D}$) based portion of non-photochemical quenching (Figure 4.4), linear electron transport rates (ETR), excitation pressure of PSII (1-qP), and combined ΔpH-dependent and ΔpH-independent non-photochemical quenching (qN) (Fig. 4.5) was performed by Marc Rosembert. Furthermore, basal quenching (qo) relative to non-photochemical quenching was assessed (Fig. 4.6). Marc has grown wild type plants, as well as *ame3* mutants under control and cold acclimation conditions in order to assess the effect of cold acclimation, as well as the deletion of *ame3* on Photosystem I (P_{700}) performance, presented in Table 4.3. The effect of the deletion of *ame3* on both stromal and intersystem electron pool sizes (Table 4.3), the reduction of the plastoquinone pool in darkness (Fig. 4.9) and the capacity of *ame3* mutants to undergo state transitions (Fig. 4.10) was also evaluated by Marc. While Marc Rosembert has performed RNA extractions, primer design and qPCR analyses monitoring PsbS, NDH-H, PGR5 and PTOX (Fig. 4.11) were done by David P. Sprott (AAFC). Marc has prepared samples from wild type *Arabidopsis*, as well as *ame3* mutants which were used to assess chlorophyll a and chlorophyll b content (Table 4.2). Furthermore, Marc has also worked on protein extractions and fractionations used in subsequent SDS-PAGE and Western blots comparing protein abundance of Photosystem II related proteins between wild type and *ame3* mutants under non-acclimated conditions, and after five weeks of cold acclimation (Fig. 4.12A). Moreover, these samples were used in the evaluation of the phosphorylation status of a subset of proteins associated with PSII (Fig. 4.12B), and the protein abundance of proteins associated with PSI (Fig. 4.12C). All statistical analyses presented in this chapter were done by Marc.

This chapter was written as a manuscript, in preparation for submission by Marc Rosembert, David P. Sprott, Jas Singh, Douglas A. Johnson and Leonid V. Savitch, titled **"Photosynthetic characterization of an *Arabidopsis* At-AME3 loss-of-function mutant undergoing cold acclimation".** I have written the first draft of this manuscript, and will work on subsequent revisions. Subsection 4.3, stating the hypotheses and research objectives of the study was added for the thesis.

4.1 Abstract

Exposure to low temperatures results in an imbalance between temperature insensitive and temperature sensitive processes associated with photosynthesis. Plants, however, have evolved various short term and long term mechanisms allowing them to restore photostasis. A LAMMER kinase mutant (*at-ame3*) was shown to be jeopardized with regards to two major processes, namely the cold acclimation induced recovery of photosynthetic performance, and the acquisition of freezing tolerance. These findings prompted a detailed photosynthetic characterization of this mutant undergoing cold acclimation. Results from this study have shown that after three weeks of exposure to low temperatures, *at-ame3* mutants exhibit enhanced excitation pressure (1-qL), heat dissipation via reaction center quenching ($\phi_{f,D}$), decreased fraction of energy used for photochemical processes (ϕ_{PSII}) and decreased linear electron transport rates (ETR) at the level of PSII performance. Decreased intersystem and stromal pool sizes were also observed. Moreover, unlike wild type *Arabidopsis thaliana*, cold acclimation conditions resulted in limitations with respect to photoprotective mechanisms such as state-1 state-2 transitions, cyclic electron transport via NDH-H and PGR5, and chlororespiration by means of PTOX-mediated electron transport. Prolonged exposure (five weeks of cold acclimation) to low temperatures exacerbated these trends. Limitations in Photosystem II performance and photoprotective mechanisms were associated with a decreased abundance of Photosystem II and Photosystem I light harvesting complex and reaction centre proteins.

4.2 Introduction

Photosynthesis involves the integration of extremely rapid biophysical and photochemical processes such as light absorption and subsequent energy transfer, with much slower biochemical redox reactions, which play a role in photosynthetic electron transfer, reduction of CO_2 and carbohydrate synthesis (Hüner and Grodzinski, 2011; Hüner et al., 2002).

ATP generated by means of proton motive force generated by Photosystems II and I is used in the fixation of CO_2 by means of catalytic enzymatic reactions via the Calvin cycle (reviewed in Ensminger et al., 2006; Hüner and Grodzinski, 2011; Hüner et al., 2013a). Under optimal growth temperatures, the slower, temperature sensitive biochemical reactions involved in CO_2 reduction, carbohydrate synthesis and export are capable of keeping pace with the much quicker, temperature independent photophysical processes of Photosystems II and I, which are responsible for absorbing and trapping light energy (Hüner and Grodzinski, 2011). This balance between temperature insensitive photochemical reactions (light reactions) and temperature sensitive biochemical reactions (carbon fixing reactions) is called photostasis (Ensminger et al., 2006; Hüner and Grodzinski, 2011; Wilson et al., 2006) (Figure 1.5A). Conversely, exposure to various abiotic stresses, including fluctuations in light irradiance, drought and low temperatures can result in an imbalance between the photochemical reactions of photosynthesis, and the biochemical reactions used in carbon fixing reactions which harvest the energy from photochemical reactions (Ensminger et al., 2006).

Exposure to low temperatures has been associated with the inactivation of ribulose-1,5-bisphosphate carboxylase (Rubisco), stromal fructose-1,6-bisphosphatase (sFBPase) and

sedoheptulose-1,7-biphosphatase both in chilling sensitive and chilling tolerant plant species (Strand et al., 1999), leading to a pronounced reduction in rates of the enzymatic reactions used in the reduction of CO_2 into triose phosphate. This in turn results in an over-reduction of the plastoquinone pool as well as other components of the intersystem electron transport pool (Hüner et al., 1998, 2013a). These changes, also known as excitation pressure, can be detected as an accumulation of closed PSII centres and quantified *in vivo* as an increase in 1-qP or 1-qL (Hendrickson et al., 2004; Hüner et al., 1998, 2013a). Conversely, a decrease in PSII activity is observed, as linear electron rates (ETR) and photosystem II photochemistry rates decrease under cold stress conditions (Hüner et al., 1993; Savitch et al., 2001, 2009) (Fig. 1.5B). If the absorbed energy exceeds both the capacity for non-photochemical quenching and the capacity for photochemistry, this can result in an accumulation of Reactive Oxygen Species (ROS), in turn leading to photooxidative damage and photoinhibition of Photosystem II and Photosystem I (Aro et al., 1993; Ivanov et al., 2012; Long et al., 1994; Savitch et al., 2001, 2011; Sonoike, 2011; Sonoike et al., 1997; Zhang and Scheller, 2004). However, plants have evolved a wide variety of mechanisms allowing them to restore photostasis, thus mitigating damages caused by this imbalance and maintaining an optimal electron flow.

One of the mechanisms used in restoring photostasis involves antennae-based non-photochemical quenching via the xanthophyll cycle (Hüner et al., 2008). PsbS, a Photosystem II subunit belonging to the light harvesting complex superfamily, also plays an essential role in dissipating excess energy (Hüner et al., 2008; Li et al., 2002). Reaction centre quenching is another method used to prevent further damage to other active PSII reaction centres (Ensminger et al., 2006; Ivanov et al., 2001; Krause and Weis, 1991).

State transitions provide a rapid (within minutes of exposure to high excitation pressure) means by which plants are able to adjust photosynthetic rates once exposed to these stresses involves a reduction in efficiency in the energy transfer to photosystem II by diverting energy to photosystem I (Ensminger et al., 2006; Lunde et al., 2000; Minagawa, 2011) (Refer to Section 1.3). Furthermore, on a longer time scale, the physical size of light harvesting complexes can be modulated by regulating the transcription and subsequent translation of *Lhcb* genes (Ensminger et al., 2006; Hüner et al., 2013b). Taken together, these mechanisms provide a means to reduce the amount of energy absorbed by Photosystem II (Horton et al., 2008; Hüner and Grodzinski, 2011).

At the level of Photosystem I, the water-water cycle, or Mehler reaction plays a photoprotective role by transferring excess electrons coming from Photosystem II back to O_2 (Asada, 1999). Photorespiration reduces photosynthetic performance by generating phosphoglycolate (2PG), which is eventually converted to 3-phosphoglycerate (3PGA), a Calvin cycle intermediate, via several enzymatic reactions 3PGA that consume ATP and NADPH. (Badger et al., 2000; Bauwe et al., 2010; Takahashi and Badger, 2011; Wingler et al., 2000) (Refer to Section 1.3). Cyclic electron transport by means of the NDH and PGR5 dependent pathways are thought to play a role in diverting excess energy through the generation of a proton motive force across the thylakoid membrane, in turn driving ATP synthesis, but not NADPH (Shikanai, 2007; Yamori et al., 2016).

Chlororespiration has been shown to take place via plant plastid terminal oxidase, or PTOX, which can catalyse the oxidation of plastoquinol and reduction of O_2 to H_2O. Furthermore, PTOX has been shown to increase in abundance under exposure to low temperatures, and has been shown to play a role as an alternate electron sink under exposure

to low temperatures (Ivanov et al., 2012; Vanlerberghe et al., 2015). Taken together, by diverting excess electrons not being used in carbon assimilation, both cyclic electron transport pathways, and the PTOX-dependent electron transport pathway play an important role in mitigating reactive oxygen species (ROS) formation. Cold acclimation conditions have been reported to be associated with a recovery of photosynthetic performance (Savitch et al., 2001; Strand et al., 1997, 2003), as well as an increased tolerance to photoinhibition (Sane, 2003) in *Arabidopsis*. This recovery of photosynthetic performance and enhanced tolerance to photoinhibition can be attributed in part to the short term photoprotective mechanisms (Fig. 1.5C), in addition to an observed elevation of the levels and/or activities of Calvin cycle enzymes and enzymes involved in cytosolic sucrose biosynthesis. Cold tolerant species such as *Arabidopsis thaliana* have been reported to upregulate the transcription and subsequent translation of Rubisco bisphosphatase (RuBP), as well as Sucrose Phosphate Synthase (SPS) and cytosolic fructose-1,6-bisphosphatase (cFBPase), which are involved in cytosolic sucrose and fructose biosynthesis, respectively (Holaday et al., 1992; Strand et al., 1999, 2003), as a long-term strategy used in the reduction of photostasis. Taken together, plants have evolved a variety of short and long term mechanisms allowing them to restore photostasis in response to abiotic stresses, including low temperatures.

A preliminary study has reported that *at-ame3* mutants were not only jeopardized in their ability to recover their photosynthetic performance under cold acclimation conditions, but in their capacity to acquire freezing tolerance (Refer to Chapter 3). While At-AME3 was suggested to play an important role in the cold acclimation response, these findings raised

questions as to the extent of limitations with respect to photosynthetic performance imposed by the deletion of At-AME3 kinase.

4.3 Hypotheses and objectives

For this study, it was hypothesized that *at-ame3* mutants are jeopardized with respect to their photosynthetic performance at the level of Photosystem II and Photosystem I under cold stress and acclimation conditions and 2) that photoprotective mechanisms are severely limited in *at-ame3* mutants.

The objective of this study consisted of gaining a better understanding of the limitations with respect to the cold acclimation induced recovery of photosynthetic performance observed in At-AME3 kinase mutants. This objective was attained by means of a detailed photochemical characterization of photosynthesis in *ame3* mutants undergoing cold acclimation, compared to wild type *Arabidopsis* grown and developed under the same conditions.

4.4 Materials and methods

4.4.1 Plant growth conditions

Seeds of wild type (ecotype Columbia) and transgenic *Arabidopsis thaliana* homozygous line CS835176 obtained from SALK (http://www.arabidopsis.org) containing a T-DNA insertion within the promoter region of At-AME3, a LAMMER-type protein kinase, were germinated in soil flats and seedlings were grown for four weeks in a Conviron E-15 cabinet under controlled environmental conditions with a temperature regime of 20°C/16°C (day/night), a 16-h photoperiod and a photon flux density (PFD) of 150 µmol

m^2s^{-1} for control (non-acclimating) conditions. Cold acclimated plants were obtained by transferring non acclimated, four week old plants to a temperature regime of 4°C/4°C (day/night) with light conditions identical to the control grown plants for three weeks and five weeks. During growth at low temperature, only new leaves developed at 4°C for three weeks and five weeks were considered cold acclimated.

4.4.2 Modulated chlorophyll a fluorescence measurements

4.4.2.1 PSII measurements

Chlorophyll fluorescence was measured from detached leaves from wild type *Arabidopsis thaliana* and *ame3* knockouts grown under control conditions, control conditions measured at 5°C, three weeks and five weeks cold acclimation conditions using a PAM-101 modulated fluorescence system (Heinz-Walz GmbH, Effletrich, Germany). Maximum fluorescence at closed PSII centres (F_m) were induced by means of a Schott KL1500 LCD lamp (Schott Glaswerke, Mainz, Germany) controlled by a Walz PAM 103 Trigger Control Unit (Heinz-Walz GmbH, Effletrich, Germany). For state transition measurements, a blue light source, consisting of a Schott KL1500 LCD lamp and a Kodak Wratten gelatin filter was used. Moreover, far red light was provided by a Schott RG715 filter, in conjunction with a Schott KL1500 LCD lamp.

All leaves were measured at ambient CO_2 levels. To measure non-acclimated leaves measured at 5°C as well as three weeks and five weeks cold acclimated samples, the measuring chamber was maintained at a temperature of 5°C by means of a circulating water bath. Leaves were dark adapted for 30 minutes, then F_o , which is defined as the lowest level of chlorophyll fluorescence and F_m, which is designated as the maximum level of fluorescence after a flash of 10,000 µmol photons m^2 s^{-1} is applied, causing reaction centres

to close and all the light energy to be given off as fluorescence. Following the first flash, actinic light of 215 µmol photons m^2 s^{-2}, or light capable of driving photosynthesis, was turned on. Light pulses of 10,000 µmol photons m^2 s^{-2}, with a duration of 800 ms were applied at 40 sec intervals, resulting in the closing of reaction centres. Transient increases in fluorescence, recorded as peaks on the fluorescence trace designate F_m`. Light pulses were applied until steady state, designated as $F_s$ and F`$_m$ was reached. At this point, actinic light was turned off, and F_o', which is determined as the minimal level of fluorescence after actinic light is turned off was measured (Fig. 4.2A). This process was then repeated using actinic light intensities of 350, 460, 700, 800 and 1100 µmol photons m^2 s^{-2}.

The nomenclature of van Kooten and Snel (1990) was used to define chlorophyll fluorescence parameters. The excitation pressure of PSII, or the relative reduction state of Photosystem II at the growth temperature and growth irradiance measured was designated as 1-qP (Hüner et al., 1998), and calculated using the following equation:

$$1 - qP = 1 - \frac{F_m` - F_s}{F_m` - F_0`} \quad (1)$$

ΔpH-dependent and ΔpH-independent non-photochemical quenching, designated as qN, was calculated using the following equation:

$$qN = 1 - \frac{F_m` - F_0`}{F_m - F_0} \quad (2)$$

Moreover, basal quenching, which reflects antenna quenching, denoted as q_0, was calculated using the following equation:

$$q_0 = \frac{F_0 - F_0`}{F_0} \quad (3)$$

The model proposed by Hendrickson et al. (2004) for the partitioning of absorbed light energy was used to estimate the allocation of photons absorbed by the Photosystem II (PSII) antennae for photosynthetic electron transport and PSII chemistry, or yield of PSII, designated as:

$$\Phi_{PSII} = (F_m^{`} - F_s)/F_m^{`} \qquad (4)$$

Moreover, the quantum efficiencies of regulated ΔpH- and/or xanthophyll-dependent non-photochemical dissipation processes within the PSII antennae, or antennae based quenching, designated as Φ_{NPQ}, were calculated using the following equation:

$$\phi_{NPQ} = \frac{F_s}{F_m^{`}} - \frac{F_s}{F_m} \qquad (5)$$

Additionally, $\phi_{f,D}$ can be used to quantify the fraction of light absorbed by PSII antennae that is emitted as heat by the reaction centre, otherwise known as reaction centre quenching, using the following equation, also proposed by Hendrickson et al (2004).

$$\phi_{f,D} = \frac{F_s}{F_m} \qquad (6)$$

The operating efficiency of PSII (ϕ_{PSII}) was used to estimate the linear electron transport rate (ETR), using the following equation:

$$ETR = \Phi_{PSII} \times PPFD \times A_{leaf} \times fraction_{PSII} \qquad (7)$$

Where PPFD represents the photosynthetically active photon flux density, or light intensity incident on the leaf. As 84% of incident PPFD is assumed to be absorbed by mature green leaves, A_{leaf} is assumed to be 0.84. Similarly, $fraction_{PSII,}$ representing the percentage

of light absorbed by photosystem II is frequently assumed to be 0.5, as light is assumed to be absorbed equally by Photosystems I and II (Baker, 2008; Maxwell and Johnson, 2000; Murchie and Lawson, 2013).

The extent of post-illumination transient increases in fluorescence once $F`_o$ is reached can be used as an estimate of the reduction of the plastoquinone pool in the absence of light by stromal reductants (Farineau, 1999; Ivanov et al., 2006; Mano et al., 1995; Savitch et al., 2011). Therefore, the reduction state of the plastoquinone pool in detached leaves of wild type *Arabidopsis*, as well as *ame3* mutants was assessed by monitoring the post-illumination transient increase in chlorophyll a fluorescence in darkness at the aforementioned growth conditions (Fig. 4.2B).

The capacity to undergo state transitions was measured as described by Lunde et al. (2000) and Ivanov et al., (2006). Leaves were dark adapted for 30 minutes, and state 2 was induced by exposing the dark-adapted leaves to a blue light at a light intensity of 80 µmol photons $m^{-2}s^{-1}$ favoring PSII for 15 minutes (Fig. 4.2C). Far-red light, which favors PSI, was then superimposed to the blue light in order to induce state 1. After 20 minutes the maximum fluorescence yield in state 1 ($F_m`1$) was determined. The far red light was then turned off, inducing state 2. After 20 minutes in the presence of blue light, the maximum fluorescence yield in state 2, or $F_m`2$ was measured. The relative change in state transition, ΔF was calculated as follows:

$$\Delta F = \left[F_m`1 - F_m`2/F_m`1\right]x100 \qquad (8)$$

Figure 4.1: Representative traces of modulated chlorophyll a fluorescence measurements.

A typical chlorophyll fluorescence trace used in the generation of light response curves is depicted in Panel A. A far-red dim light is turned on to measure background fluorescence with all PSII centres opened in the absence of light, or F_o. A saturating flash of light is then applied, causing all of the PSII reaction centres to be closed. This allows the measurement of the maximum fluorescence level in darkness (F_m). A light is then turned on at this point to drive photosynthesis, with saturating flashes of light at an intensity of 10, 000 µmol m^{-2} s^{-1}, at a certain interval that is determined by the user. Fluorescence traces will eventually reach a point called steady state, where F_s remains constant, and the saturating flashes of light ($F`_m$) will be measured at approximately the same intensity. Once steady state is reached, the light is turned off (AL light off), which allows to measure the background fluorescence in darkness after exposure to light, $F`_o$. Furthermore, transient increases in modulated chlorophyll a fluorescence in the absence of light, highlighted in Panel B, was used to assess the reduction state of the plastoquinone pool by stromal reductants. A chlorophyll fluorescence trace used in the assessment of the capacity to undergo state transitions is represented in Panel C. Leaves were dark adapted for 30 minutes, and state 2 was induced by exposing the dark-adapted leaves to a blue light at a light intensity of 80 µmol photons $m^{-2}s^{-1}$ favoring PSII for 15 minutes . Far-red light, which favors PSI, was then superimposed to the blue light in order to induce state 1. After 20 minutes the maximum fluorescence yield in state 1 ($F_m`1$) was determined. The far red light was then turned off, inducing state 2. After 20 minutes in the presence of blue light, the maximum fluorescence yield in state 2, or $F_m`2$ was measured.

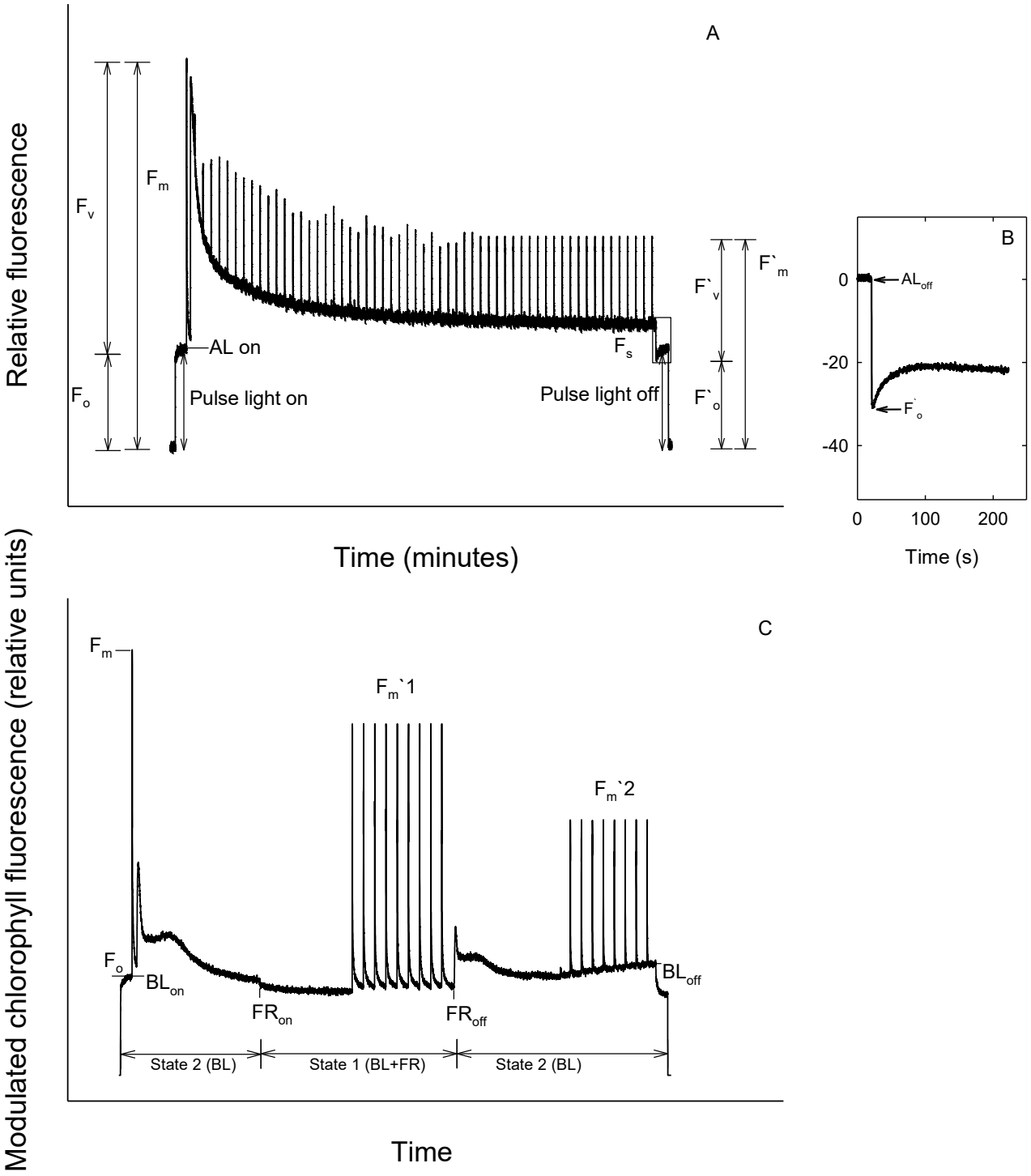
A
Relative fluorescence
F_v
F_m
F_o
AL on
Pulse light on
F_s
Pulse light off
$F`_v$
$F`_m$
$F`_o$
Time (minutes)
B
0
-20
-40
AL_{off}
$F`_o$
0
100
200
Time (s)
C
Modulated chlorophyll fluorescence (relative units)
F_m
$F_m`1$
$F_m`2$
F_o
BL_{on}
FR_{on}
FR_{off}
BL_{off}
State 2 (BL)
State 1 (BL+FR)
State 2 (BL)
Time

4.4.3 P_{700} absorbance measurements

All measurements were performed using a PAM-101 modulated fluorescence system (Heinz Walz, Effletrich, GmbH), equipped with a ED-P700DW dual wavelength emitter-detector, as well as a PAM-102 detection unit (Klughammer and Schreiber, 1991, Ivanov et al., 1998, Savitch et al., 2011). Far-red light was provided by a Schott KL-1500 LCD lamp, in conjunction with a Schott RG715 red light filter (λ_{max}=715nm, 10Wm^{-2}). Single turnover (ST) saturating flashes, followed by multiple turnover (MT) saturating flashes (50ms), were applied using the XST-103 and XMT-103 power/control units (Heinz Walz, GmbH), respectively.

4.4.3.1 Steady-state oxidation of Photosystem I (P_{700})

Leaves from wild type *Arabidopsis*, as well as At-AME3 kinase knockouts grown under control, cold stress and cold acclimation conditions were used to assess the extent of P_{700} (PSI) photooxidation *in vivo* by measuring the absorbance change at 820nm. These changes in absorbance, which are observed as an increase in absorbance in the presence of far red light, and labeled as ΔA_{820}, reflect the oxidation of P_{700} to P_{700}^{+} (Schreiber et al, 1998) (Fig 4.2A,C). Once steady state oxidation has been reached, a single turnover (ST) flash was applied. Once steady state was reached, a multiple turnover (MT) flash was applied. Once steady state was reached, the actinic light was turned off. The reduction kinetics of P_{700}^{+} in darkness, which has been shown to reflect cyclic electron transport rates around Photosystem I (Maxwell and Biggins, 1976), as well as the interaction between of stromal components with the intersystem electron chain (Asada et al., 1992) (Fig. 4.2A). The rate of P_{700}+

reduction in darkness, measured as $t_{1/2}$, was measured as the amount of time taken for the absorbance trace to reach the halfway point between steady state absorbance and basal absorbance. The area between the oxidation curve of P_{700} after single turnover and multiple turnover excitation and the stationary level of P_{700}+ under far-red light illumination represent the single turnover and multiple turnover areas, which were used to assess the intersystem electron pool size, as described by Asada et al., (1992) and Ivanov et al., (1998). The following equation was used to assess intersystem electron pool size:

$$e^{-}/P_{700} = {}^{MT_{area}}/_{ST_{area}} \quad (9)$$

The functional pool size of electrons that can be donated to P_{700}+ from stromal sources was estimated by defining the areas between the stationary level of P_{700}+ under illumination under FR light and the oxidation curve of P_{700} by FR light after a MT flash (MT), as well as after the illumination with actinic light (AL), as described by Asada et al. (1992) and Savitch et al., (2001) (Fig. 4.2C). All stromal pool size measurements were achieved using the following equation:

$$Stromal\ e^{-}pool/P_{700} = (MT_{area}/ST_{area}) \times [(AL_{area}/MT_{area}) - 1] \quad (10)$$

Single turnover area (ST_{area}) measurements were extracted from traces used in the assessment of intersystem pool sizes. Moreover, the contribution of linear electron transport from Photosystem II in the reduction of P_{700} was assessed by measuring the amount of photooxidation induced by actinic light in the presence and absence of 3-(3`,4`-dichlorophenyl)-1,1-dimethylurea (DCMU). DCMU prevents electron donation from Photosystem II to Photosystem I by inhibiting Photosystem II. Detached leaves from wild type *A. thaliana* as well as *ame3* transgenic lines grown under control, three weeks and five

weeks of cold acclimation were vacuum infiltrated with 20 μM DCMU twice for a duration of 10 minutes per incubation (Fig. 4.2B). P_{700} oxidation was induced using actinic white light, at a light irradiance of 500umol photons $m^{-2}s^{-1}$, either in the presence or absence of 20uM DCMU, and evaluated as the change in absorbance occurring at 820nm ($\Delta A_{820\text{-}860}$). All ratios were calculated using the following equation:

$$Ratio\ \Delta A_{820-860}(+DCMU)/\Delta A_{820-860}(-DCMU) = \left(\frac{\Delta A_{820-860}(+DCMU)}{\Delta A_{820-860}(-DCMU)}\right)\times 100 \quad (11)$$

The effects of the deletion of At-AME3 kinase, as well as low temperatures on transient electron flow arriving from PSII was measured by monitoring the reduction and subsequent re-oxidation of P_{700}^{+} by means of a single turnover flash of white light (Losciale et al., 2008; Savitch et al., 2009).

Figure 4.2: Representative P_{700} traces highlighting PSI measurements.

Panel A represents a typical P_{700} absorbance trace used in the determination of P_{700} absorbance estimation of the intersystem electron pool size. Panel B depicts P_{700} traces used to determine the contribution of Photosystem II in linear electron transport. Panel C depicts traces used in the estimation of the stromal pool size.

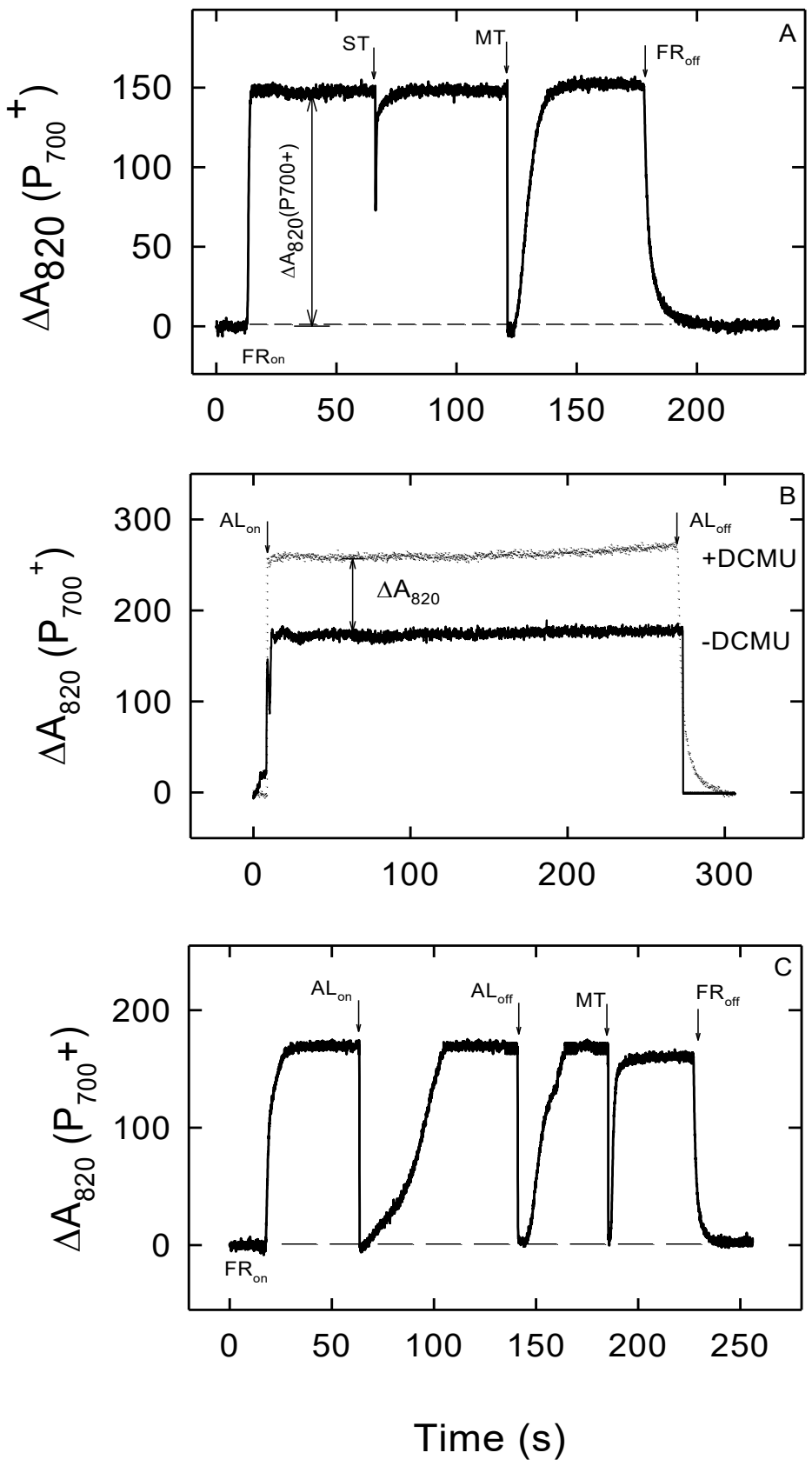
A
ST
MT
FR$_{off}$
FR$_{on}$
$\Delta A_{820}(P700+)$
ΔA_{820} (P_{700}^+)
150
100
50
0
0
50
100
150
200
B
AL$_{on}$
AL$_{off}$
+DCMU
-DCMU
ΔA_{820}
ΔA_{820} (P_{700}^+)
300
200
100
0
0
100
200
300
C
AL$_{on}$
AL$_{off}$
MT
FR$_{off}$
FR$_{on}$
ΔA_{820} (P_{700}^+)
200
100
0
0
50
100
150
200
250
Time (s)

4.4.4 qPCR analysis of photosynthesis related genes

RNA used for qPCR analyses were extracted using a phenol/guanidine isothiocyanate solution (TRIzol® Reagent, Life Technologies) and chloroform, according to the manufacturer's instructions. DNAse treatments were carried out using the Invitrogen Ambion DNAse I (Burlington, ON, Canada) according to the manufacturer's instructions. Sample quality ($A_{260/280}$) and yield were assessed using the Pharmacia Biotech GeneQuant RNA/DNA Calculator (Cambridge, England). cDNA synthesis was done suing the qScript cDNA Synthesis Kit (Quanta Biosciences, Gaithersburg, MD) using 1 µg of mRNA template. The qScript cDNA SuperMix contains a mixture of oligo dT and random oligo primers. Quantitative PCR analyses were done to assess the expression levels of PsbS (AT1G44575) (F: 5`-TCT TGT TCA CTC TGT TGG GAG CCA -3`) (R: 5`-GTT CGG CTT CGT GAA CCC AAA CAA-3`), NDH-H (ATCG01110) (F: 5`-AGA ACG GGT TGA AGG AGT TGG GAT-3`) (R: 5`-ACG AAC ATC CCA TGG TAT TCC GGA TG-3`), PGR5 (AT2G05620) (F:5`-AGC CAT TGG CTT ACA CTC TCA GGT-3`) (R:5`-AGC CTG ATA AGC CCT TGT CTC TGT-3`) and PTOX (AT4G22260) (F:5`-TTC TGG CTC AGC ACA TAG CAA CCT-3`) (R:5`-TGC ATG ACT CTC CAC ACA TTC CGA-3`) in leaves from wild type *Arabidopsis thaliana* and *ame3* knockouts grown under control and cold acclimation conditions. PCR optimization steps ($MgCl_2$ gradient and annealing temperature gradient), using cDNA from non-acclimated wild type *Arabidopsis thaliana* as a template and the primer pairs indicated above were also carried out as described in Chapter 2. To ensure that amplification that was observed is not due to DNA contamination, PCR reactions with no RT templates (non-RT) were also performed (data not shown).

All qPCR reactions were carried out using Applied Biosystems SYBR® Green PCR Master Mix (2x) in accordance with the manufacturer's instructions. Amplification was performed using a StepOne Plus Real-Time PCR System (Applied Biosciences). The amplification cycles were carried out as follows: the initial denaturing step was done at 95°C for 10 minutes, followed by 40 cycles at 95°C for 15 seconds for denaturation, 60°C for 45 seconds for annealing, and extensions were done at 72°C for 1 minute. The data was then analyzed using StepOne software version 2.2.

4.4.5 Composition and abundance of photosynthesis related proteins

Samples used for total protein extracts and subsequent SDS-PAGE gel analyses were homogenized in 5.2mL of buffer (20mM Tricine pH8.4, 10mM EDTA, 20mM $MgCl_2$, and 20mM KCl, 20mM PMSF, 20mM Benzamidine, 20mM DTT, 10mM 2-Mercaptoethanol, 20mM Sodium Fluoride, protease inhibitor cocktail) using a glass homogenizer (Corning). Samples used in chlorophyll content analyses were homogenized using the same homogenization buffer. An aliquot (200µL) of the homogenized sample was transferred to a microcentrifuge tube containing 800µL of ice-cold acetone to a final concentration of 80% in order to assess chlorophyll concentrations, as described by Porra et al. (1989). Once chlorophyll concentrations were assessed, using a Thermo-Fisher Evolution 3000 UV-visible spectrophotometer, samples were re-suspended and solubilized in homogenization buffer with 2% (v/v) SDS to a final concentration of 1µg/µL of chlorophyll.

Solubilized samples containing equal amounts of chlorophyll (20 µg per lane) were loaded into discontinuous polyacrylamide gel systems consisting of 4% (w/v) stacking and 12.5% (w/v) separating gels. Electrophoresis was performed using a Mini-Protean II apparatus (Bio-Rad) at a constant voltage of 100V for approximately 2.5h, until the dye front

had run off the gel. The Kaleidoscope prestained protein standards (BioRad) was used as a molecular marker. To ensure equal protein loading, and sample integrity, an aliquot of each sample was added to 6X loading buffer (50 mM Tris-HCl, 0.002% Bromophenol Blue, 2.5% Glycerol, 2% SDS, and 143 mM 2-Mercaptoethanol), and loaded on discontinuous polyacrylamide gel systems consisting of 4% (w/v) stacking and 12.5% (w/v) separating gels. Electrophoresis was performed using a Mini-Protean II apparatus (Bio-Rad) at a constant voltage of 100 V for approximately 2.5 h, until the dye front had run off the gel. The gel was incubated overnight in a Coomassie Blue staining solution (0.1% (w/v) Coomassie G-250 (Bio-Rad), 10% (v/v) Acetic acid, 50% (v/v) Methanol), then destained for three hours in a destaining solution (40% (v/v) Methanol, 10% (v/v) acetic acid), with gentle agitation, until the background staining is removed. Visual inspection of the large subunit of Rubisco (RBCSL) was used as a reference protein to ascertain equal loading, and are unavailable.

SDS-PAGE gels that were used for immunoblotting were transferred from the gel onto an Immun-Blot PVDF membrane (0.2µm pore size; Bio-Rad) using the mini Protean Tetra system from Bio-Rad at a constant voltage of 100V for 1.5 hours, at 4°C. Once the transfer has finished, membranes were incubated overnight in 2% ECL Advance Blocking Agent (GE/Amersham Biosciences) in TBS 0.1% Tween-20. The membranes were subsequently probed with antibodies raised against PsbA (D1), PsaA/B, PsbS, ATPase, Photosystem-II associated light harvesting proteins (Lhca1, Lhca2, Lhca3 and Lhca4) and Photosystem-I associated light harvesting proteins (Lhcb1, Lhcb2, Lhcb3, Lhcb4, Lhcb5 and Lhcb6) (Agrisera, Sweden). Moreover, membranes were probed with antibodies raised against ELIP and PTOX/IMMUTANS proteins. The dilutions used for primary antibodies were 1:3000 for D1, 1:3000 for PsaB, 1:3000 for PsbS, 1:5000 for ATPase, 1:3000 for all

PSII light harvesting proteins (Lhca1-Lhca4) and 1:5000 for all PSI light harvesting proteins. To assess the phosphorylation pattern of D1 and LHCII (Photosystem II light harvesting complex) polypeptides, some membranes were probed with a polyclonal anti-rabbit phosphoaminocid (Phosphothreonine, PhThr) antibodies, at a dilution of 1:2000 (Zymed Laboratories, Inc., San Fransisco, CA, USA). All membranes were incubated for an hour at room temperature, followed by two 15 minute washes. The blots were subsequently incubated in 2% blocking buffer with either goat anti-rabbit or rabbit anti-chicken IgG secondary antibodies, conjugated with horseradish peroxidase, at dilutions ranging from 1:20 000 to 1:100 000 when using ECL chemiluminescent detection systems, or 1:3 000 000 when using ECL advance as a chemiluminescent detection system. Blots were incubated for 1 hour, followed by 2 15-minute washes in 1X TBST. Amersham ECL Prime Western blotting detection reagents (GE Healthcare/Amersham Pharmacia Biotech, Buckinghamshire, UK) were used to visualize PTOX and PsbS polypeptides, whereas Amersham ECL Western blotting reagents were used for the detection of the remaining polypeptides.

4.4.6 Statistical analyses

For chlorophyll a fluorescence measurements, five leaves were collected at random from wild type *Arabidopsis*, as well as *ame3* mutants grown under control conditions, under control conditions, but measured at 5°C, for plants grown and developed at low temperatures (4°C) for three weeks and five weeks, while control and five weeks cold acclimated samples were harvested for state-1 state-2 transition measurements. Each collected leaf was considered a technical replicate, where each leaf collected for one experiment was considered a biological replicate. Therefore, chlorophyll a fluorescence experiments are representative of leaf tissue collected from fifteen different plants. Modulated chlorophyll a fluorescence

was first measured at 20°C, using different light intensities in order to generate a light response curve for various parameters, such as the linear electron transport rate, and photochemical efficiency. This data was then compared with plants that were also grown at 20°C, but measured at 5°C, as well as newly developed, cold acclimated leaves from plants that have remained at 5°C for three and five weeks.

For chlorophyll content measurements, 4 leaves were harvested at random from wild type *Arabidopsis* and *ame3* mutants grown under optimal growth conditions, after three weeks of cold acclimation, and after five weeks of cold acclimation. Each leaf was considered a technical replicate. This experiment was performed in duplicate, for a total of 8 leaves measured.

For P_{700} measurements, six leaves were collected at random from wild type *Arabidopsis* and *ame3* mutants grown under control conditions, under control conditions, but measured at 5°C, for plants exposed to low temperatures for three and five weeks. Leaves collected at random were represented as technical replicates, repeated in triplicate. Furthermore, each experiment was considered a biological replicate, for a total of 18 leaves used for P_{700} measurements. All chlorophyll fluorescence measurements, P_{700} measurements, state transitions, and chlorophyll fluorescence decay results were analyzed for variance by means of one-way ANOVAs. Subsequently, Tukey's Honest Significant Difference was used as a post-hoc statistical analysis to determine means that are significantly different from each other. All statistical analyses were done in R version 3.1.0.

4.5 Results

4.5.1 Effect of cold stress, acclimation and ame3 mutation on the maximal photochemical efficiency, linear electron transport rates, non-photochemical quenching, energy partitioning and chlorophyll content

Initial chlorophyll fluorescence measurements (Refer to Table 4.1) have shown that prolonged exposure (5 weeks) to low temperatures have led to a recovery in maximal photochemical efficiency (F_v/F_m) in cold acclimated wild type *Arabidopsis*, as values were comparable to non-acclimated wild type *Arabidopsis*. In contrast, maximal photochemical efficiency of non-acclimated *ame3* mutants were comparable to non-acclimated *Arabidopsis*. Prolonged exposure to low temperatures, however, have led to significant photoinhibition, as evidenced by a sharp decrease in F_v/F_m values in cold acclimated *ame3* mutants relative to non-acclimated *ame3* (Table 4.1). These findings prompted a chlorophyll content comparison between wild type and *ame3* undergoing cold acclimation.

A 36% decrease in total chlorophyll content was observed in cold acclimated leaves developed at low temperatures for three weeks (Table 4.2). Although a decrease in total chlorophyll content was observed, this was not associated with a decrease in Chl a/Chl b ratio, as a marginal decrease (5%) was observed in three weeks cold acclimated *Arabidopsis* samples. Five weeks exposure to low temperatures have led to a sharp increase (48%) in chlorophyll content in five weeks cold acclimated leaves compared to three weeks cold acclimated wild type leaves (Table 4.2). Furthermore, no changes in the chlorophyll a/chlorophyll b ratio were observed after five weeks of cold acclimation relative to three

weeks cold acclimated samples. In comparison, a 16% decrease in total chlorophyll content was observed in non-acclimated *ame3* mutants relative to non-acclimated *Arabidopsis*. Chl a/Chl b ratios were comparable to non-acclimated wild type (Table 4.2). Exposure to low temperatures led to a 50% decrease in total leaf chlorophyll content compared to non-acclimated *ame3*. While prolonged exposure to low temperatures was associated with a recovery of chlorophyll content in wild type *Arabidopsis*, cold acclimation conditions have led to a pronounced decrease (72%) in chlorophyll content compared to cold acclimated wild type *Arabidopsis*. Moreover, this was associated with a decrease in antennae size, seen as an increase in Chl a/Chl b ratio (Table 4.2).

Energy partitioning comparisons between wild type and *ame3* mutants have shown that non-acclimated leaves from *Arabidopsis thaliana* measured at 5°C exhibit a decrease in energy used in photochemical processes (Φ_{PSII}) (Fig. 4.3A). A similar trend was also observed in *ame3* mutants (Fig. 4.3B). This decrease in energy used in photochemical processes was associated with an increase in antennae based non photochemical quenching (Φ_{NPQ}) (Fig. 4.3C-D), and marginal changes in reaction centre based quenching ($\Phi_{f,D}$) (Fig. 4.3E-F) in both wild type and *ame3* mutants. Exposure to low temperatures for three weeks has resulted in an overall increase in the proportion of total energy used for photochemistry (Φ_{PSII}) in cold acclimated leaves grown and developed for three weeks at 5°C of wild type *Arabidopsis*, leading to an overall decrease in antenna-based non-photochemical quenching. In accordance with previous observations, prolonged exposure to low temperatures have led to a recovery in terms of energy partitioning, as cold acclimated leaves grown and developed at 5°C for five weeks can divert more energy towards photochemistry, resulting in a greater decrease in antennae based non-photochemical quenching (Φ_{NPQ}) compared to three weeks

cold acclimated wild type samples. It should be noted that marginal changes in reaction centre quenching was observed under every condition tested (Fig. 4.3E). While cold acclimation conditions have led to a gradual recovery in wild type *Arabidopsis*, this trend was not observed in *ame3* mutants, as three weeks cold acclimated leaves were observed to possess an attenuation in the proportion of energy used for photochemistry (Fig. 4.3B). Interestingly, in contrast to wild type *Arabidopsis* these results were associated with a drastic increase in reaction centre ($\Phi_{f,D}$) based quenching (Fig. 4.3F) and marginal changes in antenna based quenching (Fig. 4.3D) relative to non acclimated samples measured at 5°C.

The observed decrease in the proportion of energy used in photochemistry in non-acclimated wild type *Arabidopsis* leaves at 5°C was associated with significant decreases with respect to linear electron transport rates (ETR) in both wild type *Arabidopsis* (Fig. 4.4A) and *ame3* mutants (Fig. 4.4B). Conversely, an increase in excitation pressure of PSII (1-qP) (Fig 4.4C-D) and combined ΔpH-dependent and ΔpH-independent non-photochemical quenching (qN) (Fig. 4.4E-F) was observed when compared to control conditions in both wild type *Arabidopsis* and *ame3* mutants at every light intensity tested. Newly developed, cold acclimated leaves from wild type *Arabidopsis* that have been exposed to low temperatures (5°C) for three weeks show a reversal of the trends observed, as the linear electron transport rates (ETR) increased, while excitation pressure of PSII (1-qP) was observed to decrease relative to non-acclimated leaves measured at 5°C.

Table 4.1: Comparison of maximal photochemical efficiency (F_v/F_m) of wild type *Arabidopsis* and *ame3* kinase mutants under non-acclimated and after five weeks of cold acclimation.

All measurements were performed at a light irradiance of 350 PPFD. Asterisks denote a statistically significant difference between non-acclimated and cold acclimated controls, with a p-value that is less than or equal to 0.01 ($P \leq 0.01$), as determined by post-hoc Tukey Honest Significant Difference analyses

Growth conditions	WT	*ame3*
Non-acclimated	0.806 ± 0.003	0.796 ± 0.002
5w CA	0.798 ± 0.007	0.393 ± 0.053***

Table 4.2: Leaf chlorophyll/weight (µg/g) ratio comparison between wild type *Arabidopsis thaliana* and *ame3* knockouts grown under control and cold acclimation conditions.

Asterisks denote statistically significant differences between wild type samples and *ame3* mutants, based on Tukey's Honest Significant Difference analyses (**= p-value ≤ 0.05, *** = p value ≤ 0.01)

	Chl a	Chl b	Leaf chlorophyll content (µg/g fresh weight)	Chl a/Chl b ratio
WT Control	736 ± 79	210 ± 24	946 ± 39	3.51 ± 0.03
***ame3* Control**	619 ± 48	178 ± 5	796 ± 23	3.43 ± 0.04
WT 3w CA	515 ± 25	154 ± 16	668 ± 31	3.36 ± 0.06
***ame3* 3w CA**	311 ± 23**	89.6 ± 16**	401 ± 28**	3.35 ± 0.09
WT 5w CA	993 ± 42	289 ± 14	1281 ± 55	3.53 ± 0.05
***ame3* 5w CA**	282 ± 25***	72.3 ± 8.5***	354 ± 33***	4.03 ± 0.09

Figure 4.3: Effects of photon flux density on the yield of photosystem II , antenna-based portion of non-photochemical quenching, and PSII reaction centre-based portion of non-photochemical quenching within thylakoid membranes of *Arabidopsis thaliana* and *at-ame3* mutants grown under non acclimated, cold stress, and acclimation conditions.

Leaves from wild type (A, C, E) and *at-ame3* (B,D,F) mutants grown under non-acclimated (white circles), non acclimated, measured at 5°C (grey circles), three weeks (black triangles) and five weeks cold acclimated (black squares) conditions were used in the assessment of the effect of photosynthetic photon flux density on the yield of photosystem II (Φ_{PSII}), antenna-based portion of non-photochemical quenching (Φ_{NPQ}), and PSII reaction centre-based portion of non-photochemical quenching ($\Phi_{f,D}$). Each light response curve is representative of five leaves harvested at random per batch from either wild type *Arabidopsis* or *at-ame3* mutant lines, repeated three times, for a total of fifteen individual chlorophyll fluorescence runs (n=15 ± SE).

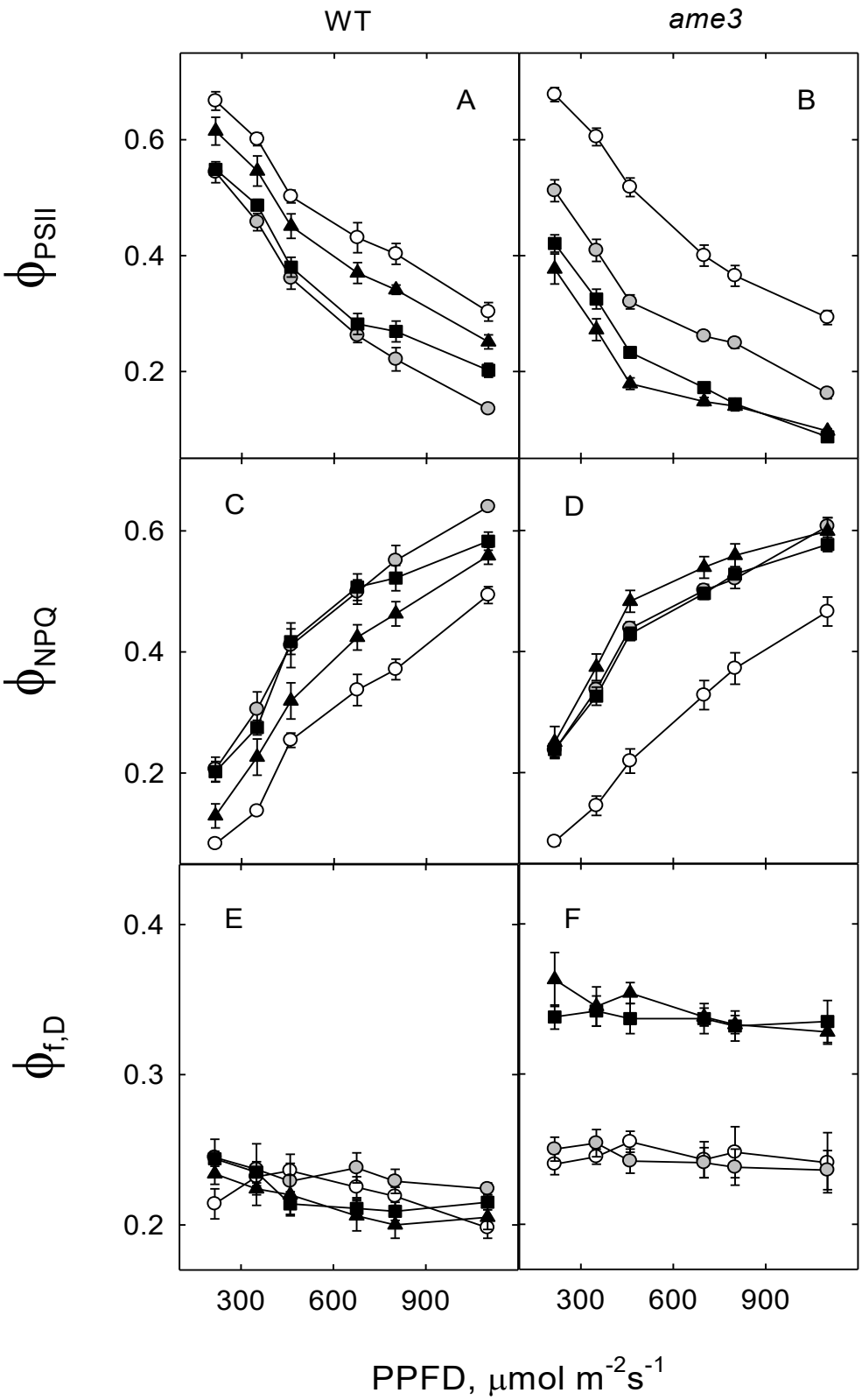
WT
ame3
A
B
C
D
E
F
ϕ_{PSII}
ϕ_{NPQ}
$\phi_{f,D}$
0.6
0.4
0.2
0.3
300
600
900
PPFD, μmol $m^{-2}s^{-1}$

Similar trends were not observed in three weeks cold acclimated leaves from *ame3* mutants, as they exhibited decreased linear electron rates (ETR), increased excitation pressure (1-qP) and marginal changes in total heat dissipation parameters (qN) compared to non acclimated leaves measured at 5°C. Extended exposure (5 weeks) to low temperatures have resulted in a stronger recovery relative to three weeks cold acclimated samples, as evidenced by linear electron transport rates (ETR) being closer to those of non-acclimated leaves in wild type *A. thaliana*. Consequently, this led to similar observations with respect to the excitation pressure of PSII (1-qP) and combined non-photochemical quenching (qN) parameters. In contrast, prolonged exposure to low temperatures have exacerbated the limitations observed in cold acclimated leaves of *ame3* mutants, as evidenced by the even greater suppression in linear electron transport rates (Fig 4.4A) and increased excitation pressure (1-qP) (Fig. 4.4D). It should be noted that while prolonged exposure to low temperatures did not increase total heat dissipation (qN) (Fig. 4.4F) values, it did have an effect on the distribution of heat dissipation as more energy was dissipated via reaction centre quenching ($\Phi_{f,D}$) relative to antenna based quenching (Φ_{NPQ}).

Figure 4.4: Effects of the deletion of At-AME3 on linear electron transport rates, excitation pressure of Photosystem II and combined non-photochemical quenching within thylakoid membranes of *Arabidopsis thaliana* under non-acclimated, cold stress, and acclimation conditions.

Leaves from wild type (A, C, E) and *at-ame3* (B, D, F) mutants grown under non-acclimated (white circles), non-acclimated plants measured at 5°C (grey circles), three weeks (black triangles) and five weeks cold acclimated (black squares) conditions were used in the assessment of photon flux density on linear electron transport rates (ETR), excitation pressure of PSII (1-qP), and combined ΔpH-dependent and ΔpH-independent non-photochemical quenching (qN). Each light response curve is representative of five leaves harvested at random per batch from either wild type *Arabidopsis* or *at-ame3* mutant lines, repeated three times, for a total of fifteen individual chlorophyll fluorescence runs (n=15±SE).

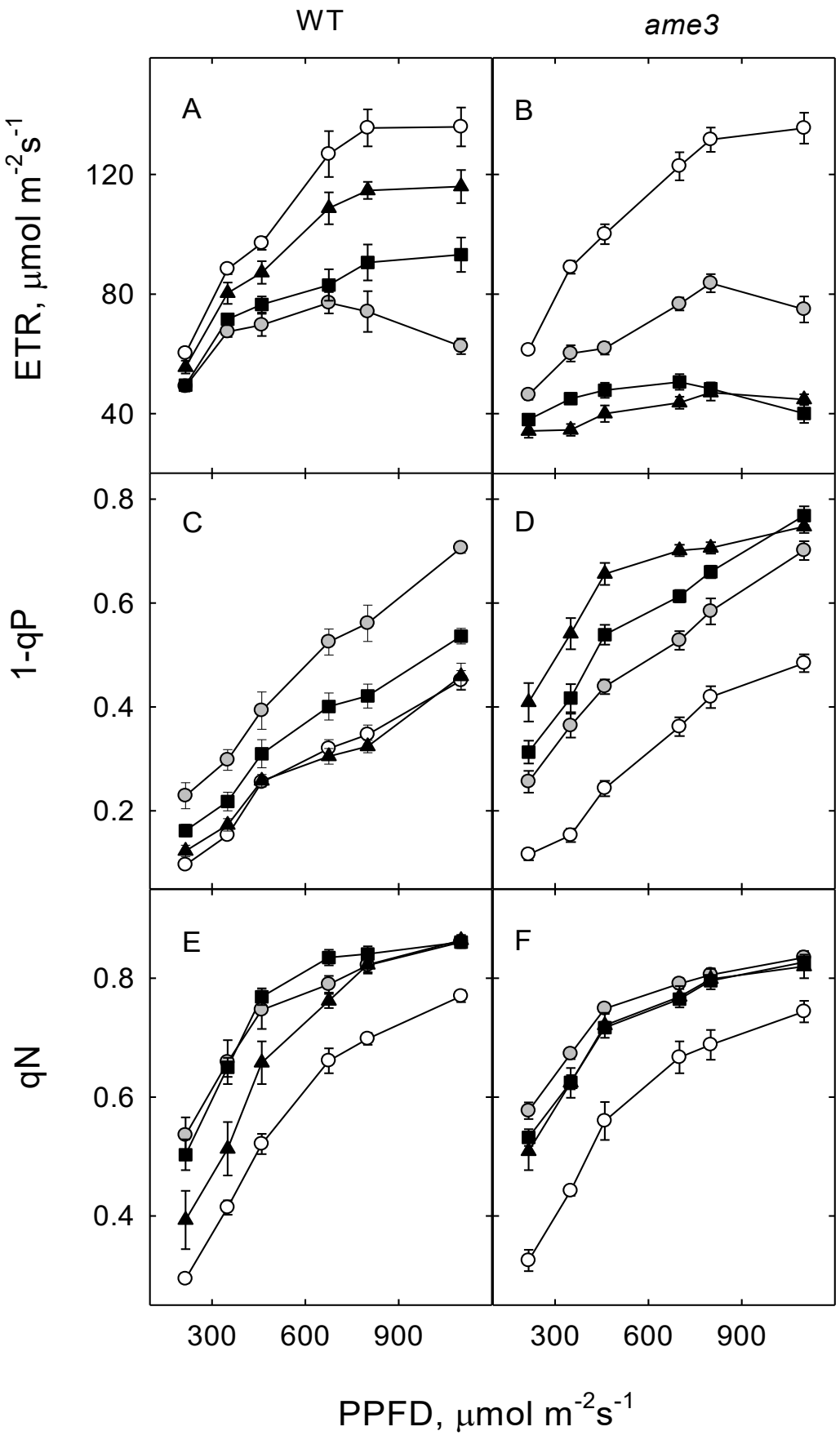
WT
ame3
A
B
C
D
E
F
ETR, μmol m-2s-1
1-qP
qN
120
80
40
0.8
0.6
0.4
0.2
300
600
900
PPFD, μmol m-2s-1

This increase in reaction centre quenching observed exclusively in cold acclimated *ame3* mutants raised the question as to the relative contribution of antennae quenching with respect to non-photochemical quenching in wild type *Arabidopsis* and *ame3* mutants undergoing cold acclimation. Thus, qo, which is a measure of antennae quenching (Bukhov et al., 2001), was plotted as a function of qN (Hüner et al., 2008) (Fig 4.5). Should all non-photochemical quenching originate from antennae quenching, a linear relationship between qo and qN would be expected. Conversely, a curvilinear relationship is expected if contributions other than antennae quenching play a role in non-photochemical quenching. In accordance with previous reports (Hüner et al., 2008; Sane, 2003), a curvilinear relationship was observed between qN and qo in non-acclimated wild type *Arabidopsis thaliana,* where up to 40% of the non-photochemical quenching is independent of qo (Fig. 4.6). Cold acclimation conditions have led to an increase in the curvilinear relationship between qo and qN, where up to 50% of the non-photochemical quenching appears to be independent of antennae quenching.

In comparison, non-acclimated *ame3* mutants were also observed to exhibit non-photochemical quenching by means of methods other than antennae quenching, similarly to non-acclimated wild type, as evidenced by the curvilinear relationship between antennae quenching and total non-photochemical quenching (Fig. 4.5). Furthermore, up to 50% of non-photochemical quenching in *ame3* mutants can be attributed to means other than antennae based quenching. While exposure to low temperatures have led to an increase in the contributions other than antennae quenching in the total non-photochemical quenching, this trend was exacerbated in *ame3* mutants, as up to 70% of the total non-photochemical quenching can be attributed to means other than antennae quenching (Fig. 4.5). This

observation would support the increase in reaction centre based quenching ($\Phi_{f,D}$) observed only in cold acclimated *ame3* mutants (Fig. 4.5).

The attenuated linear electron flow observed in *ame3* mutants raised the question as to whether these observations could be attributed to an impairment in the number of functional PSII centres. An estimation of the functional fraction of PSII in wild type *A. thaliana* and *ame3* mutant lines has shown that under non-acclimated conditions, both wild type and *ame3* mutants exhibit comparable transient electron flow (Fig. 4.6A). Cold acclimated leaves from wild type *Arabidopsis* grown and developed for five weeks were observed to have a single turnover flash-induced reduction of P_{700}^{+} trace that is comparable to its non-acclimated counterpart (Fig. 4.6B), while a shallower trace was observed for five weeks cold acclimated *ame3* mutants. As flash-induced transient kinetics are representative of functional PSII centres, these results would suggest that cold acclimation conditions have led to a recovery in functional PSII reaction centres in wild type *Arabidopsis*, while *ame3* possess a smaller amount of functional PSII reaction centres after cold acclimation compared to non-acclimated conditions. This observation agrees with the attenuated linear electron flow and subsequent proportion of energy used in photochemistry observed in cold acclimated *ame3* mutants (Figs. 4.3-4.4).

Figure 4.5: Relationship between non-photochemical (qN) and basal fluorescence (qo) at varying light intensities in leaves of wild type *Arabidopsis thaliana* and *ame3* mutant lines under non-acclimated and after cold acclimation conditions.

Leaf tissue from wild type *Arabidopsis thaliana*, grown under non-acclimated conditions (white circles), and after five weeks of cold acclimation (black circles) were compared to leaves of *ame3* mutants grown under non-acclimated (white squares), and newly developed five weeks cold acclimated leaves (black squares). Each curve is representative of five leaves harvested at random per batch from either wild type *Arabidopsis* or *ame3* mutant lines, repeated three times, for a total of fifteen individual chlorophyll fluorescence runs (n=15 ± SE). qN values are represented as a percentage of the maximal qN value recorded at a light intensity of 1100 μmol m^{-2} s^{-1}.

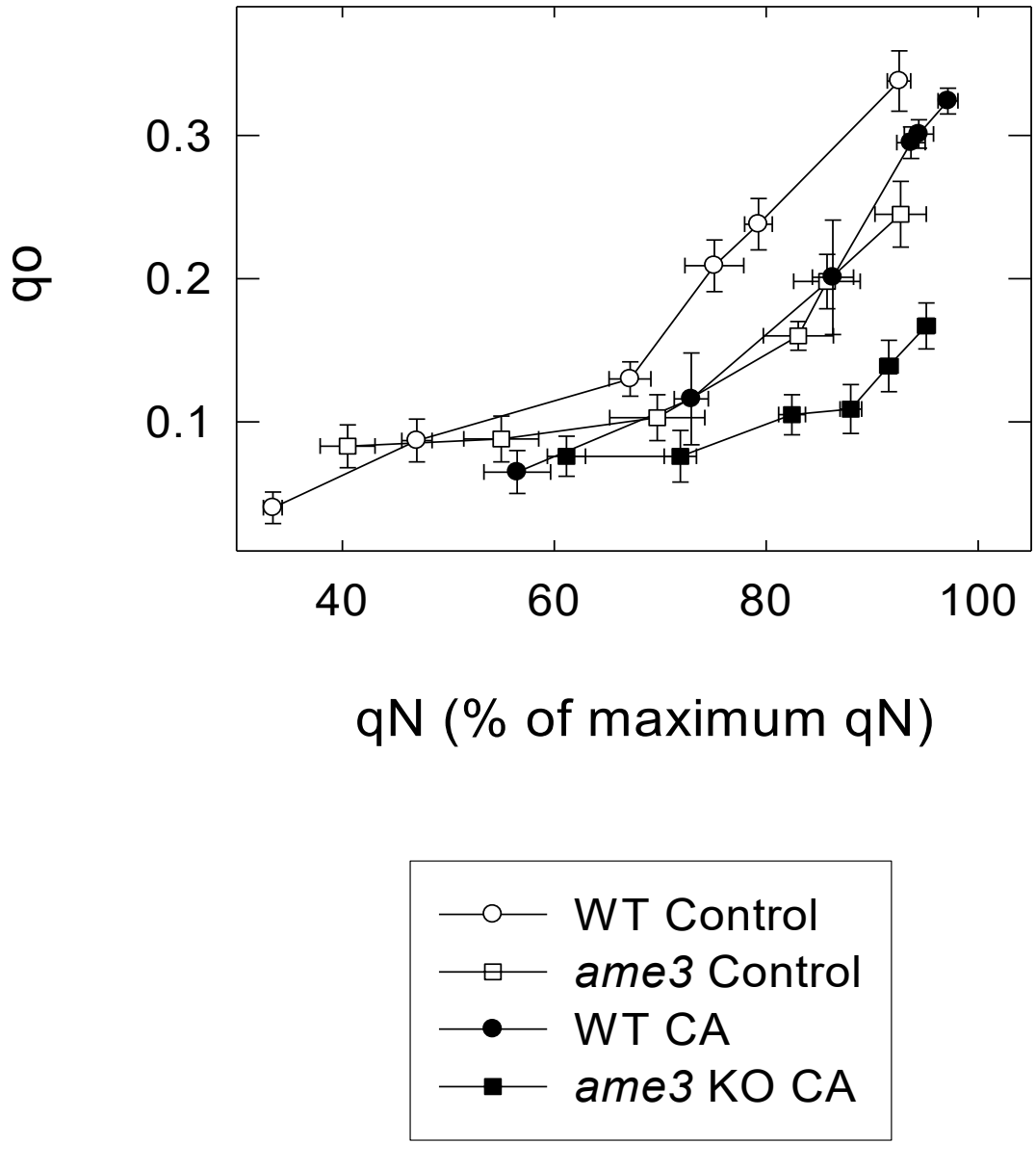
qo
0.3
0.2
0.1
40
60
80
100
qN (% of maximum qN)
WT Control
ame3 Control
WT CA
ame3 KO CA

Figure 4.6: Flash-induced transient kinetics of the P_{700} reduction induced by single turnover flash in leaves from wild type (solid lines) *Arabidopsis* and At-AME3 kinase knockouts (dotted lines) grown under control (20^{o}C) and cold acclimation conditions.

The functional fraction of PSII in leaves from wild type *Arabidopsis* and *ame3* mutants grown under control conditions and after cold acclimation conditions were assessed by monitoring the kinetics of P_{700} reduction and subsequent oxidation induced by a single turnover (ST) flash. The data represents an average of four biological replicates, with n=4 for each experiment.

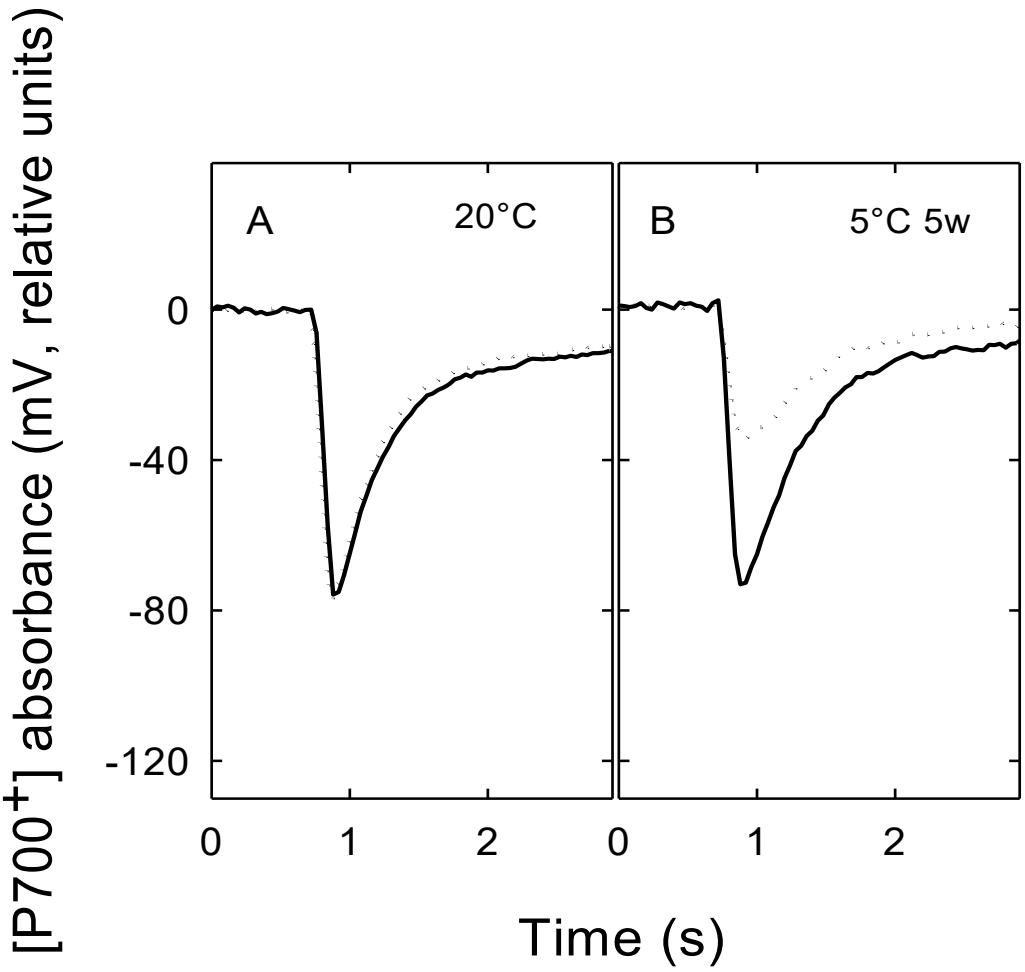
[P700+] absorbance (mV, relative units)
A
20°C
B
5°C 5w
0
-40
-80
-120
0
1
2
0
1
2
Time (s)

4.5.2 *Effect of cold stress, cold acclimation and the deletion of ame3 kinase on P_{700} absorbance, stromal and intersystem electron pool sizes, cyclic electron transport and the contribution of Photosystem II in the reduction of Photosystem I*

In order to measure whether Photosystem I is photoinhibited in response to low temperatures, P_{700} (PSI) photooxidation was monitored *in vivo* by measuring the absorbance change at 820nm. These changes in absorbance, labeled as ΔA_{820}, reflect the oxidation of P_{700} to P_{700}^{+} (Schreiber et al, 1998). Measuring non-acclimated leaves at 5°C led to a 26% increase in steady-state oxidation of PSI (ΔA_{820}) compared to non-acclimated controls (Table 4.3). This was associated with a marginal (7%) increase in stromal pool size, and a 37% decrease in intersystem (e^{-}/P_{700} (MT/ST)) electron pool size. Furthermore, these findings were associated with an attenuation in cyclic electron transport as seen by a 51% increase in P_{700} reduction kinetics ($t_{1/2}$), while a slight (8%) decrease in the ΔA_{DCMU} / ΔA ratio was observed. Low temperature exposure for three weeks led to photoinhibition at the level of Photosystem I, as seen by the 46% decrease in photooxidative capacity (ΔA_{820}) observed in newly developed, cold acclimated leaves from *Arabidopsis* relative to non-acclimated controls. This observation was associated with a 22% increase in stromal pool size, a slight increase in intersystem electron pool size and a recovery with respect to cyclic electron transport, as evidenced by $t_{1/2}$ values which are identical to non-acclimated wild type (Table 4.2). Moreover, a decrease (12%) in the contribution of PSII in the reduction of PSI based on the decrease in the ΔA_{DCMU} / ΔA ratio relative to non-acclimated wild type. In accordance with Photosystem II measurements, five weeks growth and development at low temperatures were associated with a recovery in PSI absorbance, intersystem electron pool size and reduction kinetics of P_{700} in darkness (Table 4.3). Moreover, these conditions have led to a 42% increase in stromal pool size, and a decrease in the ΔA_{DCMU} / ΔA ratio.

In comparison, although Photosystem I absorbance, cyclic electron transport and the contribution of PSII in the reduction of PSI in *ame3* mutants were comparable to its non-acclimated wild type counterpart, *ame3* mutants were observed to constitutively possess significantly smaller stromal (58%) and intersystem (44%) electron pool sizes (Table 4.3). Non-acclimated *ame3* leaves measured at 5°C exhibited comparable P_{700} oxidation values to wild type *Arabidopsis* grown under the same condition (Fig. 4.7). Concomitantly, while marginal changes in stromal and intersystem electron pool sizes were observed in non-acclimated *ame3* measured at 5°C compared to non-acclimated *ame3*, it should be noted that both stromal and intersystem electron pool sizes remained significantly reduced (56% and 52% reductions, respectively) compared to their wild type counterparts. These observations were associated with a 45% increase in $P700^{+}$ reduction kinetics and an increased (17%) contribution of Photosystem II in the reduction of PSI, as indicated by increased $t_{1/2}$ values and ΔA_{DCMU} / ΔA ratios in non-acclimated leaves from *ame3* mutants measured at 5°C compared to non-acclimated controls (Fig. 4.7).

Similarly to wild type, three weeks cold acclimated leaves from *ame3* mutants were also photoinhibited, as seen by a 53% decrease in ΔA_{820} values, which constituted a 20% greater photoinhibition relative to their wild type counterpart. While stromal and intersystem electron pool sizes have seen an increase in *ame3* mutants compared to non-acclimated conditions, they are still significantly (36% and 53%, respectively) smaller than those of three weeks cold acclimated wild type *Arabidopsis*. Moreover, P_{700}^{+} oxidation in the absence of light is slower in *ame3* (40% slower) than wild type *Arabidopsis*, as indicated by increased $t_{1/2}$ values. In contrast to three weeks cold acclimated wild type *Arabidopsis* which has seen a decrease in ΔA_{DCMU} / ΔA ratios, an increase in the contribution of Photosystem II in the

reduction of PSI was observed in *ame3* mutants, as indicated by a 10% increase in the ΔA_{DCMU} / ΔA ratio in three weeks cold acclimated *ame3* leaves compared to non-acclimated wild type. These values were 15% greater in three weeks cold acclimated *ame3* compared to its wild type *Arabidopsis* counterpart.

In contrast to wild type *Arabidopsis*, exposure to low temperatures for five weeks have not led to a recovery in P_{700} absorbance, as seen by the 55% decrease in ΔA_{820} values relative to non-acclimated *ame3*. In a similar fashion to 3 weeks cold acclimated *ame3*, 5 weeks cold acclimated *ame3* samples are heavily (56%) photoinhibited compared to 5 weeks cold acclimated wild type samples. Furthermore, both stromal and intersystem electron pool sizes remained significantly reduced compared to their wild type counterparts. Reduction kinetics of P_{700} in darkness were 31% slower in cold acclimated *ame3* compared to wild type *Arabidopsis* measured under the same conditions. In addition, *ame3* mutants were observed to rely more on Photosystem II in the reduction of PSI, as evidenced by the 20% increase in the ΔA_{DCMU} / ΔA ratio relative to 5 weeks cold acclimated wild type *Arabidopsis* samples.

In addition to the stromal pool size measurements, the contribution of stromal pool electrons in the reduction of plastoquinone was assessed. Under control conditions, a minor increase in F_o` was observed for both wild type and *ame3* mutants, indicating negligible reduction of the plastoquinone pool from the stromal electron pool (Fig. 4.8A). Non-acclimated leaves from wild type *Arabidopsis* and *ame3* measured at 5°C were also observed to exhibit a minor increase in $F_o$`, indicating a minimal contribution of the stromal electron pool in the reduction of the plastoquinone pool (Fig. 4.8B). The negligible differences in traces from wild type *Arabidopsis* and *ame3* agree with the marginal changes in stromal pool size measured under non-acclimated conditions. A rise in F_o` was observed in leaves from

wild type *Arabidopsis* developed at low temperatures for three weeks, suggesting a contribution of the stromal electron pool in the reduction of the plastoquinone in the dark. These results are supported by an observed increase in stromal electron pool size in cold acclimated leaves of *Arabidopsis thaliana* developed for three weeks at low temperatures (Table 4.3). Conversely, a marginal increase in F_o` was observed in three weeks cold acclimated leaves of *ame3* mutants (Fig. 4.8C), which was associated with a marginal increase in stromal pool size (Table 4.2). Exposure to low temperatures for five weeks exacerbated the stromal pool contribution to the reduction of plastoquinone, as evidenced by the sharp rise in F_o` observed in five weeks cold acclimated leaves from *Arabidopsis thaliana*. In contrast, minimal changes in $F_o$` were observed in five weeks cold acclimated leaves from *ame3* (Fig. 4.8D). This observation is supported by the increased stromal pool size monitored in cold acclimated leaves of wild type *Arabidopsis thaliana*, in contrast to the marginal changes in stromal pool size observed in five weeks cold acclimated *ame3* mutants (Table 4.3).

Table 4.3: Comparison of the far-red light-induced steady-state oxidation of P_{700} (ΔA_{820}, P_{700}^{+}), intersystem electron pool size ((e^{-}/P_{700}) (MT/ST)), reduction kinetics of P_{700}^{+} $t_{1/2}^{P700red}$ (s), stromal pool size and the contribution of Photosystem II in the oxidation of P_{700} (ΔA_{DCMU} / ΔA ratio) between wild type *Arabidopsis thaliana* and At-AME3 kinase knockouts grown under control, cold stress and cold acclimation conditions.

Asterisks denote statistical significance, with a p-value lesser or equal to 0.05 ($P \leq 0.05$) between wild type and *ame3* in accordance with Tukey's Honest Significant Difference test.

	ΔA_{820}, $P700^{+}$	e^{-}/P700 (MT/ST)	$t_{1/2}^{P700red}$ (s)	Stromal pool	ΔA_{DCMU} / ΔA ratio (%)
WT Control	158 ± 3	32.5 ± 1.13	3.11 ± 0.09	74.0 ± 3	165 ± 7
***ame3* Control**	144 ± 4	18.2 ± 0.59**	3.50 ± 0.07	31.6 ± 2**	162 ± 6
WT 20°C-->5°C	203 ± 6	20.6 ± 0.93	6.27 ± 0.18	79.3 ± 6	152 ± 2
***ame3* 20°C-->5°C**	214 ± 9	15.6 ± 0.57**	6.34 ± 0.14	32.2 ± 3**	194 ± 4**
WT 3w CA	84.1 ± 2	28.5 ± 0.96	3.10 ± 0.04	102 ± 8	145 ± 3
***ame3* 3w CA**	67.1 ± 1**	17.2 ± 0.58**	5.24 ± 0.08**	48.6 ± 3**	171 ± 2**
WT 5w CA	163 ± 4	28.1 ± 0.93	3.65 ± 0.11	129 ± 6	141 ± 4
***ame3* 5w CA**	71.6 ± 2**	12.8 ± 0.71**	5.26 ± 0.1**	47.4 ± 4**	177 ± 7**

Figure 4.7: Typical traces used in the determination of P_{700} absorbance, measured as ΔA_{820}, as well as intersystem electron size in leaves of wild type *Arabidopsis* grown under non-acclimated (A) growth conditions, as well as after three weeks (B) and five weeks (C) growth and development at low temperatures, compared to At-AME3 knockouts (D-F) grown under the same conditions.

Single turnover (ST), followed by multiple turnover (MT) flash pulses of saturating light were applied once the leaves had reached a steady state of P_{700} oxidation (P_{700}^{+}) by far-red (FR) light illumination. Intersystem electron transport was assessed by measuring the area between the oxidation curves of P_{700} after single and multiple turnover flashes. Each traces are representative of five leaves collected at random, from wild type *Arabidopsis* or *ame3* mutants, repeated three separate times (n=15).

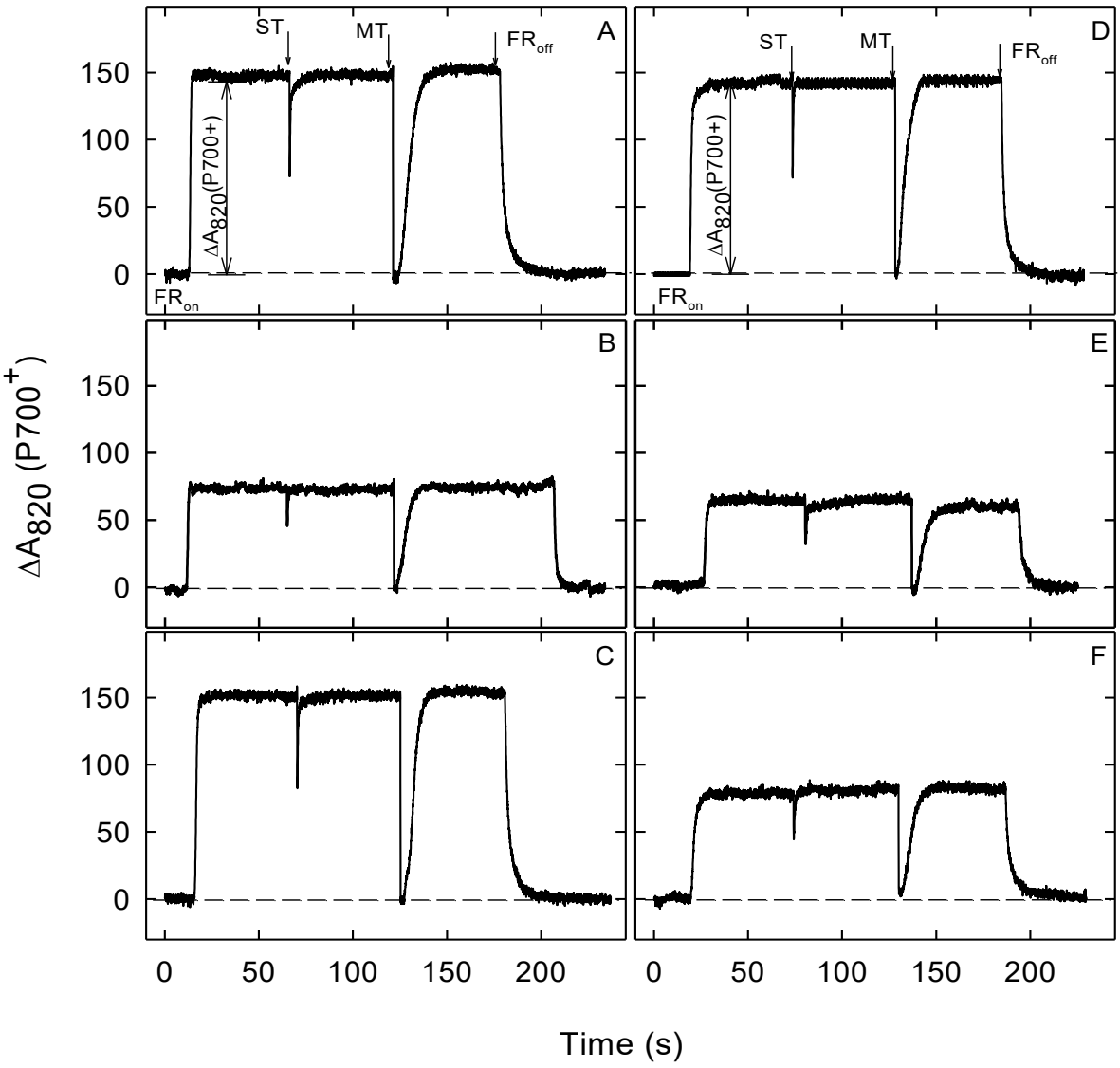
ST
MT
FR$_{off}$
A
D
ΔA_{820}(P700+)
FR$_{on}$
B
E
C
F
ΔA_{820} (P700$^+$)
Time (s)
0
50
100
150
200

Figure 4.8: Effect of the deletion of At-AME3 on post-illumination chlorophyll fluorescence transients from F_s to F_o` after the actinic light was turned off in leaves grown under control (A), grown under control conditions, but measured at 5°C (B), after 3 weeks (C) and 5 weeks (D) of cold acclimation.

Post illumination chlorophyll fluorescence, which is reflective of the reduction of the plastoquinone pool in darkness, was measured in leaves of wild type *Arabidopsis* and *ame3* kinase mutants under control conditions, control conditions measured at 5°C, three weeks and five weeks of cold acclimation. The traces represent averages from four measurements in three independent experiments (n=12).

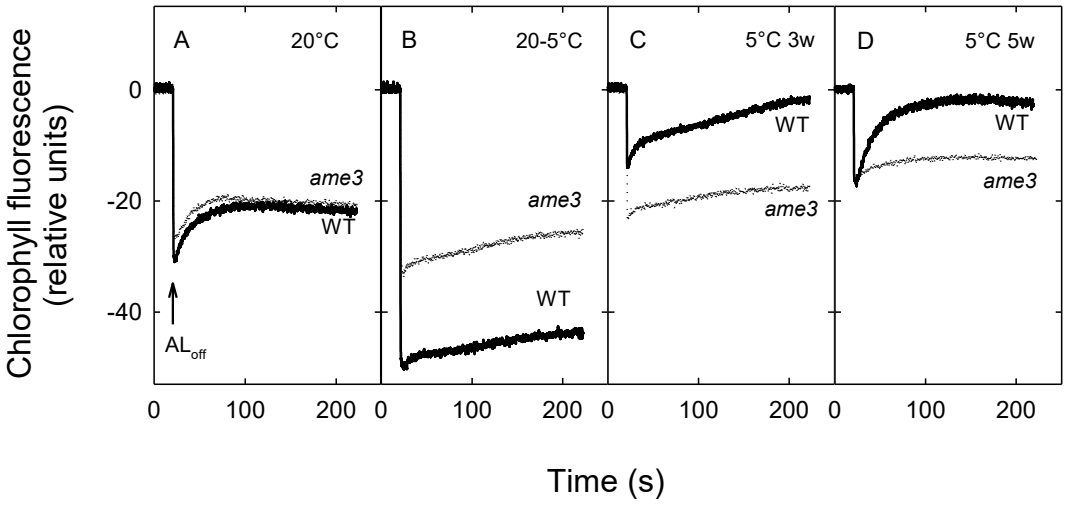
A
20°C
B
20-5°C
C
5°C 3w
D
5°C 5w
Chlorophyll fluorescence
(relative units)
0
-20
-40
ame3
WT
AL$_{off}$
0
100
200
Time (s)

4.5.3 Effect of cold acclimation and ame3 kinase mutation on the capacity to undergo state transitions

Modulated chlorophyll a fluorescence experiments, in conjunction with Photosystem I experiments have revealed that the deletion of At-AME3 kinase led to limitations in the photosynthetic performance of photosystems II and I. These findings have raised the question as to whether the ability to undergo state transitions was also altered in *ame3* mutants. Under non-acclimated conditions, leaves of wild type *Arabidopsis thaliana* have a measured ΔF value of 24.10 (Fig. 4.9A). Conversely, cold acclimation conditions have led to a decrease in the capacity to undergo state transitions, as evidenced by a 30% decrease in ΔF values in five weeks cold acclimated leaves from wild type *Arabidopsis thaliana* (Fig. 4.9C).

In comparison, the capacity to undergo state transitions was constitutively impaired in *ame3* mutant lines, as leaves from non-acclimated *ame3* mutants have exhibited a 30% decrease in their capacity for undergoing state transitions compared to non-acclimated wild type *Arabidopsis* (Fig. 4.9B). Furthermore, long term exposure to low temperatures have exacerbated this trend, as a 52% decrease in the capacity to undergo state transitions was observed in five weeks cold acclimated leaves from *ame3* mutant lines relative to non-acclimated controls (Fig. 4.9D).

Figure 4.9: Comparison of the capacity to undergo state transitions between wild type *Arabidopsis thaliana* and *ame3* mutants under non-acclimated and after cold acclimation conditions.

Mean values were calculated ± SE from 5 leaves in 3 experiments. Asterisks denote statistical significance between parameters measured under control conditions compared to cold acclimation conditions, with *** $P \leq 0.01$, in accordance with Tukey's Honest Significant Difference test.

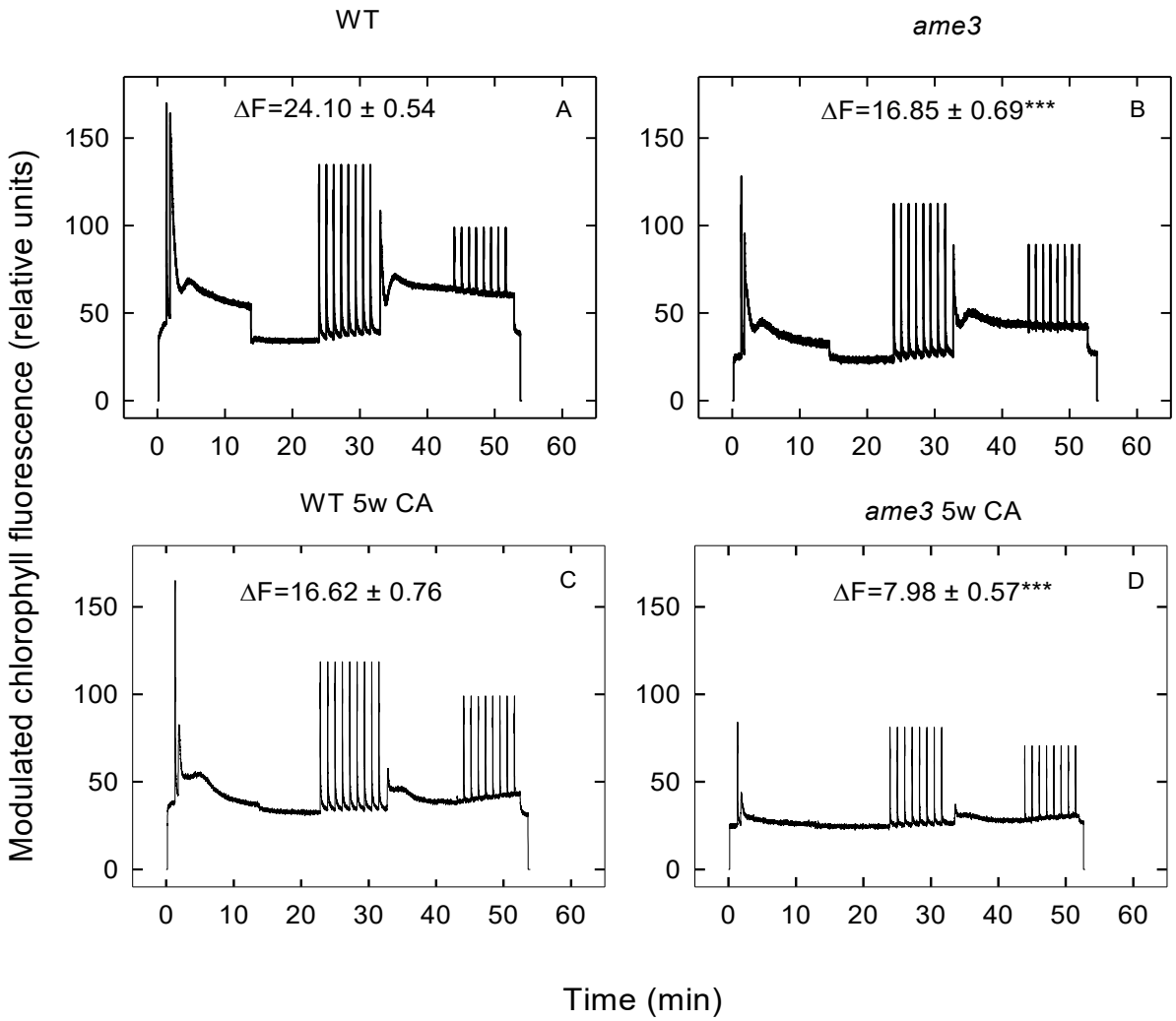
WT
ΔF=24.10 ± 0.54
A
ame3
ΔF=16.85 ± 0.69***
B
WT 5w CA
ΔF=16.62 ± 0.76
C
ame3 5w CA
ΔF=7.98 ± 0.57***
D
Modulated chlorophyll fluorescence (relative units)
Time (min)

4.5.4 Effect of cold acclimation and ame3 mutation on the expression profile of PsbS, NDH-H, PGR5, PTOX and protein abundance

To gain further insight on the limitations at the level of non-photochemical quenching, cyclic electron transport and chlororespiration, transcript levels of PsbS (Figure 4.10A), NDH-H (Fig. 4.10B), PGR5 (Fig. 4.10C) and PTOX (Fig. 4.10D) were monitored in wild type and ame3 mutants under control and after five weeks of cold acclimation. Cold acclimation conditions have led to a decrease in the transcript levels of PsbS (Figure 4.10A), NDH-H (Fig. 4.10B), PGR5 (Fig. 4.10C) and PTOX (Fig 4.10D) compared to optimal growth conditions. In comparison, *ame3* mutants were observed to possess reduced transcript levels of *PsbS*, *NDH-H* and *PTOX* under optimal growth conditions. It should be noted that marginal differences in PGR5 transcript levels were observed between non-acclimated wild type and *ame3* mutants. Cold acclimation conditions have exacerbated this trend, as transcript levels of *psbS*, *NDH-H*, *PGR5* and *PTOX* show greater attenuation than their wild type *Arabidopsis* counterparts.

Assessing the abundance of proteins associated with PSII has revealed no differences in D1 and light harvesting complex proteins between non-acclimated leaves and cold acclimated leaves from wild type *Arabidopsis* (Figure 4.11A). Although a decrease in PsbS and PTOX transcript levels was observed, this was not associated with a decrease in PsbS or PTOX protein abundance after cold acclimation in wild type *Arabidopsis*. Conversely, cold acclimation conditions have led to a decrease in D1 and light harvesting complex proteins in *ame3* mutants (Fig. 4.11A). The decrease in D1 and Lhcb protein abundance support the suppressed photosynthetic performance of five weeks cold acclimated *ame3* mutants. In a similar fashion to wild type *Arabidopsis*, decreased

transcript levels of PsbS and PTOX were not associated with a decrease in PsbS or PTOX protein abundance. Of note was that *ame3* mutants constitutively possess a mitigated abundance of these proteins under non-acclimated conditions relative to its wild type counterpart, and the same trend remains after five weeks of cold acclimation.

Monitoring the phosphorylation status of a subset of PSII proteins using phosphothreonine antibodies has shown an increase in the phosphorylation status of light harvesting complex proteins, as well as mobile phosphoproteins TSP9 and PsbH, which appear to play a role in state transitions (Hansson et al., 2007) (Refer to Section 1.3), in cold acclimated wild type *Arabidopsis* samples (Fig. 4.12B). In addition, no changes in the phosphorylation status of D1 and D2 was observed after cold acclimation in wild type *Arabidopsis*. In contrast, the phosphorylation status of D1 and D2 is greatly attenuated in non-acclimated *ame3* mutants compared to non-acclimated wild type *Arabidopsis*. While cold acclimation conditions have led to an overall increase in LHCII, TSP9 and PsbH phosphorylation status in *ame3*, this response is still attenuated in comparison to cold acclimated wild type *Arabidopsis.*

In addition to the evaluation of proteins associated with Photosystem II, the protein abundance Photosystem I reaction centre subunits (PsaB, PsaL, PsaH, PsaF), in addition to light harvesting complex proteins (Lhca 1-4) were also evaluated (Fig. 4.11C). In wild type *Arabidopsis thaliana*, cold acclimation conditions have not led to any changes in the protein abundance of PsaB, PsaL, PsaH, PsaF PSI reaction centre subunits. Lhca1, Lhca2 and Lhca4 protein abundance in cold acclimated *Arabidopsis* remained comparable to non-acclimated controls. Lhca3 was observed to decrease in abundance under cold acclimation conditions. ATPase and POR protein abundance

remained unchanged under cold acclimation conditions, while an increase in early light inducible proteins ELIP1 and ELIP2 was observed.

In contrast, non-acclimated *ame3* had similar protein abundance profiles as non-acclimated wild type *Arabidopsis*. Furthermore, exposure to low temperatures have led to a decrease in Lhca3, similarly to wild type. While ATPase protein levels remained unchanged in *ame3* mutants, these mutants possessed a decreased abundance of PSI reaction centre subunits (PsaB, PsaL, PsaH, PsaF) and light harvesting complex proteins (Lhca1, Lhca2, Lhca4). These findings were associated with a decrease in POR abundance in cold acclimated *ame3* and a sharp increase in ELIP1 and ELIP2 abundance.

Figure 4.10: Effects of the deletion of At-AME3 on the transcript levels of *psbS*, *NDH-H*, *PGR5* and *PTOX* grown under control and cold acclimation conditions, as determined by qPCR analysis.

Leaf tissue from wild type *Arabidopsis thaliana* and *ame3* mutant lines grown under control conditions (White bars, diamond patterns), as well as cold acclimated leaves grown for five weeks (diagonal lines, black bars) were used in qPCR analyses to assess the expression levels of *PsbS* (A), *NDH-H* (B), *PGR5* (C), and *PTOX* (D). All bars represent averaged expression values +SE from three biological replicates, each with three technical replicates (n=9) normalized against the mean transcript levels of elongation factor 1α (elf1). The data presented in this figure was provided by David P. Sprott.

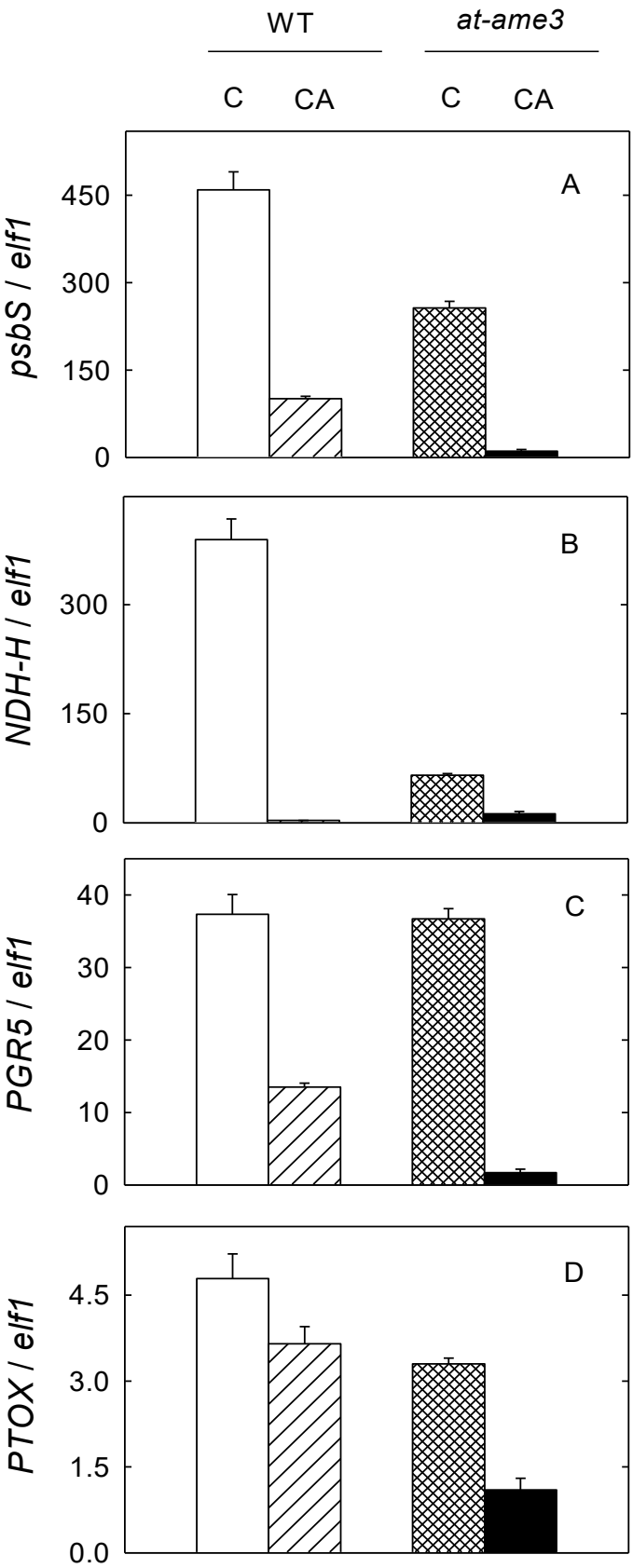
WT
at-ame3
C
CA
C
CA
A
B
C
D
psbS / elf1
NDH-H / elf1
PGR5 / elf1
PTOX / elf1
450
300
150
0
300
150
0
40
30
20
10
0
4.5
3.0
1.5
0.0

Figure 4.11: Effect of the deletion of At-AME3 on the abundance of proteins associated with Photosystem II (A), phosphorylation status of Photosystem II reaction centre and light harvesting complex proteins (B), abundance of proteins associated with Photosystem I and ELIP (C) under control (non-acclimated) and after five weeks of cold acclimation.

Western blots presented are representative of three biological replicates. Samples were loaded on equal chlorophyll basis, consisting of 20 µg per lane. Gels used to ascertain equal loading are unavailable. Panel A depicts Western blots of SDS-PAGE gels of total protein extracts probed with antibodies raised against PsbA (D1) and Photosystem II-associated light harvesting complex proteins (Lhcb1, Lhcb2, Lhcb3, Lhcb4, Lhcb5 and Lhcb6), PsbS and PTOX/IMMUTANS. Panel B depicts a Western blot of an SDS-PAGE gel probed with Phosphothreonine (PhThr), used in the detection of phosphorylated D1 and LHCII polypeptides from wild type and *at-ame3* mutants grown under control and after cold acclimation conditions. Panel C depicts representative Western blots of SDS-PAGE gels probed with antibodies raised against PsaB, Photosystem-I associated light harvesting proteins (Lhca1, Lhca2, Lhca3 and Lhca4), ATPase and ELIP proteins.

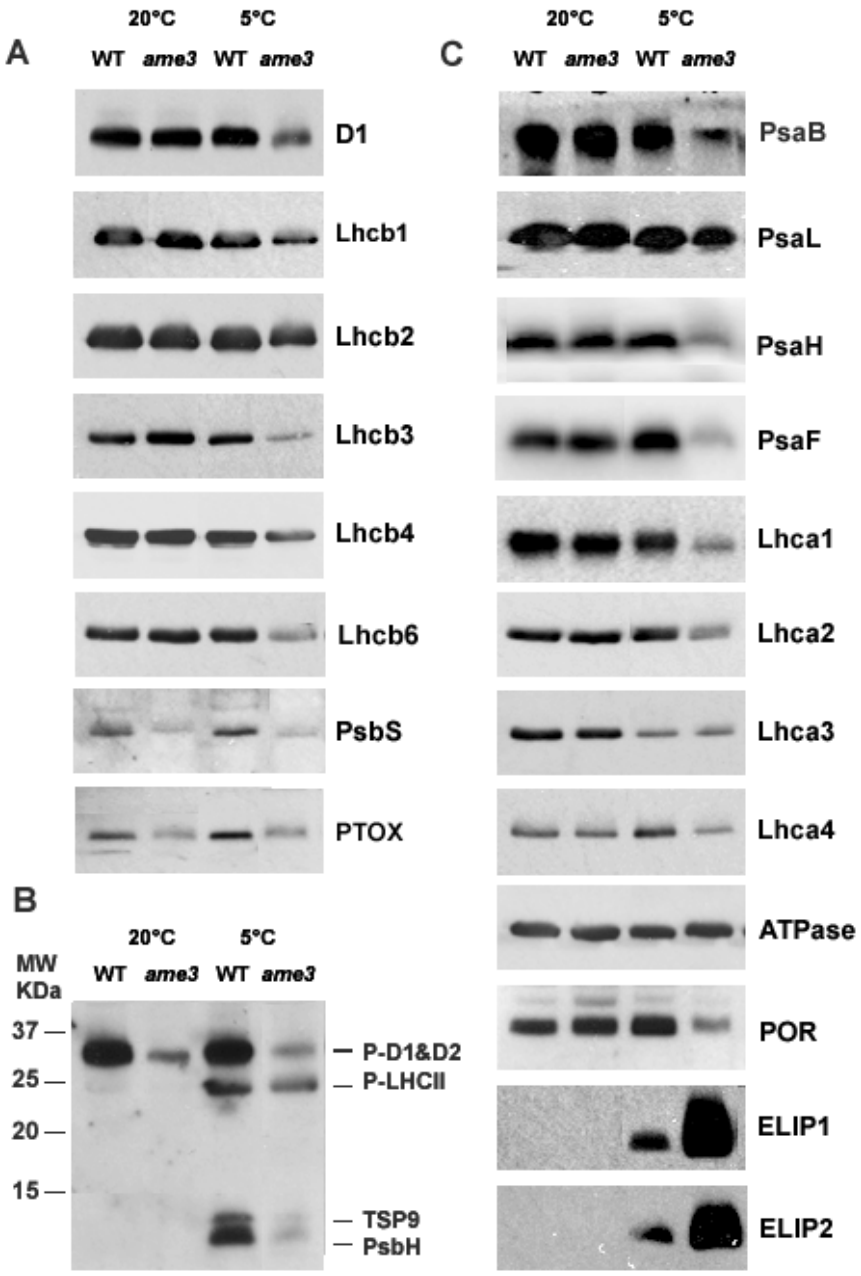
A
20°C
5°C
WT
ame3
WT
ame3
D1
Lhcb1
Lhcb2
Lhcb3
Lhcb4
Lhcb6
PsbS
PTOX
B
MW
KDa
37
25
20
15
P-D1&D2
P-LHCII
TSP9
PsbH
C
PsaB
PsaL
PsaH
PsaF
Lhca1
Lhca2
Lhca3
Lhca4
ATPase
POR
ELIP1
ELIP2

4.6 Discussion

The objective of this study consisted in defining the role of At-AME3 in the photosynthetic performance of *Arabidopsis thaliana* undergoing cold acclimation by means of a detailed photosynthetic characterization of At-AME3 kinase mutants. At the level of Photosystem II performance, results have shown that exposure to low temperatures for three weeks led to decreases in chlorophyll content (Table 4.2), in the proportion of energy used for photochemistry (Φ_{PSII}) and linear electron transport rates (ETR), increases in excitation pressure (1-qP) and total heat dissipation (qN) parameters, with most of the excess energy being dissipated via antenna based non photochemical quenching (Φ_{NPQ}) rather than reaction centre based non photochemical quenching ($\Phi_{f,D}$) (Figures 4.3-4.4). These results are in agreement with previous reports (Hüner et al., 1993, 1998, Savitch et al., 2001, 2009; Strand et al., 2003), which have shown that cold stress, which would occur on a short time scale (days), significantly reduces photochemical efficiency and photosynthetic performance of wild type *Arabidopsis* plants, as well as other plants such as corn (Savitch et al., 2009, 2011). In addition, the observed photoinhibition in three weeks cold acclimated *Arabidopsis* was correlated with a decrease in chlorophyll content (Table 4.2).

Long term exposure (five weeks) to low temperatures has previously been reported to be correlated with a strong recovery of photosynthetic performance and an enhanced photoinhibition tolerance in *Arabidopsis* (Sane, 2003; Savitch et al., 2001; Stitt and Hurry, 2002; Strand et al., 1997, 1999). Therefore, it is expected that a recovery of photosynthetic performance will be observed in wild type *Arabidopsis thaliana.* In accordance with the reports mentioned above, prolonged exposure to low temperatures have led to a recovery in photosynthetic performance, as evidenced by the decreased photoinhibition (Table 4.1),

increased proportion of energy used in photochemistry (Φ_{PSII}) (Fig. 4.3) and subsequent linear electron transport rates (Fig. 4.3-4.4). This was associated with a decrease in excitation pressure (1-qP), total heat dissipation (qN) and the proportion of energy dissipated as heat via antenna quenching (Φ_{NPQ}). A slight decrease in reaction centre based non photochemical quenching was also observed ($\Phi_{f,D}$).

In comparison, *ame3* mutants were also hindered in their photosynthetic adjustment under short term cold acclimation (3 weeks), as evidenced by the observed decrease in linear electron transport rates (ETR), and subsequent increases in excitation pressure of Photosystem II (1-qP), non-photochemical quenching (qN), antennae based heat dissipation (Φ_{NPQ}) and reaction centre quenching ($\Phi_{f,D}$) (Figs. 4.3-4.4). These trends were correlated with a significant decrease in chlorophyll content in three weeks cold acclimated *ame3* leaves.

Unlike wild type *Arabidopsis*, prolonged exposure (5 weeks) to low temperatures did not result in a recovery of photosynthetic performance, as evidenced by a significant decrease in maximal photochemical efficiency (F_v/F_m). This in turn was associated with suppressed linear electron transport rates (ETR), increased excitation pressure (1-qP) and non-photochemical quenching (qN), preferentially via reaction centre based non photochemical quenching ($\Phi_{f,D}$) (Figures 4.3-4.4). Moreover, this severe photoinhibition observed in cold acclimated *ame3* mutants was associated with a sharp decrease in chlorophyll content and an increase in chlorophyll a/chlorophyll b ratio, suggesting a decrease in antenna size (Table 4.2). This decrease in antenna size is supported by the decrease in Lhcb1, Lhcb3, Lhcb4 and Lhcb6 protein abundance observed in cold acclimated *ame3* mutants (Fig. 4.11A). Moreover, this observed decrease in chlorophyll content might be attributed to a decrease in

Protochlorophyllide OxidoReductase (POR) protein abundance (Fig. 4.11C), which is involved in chlorophyll biosynthesis (Reinbothe et al., 1996). In addition, *ame3* mutants were found to express an increased amount of ELIP1 and ELIP2 relative to cold acclimated wild type (Fig. 4.11C). As ELIPs are indicative of light stress (Fowler and Thomashow, 2002), this increased abundance of ELIPs observed in *ame3* mutants lend credence to the enhanced photoinhibition observed in these mutant lines.

In accordance with a previous report evaluating the effects of low temperature in corn (Savitch et al., 2009), it is possible that the impaired Photosystem II performance observed in *ame3* mutants under cold acclimation conditions might be attributed to a low temperature photoinactivation and subsequent deactivation of Photosystem II, as evidenced by the observed decreases in D1 protein abundance and Photosystem II light harvesting complex proteins (Lhcb 1-6) in cold acclimated *ame3* mutants (Fig. 4.11A), in conjunction with the observed decrease in the amount of functional PSII units (Fig. 4.8). It should also be noted that the deletion of At-AME3 kinase led to a decrease in the phosphorylation status of Photosystem II reaction centre subunit D1 and light harvesting complex proteins under optimal growth conditions, and after cold acclimation conditions (Fig. 4.11B).

In a similar fashion to Photosystem II performance in wild type *Arabidopsis* undergoing cold acclimation, exposure to low temperatures have led to photoinhibition at the level of Photosystem I (Table 4.3). Newly developed, cold acclimated leaves, however, can recover with respect to PSI photochemistry. This trend was observed when comparing the steady-state oxidation of P_{700}, intersystem electron pool size and the reduction kinetics of P_{700}^{+}, and is in agreement with previous reports (Ivanov et al., 2012; Savitch et al., 2001, 2011; Sonoike, 2011; Sonoike et al., 1997; Zhang and Scheller, 2004). In comparison, while non-

acclimated *ame3* leaves behaved similarly to wild type *Arabidopsis* under optimal conditions with respect to the steady state oxidation of P_{700}, reduction kinetics of P_{700}^{+} and the induced oxidation of P_{700} (Table 4.3), *ame3* mutants were observed to have significantly attenuated stromal and intersystem electron pool sizes under non-acclimated conditions. Low temperature exposure for three weeks led to a significant decrease in P_{700} oxidation rates, which was associated with an attenuation in stromal and intersystem electron pool sizes, as well as an increase in P_{700}^{+} reduction kinetics. Furthermore, unlike wild type *Arabidopsis*, five weeks exposure to low temperatures did not result in a recovery with respect to PSI photochemistry, as P_{700} oxidation rates, intersystem and stromal pool sizes and reduction kinetics were significantly attenuated compared to cold acclimated wild type *Arabidopsis*. Furthermore, this attenuation in PSI absorbance in cold acclimated leaves developed for five weeks was associated with a decrease in the abundance of PsaB, PsaL PsaH and PsaF, which constitute subunits of the Photosystem I reaction centre, as well as light harvesting complex proteins Lhca1 and Lhca2 (Fig. 4.11C) under cold acclimation conditions.

As low temperature exposure is known to impose an imbalance between the photochemical and biochemical reactions of photosynthesis, in turn leading to an increase in PSII excitation pressure (Ensminger et al., 2006; Gray et al., 1996; Hüner and Grodzinski, 2011; Öquist and Hüner, 2003), the observed increase in photoinhibition observed in leaves from wild type *Arabidopsis* exposed for three weeks, followed by the decrease in photoinhibition in leaves exposed for five weeks, would suggest that photoprotective mechanisms have played a role in the reduced photoinhibition observed in wild type *Arabidopsis*. Conversely, as *ame3* mutants were severely photoinhibited after extended

exposure to low temperatures, this would suggest that photoprotective mechanisms were jeopardized in these mutants.

Non-photochemical quenching (NPQ) through the antennae, via the xanthophyll cycle, is considered to be one of the major photoprotective mechanisms (Allen and Ort, 2001; Horton et al., 1996; Ivanov et al., 2012; Li et al., 2000; Niyogi, 1999). As expected, exposure to low temperatures was associated with an increase in the proportion of energy dissipated as heat via antenna based non-photochemical quenching (Φ_{NPQ}) in cold acclimated wild type *Arabidopsis* and *ame3* compared to their non-acclimated counterparts (Fig. 4.3). While cold acclimation conditions have led to a decrease in PsbS transcript levels in both wild type *Arabidopsis* and *ame3*, this was not correlated with a decrease in PsbS abundance in wild type *Arabidopsis*. As it is known that post-transcriptional mechanisms such as RNA stability play critical roles during cold acclimation (Chinnusamy et al., 2007; Mazzucotelli et al., 2008) this observation might be attributed to an increase in PsbS transcript stability in response to cold acclimation. Conversely, *ame3* mutants possessed a lower PsbS abundance relative to their wild type counterpart, and this trend was maintained after cold acclimation conditions. Since PsbS is known to play a role in the photoprotection of PSII (Li et al., 2002; Müller-Moulé et al., 2001; Peterson and Havir, 2001, 2003; Roach and Krieger-Liszkay, 2012), the decreased abundance of PsbS would suggest that this photoprotective mechanism is jeopardized in *ame3* mutants undergoing cold acclimation. In addition to an enhancement in heat dissipation through the antennae, *ame3* mutants exhibited a significant enhancement in reaction centre quenching ($\Phi_{f,D}$) (Figure 4.3). As reaction centre quenching is thought to involve inactive, closed PSII reaction centres (Ensminger et al., 2006; Ivanov et al., 2001; Krause and Weis, 1991), the observed increase in reaction centre quenching observed

exclusively in *ame3* mutants compared to wild type undergoing cold acclimation could be attributed to an increased proportion of damaged/inactive PSII reaction centres.

Assessing the capacity of wild type and *ame3* mutants to undergo state transitions has shown that in accordance with previous reports in corn (Savitch et al., 2011) and *Arabidopsis* (Ivanov et al., 2012), cold acclimation conditions have led to an overall decrease in state-1 state-2 transitions in wild type *Arabidopsis thaliana*. While a similar trend has been observed in *ame3* mutants, it should be noted that unlike wild type *Arabidopsis*, *ame3* mutants possess a reduced capacity to undergo state transitions under control conditions, and that cold acclimation exacerbated this trend (Figure 4.10). This was associated with a reduced abundance of reversibly phosphorylated (Tikkanen and Aro, 2012) Photosystem II light harvesting complex proteins Lhcb1 and Lhcb2 (Fig. 4.11A), as well as PsaH and PsaL (Fig. 4.11C), which are components of the Photosystem I reaction centre. As these aforementioned proteins have been reported to play an essential role in state-1 state-2 transitions (Ivanov et al., 2006; Lunde et al., 2000; Minagawa, 2011; Tikkanen and Aro, 2012), their decreased abundance in *ame3* mutants could account for the impediment in state-1 state-2 transitions observed in *ame3* mutants. Furthermore, the phosphorylation status of light harvesting complex proteins and TSP9 were attenuated in newly developed, cold acclimated leaves from *ame3* mutants compared to their wild type counterpart (Fig. 4.11B). Since LHCII phosphorylation is essential to their mobility (Minagawa, 2011), the attenuated phosphorylation profile observed in cold acclimated *ame3* mutants would support the observed reduction in state transitions.

Chlororespiration, which occurs via PTOX (Ivanov et al., 2012; Vanlerberghe et al., 2015) is another photoprotective mechanism that is known to play an essential role under

cold acclimation. While cold acclimation conditions have led to a decrease in PTOX transcripts, an increase in PTOX protein abundance was observed, as was observed with PsbS. These results are in agreement with a study from Ivanov et al. (2012), who have shown that cold acclimation conditions have led to an increase in PTOX protein abundance (Fig. 4.11). In comparison, lower PTOX transcript levels were observed in *ame3* mutants grown under optimal growth conditions (Fig. 4.10). Cold acclimation conditions have led to a stronger attenuation of PTOX transcript levels, which led to a similar trend in terms of PTOX protein abundance. These results have shown that unlike wild type, *ame3* mutants are impaired in their capacity to use chlororespiration as a photoprotective mechanism.

Cyclic electron transport, via the NDH-H and PGR5 pathways, provide a means to divert excess electrons (Refer to Chapter 1, Section 1.3). Evaluating the transcript levels of NDH-H and PGR5, which play an essential role in cyclic electron transport (Munekage et al., 2004; Shikanai, 2007, 2014), has revealed a sharp decrease in NDH-H transcripts after five weeks of cold acclimation in wild type *Arabidopsis* (Fig. 4.10). Note that the Y axes have different scales. While PGR5 transcript levels were also found to decrease under cold acclimation conditions, PGR5 transcript levels were still greater, than NDH-H transcript levels, in cold acclimated wild type. These results were associated with an increase in P_{700}+ reduction kinetics ($t_{1/2}$) rates, followed by a subsequent recovery after five weeks of exposure to low temperatures (Table 4.3), as well as changes in post-illumination chlorophyll fluorescence in darkness, suggesting that cyclic electron transport has taken place.

Conversely, At-AME3 mutants appear to be jeopardized with respect to cyclic electron transport, as decreases in transcript levels of NDH-H and PGR5 were observed under optimal growth conditions (Figure 4.10). This was correlated with an increase in reduction kinetics

of P_{700}^{+} ($t_{1/2}$ values), which are indicative of cyclic electron transport (Asada et al., 1992; Maxwell and Biggins, 1976). Marginal changes in post-illumination chlorophyll fluorescence in *ame3* mutants relative to wild type *Arabidopsis* (Table 4.3) after three weeks and five weeks of cold acclimation support this hypothesis. While linear electron transport rates were severely limited in cold acclimated *ame3* knockouts, a greater contribution of electrons coming from Photosystem II was observed in comparison to cold acclimated wild type. This reliance on the severely limited electron flow from Photosystem II might be attributed to the attenuated cyclic electron transport in *ame3*, which was not observed in cold acclimated *Arabidopsis.*

Taken together, detailed photosynthetic analyses have shown that under optimal, non-acclimated conditions, *ame3* are comparable to their wild type *Arabidopsis* counterpart (Figure 4.12A), apart from a constitutively attenuated stromal and intersystem electron pool size. Although exposure to low temperatures led to photoinhibition in both wild type and *ame3* mutants, newly developed, cold acclimated wild type *Arabidopsis* leaves exposed to low temperatures for three weeks have shown a recovery at the level of Photosystem II and Photosystem I. These findings are associated with an increase in photoprotective mechanisms, such as cyclic electron transport, predominantly via the PGR5 pathway, state-1 state-2 transitions, and contributions from PTOX, all of which contribute in maintaining photostasis in cold acclimated leaves from *Arabidopsis thaliana* (Figure 4.12B). Conversely, *ame3* mutants are unable to recover in terms of their photosynthetic performance. This can be attributed to photoprotective mechanisms being severely limited in these mutants, resulting in an increase in photoinhibition at the level of Photosystem II and Photosystem I, increased excitation pressure, reduced linear electron transport rates and enhanced heat

dissipation via reaction centre quenching that was observed after three weeks of cold acclimation, and was exacerbated under prolonged exposure to low temperatures (Fig. 4.12C).

Figure 4.12: Schematic diagram depicting an overview of the energy partitioning of absorbed light by Photosystem I and Photosystem II under optimal growth conditions and after cold acclimation conditions in wild type *Arabidopsis* and *ame3* mutants.

Under optimal growth conditions, (Panel A) the rate of consumption of electrons through carbon, N and S reduction is capable of keeping pace with the rate at which the photophysical processes used absorb light energy, resulting in a preferential reduction of the plastoquinone (PQ) pool, with minimal excitation pressure and heat dissipation. Thus, under these conditions, linear electron flow from Photosystem II to Photosystem I takes precedence over cyclic electron flow in both wild type *Arabidopsis thaliana* and *ame3* mutants. Although cold stress conditions result in the reduction of linear electron transport rates due to consumption of electrons being unable to keep up with the amount of light energy absorbed by Photosystem II, resulting in an imbalance in photostasis, cold hardy plants such as Arabidopsis thaliana exhibit a strong recovery of photosynthetic performance. This can be achieved through a variety of photoprotective mechanisms in place to restore photostasis (Panel B). Cyclic electron transport through the NDH and predominantly the PGR5 pathways provide means of diverting excess electrons from the linear electron flow by recirculating them, allowing the reduction of the plastoquinone pool. In addition to PGR5 and NDH circular electron transport pathways, chlororespiration via Plastid Terminal oxidase, or PTOX, is also capable of diverting electrons by oxidizing the plastoquinone pool. Conversely (Panel C), photoprotective mechanisms in *ame3* are severely jeopardized, thus photostasis is not restored, resulting in severe photoinhibition at the level of Photosystems II and I. Modified from Ivanov et al., 2012.

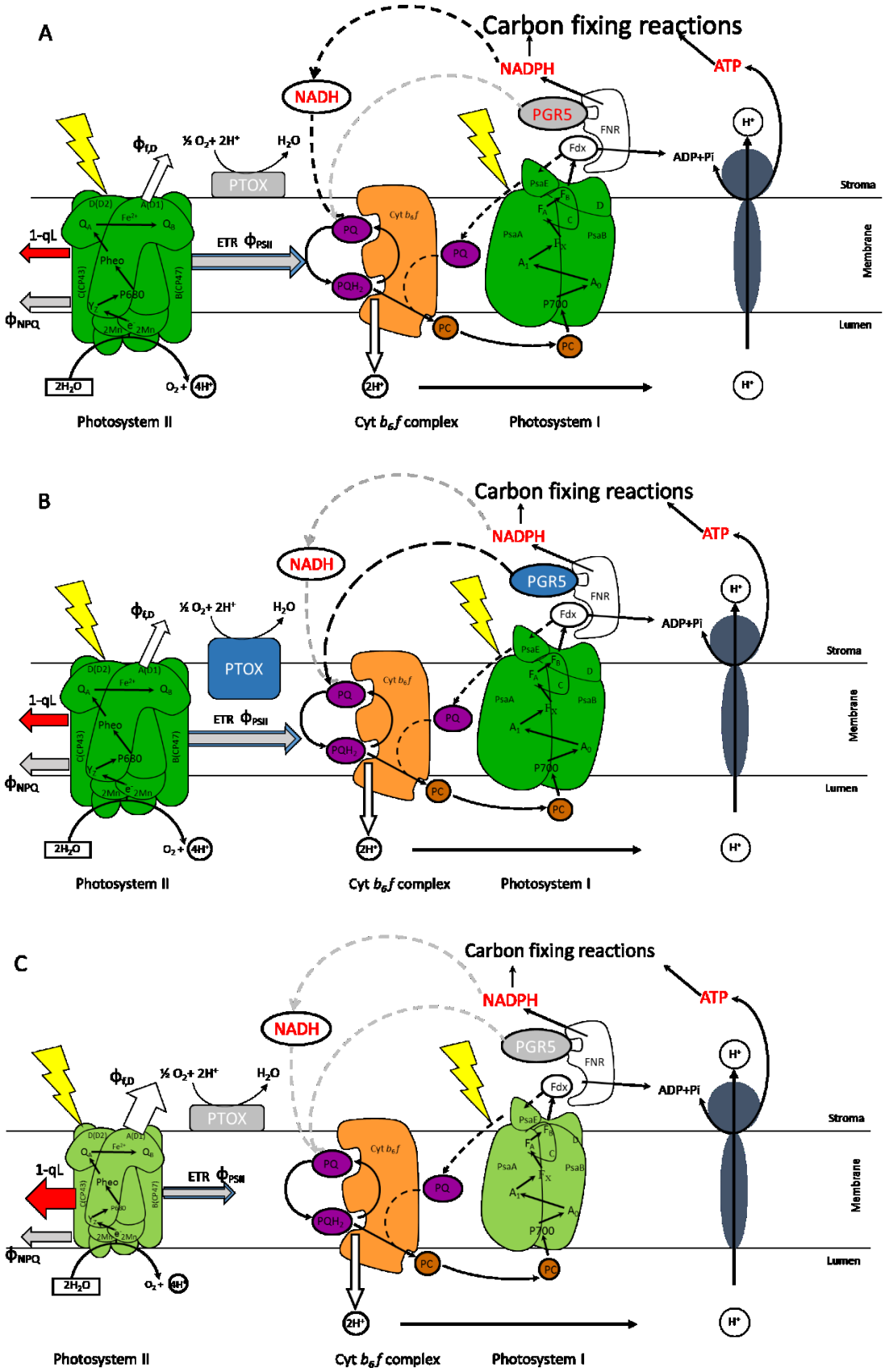
A
Carbon fixing reactions
NADPH
ATP
NADH
PGR5
FNR
Fdx
ADP+Pi
PTOX
ETR ΦPSII
1-qL
ΦNPQ
Stroma
Membrane
Lumen
Photosystem II
Cyt b6f complex
Photosystem I
B
Carbon fixing reactions
NADPH
ATP
NADH
PGR5
FNR
Fdx
ADP+Pi
PTOX
ETR ΦPSII
1-qL
ΦNPQ
Stroma
Membrane
Lumen
Photosystem II
Cyt b6f complex
Photosystem I
C
Carbon fixing reactions
NADPH
ATP
NADH
PGR5
FNR
Fdx
ADP+Pi
PTOX
ETR ΦPSII
1-qL
ΦNPQ
Stroma
Membrane
Lumen
Photosystem II
Cyt b6f complex
Photosystem I

4.7 Conclusion

The impact of At-AME3 LAMMER kinase on two major processes known to take place during cold acclimation has prompted a more detailed photosynthetic analysis of At-AME3 mutants undergoing cold acclimation compared to wild type *Arabidopsis*. Results from this study have shown that exposure to low temperatures initially result in photoinhibition in both wild type *Arabidopsis*, as well as At-AME3 mutants. While newly developed leaves from wild type *Arabidopsis* are capable of recovering at the level of Photosystem II and Photosystem I photochemistry, and extended exposure enhanced this observed recovery, this trend was not observed in *ame3* mutants. Growth and development for three weeks at low temperatures resulted in photoinhibition at the level of Photosystems II and I. This photoinhibition was associated with an enhanced excitation pressure (1-qL), heat dissipation via reaction center quenching ($\phi_{f,D}$), decreased fraction of energy used for photochemical processes (ϕ_{PSII}) and decreased linear electron transport rates (ETR) at the level of PSII performance. A decrease in intersystem and stromal pool sizes were also observed. Furthermore, photoprotective mechanisms such as state-1 state-2 transitions, cyclic electron transport via NDH-H and PGR5, and chlororespiration by means of PTOX-mediated electron transport were all severely limited in *ame3* mutants exposed to low temperatures for three weeks. Extended (5 weeks) exposure to low temperatures exacerbated these trends.

Chapter 5: Defining interacting partners of At-AME3 using yeast 2-hybrid assays.

Marc Rosembert

All RNA extractions, and RT-PCR reactions used in the generation and visualisation (Fig, 5.1) of Gateway compatible SR gene products were performed by Marc Rosembert. Marc has also designed all the primers presented in Tables 4.1 and 4.2, which were used in the generation of Gateway-compatible gene constructs. I have generated At-RSZ22, At-RSZ21, At-SR45, At-SR34, At-RS41, At-RS2Z32, At-RS40 and At-SCL30a SR entry clones and subsequent LR recombination reactions, to generate pDEST-AD vectors of SR genes of interest. All sequencing reactions used to confirm the presence of SR genes of interest were processed by the MBB group (ECORC). All yeast transformations, autophosphorylation assays (Fig. 5.4), yeast mating and replica plating highlighted in materials and methods were performed by Marc Rosembert. Marc has also analysed all results from the yeast 2-hybrid mating (Fig. 5.5). Subsection 5.3, stating the hypothesis and research objective of this study, was added for the thesis. I would like to thank Loreta Gudynaite-Savitch and Maher Mounzer for their help with planning, experimental design and data analysis.

5.1 Abstract

The objective of this study was to address whether At-AME3, a LAMMER-type kinase, is capable of physically interacting with a subset of Serine/Arginine-rich proteins (At-RSZ22, At-RSZ22a, At-RS41, At-SR34b, At-RS40, At-SCL30, At-SCL30a, At-SR34, At-RS2Z33, At-RS31, At-SCL33) and SR-like (At-SR45 and At-SR45a) proteins that were differentially expressed in response to cold stress and acclimation conditions. Yeast 2-hybrid assays have revealed that At-AME3 is capable of physically interacting with five SR proteins (At-SR34a, At-RSZ21, At-RS41, At-RSZ22a, At-SCL30), and one SR-like protein (At-SR45). While interactions between At-AME3, At-SCL30 and At-RSZ21 have been reported, four novel interactions between SR proteins (At-SR34a, At-RSZ22a, At-RS41 and At-SR45) and At-AME3 LAMMER kinase have been found in this study.

5.2 Introduction

Physical interactions between proteins play an essential role in various biological processes, including signal transduction, transcription and post translational modifications such as phosphorylation (Causier and Davies, 2002). Thus, defining potential binding partners of a protein of interest can provide functional information. While a variety of methods have been developed to validate physical protein interactions, including co-immunoprecipitation and affinity chromatography, these methods require *in vitro* handling of protein extracts (Brückner et al., 2009). Conversely yeast has been extensively used as a host in the elucidation and characterization of protein-protein interactions *in vivo* (Fields and Song, 1989). The yeast two-hybrid system makes use of the transcriptional machinery of *Saccharomyces cerevisiae*, through the generation of two gene constructs. The first construct, labelled as bait, consists of a protein of interest fused to a DNA binding domain, such as yeast GAL4. The DNA binding domain of the bait will direct the construct to the nucleus of the yeast cell, and localize it to a specific promoter region, the upstream activator sequence (UAS), located upstream of a reporter gene such as *TRP1*, *LEU2*, *HIS3* and *ADE2* (Rezwan and Auerbach, 2012). The second construct, labelled as prey, consists of a second protein of interest fused to the transactivation domain. When expressed individually, either the bait nor the prey are capable of activating the reporter genes located in the yeast genome. However, when co-expressed, should the two proteins of interest interact with each other, their interaction will reconstitute a functional transcription factor, in turn leading to the recruitment of RNA polymerase II and the subsequent transcription and accumulation mRNA encoding

for reporter proteins, usually consisting of yeast proteins involved in crucial metabolic pathways, such as His3p and Ade2p (Brückner et al., 2009; Rezwan and Auerbach, 2012). The use of yeast two-hybrid has been crucial in the development of large scale mapping networks of protein-protein interactions in *Arabidopsis thaliana* (*Arabidopsis* Interactome Mapping Consortium, 2011; Mitsuda et al., 2010). Interestingly, among the numerous protein-protein interactions tested, At-AME3, a LAMMER kinase, was shown to physically interact with a subset of Serine/Arginine-rich proteins, including At-RSZ21, At-RS2Z33 and At-SCL30 (Arabidopsis Interactome Mapping Consortium, 2011) .

LAMMER kinases are dual-specificity protein kinases that are able to phosphorylate serine, threonine, and tyrosine residues (Colwill et al., 1996). Intriguingly, all members of the LAMMER protein kinase family share an enriched RS dipeptide domain at the N-terminal region, similarly to SR proteins. The C-terminus contains the kinase domain, which is also highly conserved between members of the LAMMER kinase family. In addition to a strong degree of homology across the kinase domain, all members of this family contain a unique EHLAMMERILG motif in a subdomain of the kinase domain. Although this region is not conserved in general among kinases (Colwill, 1997), studies have suggested that this unique motif lies in a position where it might contact substrates and effectors (Yun et al., 1994, Nikolakaki et al., 2002). In *A. thaliana*, three LAMMER kinases, known as AME1, AME2 and AME3 (formerly AFC2, AFC1 and AFC3, respectively) have been identified. Golovkin and Reddy (1999), using yeast 2-hybrid assay in conjunction with phosphorylation assays showed that AME1/AFC2 is able to physically interact with and phosphorylate the plant-specific SR proteins At-RSZ21, At-RSZ22, At-SCL33(At-SR33), , and At-SR45, an SR-like protein *in vitro* (Golovkin and Reddy, 1999). Furthermore, At-AME1, was also shown to be

capable of phosphorylating proteins involved in flowering (Hornyik et al., 2010), as well as proteins involved in low temperature and drought responses (Ahsan et al., 2013; Kaye et al., 1998). Interestingly, AME1 appears to be lacking an RS domain at the N-terminus, in contrast to other LAMMER kinases, suggesting that structural features other than the RS domain are also important in protein-protein interactions. Conversely, AME2/AFC1 was shown not to be capable of phosphorylating the aforementioned SR proteins, suggesting that although LAMMER kinases are highly homologous, the ability to phosphorylate SR proteins is not likely to be a feature common to all LAMMER kinases (Golovkin and Reddy, 1999).

It has been suggested that AME3/AFC3, whose transcript levels were shown to increase under cold stress and acclimation conditions in *Brassica napus* and *BnCBF* overexpressors (Refer to chapter 2), plays a role in the adjustment of photosynthesis and acquisition of freezing tolerance of *A. thaliana* undergoing cold acclimation (Refer to chapters 2-3). Moreover, AME3 is able to phosphorylate Serine, Threonine and/or Tyrosine residues in At-RSZ22, as shown for AME1/AFC2 (Ahsan et al., 2013). In addition to interactions with SR proteins, SRPK4 and SRPK-like1, At-AME3 was shown to be able to phosphorylate protein phosphatase 1 (PPI-2), which has been suggested to play a role in multiple signalling networks (Ahsan et al., 2013). FPA, which is involved in flowering (Hornyik et al., 2010) and CAP160, which is involved in low temperature and drought responses (Ahsan et al., 2013; Kaye et al., 1998) were also shown to be phosphorylated by At-AME3, (Ahsan et al., 2013)

An expression profile analysis of mRNA transcripts encoding Serine/Arginine (SR) proteins in *Brassica* has shown a differential in expression profile of SR genes and LAMMER kinases in response to cold stress, cold acclimation and *BnCBF* overexpression.

While the transcript levels of AME1 and AME2 kinase were shown to decrease in response to cold stress, cold acclimation and *BnCBF* overexpression, AME3 transcripts were shown to increase under the same conditions (Refer to Chapter 2). This was associated with an observed increase in phosphorylation, suggesting that phosphorylation plays an important role in cold acclimation. In addition, *Arabidopsis* SR mutant lines were observed to exhibit an impaired recovery of photosynthetic performance under cold acclimation conditions, while *ame3* mutant lines were observed to be severely jeopardized with respect to the cold acclimation induced recovery of photosynthetic performance, in addition to the acquisition of freezing tolerance. More detailed studies (Chapter 4) have revealed that the deletion of At-AME3 kinase had not only jeopardized PSII performance in newly developed, cold acclimated leaves, but Photosystem I as well, providing further evidence that At-AME3 plays an essential role. While previous findings have helped in defining the importance of At-AME3 kinase with respect to cold acclimation, it was unclear whether these finding could be attributed to potential interactions between At-AME3 and this subset of SR proteins which were observed to be upregulated in response to low temperatures, or due to other factors. As AME1, which is homologous to AME3 was previously shown to phosphorylate SR proteins, this raised the question as to whether At-AME3 LAMMER kinase would be capable of interacting with At-RSZ22, At-RSZ22a, At-RS41, At-SR34b, At-RS40, At-SCL30, At-SCL30a, At-SR34, At-RS2Z33, At-RS31, At-SCL33, At-SR45 or At-SR45a Serine/Arginine-rich proteins. Palusa et al. (2007) have shown no changes in the splicing patterns of (At-RSZ22, At-RSZ22a, At-RS41, At-SCL30, At-SCL30a and At-SCL33) in response to 24h exposure to low temperatures in two week old *Arabidopsis* seedlings it is important to note that this subset of SR proteins were chosen based on the observation that an overall increase in their transcript levels were observed in response to cold stress and five

weeks of cold acclimation in wild type *Brassica napus* and *BnCBF* overexpressors (Refer to Chapter 2). Furthermore, this subset of SR proteins was chosen to be tested for physical interactions with At-AME3 based on the observation that loss-of-function mutants of At-RSZ22, At-RSZ22a, At-SCL30, At-RS41 and At-SR45 were impaired with respect to the cold acclimation induced recovery of photosynthetic performance (Refer to Chapter 3).

5.3 Hypothesis and objective

For this study, it was hypothesized that At-RSZ22, At-RSZ22a, At-RS41, At-SR34b, At-RS40, At-SCL30, At-SCL30a, At-SR34, At-RS2Z33, At-RS31, At-SCL33, At-SR45 and At-SR45a will interact with At-AME3.

The objective of this study was the identification of potential Serine/Arginine-rich and SR-like proteins which have shown differential expression under cold stress and acclimation conditions that can interact with At-AME3 LAMMER kinase, by means of yeast 2-hybrid assays.

5.4 Materials and methods

5.4.1 Generating Gateway-compatible SR gene constructs

5.4.1.1 RNA isolations and reverse transcriptase reactions

RNA was isolated from wild type *Arabidopsis thaliana* frozen leaf tissue using a phenol/guanidine isothiocyanate solution (TRIzol® Reagent, Life Technologies) and chloroform, according to the manufacturer's instructions. Sample quantity and yield was assessed using the Pharmacia Biotech GeneQuant RNA/DNA Calculator (Cambridge, England). All reverse transcription (RT) reactions were carried out using the Superscript II Reverse Transcription kit from Invitrogen (Burlington, ON, Canada). 1 µg of mRNA template, 1 µL of 100 µM oligo dT, 0.5 µL of RNase inhibitors and water were added in a final volume of 11 µL, and were incubated for 10 minutes at 70°C, then cooled on ice. Superscript II 5X buffer, along with dNTPs, 0.1 M DTT and Superscript II (Invitrogen) were then added, and samples were incubated for 1 hour at 42°C. All RT reactions were carried out using an Eppendorf epigradient S thermocycler.

5.4.1.2 PCR reactions

Primers containing Gateway attB restriction sites, along with the first few bases of the SR genes of interest (Tables 5.1 and 5.2) were used to amplify Gateway-compatible gene constructs of the following SR genes: At-RSZ21, At-RSZ22, At-SR45, At-SR45a, At-RS41, At-RS2Z32, At-RS40, At-SCL30a, At-SR34a, At-SR34b, At-SR30, At-SCL28, At-SCL33, At-RS31 and At-RS31a. In addition, At-SRPK-like 1 protein kinase was amplified. The following PCR parameters were used for all reactions: an initial denaturation step at 90°C for two minutes, followed by 30 cycles at 90°C for 30 sec, 58°C annealing step for 30 seconds, and two minute extensions at 72°C. An aliquot of each PCR product was then loaded and run on 1% TAE-Agarose gels, and visualized under UV light using a ChemiDoc XR+ light cabinet (BioRad) and ImageLab visualization software (Fig. 5.1). All bands which have been identified on the gel were excised and purified using the PureLink Quick Gel Extraction Kit (Invitrogen, Carlsbad CA), per the manufacturers' protocol.

Table 5.1: attB1 primers used for generating Gateway-compatible Serine-Arginine (SR) gene constructs.

	SR protein	Accession number (TAIR)	attB1 primer sequence
SF2/ASF-like	At-SR30	At1g09140	GGGG-ACA-AGT-TTG-TAC-AAA-AAA-GCA-GGC-TTC-GAA-GGA-GAT-AGA-ACC-ATG-AGT AGC CGA TGG AAT CGT A
SR subfamily	At-SR34	At1g02840	GGGG-ACA-AGT-TTG-TAC-AAA-AAA-GCA-GGC-TTC-GAA-GGA-GAT-AGA-ACC-ATG-AGC AGT CGT TCG AGT AG
	At-SR34a	At3g49430	GGGG-ACA-AGT-TTG-TAC-AAA-AAA-GCA-GGC-TTC-GAA-GGA-GAT-AGA-ACC-ATG- AGT GGG CGA TTT TCT CG
	At-SR34b	At4g02430	GGGG-ACA-AGT-TTG-TAC-AAA-AAA-GCA-GGC-TTC-GAA-GGA-GAT-AGA-ACC-ATG- AGC AGC CGT TCG AGT AG
9G8/SRp20-like	At-RSZ21	At1g23860	GGGG-ACA-AGT-TTG-TAC-AAA-AAA-GCA-GGC-TTC-GAA-GGA-GAT-AGA-ACC-ATG- ACG AGG GTT TAT GTC GG
RSZ subfamily	At-RSZ22	At4g31580	GGGG-ACA-AGT-TTG-TAC-AAA-AAA-GCA-GGC-TTC-GAA-GGA-GAT-AGA-ACC-ATG-TCA CGT GTG TAC GTC GG
RS2Z subfamily	At-RS2Z32	At3g53500	GGGG-ACA-AGT-TTG-TAC-AAA-AAA-GCA-GGC-TTC-GAA-GGA-GAT-AGA-ACC-ATG-AAG CGT GAT TAT GCC TTT GT
SC35-like	At-SCL28	At5g18810	GGGG-ACA-AGT-TTG-TAC-AAA-AAA-GCA-GGC-TTC-GAA-GGA-GAT-AGA-ACC-ATG- GCT AGA GCG AGA AGC C
	At-SCL30a	At3g13570	GGGG-ACA-AGT-TTG-TAC-AAA-AAA-GCA-GGC-TTC-GAA-GGA-GAT-AGA-ACC-ATG- AGA GGA AGG AGC TAC ACG
	At-SCL33	At1g55310	GGGG-ACA-AGT-TTG-TAC-AAA-AAA-GCA-GGC-TTC-GAA-GGA-GAT-AGA-ACC-ATG- AGG GGA AGG AGC TAC A
Plant specific	At-RS31	At3g61860	GGGG-ACA-AGT-TTG-TAC-AAA-AAA-GCA-GGC-TTC-GAA-GGA-GAT-AGA-ACC-ATG-AGG CCA GTG TTC GTC
RS subfamily	At-RS31a	At2g46610	GGGG-ACA-AGT-TTG-TAC-AAA-AAA-GCA-GGC-TTC-GAA-GGA-GAT-AGA-ACC-ATG-AGA CAT GTG TAC GTT GGG
	At-RS40	At4g25500	GGGG-ACA-AGT-TTG-TAC-AAA-AAA-GCA-GGC-TTC-GAA-GGA-GAT-AGA-ACC-ATG- AAG CCA GTC TTC TGT GG
	At-RS41	At5g52040	GGGG-ACA-AGT-TTG-TAC-AAA-AAA-GCA-GGC-TTC-GAA-GGA-GAT-AGA-ACC-ATG- AAG CCT GTC TTT TGC GG
SR-like	At-SR45	At1g16610	GGGG-ACA-AGT-TTG-TAC-AAA-AAA-GCA-GGC-TTC-GAA-GGA-GAT-AGA-ACC-ATG-GCG AAA CCA AGT CGT
	At-SR45a	At1g07350	GGGG-ACA-AGT-TTG-TAC-AAA-AAA-GCA-GGC-TTC-GAA-GGA-GAT-AGA-ACC-ATG- GGG AAA CGT GAA ATT CAT T
Protein kinases	SRPK-like 1	At2g17530	GGGG-ACA-AGT-TTG-TAC-AAA-AAA-GCA-GGC-TTC-GAA-GGA-GAT-AGA-ACC-ATG-TCG TGT TCA TCC TCA TCT G

Table 5.2: attB2 primers used for generating Gateway-compatible Serine-Arginine (SR) gene constructs.

	SR protein	Accession number (TAIR)	attB2 primer sequence
SF2/ASF-like	At-SR30	At1g09140	GGGG-ACC-ACT-TTG-TAC-AAG-AAA-GCT-GGG-TT-TCA ACC AGA TAT CAC AGG TGA AA
SR subfamily	At-SR34	At1g02840	GGGG-ACC-ACT-TTG-TAC-AAG-AAA-GCT-GGG-TT- TTA CCT CGA TGG ACT CCT AGT G
	At-SR34a	At3g49430	GGGG-ACC-ACT-TTG-TAC-AAG-AAA-GCT-GGG-TT-TCA CAC ACT GCC TTC GCG
	At-SR34b	At4g02430	GGGG-ACC-ACT-TTG-TAC-AAG-AAA-GCT-GGG-TT- TCA TCG AGC TTT TTT TAT CGC A
9G8/SRp20-like	At-RSZ21	At1g23860	GGGG-ACC-ACT-TTG-TAC-AAG-AAA-GCT-GGG-TT- TCA CAC CCC ATT GGC ATA TG
RSZ subfamily	At-RSZ22	At4g31580	GGGG-ACC-ACT-TTG-TAC-AAG-AAA-GCT-GGG-TT-TCA GCT CCT GCT TCT GCG
RS2Z subfamily	At-RS2Z32	At3g53500	GGGG-ACC-ACT-TTG-TAC-AAG-AAA-GCT-GGG-TT-TCA AGG TGA CTC ACT GCC TTT AG
SC35-like	At-SCL28	At5g18810	GGGG-ACC-ACT-TTG-TAC-AAG-AAA-GCT-GGG-TT-TCA ACG ACT TAA GGA TCG AGA A
	At-SCL30a	At3g13570	GGGG-ACC-ACT-TTG-TAC-AAG-AAA-GCT-GGG-TT-TCA CTG GCT TGG AGA ACG G
	At-SCL33	At1g55310	GGGG-ACC-ACT-TTG-TAC-AAG-AAA-GCT-GGG-TT-TCA CTG GCT TGG TGA ACG
Plant specific	At-RS31	At3g61860	GGGG-ACC-ACT-TTG-TAC-AAG-AAA-GCT-GGG-TT- TCA AGG TCT TCC TCT TGG GA
RS subfamily	At-RS31a	At2g46610	GGGG-ACC-ACT-TTG-TAC-AAG-AAA-GCT-GGG-TT-TCA ACC TCT TGC TCT TTG AAT C
	At-RS40	At4g25500	GGGG-ACC-ACT-TTG-TAC-AAG-AAA-GCT-GGG-TT-TCA CTC GTC AGC TGG TGG
	At-RS41	At5g52040	GGGG-ACC-ACT-TTG-TAC-AAG-AAA-GCT-GGG-TT-TCA TTC CTC TGC TGG CG
SR-like	At-SR45	At1g16610	GGGG-ACC-ACT-TTG-TAC-AAG-AAA-GCT-GGG-TT-TTA AGT TTT ACG AGG TGG AGG TG
	At-SR45a	At1g07350	GGGG-ACC-ACT-TTG-TAC-AAG-AAA-GCT-GGG-TT- TTA TGG GCT GAC GGA TCT G
Protein kinases	SRPK-like 1	At2g17530	GGGG-ACC-ACT-TTG-TAC-AAG-AAA-GCT-GGG-TT-TCA AGA ACA TGA ACC TTT GAT CTG

Figure 5.1: Amplification of Gateway-compatible SR gene constructs.

The molecular marker was designated as L, while lanes 1 to 18 designate gene PCR amplification products of At-RSZ22, At-SR45, At-SR34, At-RSZ21, At-RS41, At-RS31a, At-RS2Z32, At-SR30, At-RS40, At-SCL30a, At-SRPK-like1, At-RS31, At-SR34a, At-SCL28, At-SR45a, At-SR34b, At-SCL33 and elf1a, respectively. Bands corresponding to At-RSZ22 (1), At-SR45 (2), At-SR34 (3), At-RSZ21 (4), At-RS41 (5), At-RS2Z32 (7), At-SR30 (8), At-SCL30a (10), At-RS31 (12) and At-SR34a (13) were successfully excised from the gel and purified. The purified Gateway-compatible SR gene constructs were then used for subsequent ligation reactions to generate SR entry vectors, followed by PDEST-AD vectors.

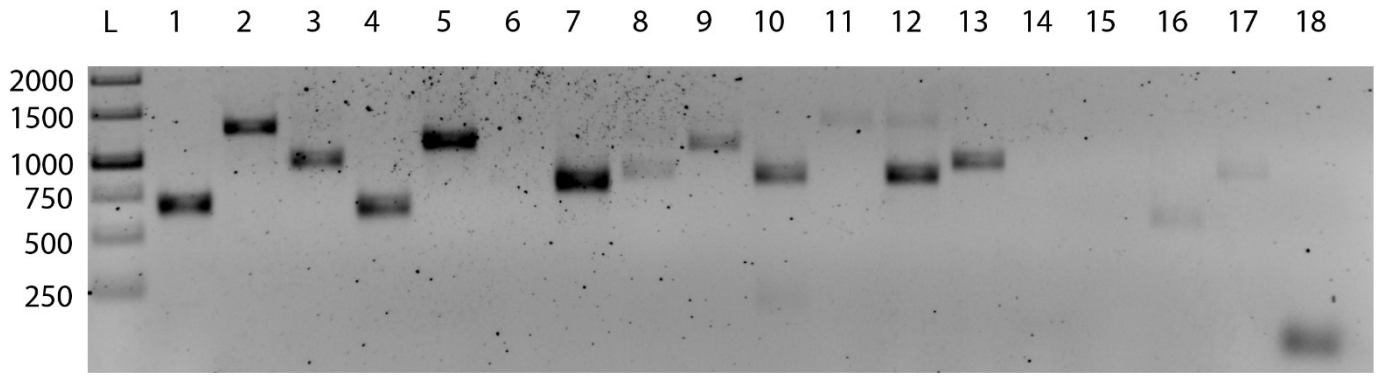
L
1
2
3
4
5
6
7
8
9
10
11
12
13
14
15
16
17
18
2000
1500
1000
750
500
250

5.4.2 Cloning SR genes of interest

5.4.2.1 Generating SR entry clones

The purified attB PCR products were subsequently used in BP recombination reactions to transfer them into donor vectors to create entry clones. Equimolar amounts of At-RSZ22, At-RSZ21, At-SR45, At-SR34, At-RS41, At-RS2Z32 and At-SCL30a attB-PCR products and PDONR 221 vectors (Invitrogen) (Fig. 5.2) were added to the Gateway BP Clonase II enzyme mix (Invitrogen), to a final volume of 10 µL. All reactions were incubated at 25°C for an hour. 1 µL of Proteinase K was then added to each reaction, and incubated for 10 minutes at 37°C.

The resulting entry vectors were then transformed into Library Efficient DH5α Competent *E. coli* cells (Invitrogen) according to the manufacturer's instructions. An aliquot of the transformed cells was spread on LB agar plates with 100 µg/mL kanamycin, and incubated at 37°C overnight to select for positive transformants. The identified transformants containing SR genes of interest were then grown in liquid cultures, and plasmids were purified using the PureLink HQ Mini Plasmid Purification Kit (Invitrogen), in accordance with the manufacturer's specifications.

Figure 5.2: Restriction map of pDONR221.

Equimolar amounts of At-RSZ22, At-RSZ21, At-SR45, At-SR34, At-RS41, At-RS2Z32 and At-SCL30a attB-PCR products and PDONR 221 vectors were used in conjunction with the Gateway BP Clonase II enzyme mix to generate SR entry clones. These SR entry clones were subsequently transformed into Library Efficient DH5α Competent *E.coli* cells. (Restriction map generated using the Lasergene SeqBuilder program from DNASTAR, Madison, WI, USA).

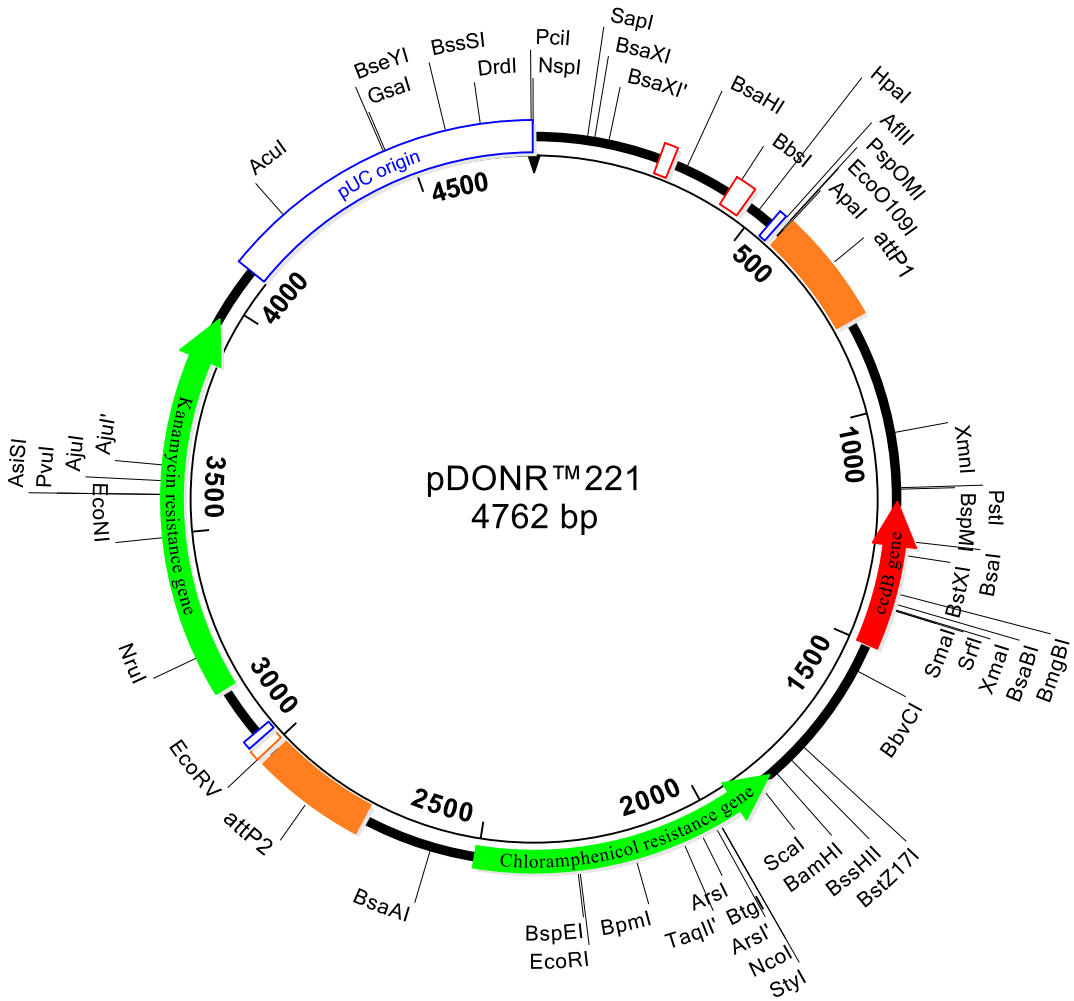
pDONR™221
4762 bp
pUC origin
Kanamycin resistance gene
Chloramphenicol resistance gene
ccdB gene
attP1
attP2
500
1000
1500
2000
2500
3000
3500
4000
4500
AcuI
BseYI
GsaI
BssSI
DrdI
PciI
NspI
SapI
BsaXI
BsaXI'
BsaHI
BbsI
HpaI
AflII
PspOMI
EcoO109I
ApaI
XmnI
PstI
BspMI
BsaI
BstXI
SmaI
SrfI
XmaI
BsaBI
BmgBI
BbvCI
ScaI
BamHI
BssHII
BstZ17I
NcoI
StyI
ArsI'
BtgI
TaqII'
ArsI
BpmI
BspEI
EcoRI
BsaAI
EcoRV
NruI
AsiSI
PvuI
AjuI
AjuI'
EcoNI

5.4.2.2 Generating destination (pDEST-AD) vectors

The purified plasmids were used in LR recombination reactions to transfer SR genes of interest, located into PDONR entry vectors, into PDEST vectors (Fig. 5.3) for subsequent yeast transformations. Equimolar amounts of plasmids containing At-RSZ22, At-RSZ21, At-SR45, At-SR34, At-RS41, At-RS2Z32 and At-SCL30 and purified PDEST-AD vectors were added to the Gateway LR Clonase II Plus enzyme mix (Invitrogen), to a final volume of 10 µL. All reactions were incubated at 25°C for an hour. 1 µL of Proteinase K was then added to each reaction, and incubated for 10 minutes at 37°C. The purified PDEST-AD were a kind donation from Dr. Marc Vidal.

The resulting entry vectors were then transformed into Library Efficient DH5α Competent *E. coli* cells (Invitrogen) according to the manufacturer's instructions. An aliquot of the transformed cells was spread on LB agar plates with 100 µg/mL ampicillin, and incubated at 37°C overnight to select for positive transformants. All successful transformants were then grown in liquid cultures, and plasmids were purified using the PureLink HQ Mini Plasmid Purification Kit (Invitrogen), in accordance with the manufacturer's instructions.

In addition to the generated PDEST vectors five commercially available PDEST clones (PDEST-DB075F09, PDEST-AD011H09, PDEST-AD100F07, PDEST-AD097E08 and PDEST-AD042C11), corresponding to At-AME3 (At4g32660), At-SC35 (At5g64200), At-SCL30 (At3g55460), At-RS2Z33 (At2g37340) and At-RSZ22a (At2g24590), respectively, were purchased as bacterial stabs from the *Arabidopsis* Biological Resource Centre (ABRC). These clones were streaked on LB plates with 100 µg/mL ampicillin and incubated overnight at 37°C. Resulting colonies were grown in liquid LB cultures, and plasmids were purified

using the PureLink HQ Mini Plasmid Purification Kit (Invitrogen), according to the manufacturer's instructions. Sample yields were assessed using the Pharmacia Biotech GeneQuant RNA/DNA Calculator (Cambridge, England). Purified plasmids were then stored at -20°C for subsequent transformations in yeast.

5.4.3 Sequencing reactions

To confirm the presence of full-length SR genes, all PDONR and PDEST vectors were sequenced. All sequencing reactions were done using the BigDye Terminator v3.1 Cycle Sequencing Kit (Applied Biosystems). 10-30 ng of purified PDEST-AD or PDEST-DB plasmids were used as template in conjunction with 2.5X Ready Reaction Premix, 5X BigDye Sequencing Buffer, attB1 (5`- GGGGACAAGTTTGTACAAAAAAGCAGGCT-3`) forward sequencing primer or attB2 (5`-GGGGACCACTTTGTACAAGAAAGCTGGGT-3`) reverse sequencing primer and distilled water for a total of 20µL. A forward sequencing reaction using an M13 primer (5`-TGTAAAACGACGGCCAGT-3`) and a pGEM-3Zf as a DNA template (both provided in the kit) was done as a positive control. Sequencing reactions were then run on Eppendorf epigradient S or Mastercycler Pro S thermocyclers, with the following parameters: initial denaturation at 95°C for 5 minutes, followed by 40 cycles at 95°C for 15 secs, a 10 sec annealing step at 55°C, and an elongation step for 4 minutes at 60°C. All sequencing reactions were processed by an ABI Prism 3100 Genetic Analyzer.

5.4.4 Yeast 2-hybrid assays

5.4.4.1 Yeast transformations

Parental haploid yeast strain Y8800 MATa was used to transform PDEST-AD-Y constructs for At-RSZ22, At-RSZ22a At-RSZ21, At-SC35 At-SR45, At-SR34, At-RS41, At-RS2Z32, At-RS2Z33 and At-SCL30 while Y8930 MATα was used to transform PDEST-DB075F09, a PDEST-DB-X construct for At-AME3. The parental yeast strains used for the transformations were kindly donated by Dr. Marc Vidal. All yeast transformations were carried out as described by Dreze et al (2010). Y8800 MATa and Y8930α haploid yeast strains were grown on YPD plates supplemented with 0.003% L-Adenine hemisulfite salt (Sigma) for 3 days at 30°C. Resulting colonies were then suspended in TE/LiAc buffer, and 1ug of plasmid DNA from AD-Y constructs were added to the Y8800 suspensions. Concomitantly, 1µg of plasmid DNA from PDEST-DB075F09 was added to Y8930. All cell suspensions were then incubated at 30°C for 30 minutes, followed by a heat shock treatment at 42°C for 5 minutes. The cells were then resuspended in YPD medium and spread on selective plates in order to select for positive yeast transformants. Y8930 cells transformed with At-AME3 as a DB-X vector were plated on Synthetic Dropout (SDO) agar plates lacking leucine, whereas Y8800 cells transformed with the AD-Y constructs corresponding to SR genes of interest were plated on SDO agar plates lacking tryptophan.

Figure 5.3: Restriction map of pDEST22 and pDEST32 destination vectors.

Panel A depicts the restriction map of the pDEST22 vector used to generate PDEST-AD vectors containing At-RSZ22, At-RSZ21, At-SR45, At-SR34, At-RS41, At-RS2Z32 and At-SCL30. Panel B depicts the restriction map of a pDEST32 vector used to generate a pDEST-DB destination vector for At-AME3. Arrowheads designate attR1 and attR2 sites, where SR genes of interest, as well as At-AME3 were inserted. Equimolar amounts of plasmids containing At-RSZ22, At-RSZ21, At-SR45, At-SR34, At-RS41, At-RS2Z32, At-RS40 and At-SCL30 and purified pDEST22 vectors were added to the Gateway LR Clonase II Plus enzyme mix entry to generate pDEST-AD and pDEST-DB destination vectors to be used as preys and bait, respectively, in yeast 2-hybrid assays. pDEST22 and pDEST32 restriction maps were obtained from Invitrogen.

A

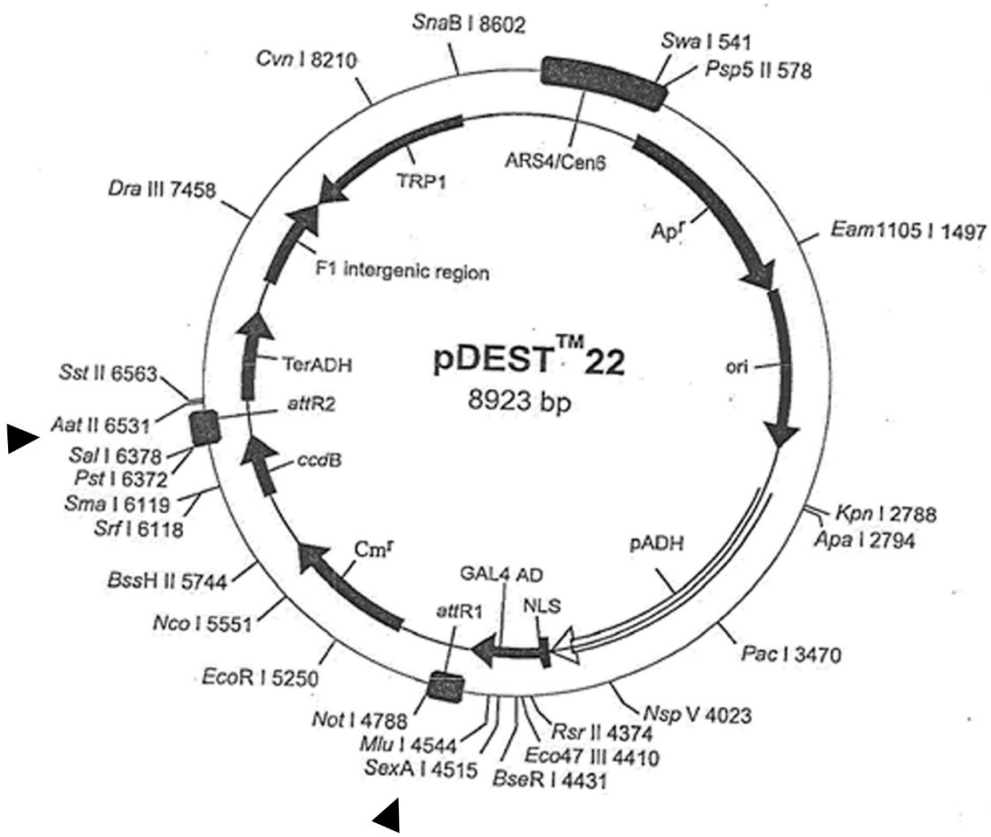
SnaB I 8602
Swa I 541
Psp5 II 578
Cvn I 8210
ARS4/Cen6
TRP1
Dra III 7458
Ap^r
Eam1105 I 1497
F1 intergenic region
pDEST™22
8923 bp
ori
TerADH
Sst II 6563
attR2
Aat II 6531
Sal I 6378
Pst I 6372
Sma I 6119
Srf I 6118
ccdB
Kpn I 2788
Apa I 2794
pADH
Cm^r
BssH II 5744
GAL4 AD
attR1
NLS
Nco I 5551
Pac I 3470
EcoR I 5250
Nsp V 4023
Not I 4788
Rsr II 4374
Mlu I 4544
Eco47 III 4410
SexA I 4515
BseR I 4431

B

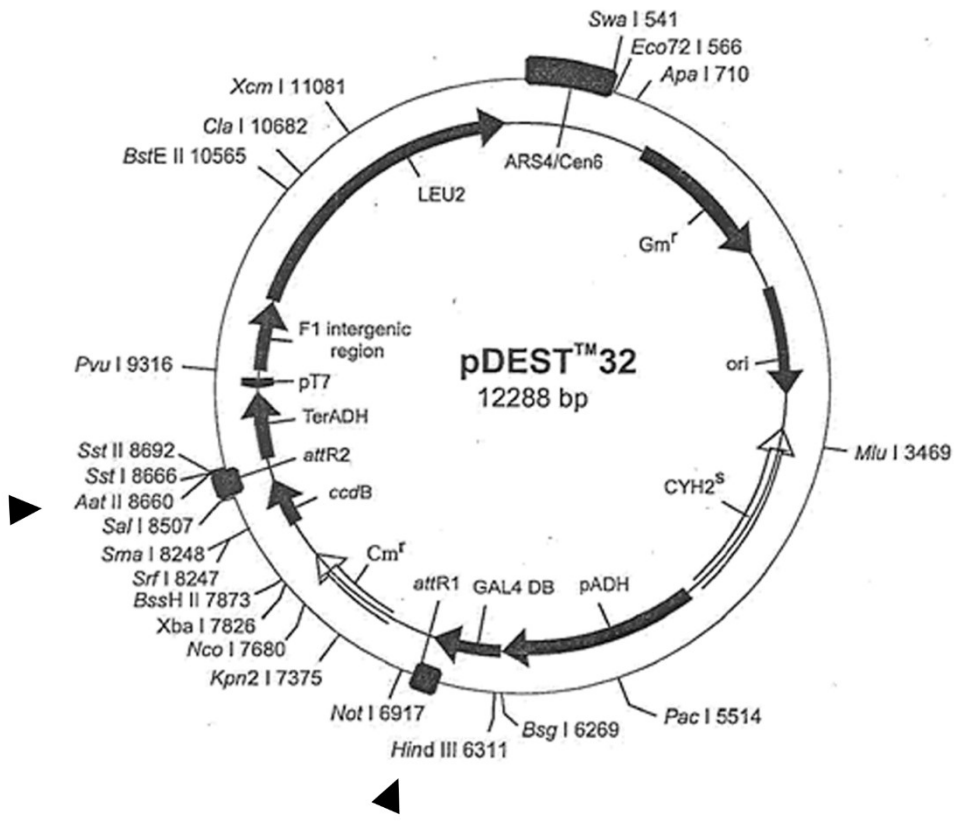
Swa I 541
Eco72 I 566
Apa I 710
Xcm I 11081
Cla I 10682
BstE II 10565
ARS4/Cen6
LEU2
Gm^r
F1 intergenic region
pDEST™32
12288 bp
ori
Pvu I 9316
pT7
TerADH
Mlu I 3469
Sst II 8692
Sst I 8666
attR2
Aat II 8660
ccdB
CYH2^S
Sal I 8507
Sma I 8248
Cm^r
Srf I 8247
attR1
GAL4 DB
pADH
BssH II 7873
Xba I 7826
Nco I 7680
Kpn2 I 7375
Not I 6917
Bsg I 6269
Pac I 5514
Hind III 6311

5.4.4.2 Self-activation tests

To test for self-activation of either AD-Y or DB-X constructs, six positive At-RSZ22, At-RSZ22a At-RSZ21, At-SC35 At-SR45, At-SR34, At-RS41, At-RS2Z33, At-SCL30 and At-SCL30a yeast transformants were picked, then patched onto SDO agar plates lacking tryptophan, adenine and histidine. At-AME3 transformants were picked and patched onto SDO agar plates lacking leucine, adenine and histidine. All SDO agar plates were supplemented with 1 mM 3-aminotriazol (3AT). All plates were incubated at 30°C for three days, and assessed for growth. Plates exhibiting growth represent auto-activation, and were not considered for the yeast 2-hybrid assay. Conversely, plates containing a lack of growth suggest that the AD-Y or DB-X construct is unable to auto-activate, and were subsequently used for yeast 2-hybrid assays.

Figure 5.4: Synthetic Dropout agar plates used for the assessment of auto-activation of At-RSZ22a At-RSZ21, At-SC35 At-SR45, At-SR34a, At-RS41, At-RS2Z33, At-SCL30 and At-SCL30a AD-Y and At-AME3 DB-X yeast transformants.

Six positive At-RSZ22a At-RSZ21, At-SC35 At-SR45, At-SR34a, At-RS41, At-RS2Z33, At-SCL30 and At-SCL30a yeast transformants were picked, then patched onto Synthetic Dropout (SDO) agar plates lacking tryptophan, adenine and histidine. At-AME3 transformants were picked and patched onto SDO agar plates lacking leucine, adenine and histidine. All SDO agar plates were supplemented with 1mM 3-aminotriazol (3AT). All plates were incubated at 30°C for three days, and assessed for growth. Plates exhibiting growth represent auto-activation, and were not considered for the yeast 2-hybrid assay. Conversely, plates containing a lack of growth suggest that the AD-Y or DB-X construct is unable to auto-activate, and were subsequently used for yeast 2-hybrid assays. Positive yeast transformants shown are representative of six streaks, which were performed in triplicates.

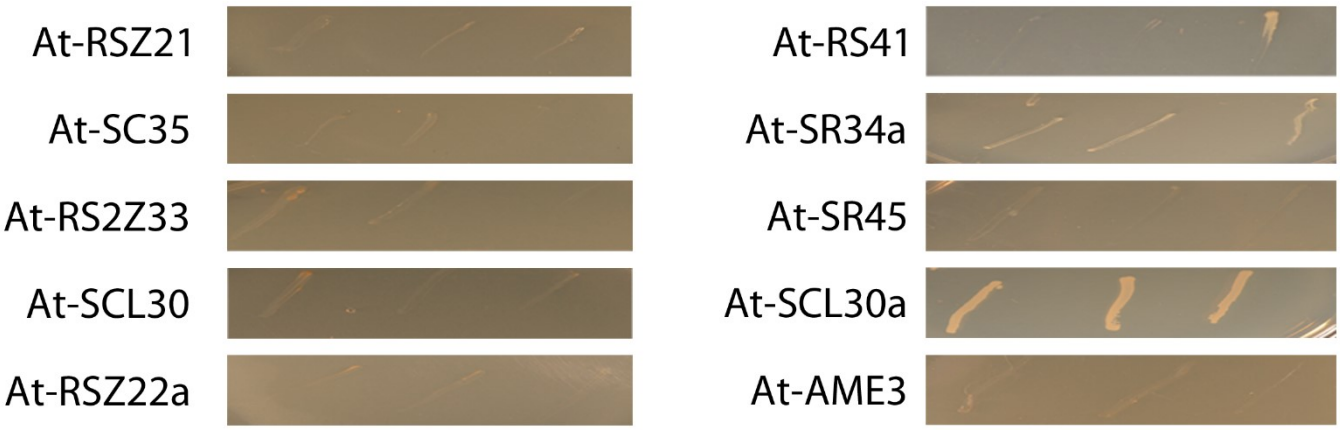
At-RSZ21
At-SC35
At-RS2Z33
At-SCL30
At-RSZ22a
At-RS41
At-SR34a
At-SR45
At-SCL30a
At-AME3

5.4.4.3 Yeast mating and replica plating

Yeast transformants that did not auto-activate were patched on secondary selection plates. At-AME3 transformants were patched on SDO –Leu plates, and SR transformants were patched on SDO –Trp plates and incubated for 3 days at 30°C. Transformants were then picked and transferred to 50mL of SDO –Leu or SDO –Trp for At-AME3 or At-SR transformants, respectively. All selective media cultures were grown overnight at 30°C using a Controlled Environment Incubator Shaker from New Bruinswick Scientific (Edison, NJ, USA). The overnight cultures were then centrifuged in an Eppendorf 5810 R and resuspended in 1.5mL of non-selective rich yeast medium (YPDA). All subsequent mating reactions were performed as described by Dreze et al. (2010). Liquid cultures of Y8930 haploid cells transformed with At-AME3 DB-X vector were mixed with Y8800 haploid cells transformed with At-RSZ22, At-RSZ22a At-RSZ21, At-SC35 At-SR45, At-SR34, At-RS41, At-RS2Z32, At-RS40, and At-SCL30 AD-Y vectors in equal amounts, and spread on YPDA media plates containing sterile cellophane sheets (Bio-Rad). All plates were then incubated for 3 hours at 30°C. Cellophane sheets were then washed in 40mL of SDO media lacking leucine and tryptophan, and centrifuged at 5000 x g for 5 minutes. The resulting pellets were then resuspended in SDO –Leu –Trp media and plated on SDO plates lacking leucine and tryptophan, in order to select for diploids cells. All plates were incubated at 30°C for 4-5 days.

Template SDO –Trp –Leu plates, which were used for replica plating, were set up by patching 5 yeast diploid cells, along with 5 control diploid strains of varying interaction strength (Refer to Table 5.3). Each experiment was performed in triplicate. The control diploid yeast cells were a kind donation from Dr. Marc Vidal. Control 1, consisting of an

empty pDEST-AD vector paired with an empty pDEST-DB vector, was used as a negative control, whereas Controls 2,3,5 and 6 all designate positive controls with varying levels of protein interaction, ranging from weak (Control 2) to strong (Controls 3,5,6). All plates were incubated at 30°C for 3 days, then replica plated using sterile velvet sheets (Scienceware) fixed to a replica plating base (Bio-Rad) on Synthetic Dropout (SDO) media plates supplemented with 1mM 3-aminotriazol, lacking leucine, tryptophan, histidine, adenine, SDO plates supplemented with 1mM 3-aminotriazol, lacking leucine, tryptophan, and histidine, SDO plates lacking leucine, tryptophan and adenine, and SDO plates lacking leucine and tryptophan. Moreover, replica plates were done on non-selective YPDA plates as a positive control. Replica plates were incubated at 30°C for 3 days, and growth on selective and non-selective plates were recorded and compared with the controls to assess the level of interaction between the SR proteins of interest and At-AME3.

Table 5.3: Identities and expected phenotypes of controls used in every yeast 2-hybrid experiment.

	Plasmid pairs	Proteins	Interaction strength
Control 1	pDEST-AD/pDEST-DB	No insert	None, background
Control 2	pDEST-AD-E2F1 pDEST-DB-CYH2-pRB	Human E2F1, aa 342-437 Human pRB, aa 302-928	Weak
Control 3	pDEST-AD-Jun pDEST-DB-Fos	Mouse Jun, aa 250-325 Rat Fos, aa 132-211	Moderately Strong
Control 5	pDEST-AD-dE2F1 pDEST-DB-dDP	Drosophila E2F, aa 225-433 Drosophila DP, aa 1-377	Strong
Control 6	pDEST-AD-dE2F1 pDEST-DB-dDP	Drosophila E2F, aa 225-433 Drosophila DP, aa 1-377	Strong

5.5 Results

5.5.1 Yeast 2-hybrid mating

PDEST-DB strains containing At-AME3, mated to transformed PDEST-AD yeast strains with At-RS2Z33 exhibited poor growth on synthetic dropout plates lacking leucine, histidine, adenine, (SDO –LTA), synthetic dropout plates lacking leucine, tryptophan and histidine supplemented with 3-aminotriazol (SDO –LTH +3AT), as well as on synthetic dropout plates lacking leucine, tryptophan, histidine and tryptophan with added 3-aminotriazol (SDO-LTAH +3AT). This observed growth of At-AME3/At-RS2Z33 diploids is consistent with the growth of Control 1 (C1) diploids, which do not contain any inserts, and are indicative of no interaction between the binding and activation domains (Table 5.3). Thus, based in the known phenotype of C1 diploid strains and the observed phenotype of At-AME3/At-RS2Z33 diploid strains, these results would suggest that At-AME3 does not interact with At-RS2Z33 (Fig. 5.5). Moreover, similarly to At-AME3/At-RS2Z33 diploids, At-AME3/At-SC35 diploids exhibit growth phenotypes comparable to C1 controls, suggesting no interaction between At-AME3 and At-SC35.

Conversely, At-AME/At-RSZ21, At-AME3/RSZ22a, At-AME3/At-SCL30, At-AME3/At-SR34a, At-AME3/At-RS41 and At-AME3/At-SR45 diploids were observed to grow at various levels on synthetic dropout plates lacking leucine and tryptophan (SDO –LT), leucine, tryptophan, adenine, (SDO –LTA), synthetic dropout plates lacking leucine, tryptophan and histidine supplemented with 3-aminotriazol (SDO –LTH +3AT), as well as on synthetic dropout plates lacking leucine, tryptophan, histidine and tryptophan with added 3-aminotriazol (SDO-LTAH +3AT). As the growth of these previously mentioned diploids was similar to controls C2, C3, C5 and C6, these results would suggest that this subset of

Serine/Arginine-rich proteins are able to physically interact with At-AME3 kinase, to varying levels of interaction strength. The growth of At-AME3/At-RSZ21 and At-AME3/At-SCL30 diploids compared to controls would suggest weak interactions between At-AME3 kinase and At-RSZ21, as well as between At-AME3 and At-SCL30. Furthermore, a moderate interaction strength was observed between At-AME3 and At-RSZ22a, At-SR34a and At-SR45, based on diploid growth on selective media plates (Fig. 5.5). The strong growth of At-AME3/At-RS41 diploids on selective media compared to controls would suggest a strong interaction between At-AME3 and At-RS41 (Fig. 5.5). It should be noted that poor growth which was observed on YPDA plates for RSZ21, SCL30 and SR45 diploids could be attributed to a low biomass being left on the replica plating sheet when stamping YPDA plates, which were done last.

Some interactions between At-AME3 and SR proteins of interest could not be tested. For example, a Gateway-compatible construct for At-RS40 was successfully amplified and excised from the gel (Fig. 5.1), but could not be transferred into a donor vector to generate an entry clone. Interactions between At-AME3 and At-SCL30a could not be evaluated, as the latter was shown to be able to undergo auto-activation (Fig. 5.4). While At-RS2Z32 constructs was successfully transferred to an AD-Y vector, subsequent yeast transformation attempts were unsuccessful. Thus At-RS2Z32 interaction with At-AME3 could not be tested. Interactions between At-SCL28, At-RS31a, At-SCL33, At-SR34b, and At-SR45a could not be tested, as Gateway-compatible SR transcripts could not be amplified.

Figure 5.5: Phenotypes of At-AME3/SR protein diploids.

At-RSZ22a At-RSZ21, At-SC35, At-SR45, At-SR34a, At-RS41, At-RS2Z33, and At-SCL30 haploid AD-Y yeast transformants, which were used as prey, were mated to a DB-X At-AME3 haploid yeast transformant as described by Dreze et al. (2010), and plated on template SDO –Trp –Leu plates, which were used for replica plating. These plates were set up by patching 5 yeast diploid cells, along with 5 control diploid strains of varying interaction strength. Control 1, consisting of an empty pDEST-AD vector paired with an empty pDEST-DB vector, was used as a negative control, whereas Controls 2,3,5 and 6 all designate positive controls with varying levels of protein interaction, ranging from weak (Control 2) to strong (Controls 3,5,6). All plates were incubated at 30°C for 3 days, then replica plated using sterile velvet sheets fixed to a replica plating base on Synthetic Dropout (SDO) media plates supplemented with 1mM 3-aminotriazol, lacking leucine, tryptophan, histidine, adenine, SDO plates supplemented with 1mM 3-aminotriazol, lacking leucine, tryptophan, and histidine, SDO plates lacking leucine, tryptophan and adenine, and SDO plates lacking leucine and tryptophan. Moreover, replica plates were done on non-selective YPDA plates as a positive control. Replica plates were incubated at 30°C for 3 days, and growth on selective and non-selective plates were recorded and compared with the controls to assess the level of interaction between the SR proteins of interest and At-AME3. Each yeast 2-hybrid mating assay presented was performed in triplicate. Please note that the poor growth of yeast diploids observed for At-AME3/At-SR45, At-AME3/At-RSZ21 and At-AME3/At-SCL30 mate pairs on YPDA plates are due to not having enough biomass on the velvet sheets used for stamping replica plates.

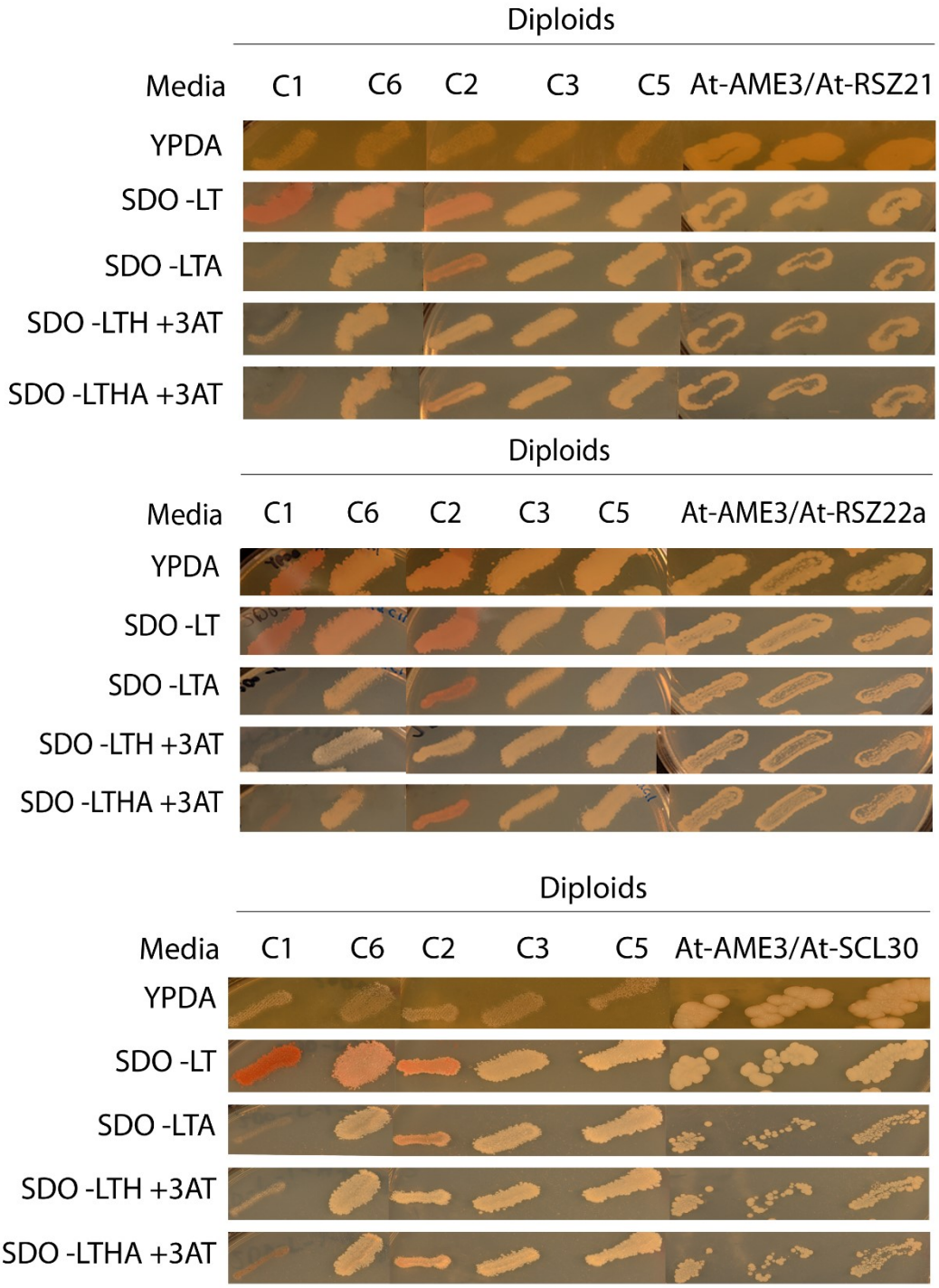
Diploids
Media
C1
C6
C2
C3
C5
At-AME3/At-RSZ21
YPDA
SDO -LT
SDO -LTA
SDO -LTH +3AT
SDO -LTHA +3AT
Diploids
Media
C1
C6
C2
C3
C5
At-AME3/At-RSZ22a
YPDA
SDO -LT
SDO -LTA
SDO -LTH +3AT
SDO -LTHA +3AT
Diploids
Media
C1
C6
C2
C3
C5
At-AME3/At-SCL30
YPDA
SDO -LT
SDO -LTA
SDO -LTH +3AT
SDO -LTHA +3AT

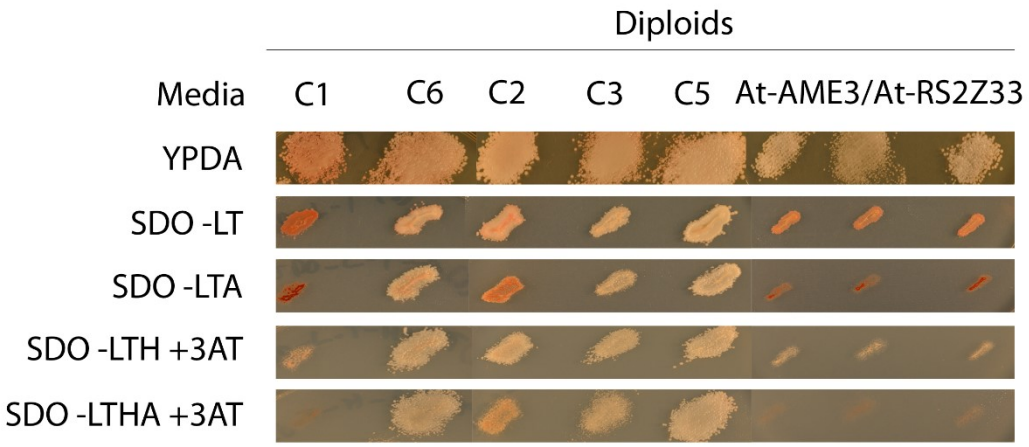
Diploids
Media
C1
C6
C2
C3
C5
At-AME3/At-RS2Z33
YPDA
SDO -LT
SDO -LTA
SDO -LTH +3AT
SDO -LTHA +3AT

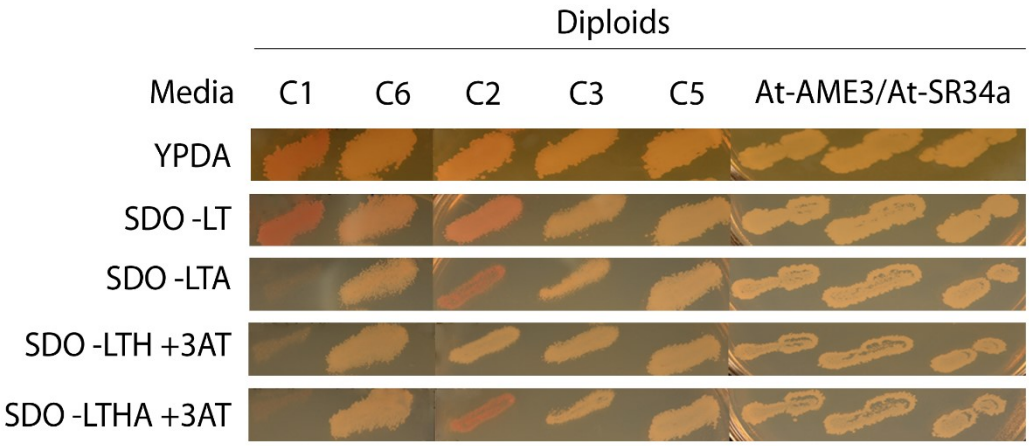
Diploids
Media
C1
C6
C2
C3
C5
At-AME3/At-SR34a
YPDA
SDO -LT
SDO -LTA
SDO -LTH +3AT
SDO -LTHA +3AT

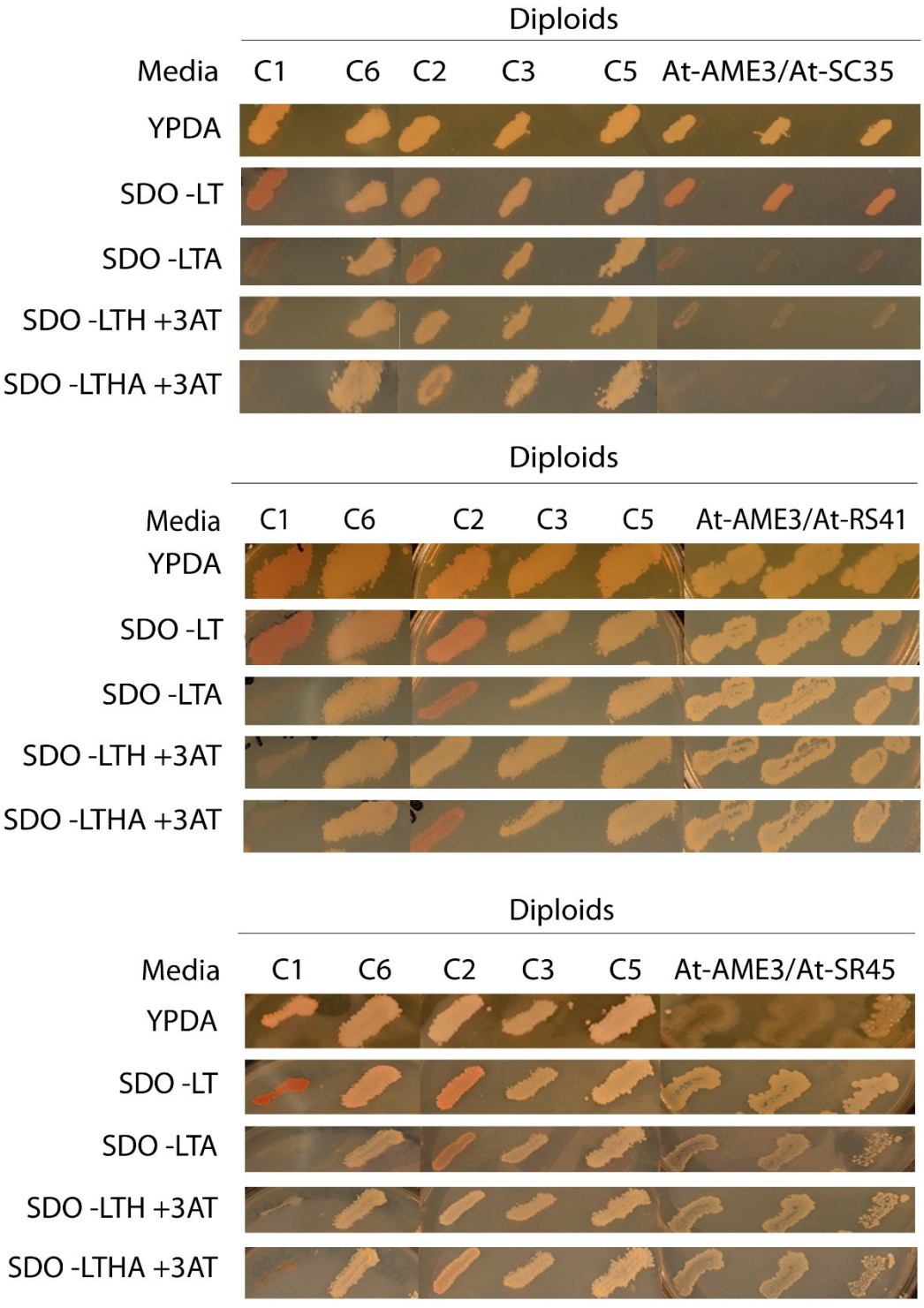
Diploids
Media
C1
C6
C2
C3
C5
At-AME3/At-SC35
YPDA
SDO -LT
SDO -LTA
SDO -LTH +3AT
SDO -LTHA +3AT
Diploids
Media
C1
C6
C2
C3
C5
At-AME3/At-RS41
YPDA
SDO -LT
SDO -LTA
SDO -LTH +3AT
SDO -LTHA +3AT
Diploids
Media
C1
C6
C2
C3
C5
At-AME3/At-SR45
YPDA
SDO -LT
SDO -LTA
SDO -LTH +3AT
SDO -LTHA +3AT

5.6 Discussion

Yeast two-hybrid provides a powerful tool in the elucidation of potential protein-protein interactions, which are key to several important biological processes, including signal transduction, transcription and post translational modifications such as phosphorylation (Causier and Davies, 2002). The objective of this study consisted in the identification of potential physical interactions between Serine/Arginine-rich proteins whose transcript levels were shown to be differentially expressed in response to low temperatures and/or *BnCBF* overexpression, and At-AME3 which has been suggested to play an essential role in the cold acclimation induced recovery of photosynthetic performance, in addition to the acquisition of freezing tolerance, by means of yeast two-hybrid assays. While the potential targets of AME3 kinase in response to cold acclimation remain elusive thus far (refer to Chapter 1), a high-throughput yeast two-hybrid assay has shown that AME3 is capable of physically interacting with At-RS21, At-SCL30 and At-RS2Z33 (Figure 1.3) (*Arabidopsis* Interactome Mapping Consortium, 2011).

The data from the present study is in partial agreement with previous reports, as At-RS21 and At-SCL30 were observed to physically interact with At-AME3 (Fig. 5.5; Fig. 5.6). In addition to confirming interactions between a subset of SR proteins and At-AME3, it should be noted that this study is also reporting potential physical interactions between At-AME3 kinase and At-RSZ22a, At-SR34a, At-RS41 and At-SR45 (Fig. 5.5; Fig. 5.6).

Conversely, At-RS2Z33, whose *Brassica napus* homolog was shown to decrease in transcript levels under cold stress, cold acclimation and *BnCBF* overexpression (Chapter 2) does not appear to physically interact with At-AME3 kinase (Fig. 5.5). This difference in results might be attributed to differences in experimental design with respect to yeast 2-hybrid controls. In this study, only diploid growth on selective plates lacking histidine (SDO –LTH +3AT) in addition to selective plates lacking histidine and adenine (SDO –LTHA +3AT) were considered positive interactions. This is in contrast to the previous study by the *Arabidopsis* Interactome Mapping Consortium, (2011), who have considered diploids capable of growing on synthetic dropout media lacking histidine (SDO –His, SDO-His +CHX) to be positive interactors. At-SC35 homologs in *Brassica napus*, whose transcript levels were observed to decrease in response to low temperatures and *BnCBF* overexpression, was also unable to interact with At-AME3. Interestingly, three SR proteins that were reported of potentially being capable of physically interacting with At-AME3 were observed to play an important role in the overall photosynthetic performance (At-SR45) or the cold acclimation induced photosynthetic performance (At-RSZ22a, At-SCL30) of *A. thaliana* when deleted (Chapter 2). However, *ame3* loss-of-function mutants were severely hampered in their ability to adjust their photosynthetic performance at the level of Photosystem II, Photosystem I and state-1 state-2 transitions under cold acclimation, in addition to their ability to acquire freezing tolerance. As AME3 was shown to interact with this subset of SR proteins and its deletion resulted in an impairment in two major processes resulting from long term exposure to low temperatures, it is possible that AME3 plays an important role in these two major processes by interacting with these Serine/Arginine-rich proteins.

While yeast 2-hybrid analyses alone cannot confirm that At-AME3 is capable of phosphorylating SR proteins, it is of note that a previous report (Ahsan et al., 2013) has shown that At-AME3 is capable of phosphorylating several targets, including an SR protein *in vitro* (Refer to Chapter 1). In addition, an earlier *in vitro* assay by Golovkin and Reddy (1999) has shown that At-AME1, which shares 76% identity to At-AME3, can phosphorylate several SR proteins, including At-RSZ21 and At-SR45, which are reported as being capable of interacting with At-AME3. As AME3, in addition to its homolog AME1, have both been shown to be capable of phosphorylating SR proteins *in vitro,* it is likely that At-AME3 is also capable of phosphorylating the previously mentioned SR proteins, which were shown to physically interact with At-AME3 kinase in this study.

Furthermore, of the three identified LAMMER kinases (AME1, AME2, AME3), only AME3 transcript levels, in conjunction with a subset of SR genes, including *Brassica* homologs of RSZ21, RSZ22a, SCL30, SR45, were observed to undergo an overall increase in expression under exposure to low temperatures and *BnCBF* overexpression (Refer to Chapter 2). As AME1 and AME3 share common targets (RSZ21, SR45, SRPK-like 1 and SRPK4), yet show differential expression profiles in response to low temperatures and BnCBF overexpression, it is possible that both LAMMER kinases target different serine, threonine and/or tyrosine residues on the same SR protein. Although it is unclear whether there are preferential phosphorylation sites between members of the LAMMER kinase family, interplay between SRPK and LAMMER kinases has been reported (Ngo et al., 2005), lending credence to this observation.

Figure 5.6: Interaction network of LAMMER, SRPK and SRPK-like proteins reported to interact with SR proteins, as determined by yeast 2-hybrid assays and *in vitro* phosphorylation assays.

Each node presented in blue represents either LAMMER kinases or SRPK and SRPK-like kinases, while Serine/Arginine-rich proteins are represented as red nodes. Grey nodes represent other proteins reported to interact with LAMMER kinases. Black lines designate physical interactions between AME3 kinase and SR proteins of interest based on yeast 2-hybrid assays performed for this study. Blue lines correspond to interacting partners based on high throughput yeast 2-hybrid assays (*Arabidopsis* Interactome Mapping Consortium, 2011), while Red lines denote results from *in vitro* phosphorylation assays reported by Golovkin and Reddy (1999) and de la Fuente van Bentem (2006, 2008). The interaction map was based on data generated using STRING v10 (Szklarczyk et al., 2015) (http://www.string-db.org/).

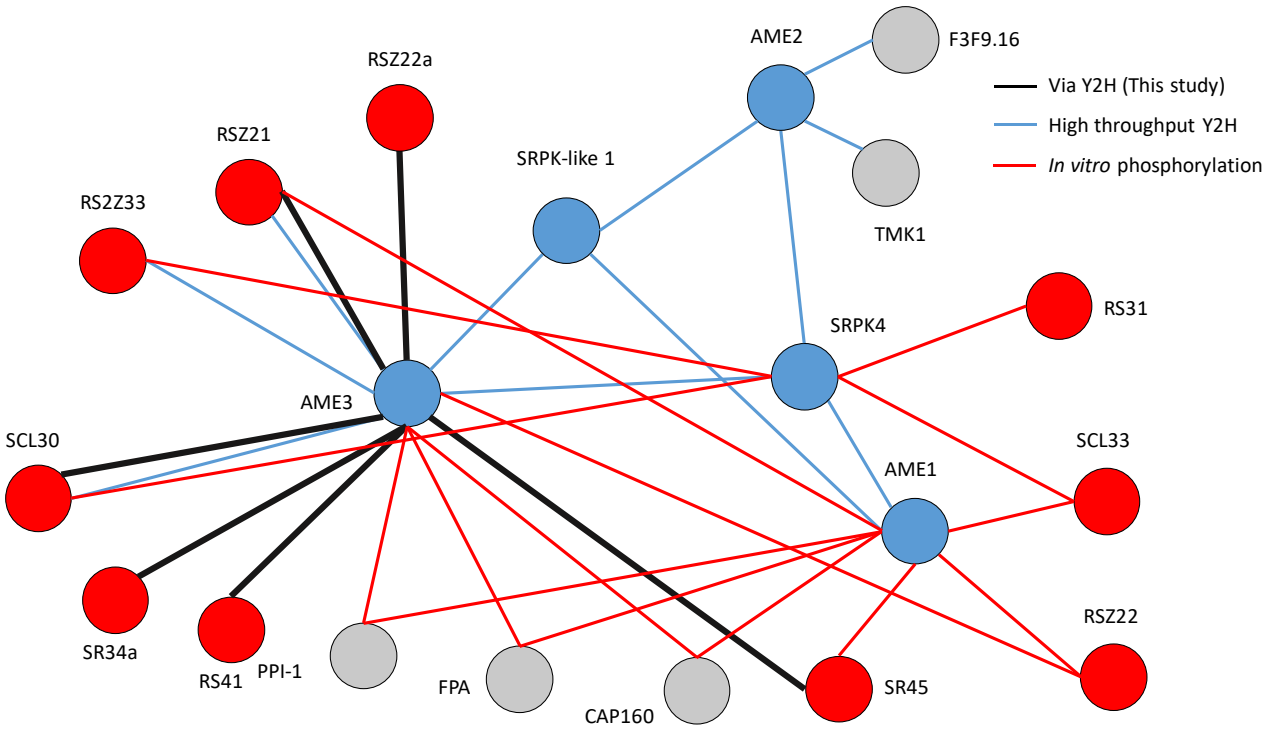
AME2
F3F9.16
RSZ22a
Via Y2H (This study)
RSZ21
High throughput Y2H
SRPK-like 1
In vitro phosphorylation
RS2Z33
TMK1
RS31
SRPK4
AME3
SCL30
SCL33
AME1
SR34a
RSZ22
RS41
PPI-1
FPA
SR45
CAP160

5.7 Conclusion

In summary, results of this study have shown that At-AME3 kinase is capable of interacting with six Serine/Arginine-rich proteins, with four (At-SR34a, At-RSZ21, At-RS41 and At-SR45) of these SR proteins being novel interactions with At-AME3. This subset of SR proteins which have been observed to interact with At-AME3 involves some SR proteins which have been shown to play a role in the cold acclimation response, and one (At-RSZ21) has not been shown to play a role in either cold stress and/or cold acclimation, suggesting that At-AME3 can not only interact with SR proteins involved in cold stress and acclimation, but also other SR proteins which are not thought to be involved in the cold acclimation response. While these results have shown that At-AME3 is able to interact with a greater subset of SR proteins than was previosuly thought, future studies might involve *in vitro* phosphorylation assays to confirm that At-AME3 is able to phosphorylate the aforementioned SR proteins which were shown to interact with At-AME3 in yeast 2-hybrid assays.

Chapter 6: Summary of results and future directions

6.1 *Summary of results*

The aim of this study was to assess the role of Serine/Arginine-rich proteins, LAMMER, SRPK and SRPK-like kinases in the cold acclimation response of *Brassica napus* and *Arabidopsis thaliana*. While it is known that abiotic stress responses, including short term exposure to low temperatures results in changes in the expression of SR genes (Fowler and Thomashow, 2002; Oono et al., 2006) or their splicing patterns (Palusa et al., 2007; Tanabe et al., 2007b), this study has expanded our current knowledge of SR gene expression in abiotic stress responses by showing that exposure to cold stress and cold acclimation conditions led to alterations in the RNA expression profiles of SR, LAMMER kinase, SRPK and SRPK-like genes in *Brassica napus*. These changes were associated with an increase in SR protein abundance and phosphorylation status. While the exact roles of SR proteins in cold acclimation remains elusive, these results highlighted their importance in this complex process.

While the results of this study, along with other research efforts have suggested a role for SR proteins in cold stress responses (Ali and Reddy, 2008a; Palusa et al., 2007), there are no functional studies defining the role of SR proteins in the cold acclimation-induced recovery of photosynthetic performance, and/or the acquisition of freezing tolerance, two major processes that are known to take place in response to cold acclimation. This study has defined a linkage between two SR proteins (At-RSZ22 and At-SR45) and overall photosynthetic performance of *Arabidopsis thaliana*, as *at-rsz22* and *at-sr45* loss-of-function

mutants were impaired with respect to their photosynthetic performance under optimal growth conditions and cold acclimation conditions.

In addition to At-RSZ22 and At-SR45, this study has identified three SR proteins (At-RSZ22A, At-SCL30, At-RS40) and one LAMMER kinase (At-AME3) that play an important role in the cold acclimation induced recovery of photosynthetic performance, as these transgenic lines were observed to be impaired in their capacity to recover in terms of their photosynthetic performance after five weeks of cold acclimation. A detailed photosynthetic characterization of At-AME3 has led to the discovery of its importance in the photosynthetic performance of *Arabidopsis thaliana* under cold acclimation conditions, as *at-ame3* loss-of-function mutants were severely limited in terms of photoprotective mechanisms, such as state-1 state-2 transitions, cyclic electron transport and chlororespiration via PTOX. Moreover, cold acclimated *ame3* mutants were observed to possess a reduced protein abundance of phosphorylated D1, light harvesting complex proteins, as well as phosphoproteins involved in state transitions. A novel discovery of this study involves the important role of At-AME3, a LAMMER kinase, in the acquisition of freezing tolerance, as *at-ame3* loss-of -function mutants were found to be unable to acquire freezing tolerance after five weeks of cold acclimation.

Taken together, the data from this study led to the following models to describe the mode of action of this subset of SR proteins and LAMMER kinases in the photosynthetic performance of *Arabidopsis thaliana* under optimal growth conditions, as well as the cold acclimation induced recovery of photosynthetic performance. Under non-acclimated growth conditions, At-RSZ22 and At-SR45 are thought to play a role in the post transcriptional regulation of photosynthesis related target genes, which are involved in modulating

photosynthetic performance. As At-AME1 has been reported to heavily phosphorylate At-RSZ22 and At-SR45, it is possible that the post transcriptional regulation of photosynthesis related target genes by these SR proteins are mediated by At-AME1. Alternatively, At-AME3 has been proposed to also play a role in the photosynthetic performance of *Arabidopsis* by phosphorylating a subset of photosynthesis related proteins, which also contribute to the photosynthetic performance of *Arabidopsis* (Fig. 6.1A). It is known that exposure to low temperatures results in the induction of the CBF and RAV1 cold responsive pathways (Haake, 2002; Hannah et al., 2005; Yang et al., 2005). Moreover, the ERD1/RD29 drought responsive pathway has been shown to be induced in response to low temperatures suggesting crosstalk between low temperature and drought responsive pathways. Exposure to low temperatures lead to the induction of At-RSZ22, At-RSZ22a, At-SCL30, At-RS40 and At-SR45 possibly through three pathways. The CBF pathway is thought to induce these SR genes as they possess predicted CRT/DRE promoter elements, based on promoter region analyses (Hehl et al., 2016). However, their induction can also be potentially mediated via the RAV1 pathway, which is not part of the CBF regulon but shows similar expression patterns as CBFs (Hannah et al., 2005), as these genes also possess predicted RAV1 promoter elements which are also induced in response to low temperatures. As it is known that there is crosstalk between cold and drought responsive pathways (Haake, 2002; Matsui et al., 2008b; Nakashima et al., 2014), low temperatures can also potentially result in the induction of these SR genes via the ERD1/RD29 pathway, by binding to predicted ABRE promoter elements found in these SR genes (Table A2.1). Concomitantly, At-AME3, which does not contain CRT/DRE promoter elements, but contains both RAV1 and ERD1/RD29 promoter elements, is induced in response to low temperatures. At-AME3 in turn has been suggested to post-translationally regulate this subset of SR proteins, which would post transcriptionally

mediate unknown target genes involved in the cold acclimation induced recovery of photosynthetic performance. Alternatively, At-AME3 has been suggested to phosphorylate target proteins other than SR proteins, which are also involved in the recovery of photosynthetic performance (Fig. 6.1B).

In summary, assessing the role of SR proteins and LAMMER kinases in the cold acclimation induced recovery of photosynthetic performance led to the discovery of two new players (At-RSZ22 and At-SR45) in the overall photosynthetic performance of *Arabidopsis thaliana* under non-acclimated growth conditions. Cold acclimation conditions have led to the discovery of a subset of SR proteins (At-RSZ22, At-RSZ22a, At-SCL30, At-RS40 and At-SR45) and one LAMMER kinase (At-AME3) playing major roles in the cold acclimation induced recovery of photosynthetic performance.

Figure 6.1: Model defining potential role of Serine/Arginine rich proteins and LAMMER kinases in the overall photosynthetic performance of *Arabidopsis thaliana* under non-acclimated conditions (A) and in the cold acclimation induced recovery of photosynthesis (B).

Under optimal growth conditions (A), At-RSZ22 and At-SR45 have been suggested to play a role in the post transcriptional regulation of target genes, potentially via interactions with At-AME1, resulting in optimal photosynthetic performance. Alternatively, it is possible that At-AME3 is capable of phosphorylating other photosynthesis related proteins which would also play a role in the photosynthetic performance of *Arabidopsis thaliana.* Under exposure to low temperatures, (B), potential CRT/DRE, RAV1 and ABRE promoter elements identified in SR proteins could induce their expression via CBF, RAV1 and ERD1/RD29 promoter elements, respectively. Furthermore, low temperatures and drought conditions can also induce the expression of RAV1 and ERD1/RD29 transcription factors, respectively, which in turn will recognize and bind to promoter elements found in At-AME3 to induce its expression. Once expressed, At-AME3 is proposed to post-translationally modulate a subset of SR proteins, which will in turn regulate target genes involved in the recovery of photosynthetic performance. Alternatively, it is possible that At-AME3 might interact with other protein targets that would play a role in the recovery of photosynthetic performance after cold acclimation. Double arrows indicate crosstalk between cold and drought responses.

A

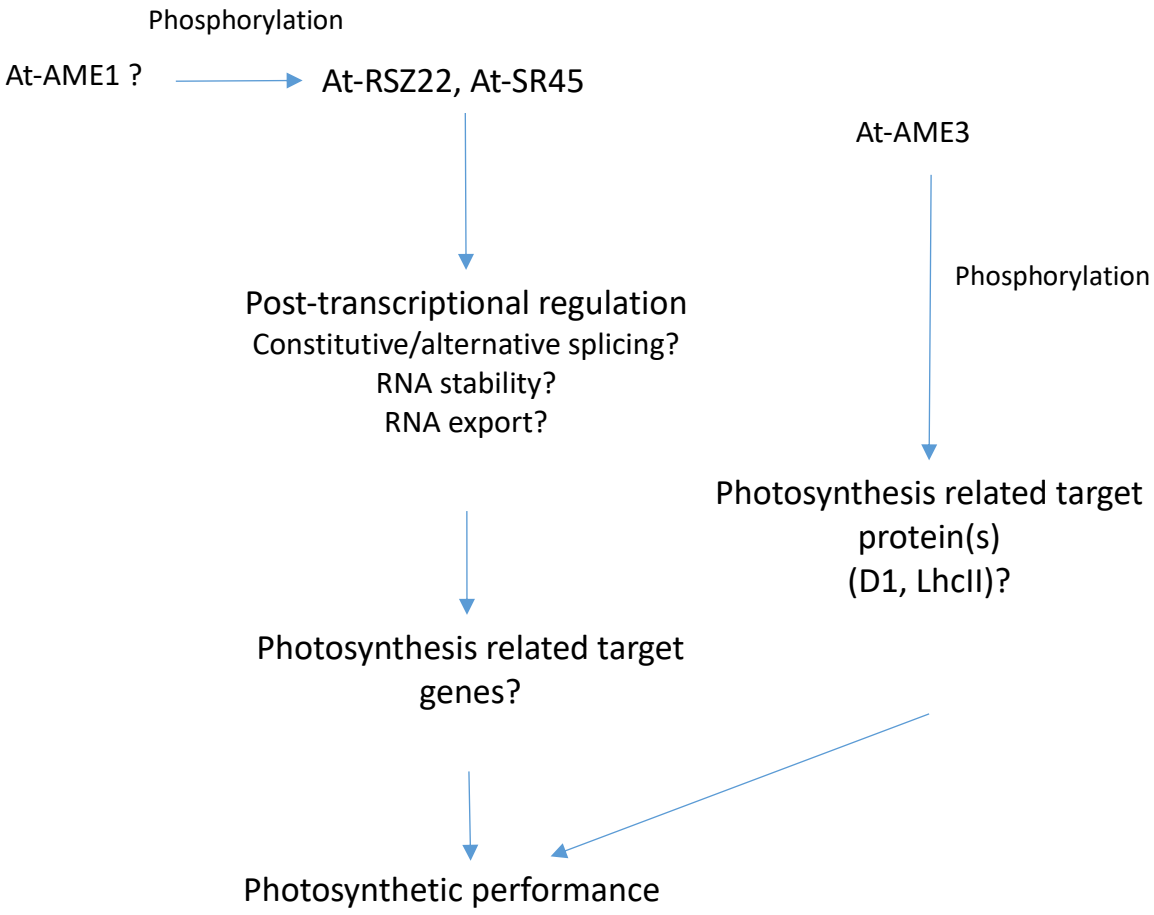
Phosphorylation
At-AME1 ?
At-RSZ22, At-SR45
At-AME3
Phosphorylation
Post-transcriptional regulation
Constitutive/alternative splicing?
RNA stability?
RNA export?
Photosynthesis related target protein(s)
(D1, LhcII)?
Photosynthesis related target genes?
Photosynthetic performance

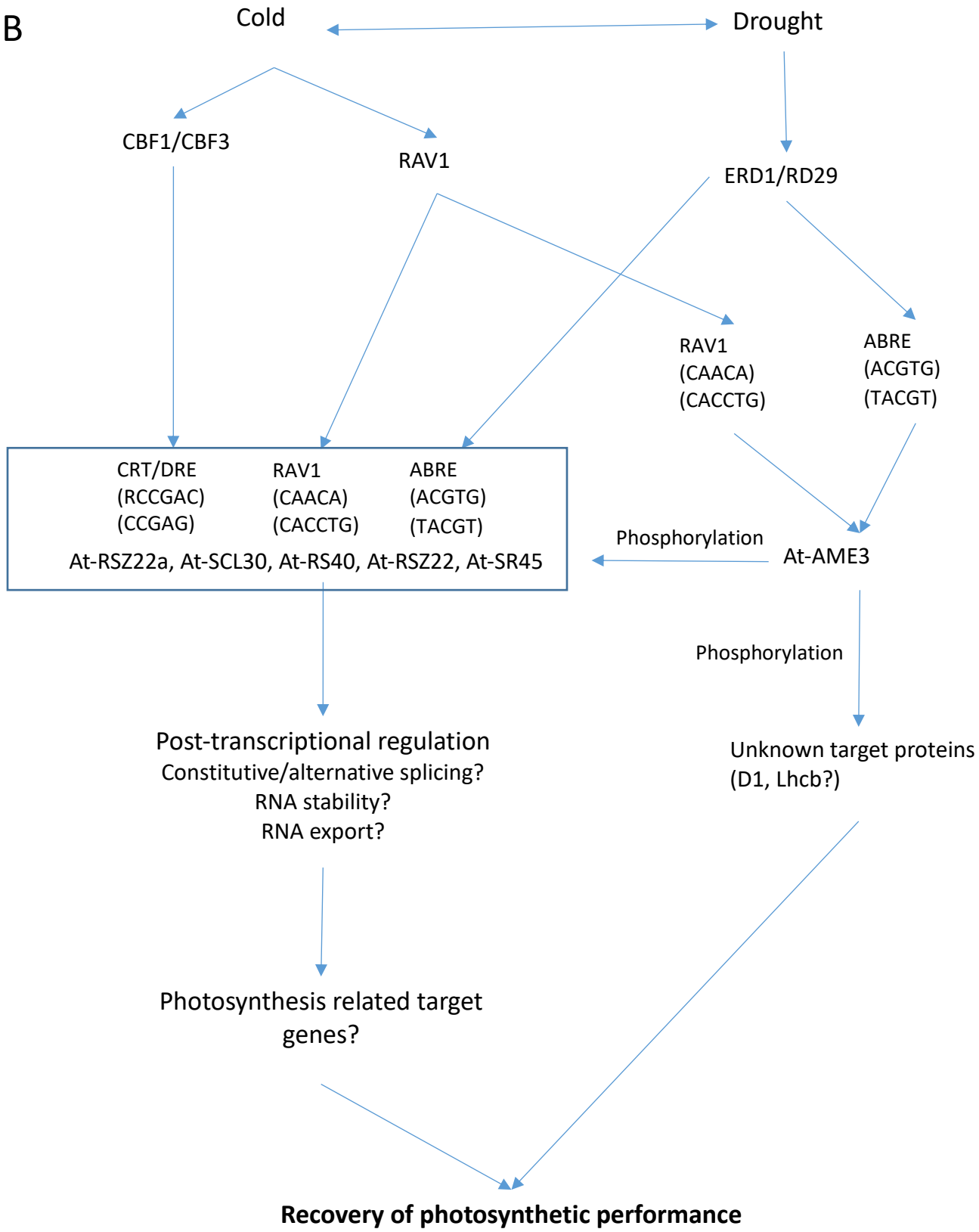
B
Cold
Drought
CBF1/CBF3
RAV1
ERD1/RD29
RAV1
(CAACA)
(CACCTG)
ABRE
(ACGTG)
(TACGT)
CRT/DRE
(RCCGAC)
(CCGAG)
RAV1
(CAACA)
(CACCTG)
ABRE
(ACGTG)
(TACGT)
At-RSZ22a, At-SCL30, At-RS40, At-RSZ22, At-SR45
Phosphorylation
At-AME3
Phosphorylation
Post-transcriptional regulation
Constitutive/alternative splicing?
RNA stability?
RNA export?
Unknown target proteins
(D1, Lhcb?)
Photosynthesis related target genes?
Recovery of photosynthetic performance

In contrast to the cold acclimation induced recovery of photosynthetic performance, electrolyte leakage assays used to assess the impact of SR proteins and LAMMER kinases have shown that a subset of SR proteins (At-RSZ22, At-RSZ22A, At-SR34B, At-SCL30A, At-RS40, At-RS41) may not be involved in the acquisition of freezing tolerance. This suggestion was attributed to the observation that loss of function mutants of the aforementioned SR proteins behaved similarly to cold acclimated wild type *Arabidopsis*. Conversely, *ame3* was jeopardized in its capacity to acquire freezing tolerance, suggesting that At-AME3 plays an essential role in the acquisition of freezing tolerance. It should be noted that while this subset of SR proteins does not appear to be involved in the acquisition of freezing tolerance specifically, it is possible that they are involved in other processes associated with cold acclimation, which were not covered in this study. For instance, as SR proteins are known to be involved in plant development (Ali et al., 2007), it is possible that they play a role in the dwarf, compact phenotype (Kurepin et al., 2013) associated with cold acclimation. The similarities with respect to the acquisition of freezing tolerance between cold acclimated wild type and SR mutants could potentially be attributed to the functional redundancy (Reddy, 2004) of SR proteins.

As SR proteins do not appear to be involved in the acquisition of freezing tolerance, these results would suggest that At-AME3 does not interact with SR proteins in order to mediate the post-transcriptional regulation of target genes involved in the acquisition of freezing tolerance as seen in the cold acclimation induced recovery of photosynthetic performance. The observation that only At-AME3 appears to be involved in the acquisition of freezing tolerance has raised the question concerning its mode of action in this process.

The following model (Fig. 6.2) is proposed as the mode of action of At-AME3 in the acquisition of freezing tolerance.

It is established that exposure to low temperatures lead to the induction of two cold responsive pathways (CBF and RAV1) and one drought responsive (ERD1/RD29) pathway. In the CBF transcriptional pathway, exposure to low temperatures leads to the SUMOylation of ICE1 by SIZ1 at the expense of its negative regulation by means of ubiquitination via HOS1 (Miura and Hasegawa, 2010; Miura et al., 2007). This in turn allows ICE1 to induce CBF expression, ultimately resulting in the induction of cold responsive genes involved in the acquisition of freezing tolerance. At-AME3, which does not contain CRT/DRE promoter elements found in cold responsive genes, is thought to be induced in response to low temperatures potentially via the RAV1 transcriptional pathway (Figure 6.2). Furthermore, drought responsive transcriptional pathways, which have been reported to be induced in response to low temperatures (Haake, 2002; Matsui et al., 2008b; Nakashima et al., 2014) are also thought to induce At-AME3 via ABRE promoter elements found in At-AME3. At-AME3 in turn, is proposed to play a role in the post translational regulation of a target protein, located upstream of ICE1 and HOS1 in the CBF transcriptional cascade. At-AME3 is thought to act upstream of ICE1 and HOS1 due to the observation that At-AME3 mutants possessed attenuated ICE1 and HOS1 transcript levels under cold acclimation conditions. These findings were associated with a decrease in CBF transcript levels, in addition to downstream targets of CBFs, which are known to possess CRT/DRE promoter elements such as COR15A, COR15B and KIN1(Fig. 6.2). While At-AME3 has been suggested to play an important role in the CBF transcriptional cascade, it is unclear whether At-AME3 has an effect on SIZ1 or acts further upstream.

In summary, this study led to the discovery of At-AME3 LAMMER kinase playing an important role in the acquisition of freezing tolerance, through the mediation of the well known CBF transcriptional pathway.

Figure 6.2: Model defining potential role of At-AME3 in the acquisition of freezing tolerance in cold acclimated *Arabidopsis thaliana*.

Exposure to low temperatures leads to the SUMOylation of Inducer of CBF1, or ICE1, while inhibiting its negative regulation by means if ubiquitination via HOS1. ICE1 in turn, induces the expression of CBF1 and CBF3. Both CBFs bind to and recognize CRT/DRE promoter elements found in cold responsive genes, such as COR15A, COR15B, LTI78 and KIN. Concomitantly, At-AME3, which does not contain potential CRT/DRE elements, is proposed to be induced in response to low temperatures via the RAV1 transcriptional pathway. Due to crosstalk between low temperatures and drought responses (Double arrow), the induction of At-AME3 under low temperatures is also thought to be mediated via the ERD1/RD29 drought responsive pathway. Thus, exposure to low temperatures induces the expression of RAV1 and ERD1/RD29 transcription factors. These transcription factors are thought to recognize and bind to potential RAV1 and ABRE promoter elements, respectively, found in At-AME3 transcripts, leading to its induction. Once induced, At-AME3 is suggested to play a role in the regulation of target proteins involved in the CBF transcriptional cascade by post-translationally mediating its target proteins acting upstream of ICE1 and HOS1.

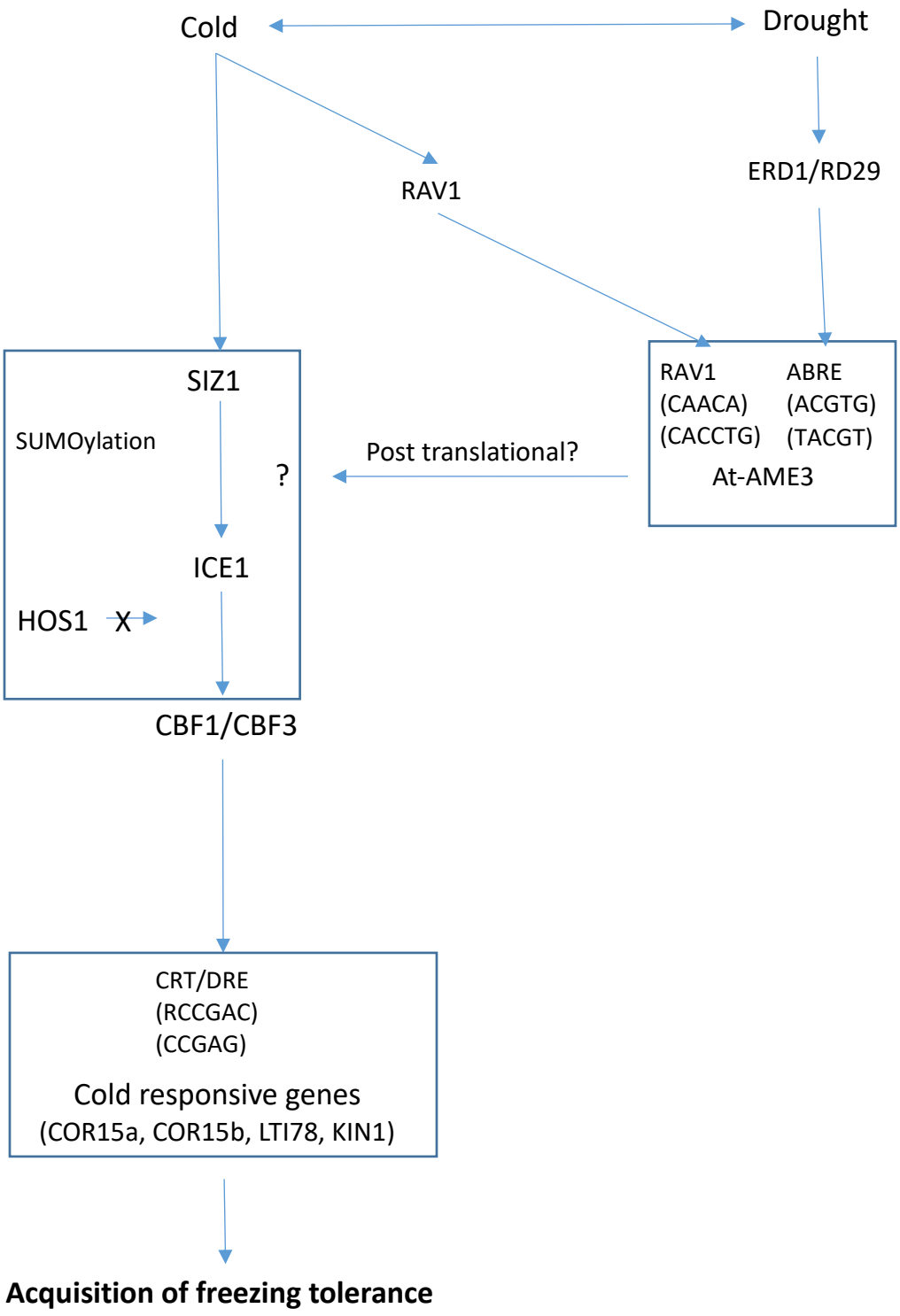
Cold
Drought
RAV1
ERD1/RD29
SIZ1
SUMOylation
?
ICE1
HOS1
X
CBF1/CBF3
Post translational?
RAV1
(CAACA)
(CACCTG)
ABRE
(ACGTG)
(TACGT)
At-AME3
CRT/DRE
(RCCGAC)
(CCGAG)
Cold responsive genes
(COR15a, COR15b, LTI78, KIN1)
Acquisition of freezing tolerance

6.2 *Future directions*

Assessing the photosynthetic performance of SR loss-of-function mutants has shown that At-RSZ22 and At-SR45 play important roles in the photosynthetic performance of *Arabidopsis thaliana* (Fig. 3.4). These observations raised some questions, namely: what are the targets of At-RSZ22 and At-SR45? Does each SR protein target a different subset of genes, or is there an overlap in the target genes in these mutant lines? Which photosynthesis related proteins are targeted by At-AME3? To define potential targets that are regulated by At-RSZ22, At-SR45 and/or At-AME3, whole genome analyses by means of RNA sequencing (RNAseq) of *at-rsz22a*, *at-scl30*, *at-sr45*, *at-rsz22* and *at-ame3* mutants grown under non-acclimated conditions and after five weeks of cold acclimation conditions would be compared to wild type *Arabidopsis* grown under the same conditions. Genes that have been identified through whole genome analyses and confirmed by qPCR to be differentially expressed in these mutant lines compared to wild type *Arabidopsis* could be considered potential targets which are regulated by these SR proteins and/or At-AME3.

Moreover, whole genome analyses, e.g. RNAseq, of *at-rsz22a*, *at-scl30*, *at-rsz22*, *at-sr45* and *at-ame3* loss-of-function mutants compared to wild type *Arabidopsis* could provide information on whether the deletion of these genes resulted in alterations in splicing patterns of potential target genes, which resulted in their poor photosynthetic performance. As an example, Jurczyk et al. (2016) reported that an enhancement in Rubisco activity was associated with an enhancement of Rubisco activase splicing variants in perennial ryegrass. Therefore, it is possible that the splicing patterns of Rubisco activase, along with other target genes have been altered under control and after five weeks of cold acclimation in *at-rsz22a*, *at-scl30*, *at-rsz22, at-sr45* and *at-ame3.* Taken together, defining potential target genes and

changes in their splicing patterns would advance our knowledge on the role of SR proteins in the photosynthetic performance of *Arabidopsis thaliana* under non-acclimated and after cold acclimation by defining target genes that are regulated by these pre-mRNA splicing factors.

Electrolyte leakage assays, in conjunction with qPCR analyses of key cold responsive genes suggest that At-AME3 could potentially act upstream of ICE1. However, potential targets regulated by At-AME3 are currently unknown. One candidate could be SIZ1, which acts upstream of ICE1. Future studies assessing SIZ1 expression and protein abundance in At-AME3 knockouts undergoing cold acclimation in comparison to wild type *Arabidopsis* may provide clues as to whether At-AME3 could potentially play a role in SIZ1 expression. Furthermore, RNAseq analyses of *at-ame3* mutants undergoing cold acclimation relative to wild type *Arabidopsis thaliana* could provide further insight on potential targets of At-AME3 which would be involved in the acquisition of freezing tolerance.

Assessing the capacity of SR knockouts to acquire freezing tolerance under cold acclimation conditions has shown that these mutants, unlike At-AME3 knockouts, are not impaired with respect to acquisition of freezing tolerance. It was unclear if these results could be attributed to SR functional redundancy (Reddy, 2004). This raised the question as to whether a subset of SR proteins might be involved in the acquisition of freezing tolerance. To address this question, future studies could involve testing the acquisition of freezing tolerance of SR double knockouts or triple knockouts generated using CRISPR/Cas9, which has been shown to be capable of editing the *Arabidopsis* genome with high efficiency (Bortesi and Fischer, 2015; Ding et al., 2016; Feng et al., 2014). The ability of these mutants to acquire freezing tolerance would be tested by means of electrolyte leakage assays, in

conjunction with qPCR analyses of genes involved in the CBF transcriptional cascade and Western blots (Refer to Chapter 3). Should SR proteins play a role in the acquisition of freezing tolerance, it is expected that these mutant lines would be impaired in their capacity to acquire freezing tolerance. This would advance our knowledge on the role of SR proteins in the acquisition of freezing tolerance, one major process which allows plants to cold acclimate. In addition the results may resolve the issues of function redundancy.

CRISPR/Cas9 could also be used to generate different At-AME3 mutants with the gene as only one T-DNA insertion line was available at the time that this study was initiated. These new At-AME3 loss-of-function mutants would be tested the same way as the At-AME3 mutant used in this study to confirm that the results presented in this study are attributed to the deletion of this LAMMER kinase.

The poor performance of *at-ame3* mutants under cold acclimation conditions has raised the question as to whether overexpressing At-AME3 would result in a constitutive enhancement of photosynthetic performance. Therefore, future studies could involve studying At-AME3 overexpressors and evaluating their photosynthetic performance by means of chlorophyll a fluorescence and P_{700} absorbance measurements under non-acclimated conditions and after five weeks of cold acclimation. Should At-AME3 overexpression result in an enhancement of photosynthetic performance, it is expected that an enhancement in photosynthetic performance would be observed under optimal growth conditions in At-AME3 overexpressors relative to non-acclimated wild type *Arabidopsis* and *at-ame3* mutants Moreover, exposure to low temperatures could lead to a greater enhancement of photosynthetic performance relative to cold acclimated wild type *Arabidopsis*. Should At-AME3 overexpression result in an improvement of photosynthetic

performance under cold acclimation conditions, these results would provide insight on improving photosynthetic performance under cold acclimation in *Arabidopsis*.

Yeast 2-hybrid assays have shown that At-AME3 can physically interact with a subset of SR proteins that play an important role in the recovery of photosynthetic performance that occurs under cold acclimation conditions (Refer to Chapter 5). It should be noted that yeast 2-hybrid assays alone cannot confirm whether At-AME3 can phosphorylate these SR proteins. Therefore, future studies could involve *in vitro* phosphorylation assays to confirm whether At-AME3 can phosphorylate these SR proteins. Enriched nuclear extracts from *at-ame3* probed with an antibody that targets phosphorylated SR proteins, e.g. mAb104, under non-acclimated and after cold acclimation conditions could be compared to their wild type counterparts to assess whether the deletion of At-AME3 had an impact on the phosphorylation status of SR proteins. Future studies could test potential interactions between SRPK-like 1 and SR proteins of interest, by means of yeast 2-hybrid assays. These findings would improve our knowledge by confirming that At-AME3 can phosphorylate SR proteins that play an important role in the recovery of photosynthetic performance that occurs under cold acclimation conditions. Moreover, defining novel interactions between SRPK-like 1 and SR proteins that were found to play a role in cold acclimation would expand on our limited knowledge of SRPK-like 1 and its targets.

In conclusion, results from this study led to novel discoveries with respect to the role of Serine/Arginine rich proteins, which are involved in constitutive and alternative splicing, and other post-splicing activities such as mRNA transport, localization and stability and LAMMER kinases, which are essential in regulating SR protein function and localization, in *Arabidopsis thaliana* undergoing cold acclimation. We are reporting for the first time that a

subset of SR proteins (At-RSZ22 and At-SR45) play a role in the overall photosynthetic performance of *Arabidopsis thaliana* under control conditions, while another subset of SR proteins (At-RSZ22, At-RSZ22a, At-SCL30, At-RS40 and At-SR45) and one LAMMER kinase (At-AME3) are major players in the cold acclimation induced recovery of photosynthetic performance. Furthermore, At-AME3 was also found to be a major player in the acquisition of freezing tolerance by regulating the CBF transcriptional cascade.

References

Achard, P., Gong, F., Cheminant, S., Alioua, M., Hedden, P., and Genschik, P. 2008. The Cold-Inducible CBF1 Factor-Dependent Signaling Pathway Modulates the Accumulation of the Growth-Repressing DELLA Proteins via Its Effect on Gibberellin Metabolism. Plant Cell **20**(8): 2117–2129 10.1105/tpc.108.058941.

Ahsan, N., Huang, Y., Tovar-Mendez, A., Swatek, K.N., Zhang, J., Miernyk, J. a, Xu, D., and Thelen, J.J. 2013. A versatile mass spectrometry-based method to both identify kinase client-relationships and characterize signaling network topology. J. Proteome Res. **12**(2): 937–948 10.1021/pr3009995.

Ali, G.S., and Reddy, A.S.N. 2006. ATP, phosphorylation and transcription regulate the mobility of plant splicing factors. J. Cell Sci. **119**(Pt 17): 3527–3538 10.1242/jcs.03144.

Ali, G.S., and Reddy, A.S.N. 2008a. Spatiotemporal organization of pre-mRNA splicing proteins in plants. In Current Topics in Microbiology and Immunology. *Edited by* A.S.N. Reddy and M. Golovkin Springer-Verlag Berlin Heidelberg . pp. 103–118.

Ali, G.S., and Reddy, A.S.N. 2008b. Regulation of alternative splicing of pre-mRNAs by stresses. In Current Topics in Microbiology and Immunology. *Edited by* A.S.N. Reddy and M. Golovkin pp. 257–275.

Ali, G.S., Palusa, S.G., Golovkin, M., Prasad, J., Manley, J.L., and Reddy, A.S.N. 2007. Regulation of plant developmental processes by a novel splicing factor. PLoS One **2**(5): e471 10.1371/journal.pone.0000471.

Allen, D.J., and Ort, D.R. 2001. Impacts of chilling temperatures on photosynthesis in

warm-climate plants. Trends Plant Sci. **6**(1): 36–42.

Arabidopsis Interactome Mapping Consortium 2011. Evidence for Network Evolution in an *Arabidopsis* Interactome Map. Science (80-.). **333**(6042): 601–607 10.1126/science.1203877.

Aro, E.-M., Virgin, I., and Andersson, B. 1993. Photoinhibition of photosystem. II. Inactivation, protein damage and turnover. Biochim. Biophys. Acta - Bioenerg. **1143**: 113–134 10.1016/0005-2728(93)90134-2.

Asada, K. 1999. The water-water cycle in chloroplasts: scavenging of active oxygens and dissipation of excess photons. Annu. Rev. Plant Biol. **50**(1): 601–639.

Asada, K., Heber, U., and Schreiber, U. 1992. Pool Size of Electrons That Can Be Donated to P700+ As Determined in Intact Leaves: Donation to P700+ from Stromal Components Via the Intersystem Chain. Plant Cell Physiol. **33**(7): 927–932.

Badger, M.R., von Caemmerer, S., Ruuska, S., and Nakano, H. 2000. Electron flow to oxygen in higher plants and algae: rates and control of direct photoreduction (Mehler reaction) and rubisco oxygenase. Philos. Trans. R. Soc. Lond. B. Biol. Sci. **355**(1402): 1433–1446 10.1098/rstb.2000.0704.

Baker, N.R. 2008. Chlorophyll fluorescence: a probe of photosynthesis in vivo. Annu. Rev. Plant Biol. **59**: 89–113 10.1146/annurev.arplant.59.032607.092759.

Barrero-Gil, J., and Salinas, J. 2013. Post-translational regulation of cold acclimation response. Plant Sci. **205**–**206**: 48–54 10.1016/j.plantsci.2013.01.008.

Barta, A., Kalyna, M., and Lorković, Z.J. 2008. Plant SR proteins and their functions. Curr. Top. Microbiol. Immunol. **326**: 83–102.

Barta, A., Kalyna, M., and Reddy, A.S.N. 2010. Implementing a rational and consistent nomenclature for serine/arginine-rich protein splicing factors (SR proteins) in plants. Plant Cell **22**(9): 2926–2929 10.1105/tpc.110.078352.

Bauwe, H., Hagemann, M., and Fernie, A.R. 2010. Photorespiration: players, partners and origin. Trends Plant Sci. **15**(6): 330–336 10.1016/j.tplants.2010.03.006.

Baxter, B. 2014. Plant acclimation and adaptation to cold environments. In Temperature and Plant Development. *Edited by* K.A. Franklin and P.A. Wigge John Wiley & Sons, Inc Oxford . pp. 19–48.

Bender, J., and Fink, G.R. 1994. AFC1, a LAMMER kinase from *Arabidopsis thaliana*, activates STE12-dependent processes in yeast. Proc. Natl. Acad. Sci. U. S. A. **91**(25): 12105–12109 10.1073/pnas.91.25.12105.

Bessonov, S., Anokhina, M., Will, C.L., Urlaub, H., and Lührmann, R. 2008. Isolation of an active step I spliceosome and composition of its RNP core. Nature **452**(7189): 846–850 10.1038/nature06842.

Black, D.L. 2003. Mechanisms of alternative pre-messenger RNA splicing. Annu. Rev. Biochem. **72**: 291–336 10.1146/annurev.biochem.72.121801.161720.

Boese, S.R., and Hüner, N.P.A. 1990. Effect of growth temperature and temperature shifts on spinach leaf morphology and photosynthesis. Plant Physiol. (1990): 1830–1836.

Bortesi, L., and Fischer, R. 2015. The CRISPR/Cas9 system for plant genome editing and beyond. Biotechnol. Adv. **33**(1): 41–52 10.1016/j.biotechadv.2014.12.006.

Brückner, A., Polge, C., Lentze, N., Auerbach, D., and Schlattner, U. 2009. Yeast two-hybrid, a powerful tool for systems biology. Int. J. Mol. Sci. **10**(6): 2763–2788

10.3390/ijms10062763.

Bukhov, N.G., Heber, U., Wiese, C., and Shuvalov, V.A. 2001. Energy dissipation in photosynthesis: Does the quenching of chlorophyll fluorescence originate from antenna complexes of photosystem II or from the reaction center? Planta **212**(5–6): 749–758 10.1007/s004250000486.

Butler, W.L. 1978. Energy distribution in the photochemical apparatus of photosynthesis. Annu. Rev. Plant Physiol. : 345–378.

Cáceres, J.F., Misteli, T., Screaton, G.R., Spector, D.L., and Krainer, A.R. 1997. Role of the modular domains of SR proteins in subnuclear localization and alternative splicing specificity. J. Cell Biol. **138**: 225–238 10.1083/jcb.138.2.225.

Cáceres, J.F., Screaton, G.R., and Krainer, A.R. 1998. A specific subset of SR proteins shuttles continuously between the nucleus and the cytoplasm. Genes Dev. **12**(1): 55–66 10.1101/gad.12.1.55.

Carvalho, R.F., Carvalho, S.D., and Duque, P. 2010. The plant-specific SR45 protein negatively regulates glucose and ABA signaling during early seedling development in *Arabidopsis*. Plant Physiol. **154**(2): 772–783 10.1104/pp.110.155523.

Carvalho, R.F., Szakonyi, D., Simpson, C.G., Barbosa, I.C.R., Brown, J.W.S., Baena-González, E., and Duque, P. 2016. The *Arabidopsis* SR45 Splicing Factor, a Negative Regulator of Sugar Signaling, Modulates SNF1-Related Protein Kinase 1 (SnRK1) Stability. Plant Cell **28**(August): tpc.00301.2016 10.1105/tpc.16.00301.

Causier, B., and Davies, B. 2002. Analysing protein-protein interactions with the yeast two-hybrid system. Plant Mol. Biol. **50**(6): 855–870 10.1023/A:1021214007897.

Cazalla, D., Zhu, J., Manche, L., Huber, E., Krainer, A.R., and Cáceres, J.F. 2002. Nuclear export and retention signals in the RS domain of SR proteins. Mol. Cell. Biol. **22**(19): 6871–6882 10.1128/MCB.22.19.6871-6882.2002.

Chinnusamy, V., Zhu, J., and Zhu, J.-K. 2007. Cold stress regulation of gene expression in plants. Trends Plant Sci. **12**(10): 444–451 10.1016/j.tplants.2007.07.002.

Cho, S., Hoang, A., Sinha, R., Zhong, X.-Y., Fu, X.-D., Krainer, A.R., and Ghosh, G. 2011. Interaction between the RNA binding domains of Ser-Arg splicing factor 1 and U1-70K snRNP protein determines early spliceosome assembly. Proc. Natl. Acad. Sci. U. S. A. **108**(20): 8233–8238 10.1073/pnas.1017700108.

Christie, P.J., Alfenito, M.R., and Walbot, V. 1994. Impact of low-temperature stress on general phenylpropanoid and anthocyanin pathways: Enhancement of transcript abundance and anthocyanin pigmentation in maize seedlings. Planta **194**: 541–549 10.1007/BF00714468.

Colwill, K. 1997. Identification of Clk/Sty as a serine/arginine-rich protein kinase (Doctoral dissertation). Retrieved from https://tspace.library.utoronto.ca/handle/1807/10888

Colwill, K., Pawson, T., Andrews, B., Prasad, J., Manley, J.L., Bell, J.C., and Duncan, P.I. 1996. The Clk/Sty protein kinase phosphorylates SR splicing factors and regulates their intranuclear distribution. EMBO J. **15**(2): 265–275.

Dahal, K.P., Gadapati, W., Savitch, L. V., Singh, J., and Hüner, N.P.A. 2012a. Cold acclimation and BnCBF17-over-expression enhance photosynthetic performance and energy conversion efficiency during long-term growth of Brassica napus under elevated

CO2 conditions. Planta **236**(5): 1639–1652 10.1007/s00425-012-1710-2.

Dahal, K.P., Kane, K., Gadapati, W., Webb, E., Savitch, L. V., Singh, J., Sharma, P., Sarhan, F., Longstaffe, F.J., Grodzinski, B., et al. 2012b. The effects of phenotypic plasticity on photosynthetic performance in winter rye, winter wheat and Brassica napus. Physiol. Plant. **144**(2): 169–188 10.1111/j.1399-3054.2011.01513.x.

Dahal, K.P., Kane, K., Sarhan, F., and Savitch, L. V. 2014. Factors as Targets for the Maintenance of Crop Yield under Suboptimal Growth Conditions. In Handbook of Plant and Crop Physiology. *Edited by* M. Pessarakli CRC Press . pp. 313–332.

Danyluk, J., Perron, A., and Houde, M. 1998. Accumulation of an acidic dehydrin in the vicinity of the plasma membrane during cold acclimation of wheat. Plant Cell … **10**(April): 623–638.

Ding, Y., Li, H., Chen, L.-L., and Xie, K. 2016. Recent Advances in Genome Editing Using CRISPR/Cas9. Front. Plant Sci. **7**(May): 703 10.3389/fpls.2016.00703.

Dong, C.-H., Agarwal, M., Zhang, Y., Xie, Q., and Zhu, J.-K. 2006. The negative regulator of plant cold responses, HOS1, is a RING E3 ligase that mediates the ubiquitination and degradation of ICE1. Proc. Natl. Acad. Sci. U. S. A. **103**(21): 8281–8286 10.1073/pnas.0602874103.

Dreze, M., Monachello, D., Lurin, C., Cusick, M.E., Hill, D.E., Vidal, M., and Braun, P. 2010. High-quality binary interactome mapping. Elsevier Inc. .

Duque, P. 2011. A role for SR proteins in plant stress responses. Plant Signal. Behav. **6**(1): 49–54.

Ehlert, B., and Hincha, D.K. 2008. Chlorophyll fluorescence imaging accurately quantifies

freezing damage and cold acclimation responses in *Arabidopsis* leaves. Plant Methods **4**: 12 10.1186/1746-4811-4-12.

Ensminger, I., Busch, F., and Hüner, N.P.A. 2006. Photostasis and cold acclimation: sensing low temperature through photosynthesis. Physiol. Plant. : 28–44 10.1111/j.1399-3054.2005.00627.x.

Farineau, J. 1999. Study of the non-photochemical dark rise in chlorophyll fluorescence in pre-illuminated leaves of various C3 and C4 plants submitted to partial anaerobiosis. Plant Physiol. Biochem. **37**(12): 911–918 10.1016/S0981-9428(99)00105-9.

Feng, Z., Mao, Y., Xu, N., Zhang, B., Wei, P., Yang, D.L., Wang, Z., Zhang, Z., Zheng, R., Yang, L., et al. 2014. Multigeneration analysis reveals the inheritance, specificity, and patterns of CRISPR/Cas-induced gene modifications in *Arabidopsis*. Proc Natl Acad Sci U S A **111**(12): 4632–4637 10.1073/pnas.1400822111.

Fields, S., and Song, O. 1989. A novel genetic system to detect protein-protein interactions. Nature **340**(6230): 245–246 10.1038/340245a0.

Filichkin, S.A., Priest, H.D., Givan, S.A., Shen, R., Bryant, D.W., Fox, S.E., Wong, W.-K., and Mockler, T.C. 2010. Genome-wide mapping of alternative splicing in *Arabidopsis thaliana*. Genome Res. **20**(1): 45–58 10.1101/gr.093302.109.

Fluhr, R. 2008. Regulation of Splicing by Protein Phosphorylation. In Nuclear Pre-mRNA Processing in Plants: Current Topics in Microbiology and Immunology. *Edited by* A.S.N. Reddy and M. Golovkin Springer-Verlag Berlin Heidelberg . pp. 119–138.

Forment, J., Naranjo, M.Á., Roldán, M., Serrano, R., and Vicente, O. 2002. Expression of *Arabidopsis* SR-like splicing proteins confers salt tolerance to yeast and transgenic plants.

Plant J. **30**(5): 511–519 10.1046/j.1365-313X.2002.01311.x.

Fowler, S.G., and Thomashow, M.F. 2002. *Arabidopsis* Transcriptome Profiling Indicates That Multiple Regulatory Pathways Are Activated during Cold Acclimation in Addition to the CBF Cold Response Pathway. Plant Cell Online **14**(8): 1675–1690 10.1105/tpc.003483.Toward.

Galau, G.A., and Dure, L. 1981. Developmental biochemistry of cottonseed embryogenesis and germination: changing messenger ribonucleic acid populations as shown by reciprocal heterologous complementary deoxyribonucleic acid--messenger ribonucleic acid hybridization. Biochemistry **20**: 4169–4178 10.1021/bi00517a033.

Gao, M.-J., Allard, G., Byass, L., Flanagan, A.M., and Singh, J. 2002. Regulation and characterization of four CBF transcription factors from Brassica napus. Plant Mol. Biol. **49**(5): 459–471 10.1023/A:1015570308704.

Gilmour, S.J., Zarka, D.G., Stockinger, E.J., Salazar, M.P., Houghton, J.M., and Thomashow, M.F. 1998. Low temperature regulation of the *Arabidopsis* CBF family of AP2 transcriptional activators as an early step in cold-induced COR gene expression. Plant J. **16**: 433–442 10.1046/j.1365-313X.1998.00310.x.

Gilmour, S.J., Fowler, S.G., and Thomashow, M.F. 2004. *Arabidopsis* transcriptional activators CBF1, CBF2, and CBF3 have matching functional activities. Plant Mol. Biol. **54**(5): 767–781 10.1023/B:PLAN.0000040902.06881.d4.

Golovkin, M., and Reddy, A.S.N. 1998. The plant U1 small nuclear ribonucleoprotein particle 70K protein interacts with two novel serine/arginine-rich proteins. Plant Cell **10**(10): 1637–1648 10.1105/tpc.10.10.1637.

Golovkin, M., and Reddy, A.S.N. 1999. An SC35-like protein and a novel serine/arginine-rich protein interact with *Arabidopsis* U1-70K protein. J. Biol. Chem. **274**(51): 36428–36438 10.1074/jbc.274.51.36428.

Gong, Z., Dong, C.-H., Lee, H., Zhu, J., Xiong, L., Gong, D., Stevenson, B., and Zhu, J.-K. 2005. A DEAD box RNA helicase is essential for mRNA export and important for development and stress responses in *Arabidopsis*. Plant Cell **17**(1): 256–267 10.1105/tpc.104.027557.

Gorsuch, P.A., Pandey, S., and Atkin, O.K. 2010. Temporal heterogeneity of cold acclimation phenotypes in *Arabidopsis* leaves. Plant. Cell Environ. **33**(2): 244–258 10.1111/j.1365-3040.2009.02074.x.

Graveley, B.R. 2000. Sorting out the complexity of SR protein functions. RNA **6**(9): 1197–1211.

Gray, G.R., Savitch, L. V., Ivanov, A.G., and Hüner, N.P.A. 1996. Photosystem II excitation pressure and development of resistance to photoinhibition (II. Adjustment of photosynthetic capacity in winter wheat and winter rye). Plant Physiol. (1 996): 61–71.

Gui, J.-F.F., Lane, W.S., and Fu, X.-D. 1994. A serine kinase regulates intracellular localization of splicing factors in the cell cycle. Nature **369**(6482): 678–682 10.1038/369678a0.

Guy, C.L., Huber, J.L., and Huber, S.C. 1992. Sucrose phosphate synthase and sucrose accumulation at low temperature. Plant Physiol. **100**(1): 502–508 10.1104/pp.100.1.502.

Guy, C.L., Kaplan, F., Kopka, J., Selbig, J., and Hincha, D.K. 2008. Metabolomics of temperature stress. Physiol. Plant. **132**(2): 220–235 10.1111/j.1399-3054.2007.00999.x.

Haake, V. 2002. Transcription Factor CBF4 Is a Regulator of Drought Adaptation in *Arabidopsis*. Plant Physiol. **130**(2): 639–648 10.1104/pp.006478.

Hannah, M.A., Heyer, A.G., and Hincha, D.K. 2005. A global survey of gene regulation during cold acclimation in *Arabidopsis thaliana*. PLoS Genet. **1**(2): e26 10.1371/journal.pgen.0010026.

Hansson, M., Dupuis, T., Strömquist, R., Andersson, B., Vener, A. V, and Carlberg, I. 2007. The mobile thylakoid phosphoprotein TSP9 interacts with the light-harvesting complex II and the peripheries of both photosystems. J. Biol. Chem. **282**(22): 16214–16222 10.1074/jbc.M605833200.

Havaux, M., and Kloppstech, K. 2001. The protective functions of carotenoid and flavonoid pigments against excess visible radiation at chilling temperature investigated in *Arabidopsis* npq and tt mutants. Planta **213**(6): 953–966 10.1007/s004250100572.

Hehl, R., Norval, L., Romanov, A., and Bülow, L. 2016. Boosting AthaMap database content with data from protein binding microarrays. Plant Cell Physiol. **57**(1): e4 10.1093/pcp/pcv156.

Hendrickson, L., Furbank, R.T., and Chow, W.S. 2004. A simple alternative approach to assessing the fate of absorbed light energy using chlorophyll fluorescence. Photosynth. Res. **82**: 73–81 10.1023/B:PRES.0000040446.87305.f4.

Henfrey, R.D., and Slater, R.J. 1988. Isolation of plant nuclei. Methods Mol. Biol. **4**: 447–452 10.1385/0-89603-127-6:447.

Henriques, F.S. 2009. Leaf Chlorophyll Fluorescence: Background and Fundamentals for Plant Biologists. Bot. Rev. **75**(3): 249–270 10.1007/s12229-009-9035-y.

Holaday, A.S., Martindale, W., Alred, R., Brooks, A.L., and Leegood, R.C. 1992. Changes in Activities of Enzymes of Carbon Metabolism in Leaves during Exposure of Plants to Low Temperature. Plant Physiol. **98**: 1105–1114 10.1104/pp.98.3.1105.

Hornyik, C., Terzi, L.C., and Simpson, G.G. 2010. The Spen Family Protein FPA Controls Alternative Cleavage and Polyadenylation of RNA. Dev. Cell **18**(2): 203–213 10.1016/j.devcel.2009.12.009.

Horton, P., Ruban, A. V., and Walters, R.G. 1996. Regulation of Light Harvesting in Green Plants. Annu. Rev. Plant Physiol. Plant Mol. Biol. **47**: 655–684 10.1146/annurev.arplant.47.1.655.

Horton, P., Johnson, M.P., Perez-Bueno, M.L., Kiss, A.Z., and Ruban, A. V. 2008. Photosynthetic acclimation: Does the dynamic structure and macro-organisation of photosystem II in higher plant grana membranes regulate light harvesting states? FEBS J. **275**(6): 1069–1079 10.1111/j.1742-4658.2008.06263.x.

Howard, J.M., and Sanford, J.R. 2014. The RNAissance family: SR proteins as multifaceted regulators of gene expression. Wiley Interdiscip. Rev. RNA **6**(February) 10.1002/wrna.1260.

Hu, Y.X., Wang, Y.X., Liu, X.F., and Li, J.Y. 2004. *Arabidopsis* RAV1 is down-regulated by brassinosteroid and may act as a negative regulator during plant development. Cell Res. **14**: 8–15 10.1038/sj.cr.7290197.

Huang, Y., and Steitz, J.A. 2001. Splicing factors SRp20 and 9G8 promote the nucleocytoplasmic export of mRNA. Mol. Cell **7**(4): 899–905 10.1016/S1097-2765(01)00233-7.

Huang, Y., and Steitz, J.A. 2005. SRprises along a messenger's journey. Mol. Cell **17**(5): 613–615 10.1016/j.molcel.2005.02.020.

Huang, G.-T., Ma, S.-L., Bai, L.-P., Zhang, L., Ma, H., Jia, P., Liu, J., Zhong, M., and Guo, Z.-F. 2012. Signal transduction during cold, salt, and drought stresses in plants. Mol. Biol. Rep. **39**(2): 969–987 10.1007/s11033-011-0823-1.

Huang, Y., Gattoni, R., Stévenin, J., and Steitz, J.A. 2003. SR splicing factors serve as adapter proteins for TAP-dependent mRNA export. Mol. Cell **11**(3): 837–843 10.1016/S1097-2765(03)00089-3.

Hüner, N.P.A., and Grodzinski, B. 2011. 1.23 - Photosynthesis and Photoautotrophy Elsevier B.V. .

Hüner, N.P.A., Palta, J., Li, P., and Carter, J. 1981. Anatomical changes in leaves of Puma rye in response to growth at cold-hardening temperatures. Bot. Gaz. **142**(1): 55–62.

Hüner, N.P.A., Öquist, G., Hurry, V., and Król, M. 1993. Photosynthesis, photoinhibition and low temperature acclimation in cold tolerant plants. Photosynth. Res. **37**: 19–39.

Hüner, N.P.A., Öquist, G., and Sarhan, F. 1998. Energy balance and acclimation to light and cold. Trends Plant Sci. **3**(98): 224–230 10.1016/S1360-1385(98)01248-5.

Hüner, N.P.A., Ivanov, A.G., Wilson, K.E., Miskiewicz, E., Król, M., and Öquist, G. 2002. Energy Sensing and Photostasis in Photoautotrophs. In Cell and Molecular Response to Stress. *Edited by* pp. 243–255.

Hüner, N.P.A., Ivanov, A.G., Sane, P. V., Król, M., Balseris, A., Rosso, D., and Savitch, L. V. 2008. Photoprotection of Photosystem II : Reaction Center. Antenna : 155–173.

Hüner, N.P.A., Bode, R., Dahal, K.P., Busch, F.A., Possmayer, M., Szyszka, B., Rosso, D., Ensminger, I., Krol, M., Ivanov, A.G., et al. 2013a. Shedding some light on cold acclimation, cold adaptation, and phenotypic plasticity. Botany **91**(3): 127–136 10.1139/cjb-2012-0174.

Hüner, N.P.A., Bode, R., Dahal, K.P., Busch, F.A., Possmayer, M., Szyszka, B., Rosso, D., Ensminger, I., Król, M., Ivanov, A.G., et al. 2013b. Shedding some light on cold acclimation, cold adaptation, and phenotypic plasticity. Botany **91**(3): 127–136 10.1139/cjb-2012-0174.

Hüner, N.P.A., Dahal, K.P., Kurepin, L. V., Savitch, L. V., Singh, J., Ivanov, A.G., Kane, K., and Sarhan, F. 2014. Potential for increased photosynthetic performance and crop productivity in response to climate change: role of CBFs and gibberellic acid. Front. Chem. **2**(April): 18 10.3389/fchem.2014.00018.

Iida, K., and Go, M. 2006. Survey of Conserved Alternative Splicing Events of mRNAs Encoding SR Proteins in Land Plants. Mol. Biol. Evol. **23**(5): 1085–1094 10.1093/molbev/msj118.

Ishitani, M., Xiong, L., Lee, H., Stevenson, B., and Zhu, J.K. 1998. HOS1, a genetic locus involved in cold-responsive gene expression in *Arabidopsis*. Plant Cell **10**(7): 1151–1161.

Ivanov, A.G., Morgan R. M., Gray, G.R., Velitchkova, M.Y., and Hüner, N.P.A. 1998. Temperature/light dependent development of selective resistance to photoinhibition of photosystem I. FEBS Lett. **430**(3): 288–292 10.1016/S0014-5793(98)00681-4.

Ivanov, A.G., Sane, P. V., Zeinalov, Y., Malmberg, G., Gardeström, P., Hüner, N.P.A., and Öquist, G. 2001. Photosynthetic electron transport adjustments in overwintering Scots pine

(Pinus sylvetris L.). Planta **213**(4): 575–585 10.1007/s004250100522.

Ivanov, A.G., Hendrickson, L., Król, M., Selstam, E., Öquist, G., Hurry, V., and Hüner, N.P.A. 2006. Digalactosyl-diacylglycerol deficiency impairs the capacity for photosynthetic intersystem electron transport and state transitions in *Arabidopsis thaliana* due to photosystem I acceptor-side limitations. Plant Cell Physiol. **47**(8): 1146–1157 10.1093/pcp/pcj089.

Ivanov, A.G., Rosso, D., Savitch, L. V., Stachula, P., Rosembert, M., Öquist, G., Hurry, V., and Hüner, N.P.A. 2012. Implications of alternative electron sinks in increased resistance of PSII and PSI photochemistry to high light stress in cold-acclimated *Arabidopsis thaliana*. Photosynth. Res. **113**(1–3): 191–206 10.1007/s11120-012-9769-y.

Jaglo-Ottosen, K.R., Gilmour, S.J., Zarka, D.G., Schabenberger, O., and Thomashow, M.F. 1998. *Arabidopsis* CBF1 overexpression induces COR genes and enhances freezing tolerance. Science **280**: 104–106 10.1126/science.280.5360.104.

Jiang, C., Iu, B., and Singh, J. 1996. Requirement of a CCGAC cis-acting element for cold induction of the BN115 gene from winter Brassica napus. Plant Mol. Biol. **30**(3): 679–684 10.1007/BF00049344.

Jiang, Y., Peng, D., Bai, L.-P., Ma, H., Chen, L.-J., Zhao, M.-H., Xu, Z.-J., and Guo, Z.-F. 2013. Molecular switch for cold acclimation -- anatomy of the cold-inducible promoter in plants. Biochem. Biokhimiĭa **78**(4): 342–354 10.1134/S0006297913040032.

Johnson, G.N. 2011. Reprint of: physiology of PSI cyclic electron transport in higher plants. Biochim. Biophys. Acta **1807**(8): 906–911 10.1016/j.bbabio.2011.05.008.

Jung, J.-H., Lee, H.-J., Park, M.-J., and Park, C.-M. 2014. Beyond ubiquitination:

proteolytic and nonproteolytic roles of HOS1. Trends Plant Sci. **19**(8): 538–545 10.1016/j.tplants.2014.03.012.

Jurczyk, B., Pociecha, E., Grzesiak, M., Kalita, K., and Rapacz, M. 2016. Enhanced expression of Rubisco activase splicing variants differentially affects Rubisco activity during low temperature treatment in Lolium perenne. J. Plant Physiol. **198**: 49–55 10.1016/j.jplph.2016.03.021.

Jurica, M.S., and Moore, M.J. 2003. Pre-mRNA Splicing. Mol. Cell **12**(1): 5–14 10.1016/S1097-2765(03)00270-3.

Kagaya, Y., Ohmiya, K., and Hattori, T. 1999. RAV1, a novel DNA-binding protein, binds to bipartite recognition sequence through two distinct DNA-binding domains uniquely found in higher plants. Nucleic Acids Res. **27**(2): 470–478 10.1093/nar/27.2.470.

Kalyna, M., Lopato, S., and Barta, A. 2003. Ectopic expression of atRSZ33 reveals its function in splicing and causes pleiotropic changes in development. Mol. Biol. Cell **14**(September): 3565–3577 10.1091/mbc.E03.

Kataoka, N., Bachorik, J.L., and Dreyfuss, G. 1999. Transportin-SR, a nuclear import receptor for SR proteins. J. Cell Biol. **145**: 1145–1152 10.1083/jcb.145.6.1145.

Kaye, C., Neven, L., Hofig, a, Li, Q.B., Haskell, D., and Guy, C. 1998. Characterization of a gene for spinach CAP160 and expression of two spinach cold-acclimation proteins in tobacco. Plant Physiol. **116**(4): 1367–1377 10.1104/pp.116.4.1367.

Knight, H., Zarka, D.G., Okamoto, H., Thomashow, M.F., and Knight, M.R. 2004. Abscisic acid induces CBF gene transcription and subsequent induction of cold-regulated genes via the CRT promoter element. Plant Physiol. **135**(July): 1710–1717

pp.104.043562.1710.

Van Kooten, O., and Snel, J.F.H. 1990. The use of chlorophyll fluoresence nomenclature in plant stress physiology. Photosynth. Res. **25**: 147–150.

Kramer, D.M., Johnson, G.N., Kiirats, O., and Edwards, G.E. 2004. New fluorescence parameters for the determination of Q A redox state and excitation energy fluxes. Photosynth. Res. **79**: 209–218.

Krause, H.G., and Weis, E. 1991. Chlorophyll Fluorescence and Photosynthesis: The Basics. Annu. Rev. Plant Physiol. Plant Mol. Biol. **42**(1): 313–349 10.1146/annurev.pp.42.060191.001525.

Król, M., Ivanov, A.G., Jansson, S., Kloppstech, K., and Hüner, N.P.A. 1999. Greening under High Light or Cold Temperature Affects the Level of Xanthophyll-Cycle Pigments, Early Light-Inducible Proteins, and Light-Harvesting Polypeptides in Wild-Type Barley and the Chlorina f2 Mutant1. Plant Physiol. **120**: 193–204 10.1104/pp.120.1.193.

Kurepin, L. V., Dahal, K.P., Savitch, L. V., Singh, J., Bode, R., Ivanov, A.G., Hurry, V., and Hüner, N.P.A. 2013. Role of CBFs as integrators of chloroplast redox, phytochrome and plant hormone signaling during cold acclimation. Int. J. Mol. Sci. **14**(6): 12729–12763 10.3390/ijms140612729.

Kurkela, S., and Franck, M. 1990. Cloning and characterization of a cold- and ABA-inducible *Arabidopsis* gene. Plant Mol. Biol. **15**(1): 137–144 10.1104/pp.111.179838.

de la Fuente van Bentem, S., Anrather, D., Roitinger, E., Djamei, A., Hufnagl, T., Barta, A., Csaszar, E., Dohnal, I., Lecourieux, D., and Hirt, H. 2006. Phosphoproteomics reveals extensive in vivo phosphorylation of *Arabidopsis* proteins involved in RNA metabolism.

Nucleic Acids Res. **34**(11): 3267–3278 10.1093/nar/gkl429.

de la Fuente van Bentem, S., Anrather, D., Dohnal, I., Roitinger, E., Csaszar, E., Joore, J., Buijnink, J., Carreri, A., Forzani, C., Lorković, Z.J., et al. 2008. Site-specific phosphorylation profiling of *Arabidopsis* proteins by mass spectrometry and peptide chip analysis. J. Proteome Res. **7**(6): 2458–2470.

Lai, M.-C., Lin, R.-I., and Tarn, W.-Y. 2003. Differential effects of hyperphosphorylation on splicing factor SRp55. Biochem. J. **371**(Pt 3): 937–945 10.1042/BJ20021827.

Lai, M.C., Lin, R.I., Huang, S.Y., Tsai, C.W., and Tarn, W.Y. 2000. A human importin-β family protein, transportin-SR2, interacts with the phosphorylated RS domain of SR proteins. J. Biol. Chem. **275**: 7950–7957 10.1074/jbc.275.11.7950.

Lazar, G., Schaal, T., Maniatis, T., and Goodman, H.M. 1995. Identification of a plant serine-arginine-rich protein similar to the mammalian splicing factor SF2/ASF. Proc. Natl. Acad. Sci. U. S. A. **92**(17): 7672–7676.

Lee, B.-H., and Zhu, J.-K. 2010. Phenotypic analysis of *Arabidopsis* mutants: electrolyte leakage after freezing stress. Cold Spring Harb. Protoc. **2010**(1): pdb.prot4970 10.1101/pdb.prot4970.

Lee, B.-H., Kapoor, A., Zhu, J., and Zhu, J.-K. 2006. STABILIZED1, a stress-upregulated nuclear protein, is required for pre-mRNA splicing, mRNA turnover, and stress tolerance in *Arabidopsis*. Plant Cell **18**: 1736–1749 10.1105/tpc.106.042184.

Lee, D., Polisensky, D.H., and Braam, J. 2005. Genome-wide identification of touch- and darkness-regulated *Arabidopsis* genes: A focus on calmodulin-like and XTH genes. New Phytol. **165**: 429–444 10.1111/j.1469-8137.2004.01238.x.

Lehti-Shiu, M.D., and Shiu, S.-H. 2012. Diversity, classification and function of the plant protein kinase superfamily. Philos. Trans. R. Soc. Lond. B. Biol. Sci. **367**(1602): 2619–2639 10.1098/rstb.2012.0003.

Lemaire, R., Prasad, J., Kashima, T., Gustafson, J., Manley, J.L., and Lafyatis, R. 2002. Stability of a PKCI-1-related mRNA is controlled by the splicing factor ASF/SF2: A novel function for SR proteins. Genes Dev. **16**(5): 594–607 10.1101/gad.939502.

Li, X.-P., Björkman, O., Shih, C., Grossman, A.R., Rosenquist, M., Jansson, S., and Niyogi, K.K. 2000. A pigment-binding protein essential for regulation of photosynthetic light harvesting. Nature **403**(6768): 391–395 10.1038/35000131.

Li, X.-P., Muller-Moule, P., Gilmore, A.M., and Niyogi, K.K. 2002. PsbS-dependent enhancement of feedback de-excitation protects photosystem II from photoinhibition. Proc. Natl. Acad. Sci. **99**(23): 15222–15227 10.1073/pnas.232447699.

Liu, Q., Kasuga, M., Sakuma, Y., Abe, H., Miura, S., Yamaguchi-Shinozaki, K., and Shinozaki, K. 1998. Two transcription factors, DREB1 and DREB2, with an EREBP/AP2 DNA binding domain separate two cellular signal transduction pathways in drought- and low-temperature-responsive gene expression, respectively, in *Arabidopsis*. Plant Cell **10**: 1391–1406 10.1105/tpc.10.8.1391.

Long, J.C., and Caceres, J.F. 2009. The SR protein family of splicing factors: master regulators of gene expression. Biochem. J. **417**(1): 15–27 10.1042/BJ20081501.

Long, S.P., Humphries, S., and Falkowski, P.G. 1994. Photoinhibition of photosynthesis in nature. Annu. Rev. Plant Physiol. Plant Mol. Biol. **45**: 633–662 10.1146/annurev.pp.45.060194.003221.

Lopato, S., Mayeda, A., Krainer, A.R., and Barta, A. 1996. Pre-mRNA splicing in plants: characterization of Ser/Arg splicing factors. Proc. Natl. Acad. Sci. U. S. A. **93**(April): 3074–3079 10.1073/pnas.93.7.3074.

Lopato, S., Kalyna, M., Dorner, S., Kobayashi, R., Krainer, A.R., and Barta, A. 1999a. atSRp30, one of two SF2/ASF-like proteins from *Arabidopsis thaliana*, regulates splicing of specific plant genes. Genes Dev. **13**(8): 987–1001.

Lopato, S., Gattoni, R., Fabini, G., Stevenin, J., and Barta, A. 1999b. A novel family of plant splicing factors with a Zn knuckle motif: examination of RNA binding and splicing activities. Plant Mol. Biol. **39**(4): 761–773 10.1023/A:1006129615846.

Lopato, S., Borisjuk, L., Milligan, A.S., Shirley, N., Bazanova, N., and Langridge, P. 2006. Systematic identification of factors involved in post-transcriptional processes in wheat grain. Plant Mol. Biol. **62**(4–5): 637–653 10.1007/s11103-006-9046-6.

Losciale, P., Oguchi, R., Hendrickson, L., Hope, A.B., Corelli-Grappadelli, L., and Chow, W.S. 2008. A rapid, whole-tissue determination of the functional fraction of PSII after photoinhibition of leaves based on flash-induced P700 redox kinetics. Physiol. Plant. **132**(1): 23–32 10.1111/j.1399-3054.2007.01000.x.

Lunde, C., Jensen, P.E., Haldrup, A., Knoetzel, J., and Scheller, H.V. 2000. The PSI-H subunit of photosystem I is essential for state transitions in plant photosynthesis. Nature **408**(6812): 613–615 10.1038/35046121.

Ma, C.T., Ghosh, G., Fu, X.-D., and Adams, J.A. 2010. Mechanism of Dephosphorylation of the SR Protein ASF/SF2 by Protein Phosphatase 1. J. Mol. Biol. **403**(3): 386–404 10.1016/j.jmb.2010.08.024.

Ma, L., Sun, N., Liu, X., Jiao, Y., Zhao, H., and Deng, X.W. 2005. Organ-specific expression of *Arabidopsis* genome during development. Plant Physiol. **138**: 80–91 10.1104/pp.104.054783.

Mahajan, S., and Tuteja, N. 2005. Cold, salinity and drought stresses: an overview. Arch. Biochem. Biophys. **444**: 139–158 10.1016/j.abb.2005.10.018.

Manley, J.L., and Krainer, A.R. 2010. A rational nomenclature for serine/arginine-rich protein splicing factors (SR proteins). Genes Dev. **24**(11): 1073–1074 10.1101/gad.1934910.

Mano, J., Miyake, C., Schreiber, U., and Asada, K. 1995. Photoactivation of the electron flow from NADPH to plastoquinone in spinach chloroplasts. Plant Cell Physiol. **36**(8): 1589–1598.

Marquez, Y., Brown, J.W.S., Simpson, C.G., Barta, A., and Kalyna, M. 2012. Transcriptome survey reveals increased complexity of the alternative splicing landscape in *Arabidopsis*. Genome Res. **22**(6): 1184–1195 10.1101/gr.134106.111.

Maruyama, K., Sakuma, Y., Kasuga, M., Ito, Y., Seki, M., Goda, H., Shimada, Y., Yoshida, S., Shinozaki, K., and Yamaguchi-Shinozaki, K. 2004. Identification of cold-inducible downstream genes of the *Arabidopsis* DREB1A/CBF3 transcriptional factor using two microarray systems. Plant J. **38**(6): 982–993 10.1111/j.1365-313X.2004.02100.x.

Maruyama, K., Takeda, M., Kidokoro, S., Yamada, K., Sakuma, Y., Urano, K., Fujita, M., Yoshiwara, K., Matsukura, S., Morishita, Y., et al. 2009. Metabolic pathways involved in cold acclimation identified by integrated analysis of metabolites and transcripts regulated by DREB1A and DREB2A. Plant Physiol. **150**(4): 1972–1980 10.1104/pp.109.135327.

Maruyama, K., Todaka, D., Mizoi, J., Yoshida, T., Kidokoro, S., Matsukura, S., Takasaki, H., Sakurai, T., Yamamoto, Y.Y., Yoshiwara, K., et al. 2012. Identification of cis-acting promoter elements in cold-and dehydration-induced transcriptional pathways in *Arabidopsis*, rice, and soybean. DNA Res. **19**(1): 37–49.

Matsui, A., Ishida, J., Morosawa, T., Mochizuki, Y., Kaminuma, E., Endo, T. a, Okamoto, M., Nambara, E., Nakajima, M., Kawashima, M., et al. 2008a. *Arabidopsis* transcriptome analysis under drought, cold, high-salinity and ABA treatment conditions using a tiling array. Plant Cell Physiol. **49**(8): 1135–1149 10.1093/pcp/pcn101.

Matsui, A., Ishida, J., Morosawa, T., Mochizuki, Y., Kaminuma, E., Endo, T.A., Okamoto, M., Nambara, E., Nakajima, M., Kawashima, M., et al. 2008b. *Arabidopsis* transcriptome analysis under drought, cold, high-salinity and ABA treatment conditions using a tiling array. Plant Cell Physiol. **49**(8): 1135–1149 10.1093/pcp/pcn101.

Maxwell, K., and Johnson, G.N. 2000. Chlorophyll fluorescence—a practical guide. J. Exp. Bot. **51**(345): 659–668.

Maxwell, P.C., and Biggins, J. 1976. Role of cyclic electron transport in photosynthesis as measured by the photoinduced turnover of P700 in vivo. Biochemistry **15**(18): 3975–3981 10.1021/bi00663a011.

Mazzucotelli, E., Mastrangelo, A.M., Crosatti, C., Guerra, D., Stanca, A.M., and Cattivelli, L. 2008. Abiotic stress response in plants: When post-transcriptional and post-translational regulations control transcription. Plant Sci. **174**(4): 420–431 10.1016/j.plantsci.2008.02.005.

Medina, J., Catalá, R., and Salinas, J. 2011. The CBFs: three *Arabidopsis* transcription

factors to cold acclimate. Plant Sci. **180**(1): 3–11 10.1016/j.plantsci.2010.06.019.

Mermoud, J.E., Cohen, P.T.W., and Lamond, A.I. 1994. Regulation of mammalian spliceosome assembly by a protein phosphorylation mechanism. EMBO J. **13**(23): 5679–5688.

Minagawa, J. 2011. State transitions--the molecular remodeling of photosynthetic supercomplexes that controls energy flow in the chloroplast. Biochim. Biophys. Acta **1807**(8): 897–905 10.1016/j.bbabio.2010.11.005.

Mishra, A., Mishra, K.B., Höermiller, I.I., Heyer, A.G., and Nedbal, L. 2011. Chlorophyll fluorescence emission as a reporter on cold tolerance in *Arabidopsis thaliana* accessions. Plant Signal. Behav. **6**(2): 301–310 10.4161/psb.6.2.15278.

Misteli, T., Cáceres, J.F., Clement, J.Q., Krainer, A.R., Wilkinson, M.F., and Spector, D.L. 1998. Serine phosphorylation of SR proteins is required for their recruitment to sites of transcription in vivo. J. Cell Biol. **143**(2): 297–307 10.1083/jcb.143.2.297.

Mitsuda, N., Ikeda, M., Takada, S., Takiguchi, Y., Kondou, Y., Yoshizumi, T., Fujita, M., Shinozaki, K., Matsui, M., and Ohme-Takagi, M. 2010. Efficient Yeast One-/Two-Hybrid Screening Using a Library Composed Only of Transcription Factors in *Arabidopsis thaliana*. Plant Cell Physiol. **51**(12): 2145–2151 10.1093/pcp/pcq161.

Miura, K., and Furumoto, T. 2013. Cold signaling and cold response in plants. Int. J. Mol. Sci. **14**(3): 5312–5337 10.3390/ijms14035312.

Miura, K., and Hasegawa, P.M. 2010. Sumoylation and other ubiquitin-like post-translational modifications in plants. Trends Cell Biol. **20**: 223–232 10.1016/j.tcb.2010.01.007.

Miura, K., Jin, J.B., Lee, J., Yoo, C.Y., Stirm, V., Miura, T., Ashworth, E.N., Bressan, R.A., Yun, D.-J., and Hasegawa, P.M. 2007. SIZ1-mediated sumoylation of ICE1 controls CBF3/DREB1A expression and freezing tolerance in *Arabidopsis*. Plant Cell **19**(4): 1403–1414 10.1105/tpc.106.048397.

Müller-Moulé, P., Li, X.-P., and Niyogi, K.K. 2001. Non-photochemical quenching. A response to excess light energy. Plant Physiol.

Munekage, Y., Hashimoto, M., Miyake, C., Tomizawa, K., Endo, T., Tasaka, M., and Shikanai, T. 2004. Cyclic electron flow around photosystem I is essential for photosynthesis. Nature **429**(6991): 579–582 10.1038/nature02598.

Murchie, E.H., and Lawson, T. 2013. Chlorophyll fluorescence analysis: A guide to good practice and understanding some new applications. J. Exp. Bot. **64**(13): 3983–3998 10.1093/jxb/ert208.

Nakashima, K., Yamaguchi-Shinozaki, K., and Shinozaki, K. 2014. The transcriptional regulatory network in the drought response and its crosstalk in abiotic stress responses including drought, cold, and heat. Front. Plant Sci. **5**(May): 170 10.3389/fpls.2014.00170.

Naseem, A., and Singla, R. 2013. Ex ante economic impact analysis of novel traits in canola. J. Agric. Resour. Econ. **38**(2): 248–268.

Nemoto, K., Seto, T., Takahashi, H., Nozawa, A., Seki, M., Shinozaki, K., Endo, Y., and Sawasaki, T. 2011. Autophosphorylation profiling of *Arabidopsis* protein kinases using the cell-free system. Phytochemistry **72**(10): 1136–1144 10.1016/j.phytochem.2011.02.029.

Ngo, J.C.K., Chakrabarti, S., Ding, J.-H., Velazquez-Dones, A., Nolen, B., Aubol, B.E., Adams, J.A., Fu, X.-D., and Ghosh, G. 2005. Interplay between SRPK and Clk/Sty kinases

in phosphorylation of the splicing factor ASF/SF2 is regulated by a docking motif in ASF/SF2. Mol. Cell **20**(1): 77–89 10.1016/j.molcel.2005.08.025.

Nishida, I., and Murata, N. 1996. CHILLING SENSITIVITY IN PLANTS AND CYANOBACTERIA: The Crucial Contribution of Membrane Lipids. Annu. Rev. Plant Physiol. Plant Mol. Biol. **47**: 541–568 10.1146/annurev.arplant.47.1.541.

Niyogi, K.K. 1999. PHOTOPROTECTION REVISITED: Genetic and Molecular Approaches. Annu. Rev. Plant Physiol. Plant Mol. Biol. **50**: 333–359 10.1146/annurev.arplant.50.1.333.

Niyogi, K.K., Grossman, A.R., and Björkman, O. 1998. *Arabidopsis* mutants define a central role for the xanthophyll cycle in the regulation of photosynthetic energy conversion. Plant Cell **10**(7): 1121–1134 10.1105/tpc.10.7.1121.

Novillo, F., Medina, J., and Salinas, J. 2007. *Arabidopsis* CBF1 and CBF3 have a different function than CBF2 in cold acclimation and define different gene classes in the CBF regulon. Proc. Natl. Acad. Sci. U. S. A. **104**: 21002–21007 10.1073/pnas.0705639105.

Oono, Y., Seki, M., Satou, M., Iida, K., Akiyama, K., Sakurai, T., Fujita, M., Yamaguchi-Shinozaki, K., and Shinozaki, K. 2006. Monitoring expression profiles of *Arabidopsis* genes during cold acclimation and deacclimation using DNA microarrays. Funct. Integr. Genomics **6**(3): 212–234 10.1007/s10142-005-0014-z.

Öquist, G., and Hüner, N.P.A. 2003. Photosynthesis of Overwintering Evergreen Plants. Annu. Rev. Plant Biol. **54**: 329–355 10.1146/annurev.arplant.54.072402.115741.

Orvar, B.L., Sangwan, V., Omann, F., and Dhindsa, R.S. 2000. Early steps in cold sensing by plant cells: the role of actin cytoskeleton and membrane fluidity. Plant J. **23**(6): 785–794

10.1046/j.1365-313x.2000.00845.x.

Palusa, S.G., Ali, G.S., and Reddy, A.S.N. 2007. Alternative splicing of pre-mRNAs of *Arabidopsis* serine/arginine-rich proteins: regulation by hormones and stresses. Plant J. **49**(6): 1091–1107 10.1111/j.1365-313X.2006.03020.x.

Peterhansel, C., Krause, K., Braun, H.-P., Espie, G.S., Fernie, a R., Hanson, D.T., Keech, O., Maurino, V.G., Mielewczik, M., and Sage, R.F. 2013. Engineering photorespiration: current state and future possibilities. Plant Biol. (Stuttg). **15**(4): 754–758 10.1111/j.1438-8677.2012.00681.x.

Peterson, R.B., and Havir, E.A. 2001. Photosynthetic properties of an *Arabidopsis thaliana* mutant possessing a defective PsbS gene. Planta **214**(1): 142–152 10.1007/s004250100601.

Peterson, R.B., and Havir, E.A. 2003. Contrasting modes of regulation of PS II light utilization with changing irradiance in normal and psbS mutant leaves of *Arabidopsis thaliana*. Photosynth. Res. **75**(1): 57–70 10.1023/A:1022458719949.

Pino, M.-T., Skinner, J.S., Jeknić, Z., Hayes, P.M., Soeldner, A.H., Thomashow, M.F., and Chen, T.H.H. 2008. Ectopic AtCBF1 over-expression enhances freezing tolerance and induces cold acclimation-associated physiological modifications in potato. Plant. Cell Environ. **31**(4): 393–406 10.1111/j.1365-3040.2008.01776.x.

Porra, R.J., Thompson, W.A., and Kriedemann, P.E. 1989. Determination of accurate extinction coefficients and simultaneous equations for assaying chlorophylls a and b extracted with four different solvents: verification of the concentration of chlorophyll standards by atomic absorption spectroscopy. Biochim. Biophys. Acta - Bioenerg. **975**: 384–394 10.1016/S0005-2728(89)80347-0.

Rausin, G., Tillemans, V., Stankovic, N., Hanikenne, M., and Motte, P. 2010. Dynamic nucleocytoplasmic shuttling of an *Arabidopsis* SR splicing factor: role of the RNA-binding domains. Plant Physiol. **153**(1): 273–284 10.1104/pp.110.154740.

Reddy, A.S.N. 2001. Nuclear Pre-mRNA Splicing in Plants. CRC. Crit. Rev. Plant Sci. **20**(6): 523–571 10.1080/20013591099272.

Reddy, A.S.N. 2004. Plant serine/arginine-rich proteins and their role in pre-mRNA splicing. Trends Plant Sci. **9**(11): 541–547 10.1016/j.tplants.2004.09.007.

Reddy, A.S.N. 2007. Alternative splicing of pre-messenger RNAs in plants in the genomic era. Annu. Rev. Plant Biol. **58**: 267–294 10.1146/annurev.arplant.58.032806.103754.

Reddy, A.S.N., and Ali, G.S. 2011. Plant serine/arginine-rich proteins: roles in precursor messenger RNA splicing, plant development, and stress responses. Wiley Interdiscip. Rev. RNA **2**(6): 875–889 10.1002/wrna.98.

Reddy, A.S.N., and Golovkin, M. 2008. Nuclear pre-mRNA processing in Plants Springer Berlin Heidelberg Berlin, Heidelberg .

Reinbothe, S., Reinbothe, C., Apel, K., and Lebedev, N. 1996. Evolution of chlorophyll biosynthesis - The challenge to survive photooxidation. Cell **86**(5): 703–705 10.1016/S0092-8674(00)80144-0.

Rezwan, M., and Auerbach, D. 2012. Yeast "N" -hybrid systems for protein-protein and drug-protein interaction discovery. Methods **57**(4): 423–429 10.1016/j.ymeth.2012.06.006.

Richards, E., Reichardt, M., and Rogers, S. 1994. Preparation of genomic DNA from plant tissue. Curr. Protoc. Mol. Biol. (1994): 1–7.

Richardson, D.N., Rogers, M.F., Labadorf, A., Ben-Hur, A., Guo, H., Paterson, A.H., and Reddy, A.S.N. 2011. Comparative analysis of serine/arginine-rich proteins across 27 eukaryotes: insights into sub-family classification and extent of alternative splicing. PLoS One **6**(9): e24542 10.1371/journal.pone.0024542.

Roach, T., and Krieger-Liszkay, A. 2012. The role of the PsbS protein in the protection of photosystems I and II against high light in *Arabidopsis thaliana*. Biochim. Biophys. Acta **1817**(12): 2158–2165 10.1016/j.bbabio.2012.09.011.

Roscigno, R.F., and Garcia-Blanco, M.A. 1995. SR proteins escort the U4/U6.U5 tri-snRNP to the spliceosome. RNA **1**(7): 692–706.

Roth, M.B., Murphy, C., and Gall, J.G. 1990. A monoclonal antibody that recognizes a phosphorylated epitope stains lampbrush chromosome loops and small granules in the amphibian germinal vesicle. J. Cell Biol. **111**(6 I): 2217–2223 10.1083/jcb.111.6.2217.

Sakuma, Y., Liu, Q., Dubouzet, J.G., Abe, H., Shinozaki, K., and Yamaguchi-Shinozaki, K. 2002. DNA-binding specificity of the ERF/AP2 domain of *Arabidopsis* DREBs, transcription factors involved in dehydration- and cold-inducible gene expression. Biochem. Biophys. Res. Commun. **290**(3): 998–1009 10.1006/bbrc.2001.6299.

Sane, P. V. 2003. Changes in the Redox Potential of Primary and Secondary Electron-Accepting Quinones in Photosystem II Confer Increased Resistance to Photoinhibition in Low-Temperature-Acclimated *Arabidopsis*. PLANT Physiol. **132**(4): 2144–2151 10.1104/pp.103.022939.

Sanford, J.R., Gray, N.K., Beckmann, K., and Cáceres, J.F. 2004. A novel role for shuttling SR proteins in mRNA translation. Genes Dev. **18**(7): 755–768 10.1101/gad.286404.

Sanford, J.R., Ellis, J.D., and Cáceres, J.F. 2005. Multiple roles of arginine/serine-rich splicing factors in RNA processing. Biochem. Soc. Trans. **33**(Pt 3): 443–446 10.1042/BST0330443.

Savaldi-Goldstein, S., Aviv, D., Davydov, O., and Fluhr, R. 2003. Alternative Splicing Modulation by a LAMMER Kinase Impinges on Developmental and Transcriptome Expression. Plant Cell **15**(4): 926–938 10.1105/tpc.011056.

Savitch, L. V., Barker-Astrom, J., Ivanov, A.G., Hurry, V., Öquist, G., Hüner, N.P.A., and Gardeström, P. 2001. Cold acclimation of *Arabidopsis thaliana* results in incomplete recovery of photosynthetic capacity, associated with an increased reduction of the chloroplast stroma. Planta **214**: 295–303 10.1007/s004250100622.

Savitch, L. V., Allard, G., Seki, M., Robert, L.S., Tinker, N.A., Hüner, N.P.A., Shinozaki, K., and Singh, J. 2005. The effect of overexpression of two Brassica CBF/DREB1-like transcription factors on photosynthetic capacity and freezing tolerance in Brassica napus. Plant Cell Physiol. **46**(9): 1525–1539 10.1093/pcp/pci165.

Savitch, L. V., Ivanov, A.G., Gudynaite-Savitch, L., Hüner, N.P.A., and Simmonds, J. 2009. Effects of low temperature stress on excitation energy partitioning and photoprotection in Zea mays. Funct. Plant Biol. **36**(1): 37 10.1071/FP08093.

Savitch, L. V., Ivanov, A.G., Gudynaite-Savitch, L., Hüner, N.P.A., and Simmonds, J. 2011. Cold stress effects on PSI photochemistry in Zea mays: differential increase of FQR-dependent cyclic electron flow and functional implications. Plant Cell Physiol. **52**(6): 1042–1054 10.1093/pcp/pcr056.

Scheller, H.V., and Haldrup, A. 2005. Photoinhibition of photosystem I. Planta : 5–8

10.1111/j.1399-3054.2010.01437.x.

Schöner, S., and Heinrich Krause, G. 1990. Protective systems against active oxygen species in spinach: response to cold acclimation in excess light. Planta **180**: 383–389 10.1007/BF00198790.

Shen, Y., Zhou, Z., Wang, Z., Li, W., Fang, C., Wu, M., Ma, Y., Liu, T., Kong, L.-A., Peng, D.-L., et al. 2014. Global Dissection of Alternative Splicing in Paleopolyploid Soybean. Plant Cell **26**(March): 996–1008 10.1105/tpc.114.122739.

Shikanai, T. 2007. Cyclic electron transport around photosystem I: genetic approaches. Annu. Rev. Plant Biol. **58**: 199–217 10.1146/annurev.arplant.58.091406.110525.

Shikanai, T. 2014. Central role of cyclic electron transport around photosystem I in the regulation of photosynthesis. Curr. Opin. Biotechnol. **26**(Figure 1): 25–30 10.1016/j.copbio.2013.08.012.

Shinozaki, K., and Yamaguchi-Shinozaki, K. 2000. Molecular responses to dehydration and low temperature: differences and cross-talk between two stress signaling pathways. Curr. Opin. Plant Biol. **3**(3): 217–223 10.1016/S1369-5266(00)80068-0.

Shinozaki, K., Yamaguchi-Shinozaki, K., and Seki, M. 2003. Regulatory network of gene expression in the drought and cold stress responses. Curr. Opin. Plant Biol. **6**(5): 410–417 10.1016/S1369-5266(03)00092-X.

Sonoike, K. 2011. Photoinhibition of photosystem I. Physiol. Plant. : 56–64 10.1111/j.1399-3054.2010.01437.x.

Sonoike, K., Kamo, M., and Hihara, Y. 1997. The mechanism of the degradation of psaB gene product, one of the photosynthetic reaction center subunits of photosystem I, upon

photoinhibition. Photosynth. Res. : 55–63.

Steponkus, P.L. 1984. Role of the plasma membrane in freezing injury and cold acclimation. Annu. Rev. Plant Physiol. **35**(221): 543–584 10.1146/annurev.pp.35.060184.002551.

Stitt, M., and Hurry, V. 2002. A plant for all seasons: alterations in photosynthetic carbon metabolism during cold acclimation in *Arabidopsis*. Curr. Opin. Plant Biol. **5**(3): 199–206.

Stojdl, D.F., and Bell, J.C. 1999. SR protein kinases: the splice of life. Biochem. Cell Biol. **77**(4): 293–298 10.1139/o99-046.

Strand, Å., Hurry, V., Gustafsson, P., and Gardeström, P. 1997. Development of *Arabidopsis thaliana* leaves at low temperatures releases the suppression of photosynthesis and photosynthetic gene expression despite the accumulation of soluble carbohydrates. Plant J. **12**(3): 605–614.

Strand, Å., Hurry, V., Henkes, S., Hüner, N.P.A., Gustafsson, P., Gardeström, P., Stitt, M., and Umeå, S. 1999. Acclimation of *Arabidopsis* Leaves Developing at Low Temperatures. Increasing Cytoplasmic Volume Accompanies Increased Activities of Enzymes in the Calvin Cycle and in the Sucrose-Biosynthesis Pathway. **119**(April): 1387–1397.

Strand, Å., Foyer, C.H., Gustafsson, P., Gardeström, P., and Hurry, V. 2003. Altering flux through the sucrose biosynthesis pathway in transgenic *Arabidopsis thaliana* modifies photosynthetic acclimation at low temperatures and the development of freezing tolerance. Plant, Cell Environ. **26**(4): 523–535 10.1046/j.1365-3040.2003.00983.x.

Swartz, J.E., Bor, Y.C., Misawa, Y., Rekosh, D., and Hammarskjold, M.L. 2007. The shuttling SR protein 9G8 plays a role in translation of unspliced mRNA containing a

constitutive transport element. J. Biol. Chem. **282**: 19844–19853 10.1074/jbc.M701660200.

Syed, N.H., Kalyna, M., Marquez, Y., Barta, A., and Brown, J.W.S. 2012. Alternative splicing in plants--coming of age. Trends Plant Sci. **17**(10): 616–623 10.1016/j.tplants.2012.06.001.

Szklarczyk, D., Franceschini, A., Wyder, S., Forslund, K., Heller, D., Huerta-Cepas, J., Simonovic, M., Roth, A., Santos, A., Tsafou, K.P., et al. 2014. STRING v10: protein-protein interaction networks, integrated over the tree of life. Nucleic Acids Res. **43**(D1): D447–D452 10.1093/nar/gku1003.

Szklarczyk, D., Franceschini, A., Wyder, S., Forslund, K., Heller, D., Huerta-Cepas, J., Simonovic, M., Roth, A., Santos, A., Tsafou, K.P., et al. 2015. STRING v10: protein-protein interaction networks, integrated over the tree of life. Nucleic Acids Res. **43**(Database issue): D447-52 10.1093/nar/gku1003.

Tacke, R., Chen, Y., and Manley, J.L. 1997. Sequence-specific RNA binding by an SR protein requires RS domain phosphorylation: creation of an SRp40-specific splicing enhancer. Proc. Natl. Acad. Sci. U. S. A. **94**(4): 1148–1153 10.1073/pnas.94.4.1148.

Takahashi, S., and Badger, M.R. 2011. Photoprotection in plants: A new light on photosystem II damage. Trends Plant Sci. **16**(1): 53–60 10.1016/j.tplants.2010.10.001.

Tanabe, N., Yoshimura, K., Kimura, A., Yabuta, Y., and Shigeoka, S. 2007a. Differential expression of alternatively spliced mRNAs of *Arabidopsis* SR protein homologs, atSR30 and atSR45a, in response to environmental stress. Plant Cell Physiol. **48**(7): 1036–1049 10.1093/pcp/pcm069.

Tanabe, N., Yoshimura, K., Kimura, A., Yabuta, Y., and Shigeoka, S. 2007b. Differential

expression of alternatively spliced mRNAs of *Arabidopsis* SR protein homologs, atSR30 and atSR45a, in response to environmental stress. Plant Cell Physiol. **48**(7): 1036–1049 10.1093/pcp/pcm069.

Thalhammer, A., and Hincha, D.K. 2013. The Function and Evolution of Closely Related COR/LEA (Cold-Regulated/Late Embryogenesis Abundant) Proteins in *Arabidopsis thaliana*. In Plant and Microbe Adaptations to Cold in a Changing World. *Edited by* R. Imai M. Yoshida and N. Matsumoto Springer New York New York, NY . pp. 89–105.

Thalhammer, A., Bryant, G., Sulpice, R., and Hincha, D.K. 2014. Disordered cold regulated15 proteins protect chloroplast membranes during freezing through binding and folding, but do not stabilize chloroplast enzymes in vivo. Plant Physiol. **166**(1): 190–201 10.1104/pp.114.245399.

Thomashow, M.F. 1999. PLANT COLD ACCLIMATION: Freezing Tolerance Genes and Regulatory Mechanisms. Annu. Rev. Plant Physiol. Plant Mol. Biol. **50**: 571–599 10.1146/annurev.arplant.50.1.571.

Tikkanen, M., and Aro, E.-M. 2012. Thylakoid protein phosphorylation in dynamic regulation of photosystem II in higher plants. Biochim. Biophys. Acta - Bioenerg. **1817**(1): 232–238 10.1016/j.bbabio.2011.05.005.

Tillemans, V., Leponce, I., Rausin, G., Dispa, L., and Motte, P. 2006. Insights into nuclear organization in plants as revealed by the dynamic distribution of *Arabidopsis* SR splicing factors. Plant Cell **18**: 3218–3234 10.1105/tpc.106.044529.

Towbin, H., Staehelin, T., and Gordon, J. 1979. Electrophoretic transfer of proteins from polyacrylamide gels to nitrocellulose sheets: procedure and some applications. Proc. Natl.

Acad. Sci. U. S. A. **76**: 4350–4354 10.1073/pnas.76.9.4350.

Trischuk, R.G., Schilling, B.S., Low, N.H., Gray, G.R., and Gusta, L. V. 2014. Cold acclimation, de-acclimation and re-acclimation of spring canola, winter canola and winter wheat: The role of carbohydrates, cold-induced stress proteins and vernalization. Environ. Exp. Bot. 10.1016/j.envexpbot.2014.02.013.

Tunnacliffe, A., Hincha, D.K., Leprince, O., and Macherel, D. 2010. Dormancy and Resistance in Harsh Environments. **21**: 91–108 10.1007/978-3-642-12422-8.

Twyffels, L., Gueydan, C., and Kruys, V. 2011. Shuttling SR proteins: More than splicing factors. FEBS J. **278**: 3246–3255 10.1111/j.1742-4658.2011.08274.x.

Vanlerberghe, G.C., Wang, J., Cvetkovska, M., and Dahal, K.P. 2015. Modes of electron transport chain function during stress : Does alternative oxidase respiration aid in balancing cellular energy metabolism during drought stress and recovery ? In Alternative Respiratory Pathways in Higher Plants. *Edited by* K.J. Gupta L.A.J. Mur and B. Neelwarne John Wiley & Sons, Inc . pp. 157–183.

Vogel, J.T., Zarka, D.G., Van Buskirk, H.A., Fowler, S.G., and Thomashow, M.F. 2005. Roles of the CBF2 and ZAT12 transcription factors in configuring the low temperature transcriptome of *Arabidopsis*. Plant J. **41**(2): 195–211 10.1111/j.1365-313X.2004.02288.x.

Wang, B.-B., and Brendel, V.P. 2004. The ASRG database: identification and survey of *Arabidopsis thaliana* genes involved in pre-mRNA splicing. Genome Biol. **5**(12): R102 10.1186/gb-2004-5-12-r102.

Wang, H.-Y., Lin, W., Dyck, J.A., Yeakley, J.M., Songyang, Z., Cantley, L.C., and Fu, X.-D. 1998. SRPK2: a differentially expressed SR protein-specific kinase involved in

mediating the interaction and localization of pre-mRNA splicing factors in mammalian cells. J. Cell Biol. **140**(4): 737–750.

Wilson, B., and Jacobs, D. 2004. Electrolyte leakage from stem tissue as an indicator of hardwood seedling physiological status and hardiness. Proc. Fourteenth Cent. Hardwood For. Conf. (765): 373–381.

Wilson, K.E., Ivanov, A.G., Öquist, G., Grodzinski, B., Sarhan, F., and Hüner, N.P.A. 2006. Energy balance, organellar redox status, and acclimation to environmental stress. Can. J. Bot. **84**(9): 1355–1370 10.1139/B06-098.

Wingler, A., Lea, P.J., Quick, W.P., and Leegood, R.C. 2000. Photorespiration: metabolic pathways and their role in stress protection. Philos. Trans. R. Soc. Lond. B. Biol. Sci. **355**(1402): 1517–1529 10.1098/rstb.2000.0712.

Woo, H.R., Kim, J.H., Kim, J., Kim, J., Lee, U., Song, I.-J., Kim, J.-H., Lee, H.-Y., Nam, H.G., and Lim, P.O. 2010. The RAV1 transcription factor positively regulates leaf senescence in *Arabidopsis*. J. Exp. Bot. **61**(14): 3947–3957 10.1093/jxb/erq206.

Wu, J.Y., and Maniatis, T. 1993. Specific interactions between proteins implicated in splice site selection and regulated alternative splicing. Cell **75**(6): 1061–1070 10.1016/0092-8674(93)90316-I.

Xiao, S.H., and Manley, J.L. 1997. Phosphorylation of the ASF/SF2 RS domain affects both protein-protein and protein-RNA interactions and is necessary for splicing. Genes Dev. **11**(3): 334–344 10.1101/gad.11.3.334.

Xin, Z., and Browse, J. 2000. Cold comfort farm: the acclimation of plants to freezing temperatures. Plant. Cell Environ. : 893–902.

Xin, Z., Mandaokar, A., Chen, J., Last, R.L., and Browse, J. 2007. *Arabidopsis* ESK1 encodes a novel regulator of freezing tolerance. Plant J. **49**(5): 786–799 10.1111/j.1365-313X.2006.02994.x.

Yamaguchi-Shinozaki, K., and Shinozaki, K. 2006. Transcriptional regulatory networks in cellular responses and tolerance to dehydration and cold stresses. Annu. Rev. Plant Biol. **57**: 781–803 10.1146/annurev.arplant.57.032905.105444.

Yamori, W., Hikosaka, K., and Way, D.A. 2014. Temperature response of photosynthesis in C3, C4, and CAM plants: temperature acclimation and temperature adaptation. Photosynth. Res. **119**(1–2): 101–117 10.1007/s11120-013-9874-6.

Yamori, W., Makino, A., and Shikanai, T. 2016. A physiological role of cyclic electron transport around photosystem I in sustaining photosynthesis under fluctuating light in rice. Sci. Rep. **6**(February): 20147 10.1038/srep20147.

Yang, T., Zhang, L., Zhang, T., Zhang, H., Xu, S., and An, L. 2005. Transcriptional regulation network of cold-responsive genes in higher plants. Plant Sci. **169**(6): 987–995 10.1016/j.plantsci.2005.07.005.

Zahler, A.M., Lane, W.S., Stolk, J.A., and Roth, M.B. 1992. SR proteins: a conserved family of pre-mRNA splicing factors. Genes Dev. **6**(5): 837–847 10.1101/gad.6.5.837.

Zhang, S., and Scheller, H.V. 2004. Photoinhibition of photosystem I at chilling temperature and subsequent recovery in *Arabidopsis thaliana*. Plant Cell Physiol. **45**(11): 1595–1602 10.1093/pcp/pch180.

Zhang, Z., and Krainer, A.R. 2004. Involvement of SR proteins in mRNA surveillance. Mol. Cell **16**(4): 597–607 10.1016/j.molcel.2004.10.031.

Zhang, P., Deng, H., Xiao, F., and Liu, Y. 2013. Alterations of Alternative Splicing Patterns of Ser/Arg-Rich (SR) Genes in Response to Hormones and Stresses Treatments in Different Ecotypes of Rice (Oryza sativa). J. Integr. Agric. **12**(5): 737–748 10.1016/S2095-3119(13)60260-9.

Zhong, X.-Y., Ding, J.-H., Adams, J.A., Ghosh, G., and Fu, X.-D. 2009. Regulation of SR protein phosphorylation and alternative splicing by modulating kinetic interactions of SRPK1 with molecular chaperones. Genes Dev. **23**(4): 482–495 10.1101/gad.1752109.

Zhu, J., Dong, C.-H., and Zhu, J.-K. 2007. Interplay between cold-responsive gene regulation, metabolism and RNA processing during plant cold acclimation. Curr. Opin. Plant Biol. **10**(3): 290–295 10.1016/j.pbi.2007.04.010.

Zimmermann, P., Hennig, L., and Gruissem, W. 2005. Gene-expression analysis and network discovery using Genevestigator. Trends Plant Sci. **10**(9): 407–409 10.1016/j.tplants.2005.07.003.

Appendix

Table A2.1: List of predicted cold- and dehydration- responsive promoter elements recognised in genes of *Arabidopsis thaliana* SR proteins, SRPK and LAMMER kinases.

The C-Terminal Repeat/Drought Responsive Elements (CRT/DRE), are recognized by CBFs and DREB2, which are involved in ABA-independent, low temperature and dehydration pathways, respectively. RELATED TO ABI3/VP1 (RAV1) promoter elements are recognized by RAV1 in an alternative low temperature responsive, ABA-independent pathway. ABA-responsive Binding factors (AREB/ABF) recognize and bind to the ABRE promoter elements involved in the dehydration responsive, ABA dependent pathway which is known to be induced in response to low temperatures. All predicted promoter elements are located 1000 bp upstream of the start codon according to data extracted from AthaMap (http://www.athamap.de/) (Hehl et al., 2016).

Gene Name	Gene locus	CRT/DRE RCCGAC CCGAG	RAV1 CAACA CACCTG	ABRE ACGTG TACGT
		SF2/ASF-like		
At-SR30	At1g09140		**3**	**1**
At-SR34	At1g02840	**2**	**4**	**7**
At-SR34b	At4g02430	**2**	**7**	**6**
		9G8/SRp20-like		
At-RSZ21	At1g23860		**3**	**8**
At-RSZ22	At4g31580		**3**	**8**
At-RSZ22a	At2g24590		**6**	**3**
		SC35-like		
At-SC35	At5g64200	**2**	**2**	**4**
		Plant specific		
At-SCL30	At3g55460	**1**	**1**	**3**
At-SCL30a	At3g13570	**2**		**7**
At-RS31	At3g61860	**1**	**9**	**5**
At-RS2Z32	At3g53500	**3**	**4**	**8**
At-RS2Z33	At2g37340	**1**	**4**	**2**
At-SCL33	At1g55310		**7**	**7**
At-RS40	At4g25500	**1**	**5**	**5**
At-RS41	At5g52040		**2**	
		SR-like		
At-SR45	At1g16610	**1**	**7**	**4**
At-SR45a	At1g07350	**1**	**12**	**1**
		LAMMER kinases (CLK/STY)		
At-AME1	At4g24740	**1**	**2**	**6**
At-AME2	At3g53570		**11**	**5**
At-AME3	At4g32660		**7**	**14**
		SRPK		
At-SRPK1	At4g35500		**2**	**4**
At-SRPK4	At3g53030	**2**	**4**	**3**
		SRPK-like		
SRPK-like 1	At2g17530		**2**	**2**
SRPK-like 2	At5g22840	**5**	**3**	**2**
		Pre-mRNA splicing related		
At-SRL1	At5g37370		**5**	**2**

Figure A2.1: Transcription profile of Bn-RS40, Bn-AME3 and Bn-SR45a in wild type *Brassica napus*, *BnCBF5* and *BnCBF17* overexpressors under non-acclimated (C), cold stress (S) and cold acclimation (A) conditions.

Gels shown in this figure were provided by David P. Sprott and Ekaterina Ponomareva.

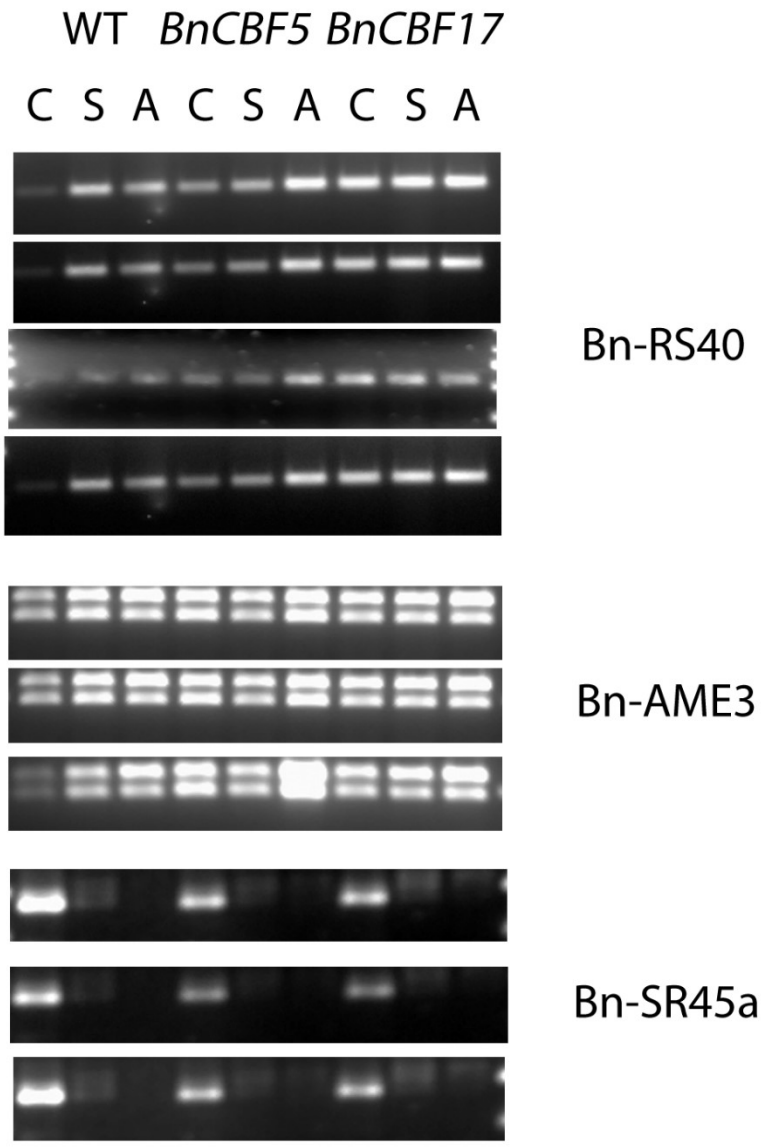
WT
BnCBF5
BnCBF17
C S A C S A C S A
Bn-RS40
Bn-AME3
Bn-SR45a

Figure A3.1 : Effects of different T-DNA insertion lines on the photochemical efficiency (F_v / F_m), excitation pressure of photosystem II (1-qL), linear electron transport rates (ETR), yield of photosystem II (Φ_{PSII}), antenna-based portion of non-photochemical quenching (Φ_{NPQ}), and PSII reaction centre-based portion of non-photochemical quenching ($\Phi_{f,D}$) of *rs41*, *sr45* and *rs40* mutants grown under control conditions, and after five weeks of cold acclimation.

White bars denote mutant lines tested under control conditions whereas grey bars represent samples from mutant lines grown under cold acclimation conditions. All leaves were measured at a Photon Flux Density (PFD) of 350 μmol m^{-2} s^{-1} (Panels A-F). Bars represent averaged values from 15 recordings + SE. Letters a-d denote statistical significance between parameters measured under control conditions compared to cold acclimation conditions, in accordance with Tukey's Honest Significant Difference test. Bars containing the letter a designate a p-value of $P \leq 0.05$ and b denoting a p-value of $P \leq 0.01$ between their non-acclimated and cold acclimated counterparts. Bars assigned with the letter c designate a statistically significant result with a p-value of $P \leq 0.01$ when compared to wild type samples, whereas the letter d designates a statistically significant difference of $P \leq 0.01$ between samples from mutant lines and wild type *Arabidopsis thaliana* grown under cold acclimation conditions.

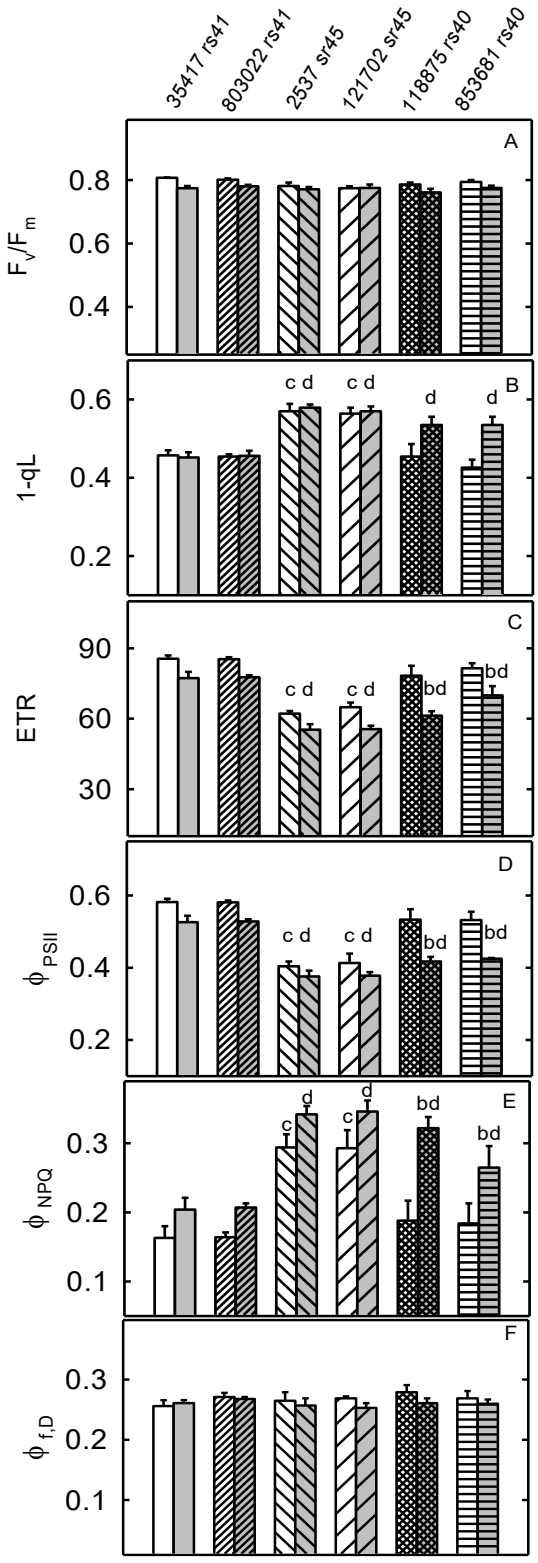
35417 rs41
803022 rs41
2537 sr45
121702 sr45
118875 rs40
853681 rs40
A
F_v/F_m
0.8
0.6
0.4
B
1-qL
0.6
0.4
0.2
c d
c d
d
d
C
ETR
90
60
30
c d
c d
bd
bd
D
ϕ_{PSII}
0.6
0.4
0.2
c d
c d
bd
bd
E
ϕ_{NPQ}
0.3
0.2
0.1
c
d
c
d
bd
bd
F
$\phi_{f,D}$
0.3
0.2
0.1

Figure A3.2: Assessment of the acquisition of freezing tolerance of wild type *Arabidopsis thaliana* compared to transgenic lines lacking SR genes or At-AME3, by means of an electrolyte leakage assay.

Leaves from wild type *Arabidopsis thaliana* plants grown under control conditions, and after cold acclimation conditions were compared to cold acclimated *rs41, sr34b, ame3, rs40, scl30, rsz22* and *sr34* mutant lines in electrolyte leakage assays. White circles denote leaves from wild type *Arabidopsis* grown under non-acclimated conditions, whereas black circles represent leaves from five weeks cold acclimated wild type *Arabidopsis*. Grey triangles pointed downwards represent leaf tissue from *at-rs41*, whereas upwards triangles represent data points from *at-sr34b* mutants. Grey squares denote data from *at-ame3* mutants, grey lozenges denote *at-rs41* data, grey circles represent *at-scl30* data, large crosses denote data from *at-rsz22* mutants while small grey crosses represent LT50 data from *at-sr34* mutants. Each point represents the mean of 3 recordings from 3 independent experiments ± SE (n=9).

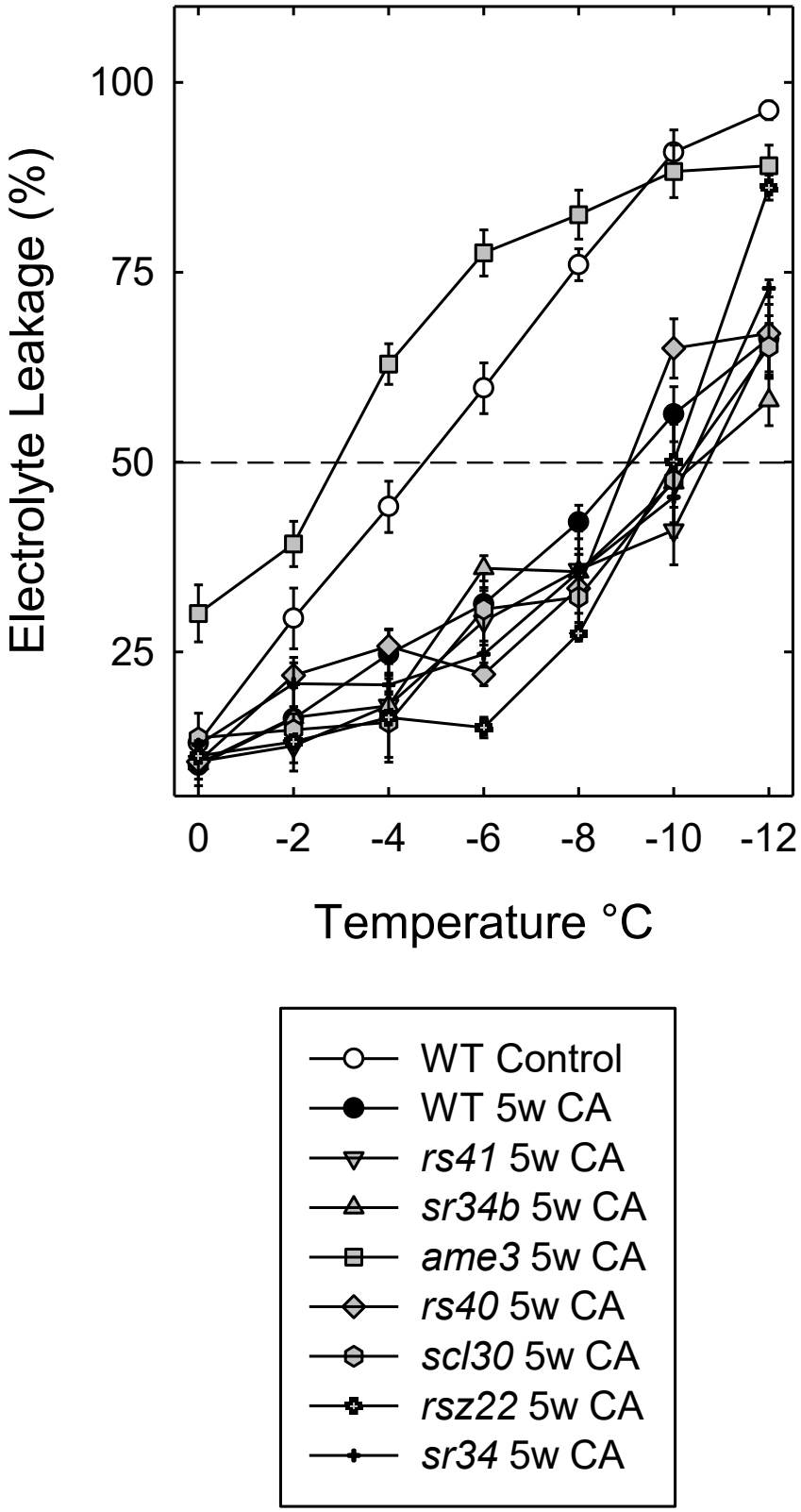
Electrolyte Leakage (%)
100
75
50
25
0
-2
-4
-6
-8
-10
-12
Temperature °C
WT Control
WT 5w CA
rs41 5w CA
sr34b 5w CA
ame3 5w CA
rs40 5w CA
scl30 5w CA
rsz22 5w CA
sr34 5w CA

Figure A3.3: Transcription profile of cold responsive genes in non-acclimated wild type *Arabidopsis* (WT), five weeks cold acclimated wild type (WT 5w CA), 5 weeks cold acclimated SR, and AME3 loss-of-function mutants.

Total RNA extracted from wild type *Arabidopsis* leaf tissue, as well as leaf tissue from cold acclimated *rs41*, *sr34b, ame3, rs40, scl30, rsz22* and *sr34* mutant lines were converted to cDNA by means of reverse transcriptase PCR, to be used for subsequent quantitative PCR analyses of the expression levels of ICE1 (A), HOS1 (B), CBF1 (C), CBF3 (D), COR15A (E), COR15B (F), KIN1 (G) and LTI78 (H). Bars represent averaged values from two independent experiments, with three technical replicates + SE (n=6). The data presented in this figure was provided by David P. Sprott.

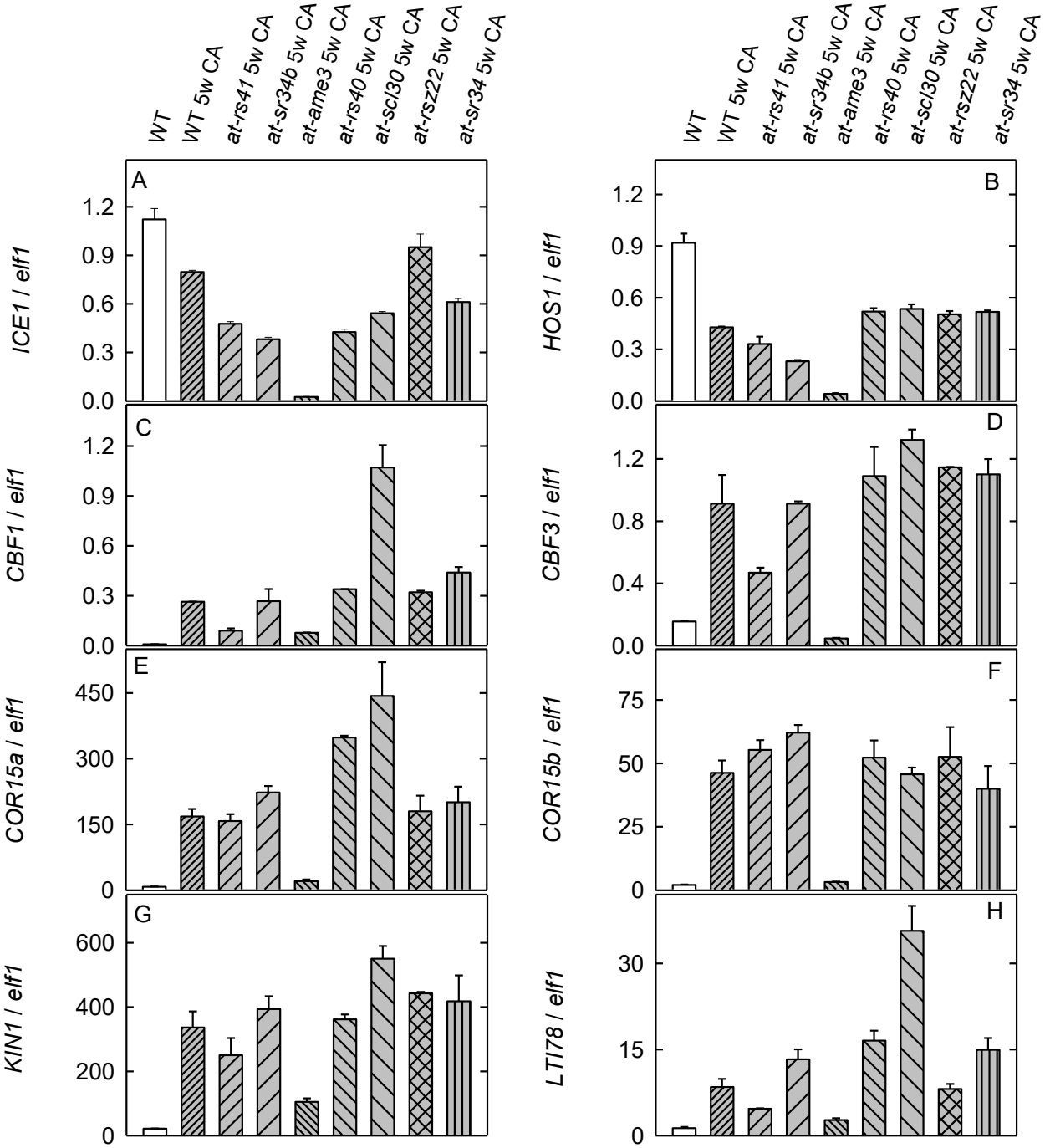
WT
WT 5w CA
at-rs41 5w CA
at-sr34b 5w CA
at-ame3 5w CA
at-rs40 5w CA
at-scl30 5w CA
at-rsz22 5w CA
at-sr34 5w CA
A
ICE1 / elf1
B
HOS1 / elf1
C
CBF1 / elf1
D
CBF3 / elf1
E
COR15a / elf1
F
COR15b / elf1
G
KIN1 / elf1
H
LTI78 / elf1